The University Of Sheffield.

Adaptation to suspension growth: analysing the surface of suspension growth adapted Chinese hamster ovary cells

by Christa G Walther

submitted for the degree of Doctor of Philosophy

Department of Chemical and Biological Engineering

January 2013

Statement of Originality:

The work presented in this thesis is to the best of my knowledge and belief original, except as acknowledged in the text. I hereby declare that I have not submitted this material, either in whole or in part, for a degree at this or any other institution.

January 2013

dedicated to my mum

Rita Wolters

*** 1932**

† 2009

Du fehlst.

Acknowledgement

I would like to thank Prof. David C. James and Dr. Mark Leonard for the opportunity to work on this project and learn about bio-pharmaceutical production in CHO cells. I am grateful for the feedback and input I got from Dr. Robin Heller-Harrison and Dr. Mark Melville, both previously at Wyeth (now Pfizer), during the first two years of the project. Also I would like to thank Pfizer for the financial support. Rob Whitfield, who has been using the same cell lines in his PhD project, was always helpful with tips on cell culture, cell splitting during times of holiday and organised the continuous flow of the proprietary media by sending lots of emails and handling the huge delivery boxes. For the supply with the media a big thank you goes as well to the media production department at Pfizer and to Steve Brennan for organising the shipments.

I am really grateful for the help I got at the Sheffield Medical School from Sue Newton and Kay Hopkinson, who answered every question about flow cytometry I had and also found alternative instruments to measure on when need arose. At the Kroto Research Institute, Dr. Nicola Green introduced me to confocal microscopy, trained me patiently on the use of the confocal microscope and helped with all questions I had.

I enjoyed working with the different nationalities and personalities in the group; to Olivia Mozley a big thank you for understanding my English when I myself wasn't too sure what I was trying to say and for discussing confocal experiment set-up. More thanks go to Dr. Paul Dobson, who undertook the effort to read a thesis draft, and to Dr. Henriette Jensen, Dr. Esther Karunakaran and Dr. Phil Jackson for their feedback on single chapters.

I would also like to thank my sister, my father and my friends in Germany who, although they found the project rather unexciting, continued to be interested in my progress. Finally, I would like to thank my husband Thomas, who besides doing a lot of cooking over the last years to keep us alive (he is now a much better cook than I am), also tried hard to learn and understand major biological terms in order to perhaps become able to understand my project. He also made sure that typical German grammar mistakes have been kept to a minimum. I promise him to not be as short tempered next year as during the last months.

Abstract

Many bio-pharmaceutical production processes are based upon the use of mammalian cell lines, such as Chinese hamster ovary (CHO) cells, capable of proliferation as single cells in suspension in a synthetic environment. Routine use of CHO cells as production vehicles requires a lengthy "adaptation" process from the wild-type adherent clone to clones capable of proliferation in a suspension environment depleted of exogenous growth factors and cell-matrix contacts. Different approaches have been applied in this study to gain a better understanding of the changes on the cell surface occurring as a response to changes in their environment, comparing four cell lines (CCL61, AML, S cells and CHO-S) adapted to suspension or adherence growth condition.

Biochemistry and mass spectrometry methods showed differences in surface protein composition for the cell lines. The comparison of the expression of cell-to-cell adhesion molecules revealed a highly variable bimodal distribution on S cells which was not seen on CCL61. Analysis of the expression level of integrins, the main interaction partner of serum components, indicated that integrin expression is not generally down-regulated on suspension-adapted CHO cells. The integrin conformation on the cell surface, analysed by confocal microscopy, revealed a specific conformation, especially with regard to integrin beta 1, characterised by an even, net-like distribution of integrin clusters over the surface of the cells. This specific integrin conformation, which has only been found on suspension-adapted cells, was underlined by a sub-cortical sheet of actin, forming a ball-like structure directly under the cell membrane; this actin conformation required re-organisation of the actin cytoskeleton from a typical fibrillar morphology in adherent cells. The actin content was higher in suspension cell lines compared to adherent cells, but actin up-regulation was also found in non-suspension adapted cells after they had been transferred into suspension.. Sphere-like integrin beta 1 clustering on CCL61 grown in suspension could be induced by treatment with cytochalasin D, followed by suspension culture without the drug, however, despite the change in integrin beta 1 conformation these cells could not grow in suspension.

The data suggests that adaptation to suspension growth requires conservation of integrins, presumably with respect to their role as structural elements anchoring the plasma membrane to the sub-cortical actin sheath, but it also requires additional changes in the interplay between integrin beta 1 and actin, for example, changes in the regulation of the associated proteins for successful suspension adaptation of CHO cells.

Table of Contents

10. Chapter

List of Tables

List of Figures

Abbreviations and Synonyms

ab	antibody
ATCC	American Type Culture Collection
ANOVA	analysis of variance
BSA	bovine serum albumin
CD29	integrin beta 1
CD324	E-cadherin
CD49a	integrin alpha 1
CD49d	integrin alpha 4
CD56	NCAM
CHO	Chinese hamster ovary
CS	complete specific staining
DIC	differential interference contrast
DMSO	Dimethylsulfoxid
DTT	Dithiothreitol
ECACC	European Collection of Cell Cultures
EDTA	Ethylenediaminetetraacetic acid
EGF	epithelial growth factor
EtOH	ethanol
ERK	extracellular signal-regulated kinases
FAK	focal adhesion kinase
FBS	fetal bovine serum
FI	fluorescence intensity
FITC	Fluorescein isothiocyanate
FSC	forward scatter
GPI	glycosylphospatidylinositol
HGF	Hepatocyte growth factor
HPLC -MS	high pressure (performance) liquid chromatography coupled to mass spectrometry
HSC	hematopoietic stem cells
IGF-1	insulin-like growth factor 1
IgG	immunoglobulin G
ILK	integrin linked kinase
ITC	isotype control

kDa	kilo Dalton
LC-MS	liquid chromatography coupled to mass spectrometry
MAP kinase	mitogen activated protein kinase
mF12	Ham's modified F-12K medium
MFI	median fluorescence intensity
NCAM	neural cell adhesion molecule
NHS	N-hydroxysuccinimide
NSO	myeloma cell line
PAM	proprietary adherent media
PBS	phosphate buffered saline
PE	phycoerythrin
PFA	para-formaldehyde
PI3	phosphoinositide 3 - kinase
PSM	proprietary suspension media
Q_p	production rate
rpm	rotations per minute
SDS	sodium dodecyl sulfate
SO	secondary antibody only
TM	trade mark
TRIS	tris(hydroxymethyl)aminomethane
VCAM-1	vascular cell adhesion protein 1
VCD	viable cell density

1. Chapter

Introduction

In this chapter the basic background of the research undertaken is explained and the objectives of the research project and different approaches used are described.

1.1 Basic background

The biopharmaceutical industry, which has grown continuously since the first human recombinant protein, human insulin, has been put onto the market in 1982 (Pavlou and Reichert, 2004) is assumed to grow further in particular due to the increase in use of human antibodies as therapeutics (van Dijk and van de Winkler, 2001; Trikha *et al.*, 2002) but also due to the possibility of high sales such as seen for Erythopeitin which has reached over 1 billion US dollar sales (Wurm, 2004). Mammalian cell lines are used widely in the biopharmaceutical industry (Godia and Cairó, 2001) for the production of recombinant products, such as antibodies (Dinnis and James, 2005) and other recombinant proteins, such as cytokines (Browne and Al-Rubeai, 2007). Mammalian cells enable post-translational modifications such as glycosylation, which are necessary to be able to use recombinant proteins widely as drugs in humans and are not possible to achieve in bacterial production processes to the same extent (Birch and Racher, 2006). The successful establishment of a mammalian production cell line, however, is far more expensive than establishing a bacterial production culture (Kuystermans *et al.*, 2007). The growing demand for therapeutic products can only be met by optimisation of specific productivity and increased viable cell density of the cell lines used (Browne and Al-Rubeai, 2007). Modern mammalian cell culture processes can now achieve product concentrations above 5g/ L (Birch and Racher, 2006) but the aim is to achieve even higher production efficiencies by not only increasing production rates (Q_p) but achievable cell densities. To reach this aim choosing cell lines showing good stability and growth in suspension conditions based on a chemically defined and animal component free medium (Birch and Racher, 2006) is required. Together with optimal cell culture condition the mammalian expression vector used for expression of the recombinant gene needs to allow efficient transcription of the gene

product and in addition needs to allow for selection of stable transfectants. Selection often occurs based on the absence of an essential metabolite in the non-transfected cells (Wurm, 2004). For stable transfectants the vector needs to be integrated into the genome to allow replication and inheritance of the vector during cell division (Ludwig, 2006). Numerous selection methods have been developed to allow reliable selection of high producing cell lines, with limited dilution cloning still being the most commonly used traditional method (Browne and Al-Rubeai, 2007) but the trend clearly goes to automated systems, such as the *Clonepix* from Genetix, which allow high throughput approaches to clone selection (Browne and Al-Rubeai, 2007). Optimisation of the specific productivity of the cell line in question is another key factor in the development of a stable production process that is to deliver appropriate amounts of product at an acceptable price (Birch and Racher, 2006). In general, for large scale production processes the preferred culture format is a single cell suspension reactor, in recent years together with chemically defined, animal component free media (Butler, 2005). As wild type mammalian cell strains usually grow adherently and require serum supplementation, establishing a cell line that is capable of growing in a serum free suspension culture is a major step in process development. It can either be applied to a non-transfected cell line, to be used for creation of a production cell line later, or to a transfected cell line that has already undergone selection with regards to transcription and translation of product and usually requires a transfer of the cell line in question into suspension conditions followed by a stepwise reduction of the serum concentration (Sinacore *et al.*, 2000). The strategy of adaptation to suspension growth is necessary as the required product concentrations with yields in the g/ L range cannot be achieved by the classical culturing approaches using adherent cell cultures in, for example, roller bottles (Wurm, 2004). Furthermore, using serum free media reduces the risk of introducing viruses or other transmissible agents; in addition, upstream processing of secreted product becomes much more feasible when no serum is supplemented. Serum is also a major cost factor in large scale production and in addition can introduce variations in production yields due to batch to batch variation (Rodrigues *et al.*, 2012). The original cell lines of Chinese hamster ovary cells (epithelial-like (ATCC)/ fibroblast-like (Puck, 1958)), NS0 cells (myeloma cells (ATCC)) and baby hamster kidney cells (fibroblasts, ECACC), which are all used frequently in the biopharmaceutical industry (Kuystermans *et al.*, 2007; Hossler *et al*., 2009), are anchorage and serum dependent and hence their growth depends on signalling interactions with serum components and inter-cellular signalling. Usually, the transformation to serum free suspension growth goes hand in hand with an increase in productivity due to the possibility of reaching high final cell densities

during the adaptation process. As noted earlier, the adaptation process is a long multi-step process; the design of serum free media is an important part of this process and no single solution even for clones from the same parental cell line has been found (Butler, 2005). Consistent control of the growth and production capability of the cell lines during adaptation is necessary and the final adaptation to serum free conditions might only be possible by supplementation of the media with defined proteins or small molecules (Rodrigues *et al.*, 2012). In general, this process is still not 100% successful which is also due to the fact that little is known about the changes in the cell itself that allow successful adaptation to a new synthetic environment. For instance, interruption of integrin cell signalling due to disruption of extracellular matrix-cell contact, due to, for example serum withdrawal, has been shown to lead to apoptosis (Streuli, 2009). The loss of cell surface contact in suspension growth will hence induce changes in the cell membrane itself. Also, changes in protein expression and cell metabolism have to occur during the adaptation process to allow for successful proliferation in the new environment. These changes might be due to changes in protein expression on the cell membrane and/or switching on/off different pathways involved in cell proliferation (Pontier and Muller, 2009).

1.2 Objectives and Approaches used

In this thesis different approaches to gain a more detailed understanding of the changes in the cell surface as a response to a change in environment have been applied. The cell surface of different cell lines growing in different environments was analysed for different parameters, comparing Chinese Hamster ovary cell lines adapted to suspension and/or adherence growth conditions. Those cell lines had not been further modified for production of biopharmaceuticals, e.g not transfected, to ensure the main selection pressure the analysed suspension cell lines have undergone was aimed at suspension adaptation only. The aim is to gain a detailed understanding of the changes that occur on and close to the cell surface due to the adaptation to the required synthetic cell culture environment and how the surface phenotype of the suspension cell line differs from the original adherent cell line as a result of the variation in culture conditions.

First, the hypothesis that changes in the surface protein composition may occur was tested. Biochemistry in combination with mass spectrometry was used to gain an overview on surface proteins expressed on the suspension cells.

Using flow cytometric analysis based on antibody staining the next step was to analyse up- and down-regulation of the expression of a chosen subset of surface proteins in the different cell lines.

One focus was on integrins, as integrins are the main molecules interacting with the serum in adherent growth conditions, using antibodies against integrin beta 1, integrin alpha 4 and integrin alpha 1; as no serum has been added in suspension conditions it was hypothesized that integrins may become down-regulated in suspension (Ruoslathi and Reed, 1994). In addition, a subset of proteins involved in cell-to-cell signalling was analysed as a second group of surface proteins involved in interaction with the environment, as several proteins of this type had been identified in the mass spectrometry analysis of the suspension cells in previous (Ahram, 2005) and in this study.

This was followed by a confocal microscopy analysis of those proteins identified as being stable expressed on the suspension cell lines, which allowed information to be gathered on structural conformation of those markers. Confocal microscopy and flow cytometry of the cytoskeleton of the cell lines was included as the cytoskeleton is known to be an important interaction partner of integrins on the intracellular side of cells (DeMali *et al.*, 2003). The information gathered was questioned by treating cells with cytochalasin D, a reagent influencing adherence and actin conformation (Lub *et al.*, 1997), to determine whether the identified phenotype characterised by a conformational change in integrin and actin expression could be induced for the adherent cell line and by this, allow successful suspension growth.

1.3 Summary of the main results

Using flow cytometric analysis as an ideal method to determine expression levels of proteins on the cell surface, it was demonstrated that integrins are not generally down-regulated in suspension adapted CHO cells, with different integrins either being up- or downregulated on the analysed suspension cell lines. This led to the conclusion that decrease in integrin expression level is not a common phenotypic feature of suspension CHO cells despite previous studies showing a loss of adhesion for cell lines down-regulating integrin expression (Giancotti and Rouslathi, 1990).

The actin content of the different cell lines was shown to depend mainly upon the cell environment by flow cytometric analysis, as actin content was shown to be up-regulated in non-suspension adapted CHO cells after being transferred into suspension conditions..

Analysing the conformation of the three integrins on the cell surface by confocal microscopy revealed a specific conformation especially with regard to integrin beta 1 for suspension adapted cells. This was characterised by an even distribution of the integrin sub-chain over the entire surface of the cells. Studying the three-dimensional geometry, this distribution formed a regular net of integrin beta 1 on the surface covering the entire cell. This net of integrin sub-chains on the cell

surface was lined by a thick sub-cortical sheet of actin forming a strong ball-like structure directly under the cell membrane, usually seen for suspension cells such as lymphocytes (Lub *et al*., 1997).

Further analysis aiming at the interaction between integrins and actin structure revealed that the specific integrin beta 1 conformation seen for suspension adapted CHO cells can be induced even in non-suspension adapted CHO cells by using Cytochalasin D as an actin structure influencing drug. Nevertheless, this treatment did not allow the cells to grow in suspension, indicating that further changes, for example in the intracellular signalling, are needed for successful growth in serum free suspension culture. The intracellular signalling changes of the cell lines in question have been analysed in a parallel PhD study using western blotting and flow cytometric analysis.

2. Chapter

Chinese hamster ovary cells as a production vehicle that requires suspension adaptation

In this chapter CHO cells are introduced as a production vehicle and the importance of a better understanding of the molecular level of suspension adaptation is explained. An overview of research on cell surface protein expression in different areas will be given to illustrate the large variety of cell surface changes occurring in adaptation (forced or by chance) to a new environment. In this context, integrins as the main surface receptor proteins which interact with extracellular matrix proteins will be introduced together with some of their interaction partners. More details about cell to cell adhesion molecules, the role, structure and characteristics of integrins and how integrins interact with the actin cytoskeleton can be found in chapters 6, 7 and 8, respectively. Furthermore, using a proteomics approach to cell surface analysis as a starting point of this project is justified.

2.1 Chinese hamster ovary cells for biopharmaceutical production

Biopharmaceuticals, meaning therapeutic proteins such as monoclonal antibodies and anti-inflammatory cytokines produced through engineering processes, will be increasingly important for future drug development and account for around a quarter of all newly developed drugs in the US market (Browne and Al-Rubeai, 2007). Mammalian cell lines are the vehicles of choice, due to their capability to produce proteins with post-translational modifications and glycosylation patterns similar to human proteins (Hossler *et al.*, 2009). The Chinese hamster ovary (CHO) cell line, established by Puck *et al.* in 1958, is one of the earliest established mammalian cell lines. It is an adherent epithelial cell line that in standard growth conditions, which include fetal calf serum, shows fibroblast-like growth patterns (Auersperg *et al.*, 2001). CHO cells have been used since 1986 as a production vehicle (Wurm, 2004; Dinnis and James, 2005) in large scale bio-pharmaceutical production due their capability to produce high protein concentrations and the consistency in product characteristics (Birch and Racher, 2006; Wurm, 2004) in combination with

their ability to produce therapeutics with highly N-linked glycosylation (Hossler *et al.,* 2009; Farges *et al.*, 2008). Hossler *et al.* (2009) clearly show the predominance of CHO as production vehicle for FDA approved glycosylated therapeutics. The original Chinese hamster ovary cell line from Puck requires serum to grow successfully (Ham, 1964) whereas today in biopharmaceutical large scale production only suspension cells in serum-free chemically defined medium are used. CHO cells have also been used for production of recombinant proteins in micro-carrier based cultures. These allow to achieve high cell densities in cultures where cells can still grow attached to a surface. Those culture conditions enable a protection of the cells from the shear forces but growth can be reduced compared to suspension culture (Spearman *et al*., 2005). Micro-carrier culture results can be greatly influenced by the culture vessel, not only with respect to growth behaviour but also heterogeneity of product with respect to glycosylation profile (Costa *et al*., 2013). The adaptation to serum free chemically defined media has been driven by factors such as high cost of serum, risk of product contamination and batch to batch variation. Nevertheless, serum is known to contain numerous factors relevant for cellular functions enabling,or example, proliferation. Hence, serum free adaptation needs to be carefully monitored to ensure stability of the cell lines in question in terms of growth, viable cell densities reached and protein production (LeFloch *et al.*, 2006). Successfully suspension adapted cells are able to grow to a high density of around 1×10^7 cells/ml (Wurm, 2004) and therefore enable a reliable, economically viable production process with product titers in the gram per liter culture volume range (Wurm, 2004). Adaptation to suspension growth in combination with serum-free culture conditions is a time consuming process (Sinacore *et al.*, 2000) that fails in some cases (Rodrigues *et al.*, 2012). A number of serum replacement components (Farges *at al*., 2008) have been tested to enhance the success of suspension adaptation. This includes insulin and zinc (Wong *et al.*, 2004) and transferin (Glassy *et al.* 1988; Schröder *et al.*, 2004). A deeper understanding of the changes that cells undergo during suspension adaptation would enhance cell engineering possibilities (Kuystermans *et al.*, 2007) or allow faster selection methods for the best suspension adapted cell lines and hence allow speeding up the complex procedure of cell line development. Understanding the basic mechanism involved in suspension cell adaptation with respect to the cell surface might also help avoid negative effects of optimization processes later in the process development besides enabling faster establishment of stable production cell lines.

2.2 Cell surface changes as a reaction to a new environment

It is proposed that the adaptation to suspension growth will include changes on the cell surface, such as changes in protein expression levels. This study concentrates on cell surface proteins found in the lipid bilayer forming the plasma membrane as those are known to be the main structure of the cell surface which enable interaction of the cell with the environment. Without any cell surface protein changes as reaction to the new environment the cell will die due to the loss of cell to matrix adhesion. Cell death due to loss of cell to matrix adhesion is called anoikis (Frisch and Francis, 1994) and describes the apoptotic reaction of cells to the absence of cell matrix interactions, stressing the importance of this interaction for cell proliferation. Anoikis has also been described as apoptosis induced by loss of cell adhesion (Ruoslathi and Vaheri, 1997). Induction of anoikis, which can be seen as an apoptotic signalling process, is mediated by different pathways. The main signal is thought to come via integrin signalling from the cell surface (Gilmor, 2005) but the specific pathways signalling anoikis depend on the cell type and the integrins involved (Chiarugi and Giannoni, 2008). The loss of binding partners for integrins, such as proteins of the extracellular matrix or serum, is responsible for the loss of the so called 'outside-in' (Arnaout *et al*., 2002) signalling and hence the starting point for anoikis. Integrins are hetero-dimers consisting of non-covalently bound class I transmembrane proteins; each integrin contains an alpha and a beta chain (Wiesner *et al.*, 2005). So far, 18 alpha and 8 beta subunits have been found in humans; those can assemble into 24 different integrin receptors (Eble and Haier, 2006, Wiesner *et al.*, 2005). The combination of the subunits determines the ligand of the integrin and hence the function, e.g. integrin alpha 1 beta 1 belongs to the group of collagen binding integrins whereas integrin alpha 4 beta 1 binds to different sites in fibronectin (Eble and Haier, 2006). Integrin signalling is split into inside-out and outside-in signalling; inside-out being defined as activational signalling based on conformational changes due to inter-cellular signalling events, outside-in signalling as the signalling events following receptor-ligand binding. Inside-out and outside-in are closely interlinked as, for example, clustering and ligand affinity, both requiring conformational changes, depend not only on the interaction with the actin cytoskeleton as their inter-cellular interaction partner but also on the shear forces (outside signals) the cell experiences (Schymeinsky *et al*., 2011).

All the anoikis signalling pathways described so far merge in the activation of caspases, leading to activation of endonucleases, DNA fragmentation and cell death. The protein Bcl-2 is a key part of the process, as demonstrated by Lee and Ruoslathi (2005). Bcl-2 protein expression has been shown

to be regulated not only by the expression of certain types of integrins but also to depend on the proteins the integrin interact with. Hence, different integrin ligands, such as vitronectin or fibronectin, influence Bcl-2 regulation (Matters and Ruoslathi, 2001). Some of the signal proteins only play a role in certain cell types, e.g. BH3-only proteins seem to be important in fibroblast anoikis. Anoikis has also been shown to be induced by a change in cell shape (Chen *et al.*, 1997); this has been proposed to be due to clustering of FAS ligands on the cell surface (Chiarugi and Giannoni, 2008). Epithelial cells have been shown to regulate anoikis through integrin /growth factor receptor cross-talk; a number of mammalian epithelial cells require a combination of adhesion signalling and growth factor signalling for survival, with only one activated pathway not being sufficient (Gilmor, 2005). Protection from anoikis has been found to occur under conditions such as cell migration and in professional non-adherent cells such as leukocytes. In these cases it has been shown that certain cytokines, depending on the cell type and surrounding, can provide survival signals during cell migration (Freitas and Rocha, 1999). Resistance to anoikis has also been seen to be induced by treatment with motility factors that cause a breakdown of normal epithelial cell-to-cell interactions (Frisch and Francis, 1994). Resistance can also be gained by cells based on other mechanisms such as autocrine growth factor loops, changes in integrin expression, ligand independent activation of growth factor receptor and up-regulation of N-cadherin on the cell surface (Chiarugi and Giannoni, 2008). The number of signalling molecules proposed to be involved in anoikis has grown over the last ten years; Redding and Juliano (2005) mention epithelial growth factor (EGF), Bim, Bcl-2 and Bax as the main apoptotic proteins involved in the signalling cascades related to anoikis, but stress the importance of further protein interactions involving integrin signalling via talin, vinculin and paxillin, proteins linking integrins to the actin cytoskeleton, together with signalling cascades linked by PI3, integrin linked kinase (ILK) and focal adhesion kinase (FAK). The interaction between EGF and integrin signalling cascades has been demonstrated to influence the actin stress fibre formation. Shahal *et al*. (2012) have shown that EGF and integrin adhesion interaction, thought to involve the signalling proteins Src, depends not only on protein levels but also on densities of points of adhesion and the form of EGF, whether it is soluble or immobilised; this indicates the importance of structural distribution in the form of clusters apart from general protein expression levels.

Changes in cell surface protein expression levels have also been seen as a reaction to fluid shear stress (Morigi *et al.*, 1995). The down-regulation of the fibronectin receptor integrin alpha 5 beta 1 has been demonstrated in three different fibroblast cell lines; this was demonstrated to happen in

conjunction with a down-regulation of the cell derived fibronectin (Dalton *et al.*, 1992). The importance of the integrin alpha 5 beta 1 receptor in survival signalling in CHO cells has been shown in a number of studies, such as by Lee and Ruoslathi (2005) who analysed in detail the signalling pathways of integrin alpha 5 beta 1 and integrin alpha V beta 1, concentrating on PI3/AKT signalling, and demonstrated that different signalling mediators such as AKT and NF-kappa B are involved in up-regulation of the anti-apoptotic protein Bcl-2. The complexity of the involved signalling pathways has been summarised by Chiarugi and Giannoni (2008) who describe three different situations, cell survival, anoikis and anoikis resistance, which differ in the signalling pathways involved. The main difference between general cell survival and anoikis resistance as described by them is to be found in constitutive activity of PI3/AKT and MAPK/ERK signalling, possibly induced by a change in the pattern on integrin expression in anoikis resistant cells. Furthermore, reactive oxygen species influence downstream integrin signalling events (Chiarugi, 2008) in combination with ligand-independent activation of growth factor receptors and can provide anoikis resistance (Chiarugi and Giannoni, 2008).

The adaptation from adherent growth to suspension growth is also found in the process of metastasis. Metastatic cancer cells have been shown to lack the dependency on extracellular matrix contact for proliferation, which is thought to be a necessary step for development of metastasis; metastatic cancer is only possible due to cells overcoming attachment and acquiring the ability to move freely around in the body while still capable of proliferation. Hence, studies related to development of metastatic cancer can give further clues regarding changes in intra- and extracellular cell signalling that is possibly involved in the transition from adherent to suspension cell growth of mammalian cell lines.

In a study by Li *et al.* (2001) E-cadherin, one of the major adhesion molecules in adherent junctions between cells, was shown to become down-regulated during melanoma development; this down-regulation could be counteracted by over-expression of desmosomal cadherins, such as Desmoglein 1, due to the cross-talk between desmosomes and adherent junctions. Chiarugi and Giannoni (2008) link anoikis resistance to up-regulation of N-cadherin expression; this indicates a role for cadherin expression in adherence regulation. Another mechanism shown to be important in melanoma cell lines is the self-stimulation by hepatocyte growth factor (HGF) which in tissue would be secreted by fibroblasts. The cell lines investigated all expressed c-Met, the HGF receptor, and showed increased proliferation when treated with HGF. Constant treatment with HGF also leads to a significant down-regulation of E-cadherin and Desmoglein 1 in melanoma cells. In contrast to

this is the up-regulation of integrin alpha 5 beta 3 in the same setting (Li *et al.*, 2001); this illustrates that integrins can provide survival signals during cell migration. Integrins have been studied as tumor suppressors, with several integrins such as integrin 5 beta 1 and integrin alpha 3 beta 1 being shown to be down-regulated in metastatic cancer cells (Eble and Haier, 2006). As the development of metastatic cancer requires a number of steps from leaving the primary tumor to establishment of metastatic growth in the new environment, the role of integrins is assumed to be a combination of up- and down-regulation, partially depending on the type of the primary tumor and the new environment (Eble and Haier, 2006). Another study on melanoma cells (Satymoorthy, 2001) concentrated on the effect of insulin-like growth factor 1 (IGF-1). The IGF-1 receptor is known to be expressed on melanoma cells and shows an increase in expression during cancer progression. Paracrine stimulation of melanoma cells by IGF-1 from fibroblasts was demonstrated to activate several effector proteins of signalling pathways, including MAP kinase and AKT in early stage melanoma cells, pathways that are also regulated in integrin downstream signalling as described before. It has been suggested that by activation of MAP kinase and AKT, IGF-1 acts as an anti-apoptotic survival factor for early stage melanoma cells. Furthermore, it was described that IGF-1 can substitute for other growth factors, such as basic Fibroblast Growth Factor (Satymoorthy, 2001). Difference in adhesion of CHO cells to a fibronectin coated surface has been reported to be influenced by insulin supplementation, with a better adhesion demonstrated in the presence of insulin (Guilherme *et al.*, 1998), again revealing the importance of growth factor signalling in adhesion regulation. As insulin, which can also interact with the IGF-1 receptor, is often included in serum-free media to enable serum-free suspension growth of cells, some of these mechanisms might play a role in suspension adaptation of cells.

The studies listed above indicate that signalling pathways affiliated to integrins and cadherins play a major role in suspension adaptation. In adherent conditions the major signalling pathways regulated by integrin signalling in combination with growth factor signalling involve FAK, which also provides a link to the cytoskeleton via adapter proteins such as talin, paxillin and vinculin (see also Fig. 8.1); FAK also interacts with PI3 via different adapter proteins, with PI3 interacting with AKT allowing anti-apototic signalling to take place as describe before (Giancotti *et al*., 1999). Furthermore, FAK can also indirectly lead to activation of the mitogen activated protein (MAP) kinase signalling pathway (Stupack and Cheresh, 2002), allowing regulation of cell cycle progression. It needs to be stressed that integrins have no catalytic function themselves (Wiesner *et al.*, 2005). Instead, they signal by binding to a large number of effector proteins; a number of those

proteins, such as talin and vinculin, bind either themselves or via a binding partner to the actin cytoskeleton of the cell, thereby linking the integrins on the cell surface to the intracellular cytoskeleton. Hence, signalling pathways such as the RhoA/ROCK pathway (Hayes *et al*., 2011) might also be affected by suspension adaptation. The effector proteins linking integrins and the cytoskeleton are known to differ between different cell types and have mainly been studied on cell lines showing anchorage dependent growth.

In addition, the integrin signalling is controlled by integrin conformation; clustering and switching between low-affinity and high-affinity conformation plays an important role in the regulation of cell growth via integrin signalling (Wiesner *et al*., 2005). For example, van Kooyk and Figdor (2000) proposed clustering as a major step in integrin activation and suggested that the release of cytoskeletal restrain is a step required for clustering. A more detailed study by Bakker *et al*. (2012) on the role of integrin clusters on leukocytes concentrated on the role of conformation, lateral mobility and ligand-induced microclustering of integrin alpha L beta 2. Leukocytes are professional suspension cells that are still capable to adhere. Bakker *et al*. (2012) concentrated on the behaviour of integrin nano-clusters that exist in non-adherent leukocytes, showing that in resting monocytes these clusters can diffuse within the cell membrane, but mobility depends on the conformation. Furthermore. they demonstrated that the mobility within the membrane is influenced by the calcium concentration of the cell environment, with low calcium concentration restricting diffusion; this was suggested to be due to conformational changes of integrin receptors in reaction to calcium concentration. The mobility of integrin alpha L beta 2 could also be linked to the actin cytoskeleton; treatment with a drug leading to the de-polymerisation of F-actin, cytochalasin D enhanced mobility besides low calcium concentration in the media demonstrating a link between integrin cluster mobility, integrin conformation and the cell environment. While the integrin nano-clusters remained intact independent of the treatment and the cell culture environment, micro-cluster formation and hence adhesions and cell spreading was restricted in a low calcium environment (0.04 mM). Bakker *et al*. (2012) could demonstrate that mobile integrin nano-clusters exist on leukocytes in different conformations, e.g. primed or not extended, and that those clusters are anchored to the cytoskeleton, depending on their conformation.

Altrock *et al*. (2012) studied the distribution of lipid rafts in hematopoietic stem cells (HSC) which are the source of leukocytes in the human body. The study on HSCs by Altrock *et al*. (2012) concentrated on the distribution of lipid rafts, transient membrane domains, characterised by enrichment of cholesterol and sphingolipids during adhesion to fibronectin, an integrin ligand.

Three-dimensional analysis using confocal microscopy revealed the occurrence of polarisation towards the adherent cell side for lipid rafts, integrin alpha 5 and integrin alpha V beta 3 demonstrating an extensive reorganisation of the cell surface during HSC adhesion. In contrast to this, integrin beta 1 remained homogeneously spread over the entire cell surface. All integrins analysed in this study showed a clustered distribution in confocal microscopy analysis.

Cytoskeletal reorganisation has been demonstrated by Barda-Saad *et al*. (2005) in a study using T cells. The study concentrated on the events occurring after activation via the T cell receptor (TCR) and showed the restructuring actin undergoes during the process of TCR activation in combination with adherence, leading to a clearly defined actin ring structure in activated cells.

Hayse *et al*. (2011) proposed that cytoskeleton remodelling also occurs in CHO cells when adapted to suspension. They studied a phosducin like protein, PhLP3, that has been linked to beta-tubulin and actin folding, and its influence on cytoskeletal remodelling by over-expression in CHO cells. Actin levels and assembly were unaltered by over-expression of PhLP3 but adherent cells were released into the supernatant; those cells did not remain viable. Knock-down of PhLP3 in CHO suspension cells resulted in a morphological change of the cells with an increase in actin stress fibre formation. In those cells the distribution of vinculin also changed. These changes were linked to a change in levels and distribution of activated MAP kinase, linking PhLP3 to cell death signalling. In the study by Hayes *et al*. (2011) knock-down of PhLP3 in suspension CHO cells seems hence to introduce a more adherent phenotype, leading to formation of actin stress fibres, focal adhesion formation and increase of MAP kinase phosphorylation.

In contrast to the studies above that are mainly based on expression level analysis and conformational studies for the cell surface proteins, another method to analyse cell surface proteins is the analysis of the shedded proteins (Ahram *et al.*, 2005b; Guo *et al.*, 2002) using mass spectrometry approaches. A number of membrane proteases, also called sheddases (Guo *et al.*, 2002), has been identified over the last years (Hopper *et al.*, 1997); membrane proteins are released by those sheddases from the membrane into the culture supernatant. It has been shown that adhesion proteins are released by this mechanism (Arribas and Borroto, 2002). The released proteins (either naturally occurring or induced by treatments) can be analysed to gain insight into the proteome composition of the cell membrane.

So far mostly separate aspects regarding the changes in cell surface and the underlying signalling pathways have been studied in the transition from an adherent mammalian cell line to a suspension cell line (or vice versa). One can assume that a complex combination of these

mechanisms plays a role in suspension adaptation of cell lines. To elucidate the large number of proteins possibly involved, a quantitative mass spectrometry based approach was proposed as a starting point in this study, as has previously been used for the analysis of the shedded proteins. Also, such an approach has been used in a number of surface protein studies to either identify cell surface proteins (Nunomura *et al.*, 2005; Schindler *et al.*, 2006) or elucidate differences between cell lines (Conn *et al.* 2008). More recent mass spectrometry studies of membrane proteins (see also chapter 5) often used a variety of enrichment steps for membrane proteins to enable comprehensive identification of membrane proteins, for example biotinylation and affinity enrichment (Zhao *et al.*, 2004) or gravity gradient centrifugation (Han *et al.*, 2008).

3. Chapter

Experimental techniques

In this chapter the methods and materials used in this study are listed including relevant details. Exceptions to the general methodology are given in the applicable result chapters.

3.1 Cell lines

The following cell lines were used within this project:

- adherent CHOK1 clone CCL61 from ATCC received from Pfizer,
- suspension adapted proprietary cell line S cells from Pfizer,
- adherent growing proprietary cell line AML from Pfizer,
- suspension CHO cell line Free Style™ CHO-S cells from Invitrogen.

Cell banks were created for each cell line by harvesting during the exponential growth phase. Cells were pelleted (200g, 5 minutes) and re-suspended in their respective media with the addition of 10% dimethylsulfoxide (DMSO) (Sigma, St. Louis, USA) at 1 x 10^7/ml. 1.5 ml aliquots were frozen at -80°C in Nunc cryovials (Thermo, Epson, Surrey) using a Mr Frosty container (Nalgene, Roskilde, Denmark) to ensure cooling at 1°C/ minute. Cells were transferred into liquid nitrogen after a minimum period of 48 h.

3.2 Cell culture conditions

3.2.1 Suspension culture

Suspension cell culture condition was 5% CO_2, 37°C and 140 rotations per minute (rpm) (standard condition for suspension growth). Suspension cells were split after 3 or 4 days (alternating) with adjustment of seeding density. Cells were seeded after 3 days using 0.4 x 10^6/ml and after 4 days with 0.2 x 10^6/ml; CHO-S cells were always seeded at 0.2 x 10^6/ml. For suspension growth of Pfizer cell lines and CCL61, proprietary suspension media (PSM) from Pfizer (Andover, USA) containing 10 mg/ml insulin was used (PSM plus); CHO-S cells were cultured in CD-CHO medium (Invitrogen, Paisley, UK) supplemented with 8 mM glutamine (Sigma Aldrich, St. Louis,

USA). Suspension cells were cultured in vented 25 ml Erlenmeyer shake flasks (Corning, Surrey, UK). Measurements of cell density and cell viability were performed using the Vi-cellXR cell viability analyser (Beckmann Coulter, High Wycombe, UK) which uses the trypan blue exclusion method. Cells were cultured up to a maximum of 30 passages (CHO-S: 20 passages).

3.2.2 Adherent culture

Adherent cell culture conditions were 5% CO_2 and 37°C (standard conditions for adherent growth). Cell cultures were split after 3 or 4 days (alternating) with adjustment of the seeding density after harvesting with 0.05% trypsin/EDTA (Gibco, Paisley, UK). For T75 flasks harvesting with 1 ml of the trypsin solution with an incubation of 5 to 10 minutes was used. CCL61 were seeded using 6500 cells/cm^2 (4 days) or 8000 cells/cm^2 (3 days). AML cells were seeded using 6500 cells/cm^2 or 13000 cells/cm^2. For adherent growth conditions 10% FBS (Biosera, Ringmer, UK) was added to the media. For adherent growth of CCL61 Ham's modified F-12K medium (mF12) (LGC, Teddlington, UK) was used; AML cells were cultured in proprietary adherent media (PAM) from Pfizer (Andover, USA). Cells were cultured in T75 flasks (Nunc, Roskilde, Denmark). Measurements of cell density and cell viability were performed using the Vi-cellXR cell viability analyser (Beckmann Coulter, High Wycombe, UK) which uses the trypan blue exclusion method. Cells were cultured up to a maximum of 30 passages.

3.3 Cell preparation for flow cytometry

Adherent cells were harvested using phosphate buffered saline (PBS) with 2 mM EDTA (Fisher Scientific, Lougborough, UK) and an incubation time of 5 to 10 minutes. Suspension and adherent cells were spun down and washed with PBS (Invitrogen, Paisley, UK) before fixation. For fixation 1 ml of a 1% para-formaldehyde (PFA) solution (from a 1 to 4 dilution of a 4% PFA in PBS stock (95%, Sigma Aldrich, Gillingham, UK)) per 5 x 10^6 was added to the cell pellet, followed by an incubation at 4°C for 20 minutes. Cells were washed with PBS and stored in PBS at a concentration of 1 x 10^7/ ml for a maximum period of 10 days.

3.4 Cell preparation for confocal microscopy

For adherent cells cover-slips (0.13 - 0.17mm thick) in 6 well plates (Nunc, Roskilde, Denmark) were prepared by incubation with 1ml of FBS overnight (minimum) at 5% CO_2, 37°C. Adherent cells were seeded at the usual seeding density for a four day split and stained before reaching 90% confluency (usually on day 3). For fixation cover-slips were washed twice with PBS and 1 ml 1%

para-formaldehyde solution was added to the well. Incubation was at room temperature for 20 minutes. The same fixation conditions were used for 2.5 x 10^6/ml suspension cells. Cells were then washed twice with PBS. Cells were not stored at this stage.

3.5 Flow cytometry – instrumentation set-up

Flow cytometric analysis was performed using a FacsCalibur (BD Biosiences, Oxford, UK). The instrument settings were chosen using unstained and, where necessary, single stained controls. Set up of instrument setting for each cell line was conducted independently to account for differences in autofluorescence due to different culture conditions. Flow cytometry data was analysed using FlowJo 7.6.5 (Freestar Inc., USA).

3.6 Confocal microsopy – instrumentation set-up

Confocal microscopy analysis was performed using an inverted Zeiss (Oberkochen, Germany) LSM510 Meta confocal microscope. Mounted cell samples were analysed using a plan apochromat 63x/ 1.4 oil DIC objective with excitation provided by an argon laser. For FITC/Alexa 488 excitation was at 488 nm and for Alexa 546 excitation was at 514 nm. Emission was collected for FITC/Alex 488 using a band pass 500-550 nm IR filter and for Alex 546 using a long pass 560 nm filter. All images were analysed using the Zeiss LSM Image Browser Version 4,2.0,121.

3.7 Actin labelling

Actin was stained using Alexa 546 phalloidin (Molecular Probes, Paisley, UK). The freeze dried phalloidin was dissolved in methanol and the resulting stock solution (200 units/ml) was aliquoted and stored at -20°C.

3.7.1 Actin: flow cytometry staining

2 x 10^6 fixed cells were washed twice with PBS. 50 µl 0.1% Triton X-100 (Molecular Biology tested, Sigma Aldrich, Gillingham, UK) was added to the pellet and incubated at room temperature for 3 minutes. Cells were washed twice with PBS (200 g, 5minutes). 200 µl 1% Bovine Serum Albumin (BSA; microbiological grade, Fisher Scientific, Loughborough, UK) in PBS with 5 µl of the prepared phalloidin stock solution was added. The cells were incubated for 20 minutes at room temperature and washed once with PBS (200 g, 5minutes). Cells were stored for a maximum of 24 hours in 500 µl of 1% BSA in PBS buffer.

3.7.2 Actin: confocal microscopy staining

2 x 10^6 fixed cells or cells fixed on a cover glas were washed twice with PBS (200 g, 5 minutes). 50 µl 0.1% Triton X-100 was added and cells were incubated at room temperature for 3 minutes. Cells were washed twice with PBS and 200 µl 1% BSA in PBS with 5 µl of the prepared phalloidin stock solution was added. The cells were incubated for 20 minutes at room temperature and washed twice with PBS. For suspension cells, cell pellets were dissolved in two drops of PBS and mounted on a glass slide; cells were mounted using approximately 50 µl ProLong Gold antifade (Invitrogen, Paisley, UK).

3.8 Integrin beta 1 labelling

The integrin beta 1 antibody used was clone 9EG7 (BD Biosciences, Oxford, UK). Isotype control was rat IgG2a, kappa, clone R35-95 (BD Biosciences, Oxford, UK).

3.8.1 Integrin beta 1: flow cytometry staining

Cells were stained for flow cytometry using 2 - 2.5 x 10^6 cells in 50 µl PBS/0.2 mM EDTA/0.5% BSA buffer. Antibody titer was 1 to 21, incubation time was 45 minutes at 4°C. Before secondary staining two washes with PBS/0.2 mM EDTA/0.5% BSA buffer were performed. As secondary antibody, mouse anti rat IgG2a PE, clone RG7/1.30 was used at a titer of 1 to 100, incubation time was 15 minutes at 4°C. Stained cells were stored for a maximum of 24 hours in 1ml of PBS/0.2mM EDTA/0.5% BSA buffer.

3.8.2 Integrin beta 1: confocal microscopy staining

Either a cover-slip with adherent cells or 2.5 x 10^6 suspension cells were washed twice with PBS and 50 µl 1 % BSA in PBS were added. Integrin beta 1 antibody was used at a titer of 1 to 21 and incubation was for 45 minutes at 4°C. Samples were washed twice with PBS and 50 µl 1% BSA buffer added. Secondary antibody, Alexa Fluor 488 goat anti mouse IgG2b (Molecular Probes, Paisley, UK) was used at 1 to 100 and incubated for 15 minutes at 4°C. Cells were washed once, for suspension cells cell pellets were dissolved in two drops of PBS and mounting was done on glass slides using approximately 50 µl ProLong Gold antifade (Invitrogen, Paisely, UK). Samples were stored for a maximum of 10 days.

3.9 Integrin alpha 1 labelling

The integrin alpha 1 antibody used was clone Ha31/8 (BD Biosciences, Oxford, UK).

3.9.1 Integrin alpha 1: flow cytometry staining

1 mg Sulfo-NHS-S-S-Biotin (Pierce, Thermo Fisher Scientific, Rockford, USA) was dissolved in 200 µl PBS/EDTA. 20 µl integrin alpha 4 antibody were diluted 1 to 5. To the prepared antibody solution 2 µl of the prepared biotin solution was added and incubated over night at room temperature while mixing. The resulting biotinylated antibody was used for cell staining. Cells were stained for flow cytometry using 2 - 2.5 x 10^6 cells in 50 µl PBS/2mM EDTA/0.5%BSA buffer. Biotinylated antibody titer was 1 to 6, incubation time was 30 minutes at 4°C. Before secondary staining two washes were performed. Secondary staining was performed using Streptavidin-FITC at a titer of 1 to 25, incubation time was 15 minutes at 4°C. Cells were stored for a maximum of 24 hours in 1ml of PBS/2mM EDTA/0.5% BSA.

3.9.2 Integrin alpha 1: confocal microscopy staining

Either a cover-slip with fixed adherent cells or 2.5 x 10^6 fixed suspension cells were washed twice with PBS and 50 µl 1 % BSA in PBS were added. Integrin alpha 1 antibody was used at a titer of 1 to 6 and incubation was for 45 minutes at 4°C. Samples were washed twice with PBS and 50 µl 1% BSA buffer added. As secondary antibody, anti-Armenian and Syrian Hamster IgG FITC (BD Biosciences, Oxford, UK) was used at 1 to 100 and incubated for 15 minutes at 4°C. Cells were washed once, for suspension cells cell pellets were resuspended in two drops of PBS and mounted glass slides using approximately 50 µl ProLong Gold antifade (Invitrogen, Paisley, UK). Samples were stored for a maximum of 10 days.

3.10 Integrin alpha 4 labelling

The integrin alpha 4 antibody used was clone R1-2 (Miltenyi Biotec, Bergisch Gladbach, Germany).

3.10.1 Integrin alpha 4: flow cytometry staining

Cells were stained for flow cytometry using 2 - 2.5 x 10^6 cells in 50 µl PBS/2 mM EDTA/0.5% BSA buffer. Antibody titer was 1 to 6, incubation time 45 minutes at 4°C. The antibody used was a direct conjugate with the PE fluorochrome. Cells were stored for a maximum of 24 hours in 1 ml of

PBS/2 mM EDTA/0.5% BSA buffer before measuring at a BD Calibur (BD Biosciences, Oxford, UK).

3.10.2 Integrin alpha 4: confocal microscopy staining

Either a cover-slip with adherent cells or 2.5 x 10^6 suspension cells were washed twice with PBS and 50 µl 1 % BSA in PBS were added. Integrin alpha 4 biotin (ready made) was used at a titer of 1 to 6 and incubation was for 45 minutes at 4°C. Samples were washed twice with PBS and 50 µl 1% BSA buffer added. Secondary antibody, Streptavidin FITC (BD Biosciences, Oxford, UK) was used at a titer of 1 to 25 and incubated for 15 minutes at 4°C. Cells were washed twice, for suspension cells pellets were dissolved in two drops of PBS and mounted on glass slides using approximately 50 µl ProLong Gold antifade (LifeTechnologies, Paisley, UK). Samples were stored for a maximum of 10 days.

3.11 Integrin alpha M – flow cytometry staining

The integrin alpha M antibody used was clone M1/70.15.11.5 (Miltenyi Biotec, Bergisch Gladbach, Germany). Cells were stained for flow cytometry using 2.5 - 5 x 10^6 fixed cells in 50 µl PBS/2mM EDTA/0.5%BSA buffer. Antibody titer was 1 to 6, incubation time was 45 minutes at 4°C. The antibody used was a direct conjugate with the PE fluorochrome. Cells were stored for a maximum of 24 hours in 1 ml of PBS/2 mM EDTA/0.5% BSA buffer.

3.12 CD56 (neural cell adhesion molecule) – flow cytometry staining

The CD56 antibody used was clone AF12-7H3 (Miltenyi Biotec, Bergisch Gladbach, Germany). Cells were stained for flow cytometry using 2.5 - 5 x 10^6 fixed cells in 50 µl PBS/2 mM EDTA/0.5% BSA buffer. Antibody titer was 1 to 6, incubation time was 45 minutes at 4°C. The antibody used was a direct conjugate with the PE fluorochrome. Cells were stored for a maximum of 24 hours in 1 ml of PBS/2 mM EDTA/0.5% BSA buffer.

3.13 E-cadherin staining – flow cytometry staining

The CD324 antibody used was clone 67A4 (Miltenyi Biotec, Bergisch Gladbach, Germany). Isotype control was mouse IgG1-APC clone IS5-21F5 (Miltenyi Biotec, Bergisch Gladbach, Germany). Cells were stained for flow cytometry using 2.5 - 5 x 10^6 fixed cells in 50 µl PBS/2 mM EDTA/0.5% BSA buffer. Antibody titer was 1 to 6, incubation time was 45 minutes at 4°C. The antibody used was a direct conjugate with the APC fluorochrome. Cells were stored for a maximum

of 24 hours in 1 ml of PBS/2 mM EDTA/0.5% BSA.

3.14 CD44 staining – flow cytometry staining

The CD44 antibody used was clone DB105 (Miltenyi Biotec, Bergisch Gladbach, Germany). Isotype control was mouse IgG1-FITC clone IS5-21F5 (Miltenyi Biotec, Bergisch Gladbach, Germany). Cells were stained for flow cytometry using 2.5 - 5 x 10^6 fixed cells in 50 µl PBS/2 mM EDTA/0.5% BSA buffer. Antibody titer was 1 to 6, incubation time was 45 minutes at 4°C. The antibody used was a direct conjugate with the FITC fluorochrome. Cells were stored for a maximum of 24 hours in 1 ml of PBS/2 mM EDTA/0.5% BSA .

3.15 Biotinylation of cells

The cell biotinylation protocol used was based on a membrane proteomics approach by Peirce *et al*. (2004). The buffer used for biotinylation (BBS buffer) consisted of 10 mM boric acid, 2.3 mM sodium tetraborate, 115 mM NaCl and the pH was adjusted to 8.1. For biotinylation of suspension cell 2.5 x 10^7 cells (or multiples of that) were washed twice with approximately 15 ml BBS buffer (200g, 5 minutes). Cells were re-suspended in 1 ml BBS buffer and 100 µl of a freshly prepared 1 mg/ml sulfo NHS-S-S biotin solution (dissolved in water) were added. Cells were incubated at room temperature for 20 minutes under mixing. Incubation was followed by two washes with BBS buffer. Cells were then re-suspended in PBS, either for counting or for preparation of cell lysis.

Adherent cells were grown until about 95% confluent in T75 flasks (CCL61 ~2 x 10^7 cells) and washed two times with approximately 15 ml BBS buffer. To each flask 3 ml BBS buffer was added, together with 300 µl of a freshly prepared 1 mg/ml sulfo NHS-S-S biotin solution. Cells were incubated for 20 minutes at room temperature on a shaking platform. The supernatant was emptied into waste before carefully washing cells twice with approximately 10 ml BBS buffer. Cells were then incubated with 1 ml of PBS/2 mM EDTA solution and pooled in PBS in preparation for cell lysis or other analysis.

3.16 Lysis of cells – final version

1 x 10^7 cells were centrifuged (200g, 5min) and 1 ml lysis buffer containing 1% Igepal CA630 (Sigma Aldrich) in PBS with protease inhibitors (Sigma Aldrich, Gillingham, UK) was added to the pellet. Cells were vortexed for 1 minute and sonicated in a water bath on ice for 15 minutes. The lysis solution was centrifugated at 22,000 g for 20 minutes at 4°C and the resulting supernatant stored at -20°C.

3.17 Cell surface protein enrichment with affinity chromatography – final version

Degassed wash buffer 1 (500 mM KCl with 1% Igepal C30 and protease inhibitors) and wash buffer 2 (PBS with protease inhibitors) were prepared. Snap cap spin columns (Thermo Fisher Scientific, Rockford, USA) were filled with 500 µl of Streptavidin Agarose resin (Thermo Fisher Scientific, Rockford, USA); columns were centrifuged for 1 minute at 1,000 g. This was followed by three washes with lysis buffer (PBS with 1% detergent) using centrifugation (1 minute at 1,000 g).

The washed resin was added to the thawed and pooled cell lysates and incubated under over-head mixing for 45 minutes at room temperature. The tubes containing the resin and the cell lysates were spun down for 1 minute at 1,000 g and the supernatant discarded. The resin was transferred back into the column using wash buffer 1. The columns with the resin were washed twice with 0.5 ml wash buffer 1, followed by another two washes with wash buffer 2; each centrifugation step was 1 minute at 1,000 g. For the elution step a stopper was used to close the column. The resin was mixed well with 300 µl of a 50 mM DTT (Fluka, Sigma Aldrich, Steinheim, Germany) solution and incubated for 30 minutes at 37°C. This was allowed to run through by gravity. 100 µl of ready-made 4x NuPage LDS buffer (Invitrogen, Paisley, UK) was added, the column was vortexed and centrifugated for 1 minute at 1,000 g. The elutions were pooled and analysed on an SDS gel.

4. Chapter

Growth characteristics of model cell lines used

In this chapter the relationship between the different cell lines are explained. Growth characteristics of the cell lines are given and their phenotype with regard to growth in either suspension or adherent conditions is explained in detail.

4.1 Introduction of cell lines and culture conditions used

To gain insight into the changes of the cell surface due to adaptation to a serum-free suspension environment four cell lines were chosen as model cell lines to be used in this study. As a starting point an adherent CHO cell line from ATCC, clone CCL61, was chosen; this cell line is the parental cell line for all other cell lines used. The clone CCL61 has been used at Pfizer, Andover, USA to generate a number of CHO production cell lines. This study is concentrated on cell lines that have not been screened for production purpose but simply adapted to suspension growth, to avoid the phenotype in question to be due to additional selection pressure. The cell line chosen is called S-cells in this study and grows well in chemically defined serum free suspension culture based on proprietary suspension media. At Pfizer the S-cell line was used to create another CHO clone, characterised by growing very well in adherent conditions using proprietary adherent media, this clone is called AML cells in this study. To ensure that the characterised phenotype is not biased by the study being based on proprietary media with unknown components the CHO clone CHO-S from Invitrogen, as another cell line growing in chemically defined serum-free suspension culture based on an entirely different media, was added to the model cell lines to be analysed in this study at a later stage. The relationship of the model cell lines is also explained in figure 4.1.

To analyse if the cell lines chosen were able to grow in either adherent and/or suspension mode two different culture conditions (see also chapter 3.2) have been used in combination with different media. The aim was to characterise the model cell lines with regard to their growth phenotypes. For adherent growth, culturing in mF12 with 10% FBS was chosen as a standard condition for the suspension cell lines CHO-S and S cells, as the parental CCL61 is adapted to this media. For

suspension growth culturing in proprietary suspension media (PSM) from Pfizer under shaking conditions was chosen as standard conditions for the adherent cell lines AML and CCL61, as the focus of this study was on the Pfizer cell lines. For an overview of the different conditions used and the cell lines they were applied to, see table 4.1

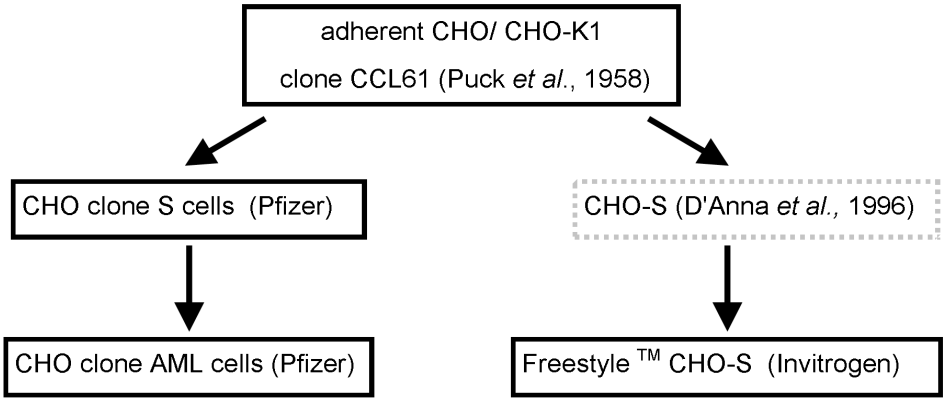

Figure 4.1 Flow diagram showing the relationship between the cell lines used in this study. Black boxes denote the cell lines actually used. All three suspension adapted cell lines, S cells, AML cells and CHO-S are closely related to the adherent CHOK1 clone CCL61.

Table 4.1 The combination of media, cell culture conditions and cell lines used to characterise the growth phenotype of the model cell lines.

Bold indicates standard growth conditions for particular cell line, *italics* indicates reversed conditions.

media	culture conditions	cell lines
Ham's modified F-12K medium + 10 % FBS	adherent (static)	**CCL61**, *S cells, CHO-S*
proprietary adherent media (PAM) from Pfizer + 10 % FBS	adherent (static)	**AML cells**
CD-CHO medium from Invitrogen + 8 mM glutamine	suspension (shaking)	**CHO-S**
proprietary suspension media (PSM) from Pfizer	suspension (shaking)	**S cells**, *AML cells, CCL61*

4.2 Cell growth characteristics in standard and reversed conditions

4.2.1 Methodology

To analyse the growth characteristics of model cell lines cells were seeded at the 4 day split seeding density and cultured in the appropriate medium and cell culture environment for seven days. Viability and viable cell density (VCD) were measured for each cell line in their standard and in the reversed condition, either adherent or suspension.

The generated growth data was used to calculate the growth rate constant μ as a parameter to describe the growth phenotype in addition to viability and viable cell density. The growth rate constant μ gives the logarithm of the rate of cell number increase in proportion to the number of cells present during a given period. μ was determined based on the following equation:

$$\ln N_t - \ln N_0 = \mu\,(t - t_0)$$

where: N_t is the number of cells at the time-point t,

N_0 is number of cells at time-point 0 (t_0)

μ is the specific growth rate.

This can also be expressed as:

$$\mu = ((2.303 \times (\log N_t - \log N_0))/\,(t - t_0)$$

4.3 Growth results

Figure 4.2 A) shows the viable cell density in suspension is highest for the CHO-S cell line and lowest for the CCL61 cells; for the CCL61 there is nearly no increase in VCD after seeding. Viability remains above 95% for all four cell lines until day 4 and drops afterwards for CCL61, S cells and AML cells. For adherent conditions (figure 4.2 B) the highest VCD is reached by AML cells, with the three other cell lines showing a very similar VCD. The difference here might be due to the difference between the media.

Figure 4.3 shows the results of the growth rate calculations. In suspension growth conditions the maximum growth rate of 0.06 h^{-1} is reached by S cells at day 2. CHO-S cells reach their maximum growth rate which is close to 0.06 h^{-1} a day later. AML cells and CCL61, the two cell lines growing in adherent mode as a standard condition, show a similar growth rate curve which peaks on day two and drops down quickly afterwards. CCL61 shows the lowest growth rate of all four cell lines in this condition with approximatively 0.03 h^{-1} on day two , which shows clearly that this cell line is

not adapted to suspension growth. There are fewer differences between the growth rate curves in adherent conditions. CHO-S peaks on day 2 before S cells on day 3, both reaching a similar maximum growth rate of around 0.06 h^{-1}. CCL61 and AML cells show a very similar growth rate curve, again with a peak at around 0.06 h^{-1} at day 3.

In suspension growth conditions from day 4 onwards the formation of small visible cell clumps was seen in all four cell lines; clumping was most pronounced in CCL61 and CHO-S and increased until the end of the cell culturing period.

As can be seen in table 4.2 the average cell size of the four cell lines shows only small differences, with CHO-S being slightly larger; the average cell size is around 14 micron when measured in suspension; it can be assumed that cells in adherent conditions show a different surface area to the one calculated here due to their stretched-out morphology, nevertheless the data given in table 4.2 is of importance when analysing cell surface expression of proteins using flow cytometry as for flow cytometric analysis all cells are measured in suspension.

Table 4.2 Cell sizes and surface areas of cell lines in standard growth conditions.
All cell lines were grown in standard growth conditions. Adherent cells were harvested with PBS/ 2 mM ETDA for 10 minutes before re-suspending them in media. Diameter was determined using the ViaCell cell counter on day four of culture. Diameter with standard deviation (number of repeats >= 11) is given. The diameter was used to calculate the cell surface area assuming a round cell.

cell line	**diameter / µm**	**surface area / µm²**
CCL61	14.47 ± 0.31	658 ± 29
S- cells	14.39 ± 0.72	654 ± 66
CHO-S	16.05 ± 1.12	816 ± 103
AML	13.73 ± 0.3	592 ± 26

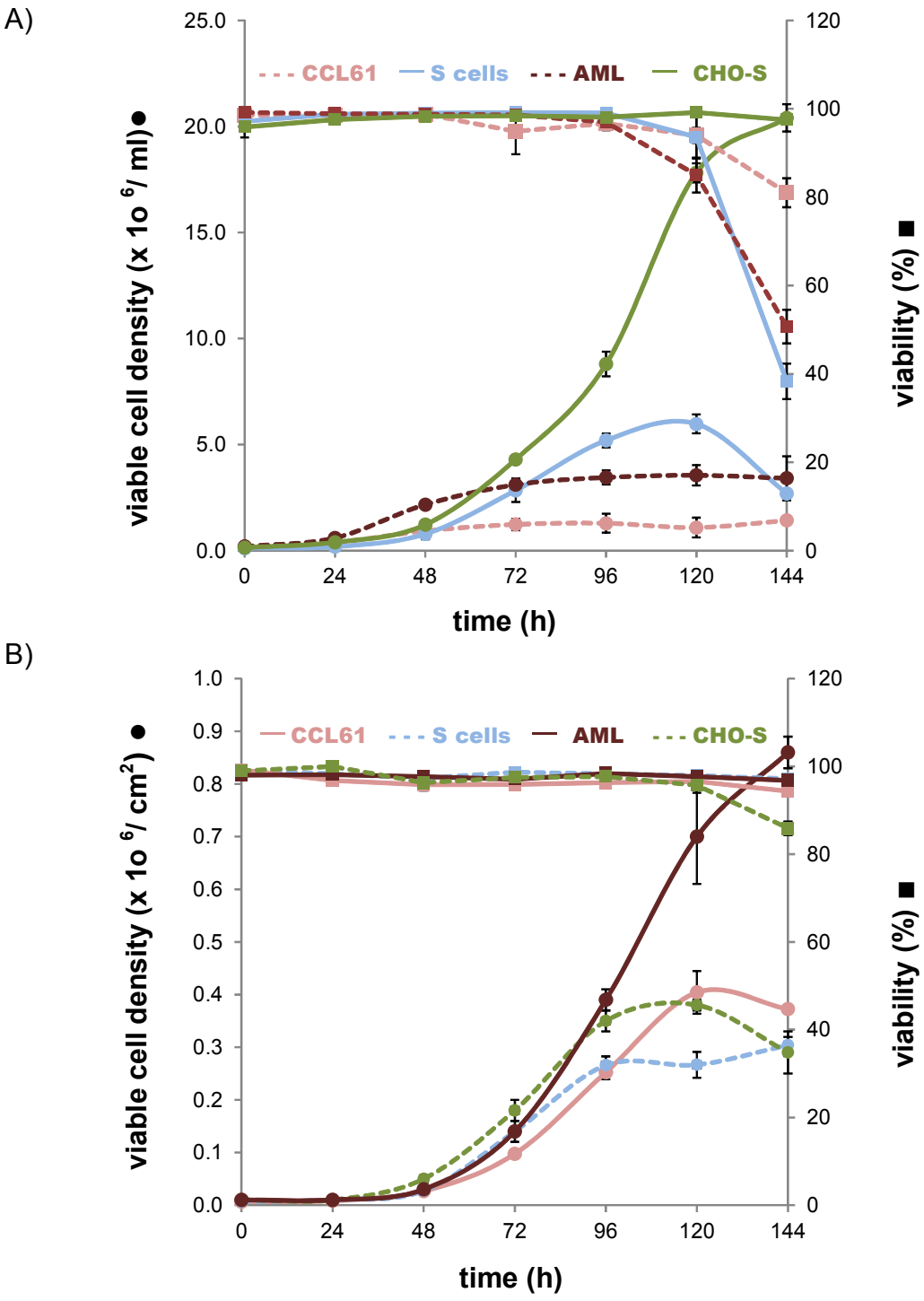

Figure 4.2: Growth results of suspension adapted cell lines S cells, AML cells, CHO-S and the non suspension adapted model cell line CCL61.

A) shows viable cell density and viability over the course of 7 days when cell lines are grown in suspension using PSM plus for CCL61, S cells and AML cells and supplemented CD CHO media for CHO-S. Dashed lines give results for non standard conditions. B) shows results when cell lines are grown in adherent mode using mF12 plus 10% FBS for CCL61, S cells and CHO-S and PAM plus 10% FBS for AML cells. Dashed lines give results for non standard conditions. Number of independent samples is 3 in all measurements.

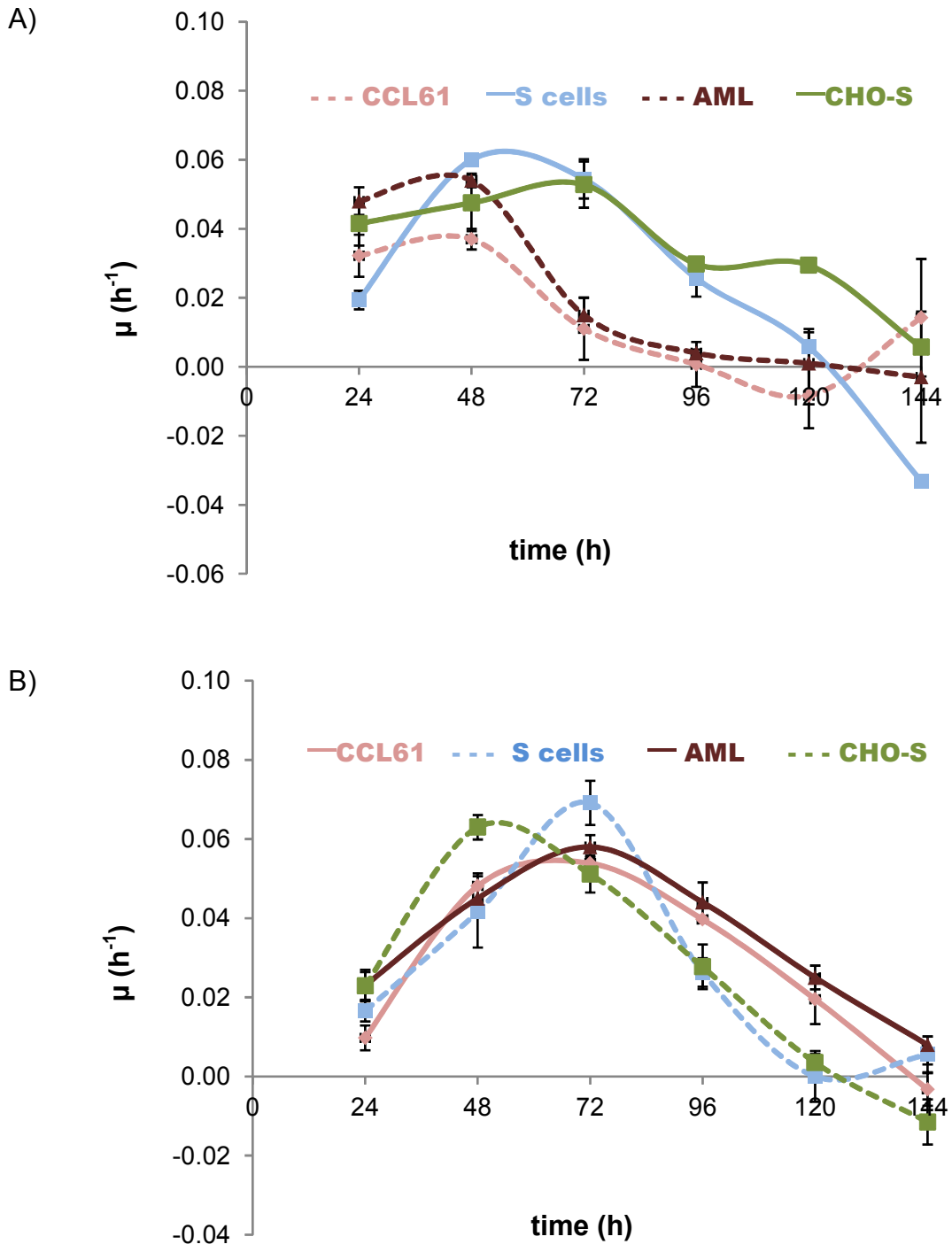

Figure 4.3: Growth rates of the suspension adapted cell lines S cells, AML cells, CHO-S and non suspension adapted cell line CCL61.
A) shows the differences in growth rate over the course of 7 days when cell lines are grown in suspension using PSM plus for CCL61, S cells and AML cells and supplemented CD CHO media for CHO-S. B) shows results when cell lines are grown in adherent mode using mF12 plus 10% FBS for CCL61, S cells and CHO-S and PAM plus 10% FBS for AML cells. Repeats of calculations based on independent samples: n= 3.

4.4 Stability of growth characteristics over time

To ensure that the growth characteristics analysed above were maintained by the cell lines during the cell culture period, two different vials of each cell line were thawed with an appropriate time gap were cultured. This allowed parallel analysis of different passages of the cell lines based on the same cell bank using the same batch of media. For CHO-S, S cells and CCL61 cultures differing by more than 20 passages were compared whereas for AML cells the comparison was done for cells differing by only 10 passages due to difficulties with media delivery.

Results of the comparison are shown in figure 4.4. For the cell lines CCL61, S cells and AML in standard growth conditions no variation in viable cell densities was seen in the comparison of passages. For CHO-S cells a difference in the maximal attainable viable cell densities is seen between the different passages: over passages the maximal viable cell density achieved decreases and a clear difference in viable cell density can already be seen on day four of culture between different early and late passages. Due to this, CHO-S cells were only used in this study when the passage number was below 20. For growth in reversed conditions all four cell lines show a similar maximal viable cell density, independent of the passage number. The larger variation seen for the CCL61 cells needs to be seen in relation to the low viable cell density reached and the high standard deviation between triplicates; both are due to the fact that these cells are not adapted to suspension growth. This data is indicative of the fact that the ability to grow successfully in reversed conditions remains stable for the chosen cell lines under the settings chosen. Hence, this ability can be seen as a characteristic of the phenotype of the four cell lines investigated.

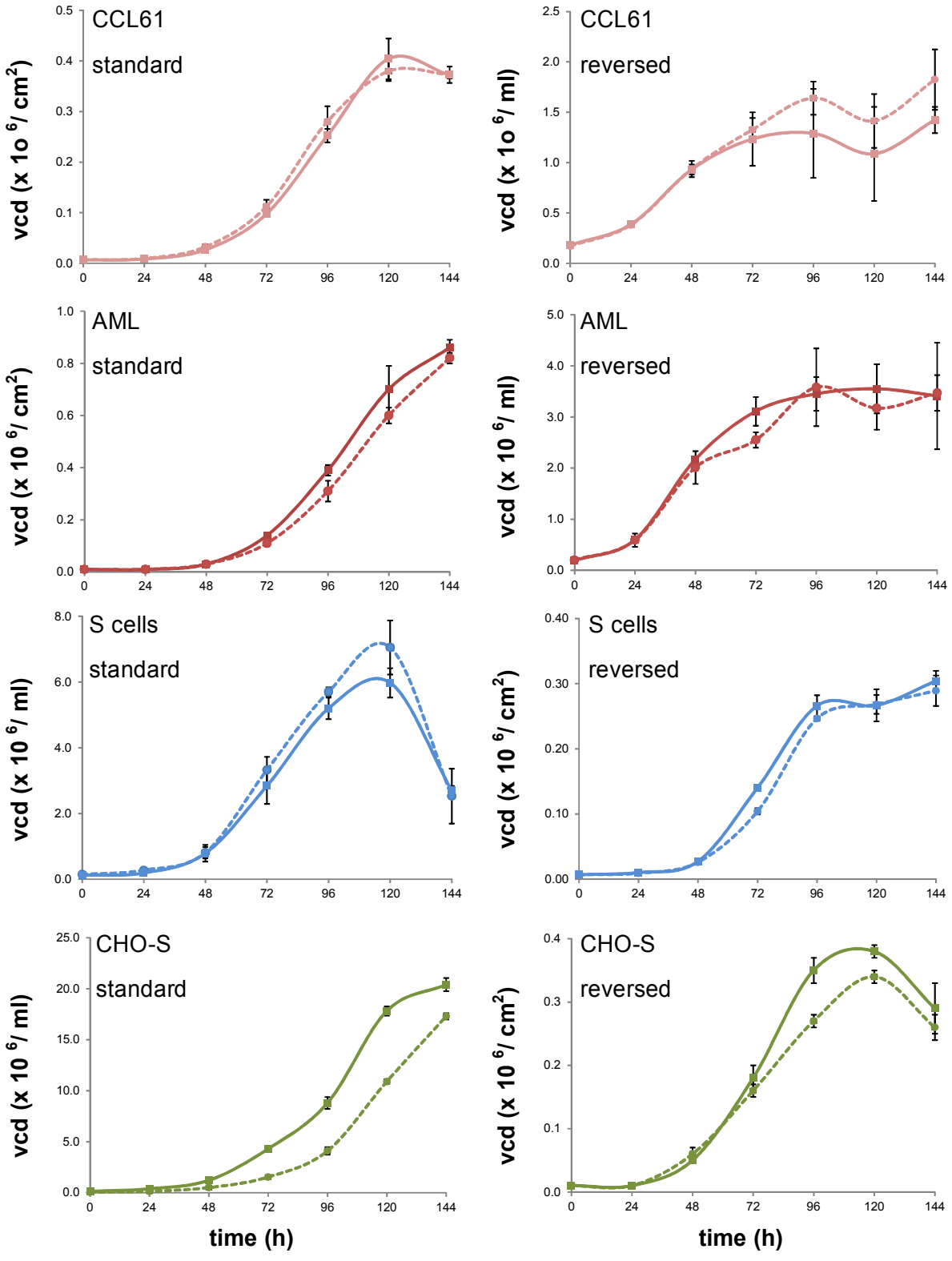

Figure 4.4: Stability of growth characteristics — comparison of viable cell density (VCD) in early and late passages of the model cell lines.

VCD of two different passages was analysed for early (solid line) and late (dashed line) passages as described in figure 4.2 at the same time point. For all measurements three independent samples were measured.

4.5 Development of adherence and confluence in adherent conditions

Further analysis of the four cell lines with regard to their growth characteristics was carried out in adherent conditions. The aim was to analyse if the four cell lines become adherent in the same time span and if they differ in the degree of confluence, i.e. the coverage of the cell culture surface reached after a period of four days; at this time point cell viability has not started to drop (see figure 4.2) and hence one can assume only a low amount of dead cells exists in each culture.

4.5.1 Methodology of adherence and confluence study

For the study of the development of adherence all four cell lines were seeded at 6500 cells/cm^2 in 6 well plates and the speed of attachment to the 6 well plate in serum containing media was documented. The confluence levels reached by the four cell lines after being cultured for four days in adherent growth conditions were also analysed.

4.5.2 Results of adherence and confluence study

As can be seen in figure 4.5, both adherent cell lines, CCL61 and AML cells, were attached after one hour in culture, with nearly all cells showing the beginning of pseudopodia formation even as early as after 30 minutes of culture, but the clearly stretched-out morphology typically seen at later stages of culture was only recognisable after 3 hours of culture and then only for some of the cells. S cells were partially attached after one hour with a number of cells showing a clear stretched-out adherent morphology and others still showing a rounded up morphology with no pseudopodia formation. CHO-S cells were not adherent after one hour of culture and did not show any proper pseudopodia formation. Even after 7 hours only a few CHO-S cells showed the typical fibroblast morphology whereas this phenotype was developed in full by CCL61 and AML cells after 3 hours. All S cells showed pseudopodia formation after 7 hours, with a large variation in the spreading of the cells. It has to be noted that due to the experimental set-up and the microscope available it was not possible to analyse the same area of culture during the time of this experiment, which accounts for the large variation in cell distribution over the field of view.

The confluence levels reached by the four cell lines after having been cultured for four days in adherent growth conditions also varied. As can be seen in figure 4.6, only AML cells become 100% confluent. CCL61 and S cells do not reach the same high degree of confluence and the culture of CHO-S cells actually shows a number of non-adherent cells which would not be accounted for in the viable cell density data due to the harvesting procedure. CCL61 cells might be contact inhibited

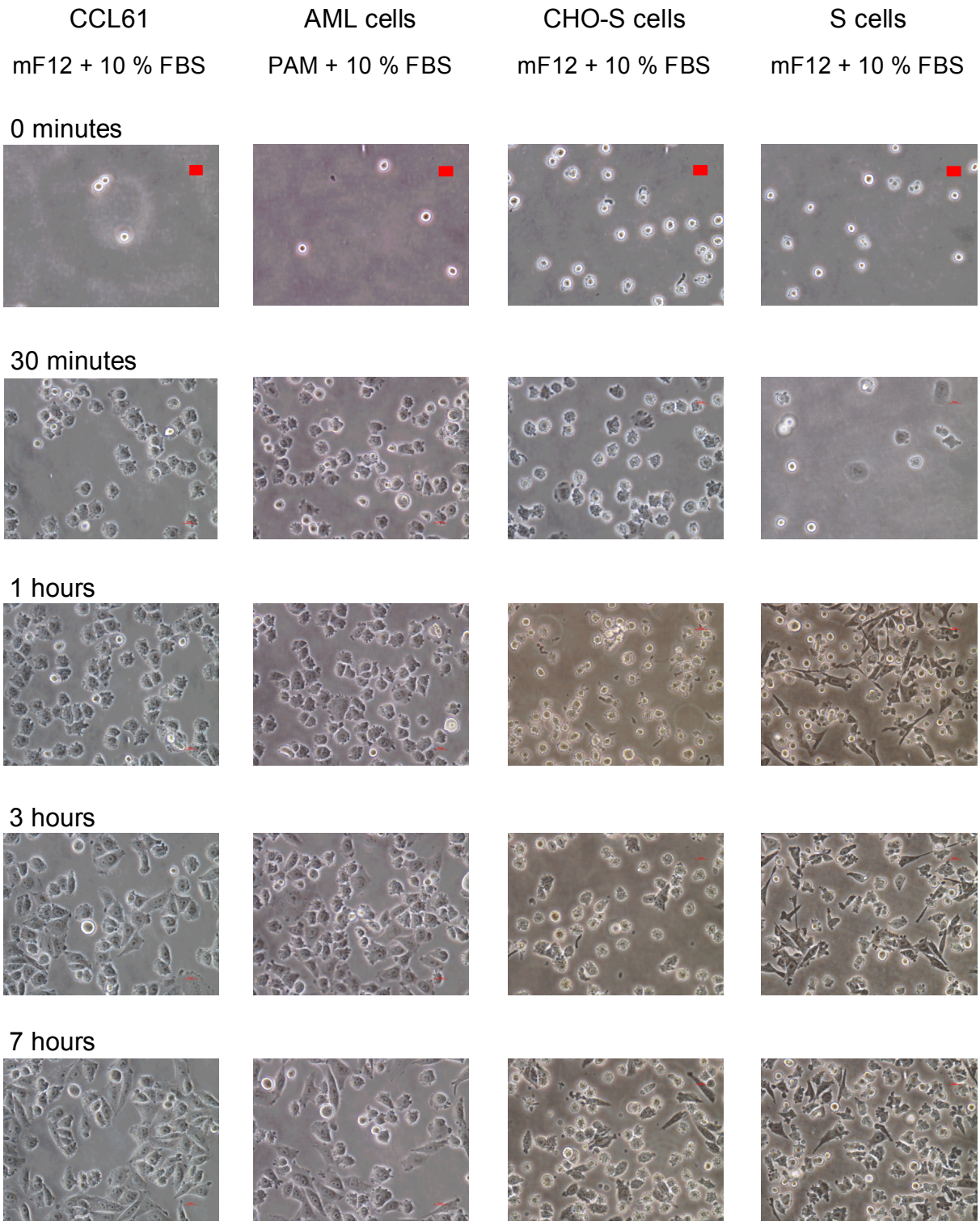

Figure 4.5: Differences in adherence development of the different CHO cell lines
Cells were cultured in 6 well plates and images were taken with a Nikon Eclipse TS100 microscope with an attached camera and a 40x objective using the NIS Elements F2.30 software at the time points indicated. The different development of the morphology after transfer into the corresponding adherent growth medium over the period of 7 hours can be seen. Cells were treated with trypsin for 10 minutes before seeding. Scale bars in top row images equal 20µm.

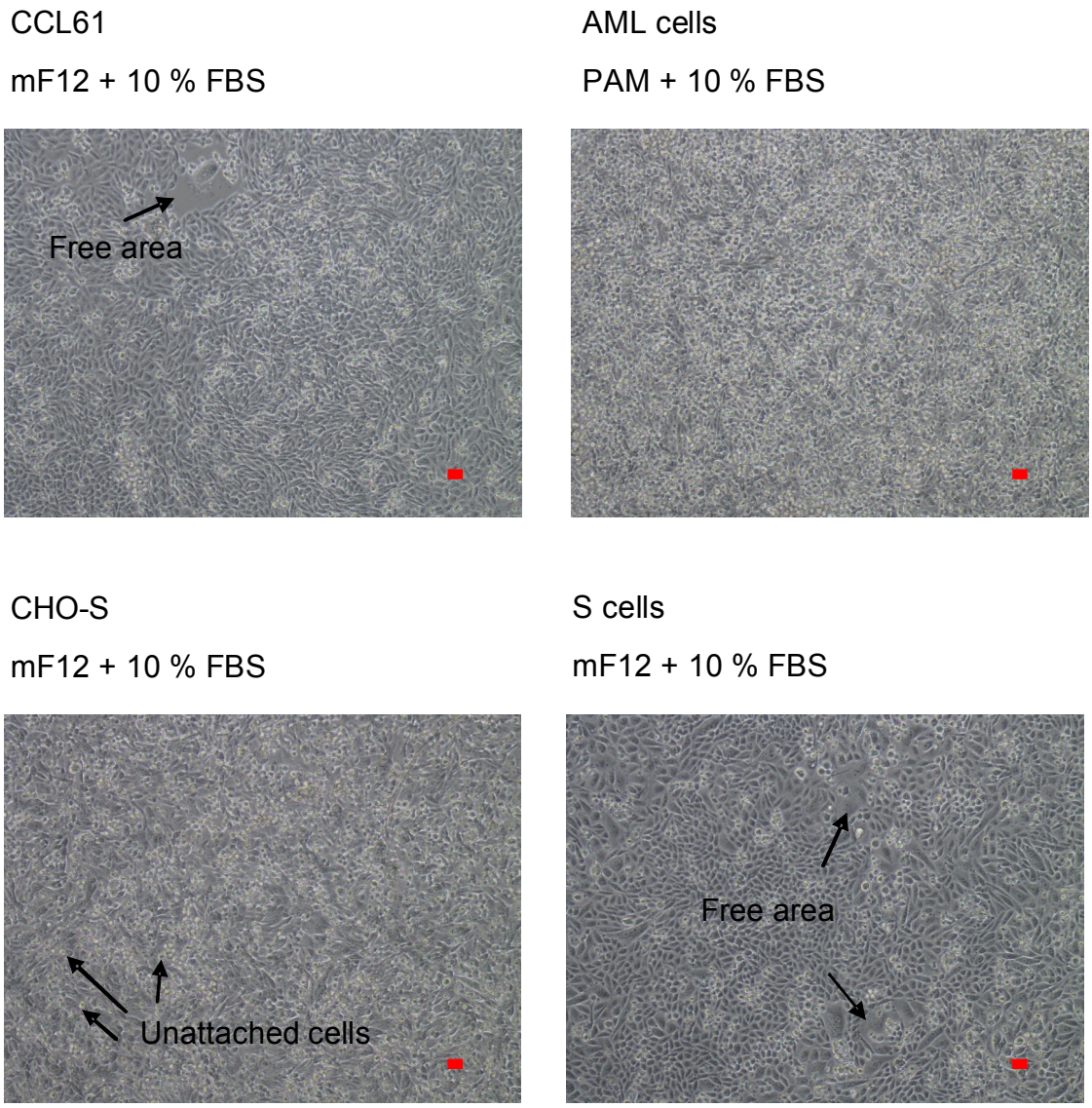

Figure 4.6: Confluence levels reached by the model cell lines after a 4 days culture period

Confluence levels reached in the respective adherent media after a period of 4 days are shown for the four cell lines in the given medium under static culture conditions. Some of the differences regarding confluence have been marked by arrows. Scale bars are 40µm long.

and hence not reach the same level of confluence as the AML cells. This difference between CCL61 and AML is also seen in the viable cell densities reached by those cell lines (see figure 4.2) and could also be related to the different media used.

4.6 Discussion of growth characteristics results

The growth data in figures 4.2 and 4.3 shows clearly that all four cell lines can proliferate in adherent growth conditions whereas only CHO-S, S cells and AML cells proliferate successfully in suspension conditions but show different maximal achievable viable cell densities in the respective growth conditions. Maximal growth rates for suspension adapted CHO cells in serum free conditions have been shown to be as low as 0.015 h^{-1} (LeFloch *et al.*, 2006); this is clearly exceeded by the suspension cell lines CHO-S, S cells and AML used in this study. The maximal growth rate of S cells, AML cells and CHO-S shows hardly any difference between suspension and adherent culture conditions, in contrast to CCL61 that show a lower maximal growth rate in suspension conditions compared to adherent conditions. The data gained for the S cells and AML cells shows similar growth characteristics as seen before at Pfizer in the cell culture conditions described, though it should be noted that the optimal CO_2 concentration for PSM and PAM would have been 7%, which could not be used in this study due to limitations in incubator availability.

The difference between CHO-S and S cells in maximal viable cell density reached might be based on the different media used in addition to their adaptation status, but AML and S cells have been cultured in the same suspensions media PSM; hence, any difference with respect to growth characteristics should indicate that those cells differ in their adaptation to suspension growth which might lead to phenotypic differences between these cell lines, as demonstrated by the confluence levels reached (see figure 4.6).

It can be summarised that CHO-S, S cells and AML cells have been adapted to suspension growth conditions, but not CCL61. Hence, differences in the surface between the two identified groups (suspension-adapted cells/ non-suspension-adapted cells) could be due to the process of suspension adaptation and hence be a reaction of the cell lines to the adaptation pressure and the new suspension environment.

Apart from the similarity in growth rates in adherent conditions, the speed of adherence development and the morphologies the four cell lines develop when becoming adherent differ. This is an indication that those cell lines are different in the way they interact with their environment and hence might indicate differences between the suspension-adapted cell lines with regard to their

surface proteins and cell signalling processes. For a summary of the results see table 4.3.

Table 4.3 Summary of cell line characteristics showing the phenotype differences between the suspension adapted cell lines and the non suspension-adapted cell line CCL61.
Each of the four cell lines shows a different phenotype for the characteristics analysed. The ability to grow successfully in suspension varies to a large degree, with viable cell densities reached between 20 x 10^6/ml (CHO-S) and 2 x 10^6/ml (CCL61, a non suspension adapted cell line). * For CHO-S cells confluence cannot be determined properly due to the appearance of non-adherent cells.

	Suspension growth	**Adherent growth**	**Adherent after 1 hour**	**100% confluence after 4 days**
CCL61	no	yes	yes	no
AML cells	yes	yes	yes	yes
CH0-S	yes	yes	no	no*
S cells	yes	yes	yes	no

5.Chapter

Analysing the cell surface proteome using a combined biochemistry/ mass spectrometry approach

In this chapter the role and structure of the proteins in the plasma membrane are summarised. Membrane proteome approaches based on mass spectrometry as a tool to study membrane proteins will be explained and different approaches of previous studies relevant to inform the strategy chosen in this project will be introduced.

5.1 Cell surface membrane proteins

Proteins can be found in all lipid bilayers that exist in cells. Cell surface membrane proteins are important in the development and physiology of cells; for example, changes in cell membrane proteins have been found to be specific for the development of a cancer cell from a healthy cell (Pontier and Muller, 2009). The lipids of the cell membrane can be seen as the backbone of the membrane structure, forming a barrier between the cytosol and cell environment, with the proteins being responsible for specific membrane functions, for instance for nutrient transport, signal transduction, adherence or as environmental sensors (Cooper and Hausmann, 2006). This multitude of functions explains why the membrane protein composition of different cell types differs to a large degree as this enables the cells to function properly in their own environment. This further strengthens our hypothesis that suspension adapted CHO cells might have a different surface protein complement compared to adherent CHO cells.

Proteins can either be attached to the membrane (intra- and extra-cellular peripheral membrane proteins) or inserted into the lipid bi-layer, in which case they are called integral membrane proteins (Macher and Yen, 2007). To allow interaction with the lipid bi-layer, integral membrane proteins usually have hydrophobic regions within their structure consisting mainly of hydrophobic amino-acids as for example phenylalanine, valine and tryptophan; therefore most integral membrane

proteins are transmembrane proteins. Transmembrane proteins are grouped into different categories depending upon their orientation with regard to the N and C termini: type 1 proteins have a cytosolic C terminus, type 2 proteins have a cytosolic N terminus and multi-pass proteins possess several membrane spanning domains with either N or C terminus or both on the cytosolic membrane side (Tan *et al.*, 2008). The membrane-spanning portion of proteins usually shows a structure of alpha helices containing about 25 hydrophobic amino acids, with the number of transmembrane domains varying between 1 and 14 (as, for example, in the *band 3* protein found in red blood cells) or even higher (Copper and Hausmann, 2006). In mammals, very often the extracellular face of the membrane proteins contains carbohydrates due to post-translational modifications of the proteins – hence, a high percentage of plasma membrane proteins are glycoproteins. Another group of integral membrane proteins is anchored to the lipid bi-layer with the help of glycolipids. One typical example of such an anchor is glycosylphospatidylinositol (GPI); the GPI anchor is bound to proteins in the endoplasmatic reticulum in exchange for the transmembrane domain.

Further to their structure, membrane proteins can be defined by their role, such as inter-cellular communications, vesicle trafficking, ion transport and propagation of signalling cascades (Speers and Wu, 2007). Proteins on the cell surface act as receptors, allowing cells to sense and react to their environment (Copper and Hausmann, 2006). For mammalian cells this includes interaction with the proteins of the extracellular matrix in tissue or interaction between cells. In tissue the cells are embedded in an extracellular matrix built from secreted proteins and polysaccharides. The plasma membrane interacts with the extracellular matrix. This interaction is found in particular between the so-called adhesion proteins of the cell membrane and the extracellular matrix. Those interactions are necessary to create a functional structure within the tissue and allow linkage of the cells to the extracellular matrix. A typical protein of the extracellular matrix is fibronectin, which is able to build up structures on its own or connect with other parts of the extracellular matrix such as collagen. Fibronectin has specific areas in its molecular structure which interact with proteins on the cell surface, for example integrins (Copper and Hausmann, 2006). Specific membrane proteins that can be classed into four groups mediate selective cell-cell adhesion: selectins, integrins, the immunoglobulin (Ig) superfamily and cadherins. The interaction between these membrane proteins is thought to occur in the culturing process of adherent cell lines. Selectins mediate transient interactions; the different selectins are expressed on different cell types, with E-selectin found on endothelial cells such as CHO cells. Selectins are cell surface receptors capable of interacting with

carbohydrates found in the form of glycoproteins on the cell surface. Cadherins are responsible for so-called stable adhesions junctions, which also involve the cytoskeleton of the cells connected. There are different sub-types of cadherins, which differ in their transmembrane and cytosolic structures. The most common structure of cadherins is a single-pass transmembrane domain and usually cadherins are glycoproteins with around 700-750 amino acids. The cadherin protein family shares a conserved extracellular domain, which is responsible for interactions between the same types of cells (homophilic actions) and shows a folding structure similar to that of the immunoglobulin (Ig) superfamily (Alberts *et al*., 2002). Membrane proteins can also act as an anchoring point for the cytoskeletal proteins and hence help define cell shape (Tan *et al.*, 2008). Another group of membrane proteins is the class of transporter proteins, which is divided into channel and carrier proteins. Channel proteins are passive transporters that do not interact directly with the transported molecule, whereas carrier proteins bind the molecule in question and undergo conformational changes during the transport process. Transporter proteins can be found, for example, to a large extent in cells lining the intestine where uptake of nutrients occurs. Hence, membrane proteins allow cells to fulfil their specific functions in the context of their environment (Wu and Yates, 2003).

5.2 Analysis and identification of membrane proteins

To analyse the diverse set of membrane proteins found in mammalian cells, membrane proteomics has developed numerous techniques over the last ten years, mainly driven by the importance of cell membrane proteins in drug discovery (Wu and Yates, 2003). Proteomic studies usually rely on the use of mass spectrometry as the best tool to analyse complex protein samples. This approach has been used successfully to address specific questions in small protein sets (Aebersold and Mann, 2003). A mass spectrometer measures the mass-to-charge ratio (m/z) of ions (Biemann, 1992). Mass spectrometry allows accurate measurements of the mass of a peptide and to obtain further information on the peptide, e.g. its amino acid sequence or posttranslational modifications. With the help of bioinformatics mass spectrometry enables identification of proteins using the data obtained with the mass spectrometer (Aebersold and Mann, 2003). A basic mass spectrometer usually consists of an ion source, a mass analyser and a detector. More complex systems combine two mass spectrometers allowing *tandem MS*; in-between the two mass analysers a so-called collusion cell allows fragmentation of the peptides; this process is called collusion induced dissociation (CID). The identification of peptides using the *tandem MS* or MS/MS method

is possible due the facts that a) the peptide bond breaks in the collusion cell and b) the resulting fragmentation follows a general pattern (Kraj and Silberring, 2008). With the help of search engines, such as *Mascot,* together with MS/MS data sets containing parent ion mass, set of resulting fragment masses and an idea of the accuracy of those masses an identification of the protein in question is possible (Thomas, 2009). As the peptides resulting from the enzymatic digest, which is part of the sample preparation, can be calculated for each protein found in the bioinformatics databases the theoretical mass of those peptides and their possible fragmentation patterns can also be calculated. Hence, by comparing the theoretical data with the data obtained in the experiment an identification of the proteins is possible (Bantscheff *et al*., 2007).

Due to the membrane protein structure which is determined by the transmembrane domain that needs to be hydrophobic to be embedded into the lipid bilayer, the standard proteomic approaches based on separation by 2D gel electrophoresis followed by mass spectrometry have failed (Ferro *et al.*, 2000; Blonder *et al.*, 2002). Furthermore, membrane proteins have a low abundance compared to intracellular proteins and their expression is highly dynamic (Macher and Yen, 2007), making their analysis even more difficult; integral membrane proteins are often under-represented in mass spectrometry studies of proteins as their large number of post translational modifications, the heterogeneity arising from this (Josic and Clifton, 2007) and their amphipathic nature (as they contain hydrophobic and hydrophilic regions) make them difficult to study (Wu and Yates, 2003). The standard procedure for a mass spectrometry proteomics study includes the following steps: protein isolation, SDS gel electrophoresis, enzymatic digest of proteins, high pressure liquid chromatography and mass spectrometry, with the last two usually being coupled into one instrument (HPLC -MS) (Aebersold and Mann, 2003). The amphipathic nature of the membrane proteins renders the classical proteomics approach based on two-dimensional gel electrophoresis useless as membrane proteins tend to be insoluble in the buffers used for iso-electric focusing (Santoni *et al*., 2000). Using one-dimensional gel electrophoresis brings the problem of increased sample complexity and does not solve the problem of insufficient enzyme digest often encountered with the membrane-spanning segment of the protein. Different approaches have been used to help the analysis of membrane proteins, such as selective stepwise dissolving of lipid membranes and using different detergents and salts. These methods, in addition to one-dimensional gel electrophoresis, have been used to reduce the complexity of the samples (Josic and Clifton, 2007). Significant advances have been made in non-gel based shot gun methods using liquid chromatography in combination with mass spectrometry (LC-MS) (Griffin and Aebersold, 2001). For this method

proteins are digested with proteases yielding a complex peptides mixture using a suitable enzyme, as for example trypsin, that is then separated by liquid chromatography and directly analysed by mass spectrometry. The liquid chromatography system used most frequently for this kind of approach is typically a nano-liquid chromatography system with a reversed phase (RP) column (Kraj and Silberring, 2008). One advantage of the shotgun proteomic approach in comparison to 2D gel-electrophoresis is that the shotgun approach has a wider dynamic range, making low abundance and highly dynamic expressed proteins more detectable with this method. Furthermore the shotgun approach allows the use of a wider range of buffer components, such as detergents in the sample preparation; nevertheless detergents usually used in the preparation of membrane proteins have to be removed for LC-MS analysis (Blonder *et al.*, 2002). The reagents that can be used in the sample preparation also depend on the type of instrument used for mass spectrometry; for example the different ion sources tolerate different reagents. Solubility of membrane proteins remains a major challenge in this approach and a great variety of methods trying to solve this problem can be found in the literature (Wu and Yates, 2003). A variety of treatments has been tested, for example, detergent containing buffer or buffers based on organic solvents. Blonder *et al.* (2002) developed a organic solvent based membrane protein preparation for proteomic analysis showing an improvement in detection of hydrophobic peptides typical for integral membrane proteins but this method was developed for prokaryotes. The method was further developed for mammalian cells avoiding the previously necessary high pH fractionating and thermal denaturation, but the protocol involves a lyophilisation step before two step fractionating is followed by mass spectrometric analysis (Blonder *et al.*, 2006). An organic solvent based method has also been used to analyse integral membrane proteins of chloroplasts (Ferro *et al.*, 2000); a variety of extraction conditions were tested to find the optimal condition but the coverage with regards to different parts of membranes of the chloroplasts changed with the extraction mixture used. Mirza *et al*. (2007) demonstrated that chloroform based extraction is also possible for epithelial cells; this method also involved protein precipitation and ultracentrifugation. Not all of those methods are compatible with a subsequent quantification of the proteins but all have been shown to improve identification of plasma membrane proteins (Wu and Yates, 2003; Josic and Clifton, 2007).

Another approach to enhance identification of membrane proteins has been to remove the required detergent such as SDS before downstream analysis as shown by Wiśniewski *et al.* (2009) who used 8 molar urea together with size exclusion chromatography to deplete SDS combining this with the enzymatic digest on a filter; this method is called FASP for filter aided sample preparation.

Furthermore, biochemical enrichment has proved to be an option for improved mass spectrometry based analysis of membrane proteins (Wu and Yates, 2003). For example, cationic silica micro-beads have been used to label and isolate proteins found in the apical membrane region of adherent epithelial cells (Josic and Clifton, 2007) but this method would not be useful for suspension cells. Another method that has been used in membrane proteomic analysis is cell surface biotinylation. Peirce *et al.* (2004) used this method to investigate differential membrane protein expression on lymphocytes. Biochemical enrichment based on protein biotinylation has been successfully used for other quantitative mass spectrometry approaches (Elia, 2008) as for example by Berro *et al.* (2007) for comparative proteomic analysis of T cells, which are also suspension cells, which makes cell surface biotinylation an attractive option for this project. In the study by Berro *et al.* (2007) the proteomics analysis was followed up by analysis of the identified proteins with flow cytometry and western blotting. Flow cytometry and western blotting has also been used by Peirce *et al.* (2004) for conformation of results.

The enrichment of biotinylated proteins is based on the strong affinity of biotin to avidin and streptavidin which can be used for affinity chromatography. A number of membrane protein studies are based on biotin derivatives such as N-hydroxysuccinimide (NHS) biotin; the reactive ester group of NHS reacts as the functional group in a nucleophilic substitution reaction with primary amines, such as found in lysine, and hence allows covalent binding of the biotin to the proteins that are to be enriched. In addition, lysine residues are numerous in proteins and their modification usually has non-detrimental effect on the protein function (Elia, 2008). Care has to be taken to avoid uptake of the chosen biotin derivative by the cells when preparing samples for membrane proteomics to avoid contamination of the samples with cytosolic proteins (Gauthier *et al.*, 2004).

Five different proteomic studies that are based on membrane biotinylation followed by enrichment were compared and used to develop a methodology for this study (see also chapter 3.15 *Biotinylation of cells*). Zhao *et al.* (2004) analysed adherent cells which were biotinylated with sulfo-NHS-S-S-biotin, a biotin cleavable due to its disulfide group (structure is shown in figure 10.1). Enrichment was based on a magnetic system and included harsh washes with high salt and high pH buffers. None of the agarose based enrichment steps in other studies included such a combination of washing steps. DDT, which reduces disulfide bonds, was used to elute biotinylated proteins from the streptavidin beads. After elution a precipitation step was added to reach higher protein concentrations. Zhang *et al.* (2003) used a similar approach of biotinylation and enrichment but give no details of elution conditions. The study demonstrated enhanced results for mass

spectrometry analysis of the plasma membrane proteins due to an decrease of contamination of the enriched protein fraction with proteins from cell organelles. Zhang *et al.* (2003) stress in their paper that sulfo-NHS-SS-biotin cannot cross the membrane. Peirce *et al.* (2004) also used biotinylation followed by non-magnetic enrichment to compare stimulated against non-stimulated cell samples. The sample preparation was monitored using confocal microscopy and western blotting; the use of the biotin label for this purpose was also noted in some of the other studies. Peirce *et al.* (2004) demonstrated that labelling with water-soluble sulfo-NHS-SS-biotin was not completely restricted to the cell surface but also included some small sub-cellular structures, in contrast to another biotin derivative that gave significant intracellular signals. To enhance the quality of the enriched membrane fraction a pre-enrichment centrifugation step was included. The affinity enrichment used streptavidin agarose beads. The overall study used a very complex sample preparation, including two-dimensional gel electrophoresis based on a non standard isoelectric focusing approach, which does not lend itself to be used in conjunction with quantification strategies on the mass spectrometry level: the actual quantification was performed by gel staining. Another study by Yu *et al.* (2006) based on biotinylation compared cleavable and non-cleavable biotin. This included a pre-enrichment step by centrifugation before the affinity chromatography step based on avidin agarose beads. For the cleavable biotin, elution from the agarose beads included DTT. Protein identification was achieved by reversed phase liquid chromatography coupled to a mass spectrometer, as with the studies mentioned before. It was noted that with this approach not only integral membrane proteins but also GPI linked proteins will be labelled. The results of the LC-MS identification were cross-checked with immuno-fluorescence microscopy for four proteins. Sostaric *et al.* (2006) used tissue as a starting material; cells from the tissue were cultured for a defined period. Adherent cultures were biotinylated using a non-cleavable biotin. After biotinylation viability of the cells was checked. In this study, as is in several of the studies mentioned earlier, IgePal CA630 (NP-40) was used in the lysis buffer as a detergent to increase solubility of the hydrophobic membrane proteins. Enrichment was based on an avidin resin and followed by different approaches for mass spectrometry analysis: one route used two-dimensional gel electrophoresis, the other one-dimensional gel electrophoresis. The latter allowed identification of a larger number of proteins.

5.3 Biotinylation of cell lines and subsequent analysis by flow cytometry

The protocol for biotinylation was developed based on the above studies and the successful biotinylation of the different cell lines was controlled by staining the cells with Streptavidin FITC. Another factor controlled during the protocol development was cell viability by measuring the cells after biotinylation on the ViCellXR cell viability analyser. The developed biotinylation approach showed successful biotinylation of more than 95% of the cells in one sample, independent of the cell line, while keeping the viability above 90%. As a next step the Streptavidin FITC staining was used to compare the amount of biotin bound to the surface of the different cell lines .

5.3.1 Methodology: Streptavidin staining of biotinylated cells

Cells were stained for flow cytometry using 5 x 10^6 cells in 50 µl PBS / 2 mM EDTA / 0.5 %BSA buffer. Staining was performed using Streptavidin FITC at a titer of 1 to 25, incubation time was 10 minutes at 4°C. Cells were washed twice with PBS, fixed with 125 µl 4% PFA (15 minutes at 4°C) and re-suspended in PBS. Storage was for a maximum of 24 hours in 1ml of PBS/2mM EDTA/0.5%BSA. Analysis of the cells was undertaken on a FacsCalibur.

5.3.2 Biotinylated cells analysed with flow cytometry: differences in staining intensity

The results of staining after biotinylation with the final biotinylation protocol (described in chapter *3.15 Biotinylation of cells*) of the different cell lines allow a comparison of the surfaces of the different cell lines. Differences in the staining intensities, measured as median fluorescence intensities (MFI), indicate differences in the amount of biotin bound to the cell surface; this can also be described as different levels of biotinylation reached due to differences in the cell surface protein complement available for biotinylation. To avoid influence by instrumentation set-up, the shift in median fluorescence intensity has been calculated between unstained and stained biotinylated cells. The resulting change in median fluorescence intensity (Δ MFI) can be compared; a smaller Δ MFI indicates that less biotin has bound to the cell surface, which can be due to:

- a lower amount of protein expressed on the cell surface,
- a different subset of proteins expressed on the cell surface or
- a different accessibility of the proteins to biotinylation.

All of these indicate differences in the cell surface proteome.

As can be seen seen in figure 5.1 the percentage of cells that become labelled with the biotin is very similar when the different cell lines are compared. The ΔMFI values clearly indicate (see also table 5.1) that there is a difference between the four model cell lines chosen for this study with respect to their cell surface.

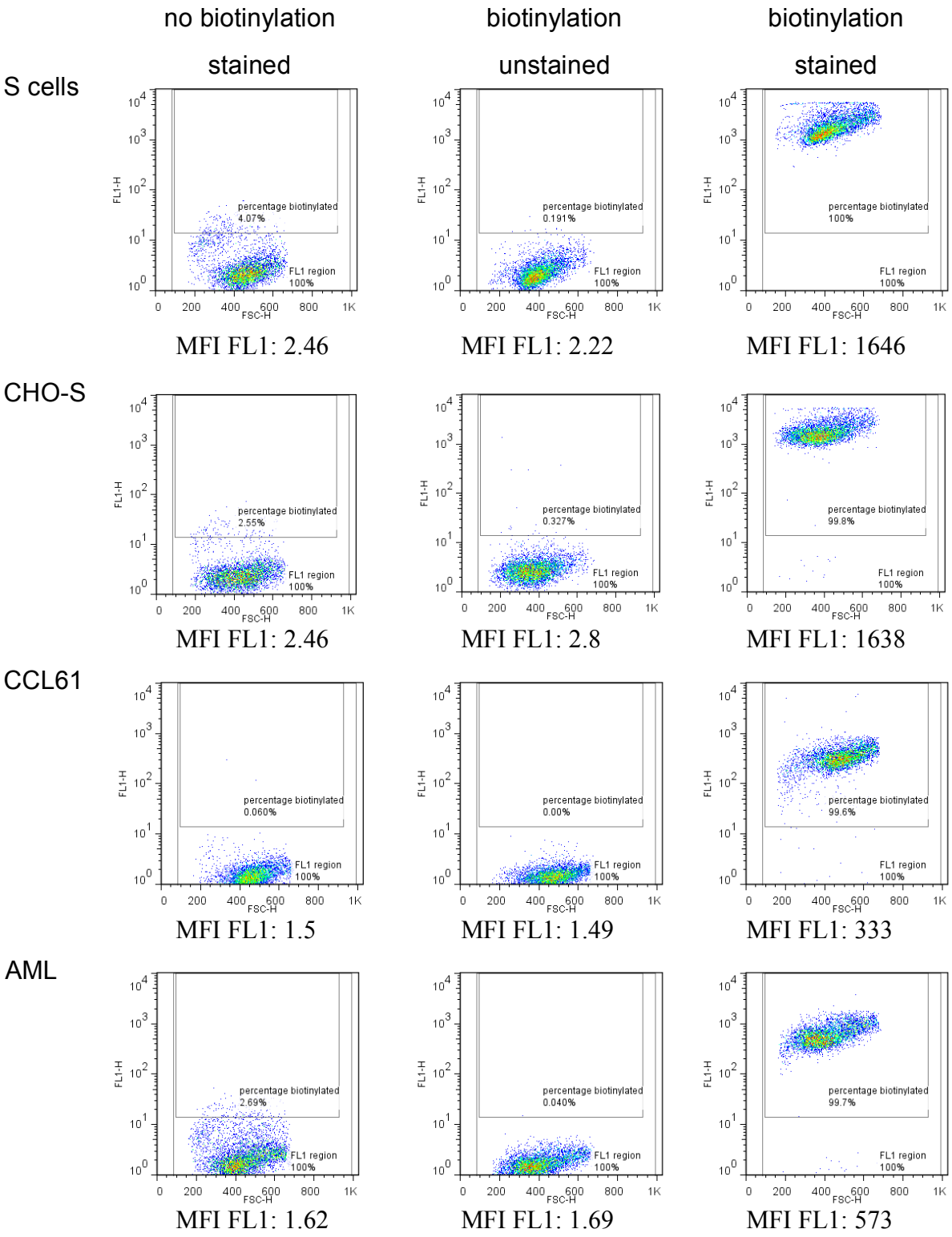

Fig. 5.1: Differences in biotinylation levels of the different cell lines analysed by flow cytometry.

Cell lines were grown in their standard growth conditions before biotinylation. Control samples with non-biotinylated cells were stained to check for unspecific staining of the fluorochrome. Unstained biotinylated cells were used for instrument set-up. MFI (median fluorescence intensity) FL1 gives the median for the y-axis calculated for the cells in the FL1 region. A forward/ side scatter gate (not shown) was used.

Table 5.1 ΔMFI values for CHO cell lines calculated using the results shown in figure 5.1. The arrow indicates the increase of biotinylation levels reached.

Cell line	Δ MFI
CCL61	331.5
AML cells	571.3
CHO-S	1635.2
S cells	1643.7

5.3.3 Discussion of biotinylation – staining results

The difference in biotinylation levels between the four cell lines is nearly a factor of 5, comparing CCL61 with S cells. The two cell lines AML cells and CCL61, which were grown in adherent conditions for this set-up, show a low biotinylation level compared to the two cell lines CHO-S and S cells grown in suspension. This might indicate that more proteins are expressed on the surface of suspension cells. But the difference in biotinylation levels could also be due to the cell surface proteins of the adherent cell lines being less accessible for biotinylation; this could be due to binding of fibronectin and other serum components to the cell surface proteins as this could reduce the number of lysine residues available for biotinylation due to a shielding effect of the extracellular matrix proteins.

5.4 Comparison of different lysis and enrichment strategies

After the biotinylation protocol was shown to be stable a larger number of cells was labelled and lysed. Initially the adherent and the suspension cells were lysed differently; lysing the adherent cells directly on the T75 flasks was performed to avoid treating the cells with an additional buffer. Lysed S cells and CCL61 were then used to establish an enrichment strategy based on the articles discussed above. For economic reasons an agarose resin based approach was used and due to availability no ultra-centrifugation step was included. The result of the affinity chromatography enrichment was controlled with SDS gel electrophoresis stained with Coomassie Blue (pre-made solution and protocol from suppliers Pierce or Invitrogen, depending on the gel system used) as this is the next step forward prior to mass spectrometry analysis.

5.4.1 Methodology: lysis of cells

Lysis of adherent and suspension cells was done differently for the first enrichment experiments: suspension cells were treated as described in chapter *3.16 Lysis of cells*. For adherent cells 1ml lysis buffer was added to a T75 flask after biotinylation and incubated for approximately 5 minutes on a shaking platform. Using vigorous pipetting the solution was then transferred into a vial and sonicated. The resulting cell solution was centrifuged at 22,000 g for 20 minutes at 4°C and the resulting supernatant stored at -20°C.

Due to difficulties reaching comparable protein enrichment results with the CCL61 cells (see figure 5.3) the lysis protocol was changed and adherent cells were harvested after biotinylation using 1 ml PBS/2mM ETDA per T75 flask, incubating at 37°C for 5 minutes. The resulting cell solution was spun down, re-suspended in PBS and lysed as described for suspension cells. This change allowed better control of the cell count during lysis of the adherent cells; for lysis on the flask, cell count was determined by harvesting and counting an additional flask that had been biotinylated as well.

5.4.2 Methodology: Streptavidin affinity chromatography

The initially established enrichment protocol used was as follows: 2 ml centrifugation columns (Pierce) were filled with 500 µl PBS to clear out air bubbles. 1 ml agarose resin was applied and washed two times with 1 ml PBS (gravity flow). This was followed by sample application. In the first washing step 3 ml lysis buffer without protease inhibitors (1% detergent) were applied on top of the columns; wash step two used 3 ml 500 mM KCl (Sigma Aldrich) + 1% detergent and wash step three was a repeat of wash step one. To prepare the column for elution 3 ml 100 mM TRIS (pH7.6) with 2% SDS was applied. Elution was performed stepwise by applying 500 µl 100 mM TRIS (pH7.6), 4%SDS and 100 mM DTT, warmed up to to 37°C, onto the column which was closed with a stopper. After incubation for 10 minutes at 37°C the column was opened to let the elution buffer run through. This step was repeated and the resulting elution fractions were pooled. This pool, containing the enriched plasma membrane protein fraction, was acetone precipitated by adding 4 times the volume of acetone, cooled down to -20°C, followed by overnight storage at -20°C. After centrifugation of the acetone protein mix at 16,000 g for 10 minutes at 4°C the protein pellet was air dried and dissolved in 100 µl elution buffer.

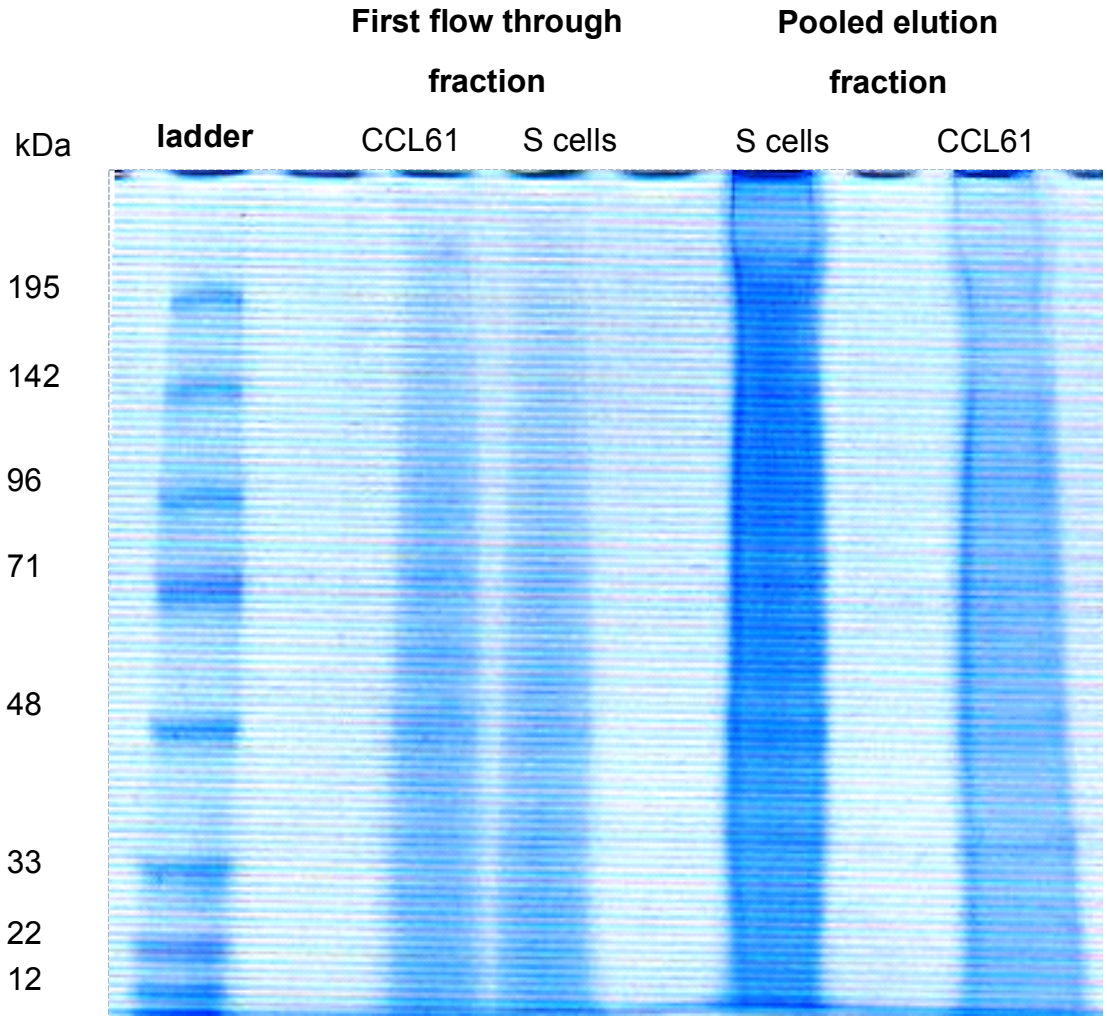

Figure 5.2: Enrichment of plasma membrane proteins from CCL61 and S cells.
1 x 10^8 biotinylated and lysed cells of each cell line were pooled and used in the Streptavidin affinity chromatography enrichment. Gel analysis of the resulting fractions was done by SDS PAGE using a 8-16% tris-glycine gel (150V for 40 minutes) and the Coomassie solution recommended by the gel supplier (Pierce). The flow through fractions (1/10 of the volume, equal to 1 x 10^7 cells) of the sample application onto the agarose resin were also run on the gel. From the elution fractions one quarter (enriched protein from 2.5 x 10^7 cells) were analysed. Proteins can be seen in the elution fraction.

5.4.3 Results of enrichment by Streptavidin affinity chromatography

A side-by-side comparison of CCL61 and S cells was performed based on the described protocol,with the adherent cells lysed on the T75 flasks. From figure 5.2 one can learn that similar amounts of proteins were detected in the first flow-through fraction; further wash fractions were not analysed as they were too diluted to give a signal. Proteins were detected in the elution fraction; for the CCL61 the amount of protein yielded by this enrichment was lower compared to the S cells.

This result correlates with the results from the biotinylation, where higher biotinylation levels were reached for the S cells compared to the CCL61. To check if the proposed protocol has actually worked and plasma membrane proteins had been enriched, the samples were used for an MS analysis. The enrichment protocol did not yield a well defined banding pattern in the gel, which is assumed to be due to the high detergent and SDS concentration in the samples as the protein pellet had been dissolved in the elution buffer after precipitation, but the blurred protein staining might also indicate degraded proteins due to proteolysis; also there were technical problems due to laboratory rearrangements with the imaging system. As the results from the mass spectrometric analysis were not satisfactory (see chapter 5.5) the enrichment step was modified to the one described in chapter *3.17 Cell surface protein enrichment with affinity chromatography;* the modification avoids the precipitation step and at the same time the samples were eluted in the correct SDS sample buffer for gel analysis; furthermore, protein-inhibitors were added to the washing steps to counter proteolysis taking place during the enrichment.

Using the same biotinylation as before, the new enrichment strategy was tested on CCL61 and on S cells in standard (suspension) and in reversed (adherent) conditions. This was done as the previous enrichment showed a difference in the amount of proteins eluted for adherent and suspension cells.

For this enrichment adherent cells were again lysed on the flask. This enrichment method proved successful (see figure 5.3) even with fewer cells in the start sample. The fact that lower amounts of cells (less than 1/3) yielded an easily visible signal on the gel indicates that the previous protocol was not optimised with regard to elution efficiency or that extensive proteolysis had taken place during enrichment.

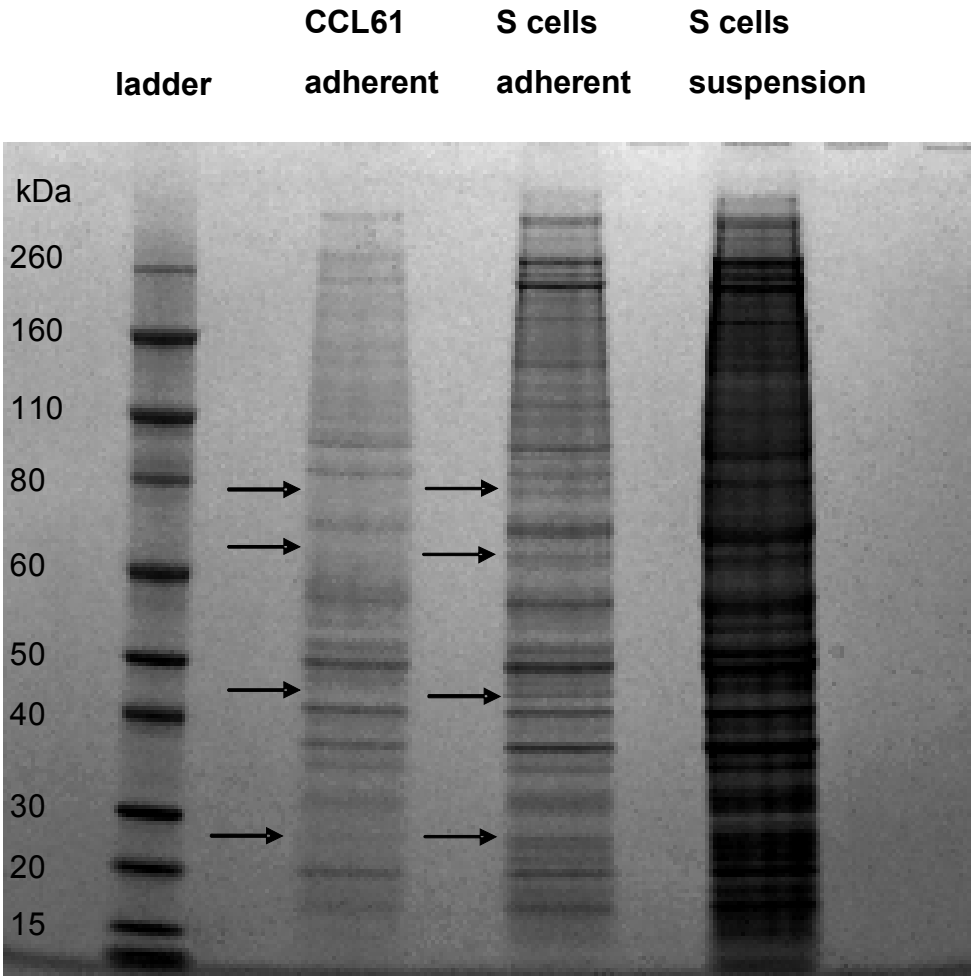

Figure 5.3: Enrichment of plasma membrane proteins from CCL61 in standard and S cells in standard and reversed conditions.

3 x 10^7 biotinylated and lysed cells of each cell line were used in the Streptavidin affinity chromatography based on the improved protocol. Gel analysis of the resulting elution fractions (1/16 of the elution fraction, equivalent to 1.8 x 10^6 cells) was done using a 4-12% Bis TRIS gel with MOPS running buffer (Invitrogen) under reducing conditions and stained using the Coomassie solution recommended by the gel supplier. In all three elution fractions proteins can be observed. Differences seen in the protein bands between the CCL61 adherent and S cells adherent, indicating a loss of protein expression in either of those cell lines, have been marked by arrows.

The latter assumption is supported by the observation that the protein bands are much clearer in figure 5.3 and it is possible to determine differences in the protein bands of the enriched membrane protein fraction between the CCL61 and the S cells, for example around 260 kDa and around 50 kDa. Although the lane for the S cells grown in suspension is somewhat overloaded, it is possible to say that the bands seen for adherent S cells (and not for CCL61) are also visible for suspension S cells. Again, even more clearly than before, the elution fraction of the suspension cells contains more protein than the elution fractions from the adherently grown cells. This might be due to the fact that the number of suspension cells was determined differently to the number of adherent cells, which was only be determined by an approximate method. Hence, as described in chapter 5.3.1 a new approach with regard to lysis of adherent cells was chosen. In addition, all four cell lines were now subject to analysis using the final protocol for biotinylation, lysis and affinity chromatography enrichment. Figure 5.4 shows that enrichment of proteins was successful for all four cell lines using the described method. There is a difference between the protein bands seen in total lysate and elution fraction, indicating a shift in protein composition within the sample. This indicates that some proteins, e.g. non-biotinylated non-membrane proteins, have been successfully removed from the enriched fraction, as would be expected. Furthermore, the eluted protein fraction shows large differences between the four cell lines; this is in line with the assumption that the four cell lines have a different membrane protein complement and the fact that the membrane protein complement is supposed to make up most of the proteins in the eluted fraction.

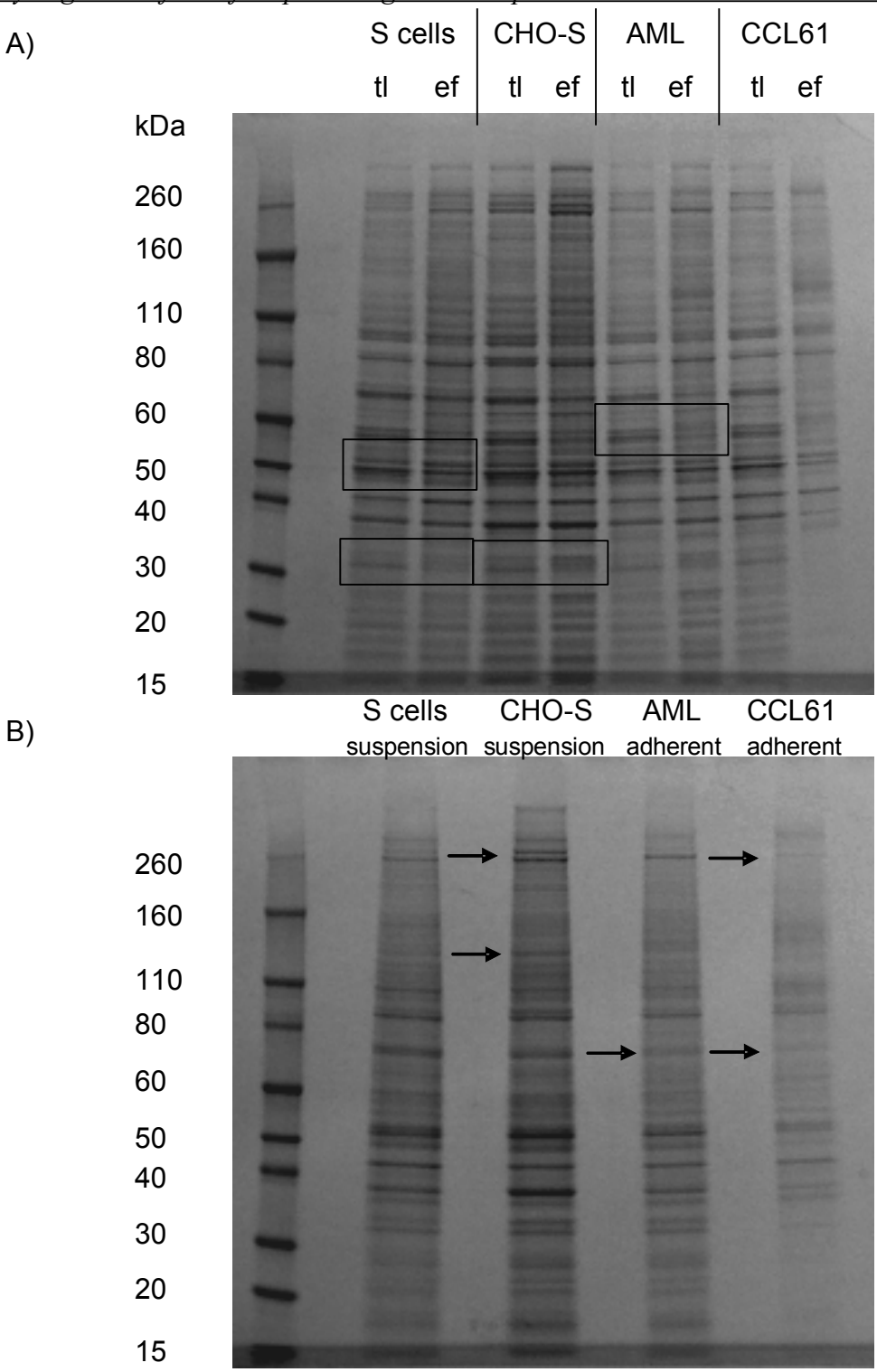

Figure 5.4: Enrichment of plasma membrane proteins from CCL61, S cells, AML cells and CHO-S.

Culture conditions: standard conditions. 3 x 10^7 biotinylated and lysed cells of each cell line were pooled, fractionated with Streptavidin affinity chromatography based on the new lysis & the improved enrichment protocol. Gel analysis of the resulting fractions was done using a 4-12% Bis TRIS gel. A) shows total lysate (tl, 1.5 x 10^4 cells) and 1/16 of the elution fraction (ef). Rectangles indicate differences in bands between tl and ef. B) only shows elution fraction. Arrows in B) denote differences in bands in comparison to S cells.

5.5 Mass spectrometry analysis

The enriched protein fractions shown in figure 5.2 (*Enrichment of plasma membrane proteins from CCL61 and S cells)* were subjected to a mass spectrometry analysis to allow a verification of the successful enrichment of cell surface membrane proteins with the established method. A gel digest was performed as part of the sample preparation as described in chapter 5.4.1, followed by a mass spectrometry run and data analysis (described in chapter 5.4.2).

5.5.1 In-gel digest of Coomassie stained proteins

Each lane from an elution fraction was cut into small pieces, resulting in 9 pieces (halved again for treatment) over the entire gel length of a 4-20% SDS page gel, and transferred into 1 ml tubes (protein low binding tubes). 500 µl de-staining solution, made of 200 mM ammonium bicarbonate with 40% acetonitrile, were added to each piece and the tubes were incubated for 30 minutes at 37°C, followed by a wash step with 200 µl acetonitrile (HPLC grade, Fisher Scientific). Both times the supernatant was carefully discarded. A trypsin stock solution was made up from 20 µg trypsin (Sigma Aldrich) in 100 µl 0.1 mM HCl. To each gel piece 50 µl of 500 mM ammonium bicarbonate with 10% acetonitrile containing 0.2 µg trypsin from the stock solution were added. The trypsin digest was performed at 37°C overnight in a shaking incubator. The resulting supernatant containing the digested proteins was transferred into fresh tubes. 200 µl acetonitrile were added and the gel pieces were again incubated at 37°C for 10 minutes. The resulting supernatant was pooled with the one gained before. Samples were dried in a vacuum concentrator 5301 (Eppendorf, UK) overnight and re-suspended in buffer containing 3% acteonitrile and 0.1% formic acid. As polymer contaminations were found in a trial mass spectrometry run, dried peptide samples were re-suspended in 20% acteonitrile and 0.1% formic acid (pH below 3) and cleaned using an in-house strong cation exchange protocol based on filter tips with porous beads resin. Samples were eluted in 20% acetonitrile, 500 mM KCl with 0.1% formic acid and dried again.

5.5.2 Mass spectrometry analysis

The tryptic peptides were reconstituted in 5 µl 3% acetonitrile with 0.1% trifluoroacetic acid and analysed using an UltiMate 3000 capillary liquid chromatography system (Dionex, Camberley, UK) coupled to an HCT Ultra ion-trap mass spectrometer (Discovery System, Bruker Daltonics, Coventry, UK). The peptides were injected onto a 5mm x 300 µm PepMap C reverse-phase trapping column (Dionex) in sample solvent at 30 µL/min, then separated on a 150mm x 300 µm Atlantis

C18 analytical column (Waters, Elstree, UK) at a flow rate of 3 µL/min. Elution was performed with a linear gradient using buffer A (3% acetonitrile and 0.1% formic acid) and buffer B (97% acetonitrile and 0.1% formic acid), starting with 3% buffer A up to 40% buffer B over 40 minutes. Data acquisition was set in the positive ion mode with a mass range of 300 – 2000 m/z. Automatic dependent tandem mass spectrometry was performed on peptides with +2, +3, and +4 charge states by collisionally-induced dissociation.

The resulting mass spectra from the peptides and the peptide fragmentations were submitted to Mascot Daemon v.2.1.3 running with Mascot Server v.2.2.01 (Matrix Science, London, UK) to conduct a search to identify the proteins present in the samples. The mgf files from the subsequent runs were merged for this search. At the time of analysis the genome of the Chinese hamster had not been sequenced (Baycin-Hizal *et al.*, 2012), hence the Mascot Daemon search was performed using the protein database for rodents (Hayduk *et al.*, 2004) provided by SwissProt (8 and 9 of February 2011). At the same time an automatic decoy database search was performed within MASCOT. Search parameters were set at a mass tolerance of 0.8 Da for both MS and MS/MS data, one missed cleavage of trypsin, oxidation of methionine. The resulting list of protein accession numbers was then used in the Uniprot database to search for proteins annotated with 'membrane' as sub-cellular location.

5.5.3 Mass spectrometry results

For the CCL61 cell line the total number of proteins identified was 119, with 34 being classed within the Uniprot database as membrane proteins. Hence, 29% of the proteins identified for CCL61 where either membrane proteins or associated with the plasma membrane. For the S cells the total number of proteins identified was 1216, with 390 being classed in Uniprot as membrane proteins. This means that 32% of the proteins identified for S cells were membrane proteins. The false discovery rate above the homology threshold and the identity threshold respectively (based on the decoy database search) were 13.5% / 6.9% for the samples from CCL61 and 9.63% / 4.62% for the samples from S cells, which indicates that the amount of sample was insufficient for both mass spectrometer runs (Mirza *et al.*, 2007). A list of the identified membrane proteins is included in chapter *10.1 Mass spectrometry: protein identification results*. Unexpectedly, for the CCL61 cells no integrins, cadherins and growth factor receptors were identified; this is also in contrast to previous results by Ahram *et al.* (2005) who analysed the shedded proteome of adherent CHO cells and identified a few integrins such as integrin alpha 11; this again indicates that the chosen sample

preparation is not suitable for the adherent CHO cells. In contrast to this, for the S cells two unexpected groups of membrane proteins were identified, inter-cellular adhesion molecules such as several cadherins, e.g. otocadherin and protocadherin, and nine different integrins including integrin alpha 4, integrin alpha 3, integrin alpha 5 and integrin beta 1. Other proteins involved in adhesion, such as CD166 and neural cell adhesion molecule 2, have been found, in addition also receptors for growth factor, including those for insulin, were identified. The later is in line with the fact that the PSM media contains insulin. Several channel proteins, for example members of the potassium voltage gated channel proteins and the sodium channel proteins, have been found; this can be seen as a clear indication that the analysed protein fraction was enriched for plasma membrane proteins as those proteins are integral membrane proteins. However, also signalling related molecules such as Focal adhesion kinase 1, a protein related to integrin signalling, has been identified in the S cells. Later re-analysis of the mass spectrometry data generated for the S cells using a CHO proteome database confirmed the expression of integrin beta 1 and CD166 on the S cells.

Due to the use of the rodents database, proteins have been identified twice in some cases, usually based on the proteins listed for *Mus musculus* and *Rattus norvegicus*. For CCL61 one membrane proteins was identified twice and for S cells 52 membrane proteins were identified twice; nevertheless, the use of the rodent data base yielded a better protein identification than using only the mouse database, as can be seen from the tables presented. The percentage of identified membrane proteins, which for both sample preparations is around 30% of the total proteins identified, can be seen as an indication that the enrichment for membrane proteins has been equally successful for both cell lines. Unfortunately, the number of total proteins identified differs largely between the suspension and adherent cell line, which is probably due to the lower protein content in the elution fraction of the adherent CCL61 cells. To overcome these problems, changes in the method were tried (no precipitation step, different cell lysis for adherent cells) but the difference between suspension and adherent cell lines with respect to total protein content in elution fraction could not be minimised, as can be seen in figure 5.4 where for the CCL61 cells small proteins are not visible, indicating that the amount is below the detection limit of the Coomassie staining.

5.6 Discussion – biochemical and mass spectrometry analysis

A successful enrichment protocol was established based on biotinylation of cell membrane proteins, followed by affinity chromatography enrichment. Biotinylation of cells and subsequent flow cytometric analysis revealed that the four cell lines differ with respect to their cell surface

proteome. This confirmed that the choice of the model cell lines for this study should allow analysis of differences in the cell surface proteome of suspension and adherent CHO cell lines. The variation in biotinylation, as seen by analysing the fluorescent staining intensities, can either be due to a difference in the amount of cell surface proteins, with the suspension CHO cells expressing more cell surface proteins compared to the adherent CHO cell lines, or due to sterical hindrance of biotinylation of cell surface proteins on the adherent cell lines. The latter could either be due to a different protein set being expressed that might be less accessible to biotinylation or due to binding of extracellular matrix proteins to the cell surface proteins. The binding of extracellular matrix proteins may have a shielding effect on the cell surface proteins or itself bind large amounts of biotin which is then not available for cell surface protein biotinylation. The latter had been taken into account in the biotinylation protocol by keeping the biotin concentration constant compared to the set-up for suspension cells while using a higher total amount of biotin, and washing steps before the biotinylation should have ensured depletion of serum proteins. In line with the flow cytometry results the enrichment for the suspension cells also yielded a higher protein content in the enriched protein fraction, independent of the method used for enrichment and cell lysis. The low protein yield after the enrichment for the adherent cells might be the reason for the lower success in protein identification with mass spectrometry analysis for the adherent cell line CCL61.

It was originally planned to use a quantitative mass spectrometry approach based on SILAC labelling (stable isotope labelling by amino acids in cell culture) to analyse the differences between the cell surface protein complement of the four different cell lines; however, the difference in enrichment efficiency yielding less sufficient proteome coverage for the adherent cells made it improbable that a quantitative comparison would be achievable. Also, the high number of sample preparation steps necessary to prepare samples for the mass spectrometry induced the risk of introducing bias into the quantification; this might also be another reason for the lower quality data gained for the CCL61 cell line. Due to these problems the mass spectrometry approach was not followed further. Instead, a more detailed analysis of the groups of proteins on S cells, as identified by mass spectrometry such as cell to cell adhesion proteins and extracellular matrix adhesion proteins, using flow cytometry was proposed to yield insight into the differences between the cell surfaces of suspension and adherent CHO cell lines.

6. Chapter

Cell-to-cell adhesion and related molecules

In this chapter the role cell-to-cell adhesion molecules might play in adaptation of adherent cells to successful suspension growth is briefly analysed. Furthermore, flow cytometry as a method to analyse cell surface protein expression is explained. Antibodies against those cell-to-cell antigens tested on CCL61 and S cells in this study are listed and results of flow cytometry staining of these antibodies that showed staining of CHO cells are given.

6.1 Cell-to-cell adhesion molecules and their role in suspension adaptation

Transition to suspension from adherent growth can be compared to the development of a phenotype similar to the one found in metastatic cancer cells. Metastatic cells loose contact with the original tumour and are capable of moving within the body using the blood and lymph system, which will lead to metastatic cancer development (Yilmaz and Christofoir, 2010). This process has been described to include up- and down-regulation of molecules involved in cell-to-cell interactions, as loss of cell-to-cell contact plays a major role in this process (Yilmaz and Christofoir, 2010). The major group of adhesion molecules in adherent junctions between cells as found in tissue are cadherins, including N-cadherin and E-cadherin (Niessen and Gumbier, 2002). E-cadherin has been shown to be involved in signalling process in anoikis (Geng *et al.*, 2012). These so called classic cadherins are homophilic adhesion molecules that are characterised by five extra-cellular protein domain repeats and linked via their cytoplasmic tail to the cytoskeleton of the cells (Yagi and Takeichi, 2000; Yap *et al.*, 2007). Some cadherins have been identified in this study, using mass spectrometry analysis, to be expressed on the cell surface of suspension adapted CHO cells (see chapter 5.4). Other molecules that show a change in expression level on metastatic tumour cells compared to healthy cells include tetraspanins such as CD81, CD44 and neural cell adhesion molecule (NCAM).

Tetraspanins have been associated with the polarisation of epithelial cells and are thought to

interact with integrins and cadherins to allow up-keep of cell polarisation (Yanez-Mo *et al.*, 2000). CD44 is the receptor for hyaluran, a component of the extra-cellular matrix in tissue, playing a role in cell-to-cell and cell-matrix interaction (Thorne *et al*., 2004); CD44 has also been shown to be relevant to cell morphology (Shi *et al.*, 2001). As well as being expressed on neural cells, NCAM has also been found on a variety of tissues and cells, including a subgroup of lymphocytes, the natural killer cells (Carter *et al.*, 1999) and has been shown to be involved in cell motility (Prag *et al.*, 2002).

6.2 Flow cytometry as a tool: protein expression level on the cell surface

The expression level of proteins on the cell surface can be analysed by antibodies conjugated to fluorochromes. As antibodies recognise specific protein antigens, fluorochrome labelled antibodies allow 'tagging' of proteins. These labels can then be used in flow cytometry, where single cell solutions flow through a flow cell and are exposed to a laser light, which leads to excitation of the fluorochromes bound to the antibodies (Nolan and Yang, 2007). With the help of flow cytometry it is therefore possible to analyse a population of cells with regard to their antigen and protein expression (Ritchie *et al.*, 2000). Depending on the staining conditions used, either cell surface proteins are stained with the antibody or intracellular antigens can be labelled; the latter require a permeabilisation step to allow the antibody to enter the cell (Knowles and McCulloch, 1992). In flow cytometry analysis the percentage of cells which express the antigen in question can be calculated in relation to the total population measured in one sample (Herzenberger *et al.*, 2006). Furthermore it is possible to analyse the 'brightness' of the stained population. In flow cytometry, 'brightness' is given as fluorescence intensity, usually measured on a logarithmic scale (Herzenberger *et al.*, 2006). As fluorochromes are bound to the antigen recognising antibodies, fluorescence intensity is also a measure of the amount of antibody bound to the cell and therefore of the actual expression level of the antigen on the cell surface. This has been used to develop assays measuring absolute units of molecules per cell (Nolan and Yang, 2007) or antibody molecules bound per cell (Arun *et al*., 2010).

Flow cytometric analysis is usually done using specialised software; in this study FlowJo version 7.6.5 (Treestar Inc., Ashland, USA) was used. Figure 6.1 shows a successful staining result. An example of a flow cytometric analysis showing the analysis methods used in this study is given.

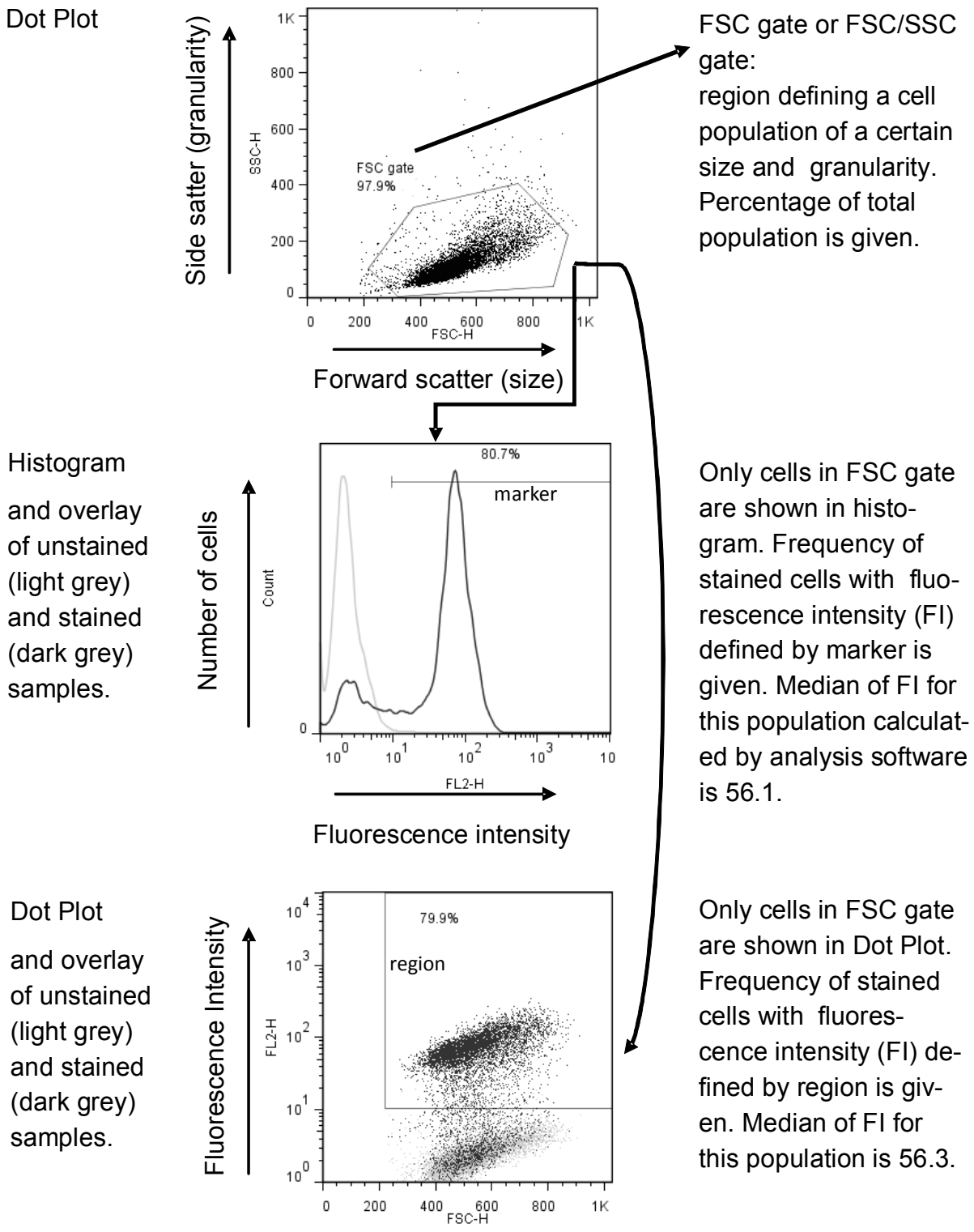

Figure 6.1: Example of flow cytometry analysis and explanation of terms used

A typical result for an antibody staining with a direct fluorochrome conjugate for a surface marker is shown. This sample shows a bi-modal staining distribution as can clearly be seen in the histogram. The most important terms used in the flow cytometry part of this study are explained.

In addition, the major terms used in this study with respect to flow cytometric analysis are explained.

6.3 Antibodies for flow cytometry analysis of CHO cells

Flow cytometry antibody conjugates are usually available for use on human, mouse or rat cells, as the main application for flow cytometry is in the area of immunology. For this study antibodies against human and mouse cells from different suppliers were tested for reaction of the antibody on CHO cells. The use of antibodies based on their cross-reactivity (antibody binding to proteins other than that of the original species) is possible due to the homology known to exist between proteins of different species (Ahram *et al.*, 2005).

The following antibody fluorochrome conjugates recognising cell-to-cell adhesion proteins were tested:

- anti mouse CD81 PE, clone Eat2, BD Biosciences,
- anti mouse CD44 FITC, clone IM7, BD Biosciences,
- anti human E cadherin antibody, polyclonal Goat IgG, R&D systems (Minneapolis, USA),
- anti mouse CD 62l FITC, clone MEL-14-H2.100, Miltenyi Biotec,
- **anti human CD324 APC (E-cadherin), clone 67A4, Miltenyi Biotec,**
- **anti human CD44 FITC, clone DB105, Miltenyi Biotec**
- **anti human CD56 APC (NCAM), clone AF12-7H3, Miltenyi Biotec**

Only the last three antibodies (bold) gave a visible shift in the staining intensities between unstained and stained cells, for both cell lines, S-cells and CCL61.

For CD44 and E-cadherin so-called isotype controls (ITC) were available. Those are antibodies of the same isotype labelled with the same fluorochrome and supplied at the same concentration as the corresponding antibody, however, the isotype antibody will not react with any cell type. Isotype controls can hence be used to identify if the antigen specific antibody has been bound non-specifically, e.g. by binding of the Fc region of the antibody to the cell, as the isotype control would be bound as well and hence give a similar signal with regard to staining intensities. As can be seen in figure 6.2 the CD44 and the E-cadherin (CD324) antibodies recognise a specific antigen on the cell surface of the S cells, as the staining with the specific antibody is brighter than for the isotype control. Unfortunately, for the CD56 clone an isotype control was not available.

CD44

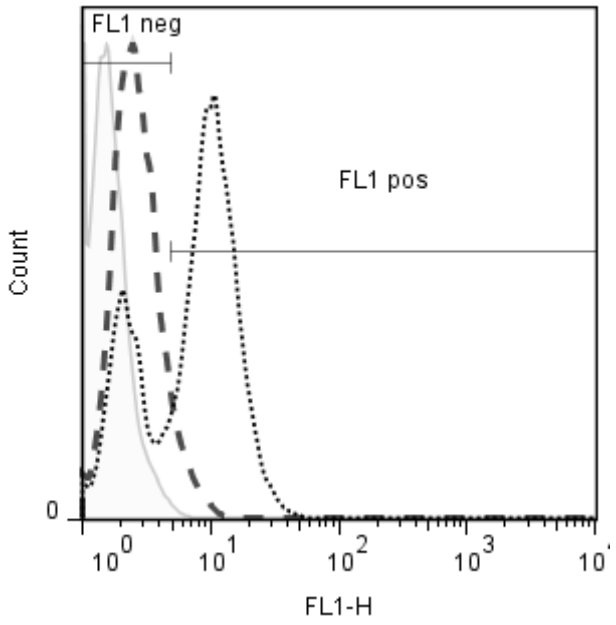

Median fluorescence intensity

	FL1 pos	FL1 neg
ITC	6.05 ± 0.04	2.51 ± 0.13
specific	10.63 ± 1.13	2.18 ± 0.02

E-cadherin

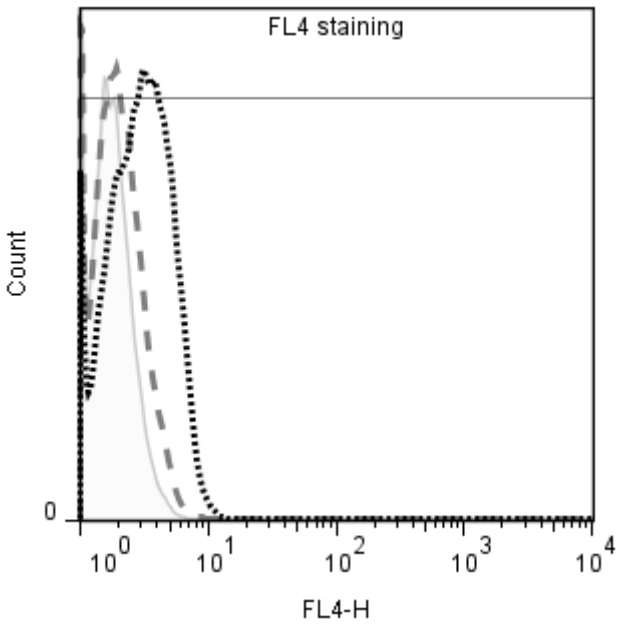

Median fluorescence intensity

	staining
ITC	1.95 ± 0.06
specific	2.95 ± 0.11

Figure 6.2: Isotype control staining for CD44 FITC and E-cadherin APC
Histograms show one set of results from staining fixed S cells. Overlays compare unstained (light grey), isotype control staining (ITC, mid grey, dashed) and antigen specific staining (dark grey, dotted). For CD44 FITC a positive and a negative population can bee seen (bi-modal distribution), whereas for E-cadherin APC only one population exists. Median fluorescence intensities have been calculated using the markers given. Data is based on a forward/side scatter gate (not shown). Standard deviation was calculated from three samples for isotype control and specific antibody.

As the antibody also revealed a positive and a negative population when used for staining S cells it was assumed that the CD56 antibody staining is also specific on the CHO cell lines.

6.4 Comparison of CD44, NCAM and E-cadherin expression on S cells and CCL61

While testing the antibodies for suitability of detection of cell-to-cell adhesion molecules it became obvious that in some cases variation of the results in the staining between different passages of suspension adapted CHO cells were relatively large. Hence, a comparison of the expression level between two passages of CCL61 and S cells was performed with the passage comparison for S cells being repeated due to the large variation seen in the first set of results.

In figure 6.3 the results of the comparison for the CCL61 cell line is shown. CD44 and CD56 show a single stained population in each passage, whereas a bimodal staining distribution with a brighter population with a size of below 50% of the total popluation is seen for E-cadherin. For CD44 the median fluorescence intensities (MFI) are quite stable, whereas a larger variation between the MFI of the two passages is seen for CD56 and E-cadherin. Overall, from these results it is concluded that the expression level of the three adhesion molecules on CCL61 cells only differs slightly between passages.

In figure 6.4 the results of the comparison of passages on S cells is shown. In the first comparison (left column) for the S cells a large variation was seen for the MFI, together with a bimodal distribution where the brighter population showed a significant difference in size between passages for all three adhesion molecules tested. When this experiment was repeated with a different set of passages the variation in the distribution pattern and MFI were even larger for CD56 and CD44. For both adhesion molecules the bimodal distribution was only visible in one of the passages tested. E-cadherin did not show a bimodal distribution in the two passages tested in the repeat experiment and only a small variation with regard to MFI. It was hence concluded that the expression level of CD44, CD56 and E-cadherin varies to a great extent on S cells over the course of culture.

CD56

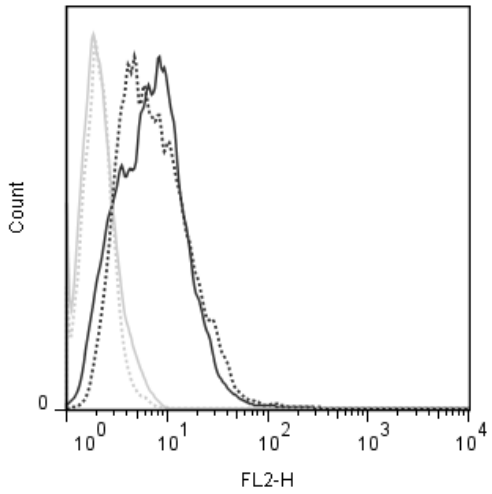

Median fluorescence intensity (MFI)

Solid dark grey line: 7.32 ± 1.16

Dotted dark grey line: 6.31 ± 0.43

E–cadherin

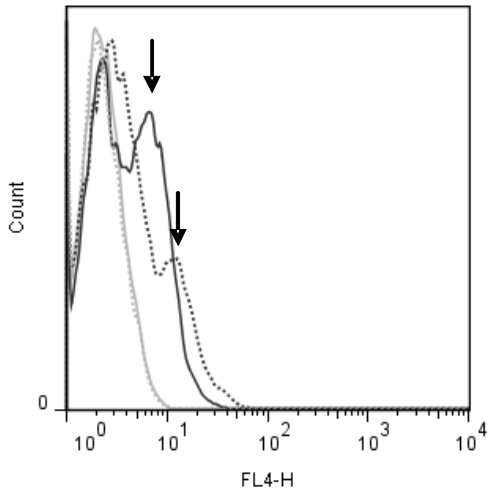

MFI

Solid dark grey line: 4.03 ± 0.47

Dotted dark grey line: 3.65 ± 0.28

CD44

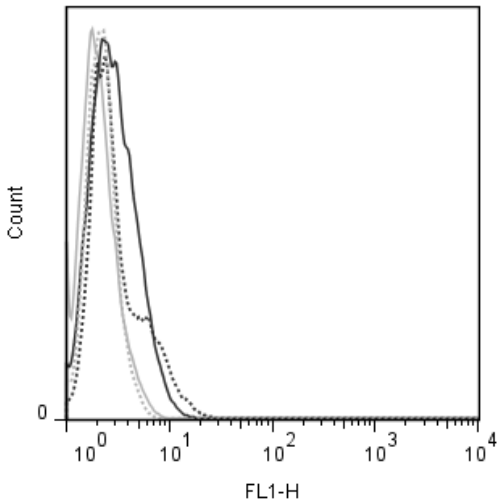

MFI

Solid dark grey line: 2.68 ± 0.06

Dotted dark grey line: 2.69 ± 0.09

Figure 6.3: Variation in expression level of CD44, CD56 and E-cadherin on the cell surface of CCL61

Two different passages were stained on the same day. Light grey lines in histograms show unstained samples, dark grey lines (dotted or solid) stained samples. Histograms show single samples, representative of triplicates (unstained: duplicates) measured. Average of fluorescence intensities of the population (FSC gate not shown) including standard deviation are given for each cell surface marker. Arrows denote bimodal distribution pattern.

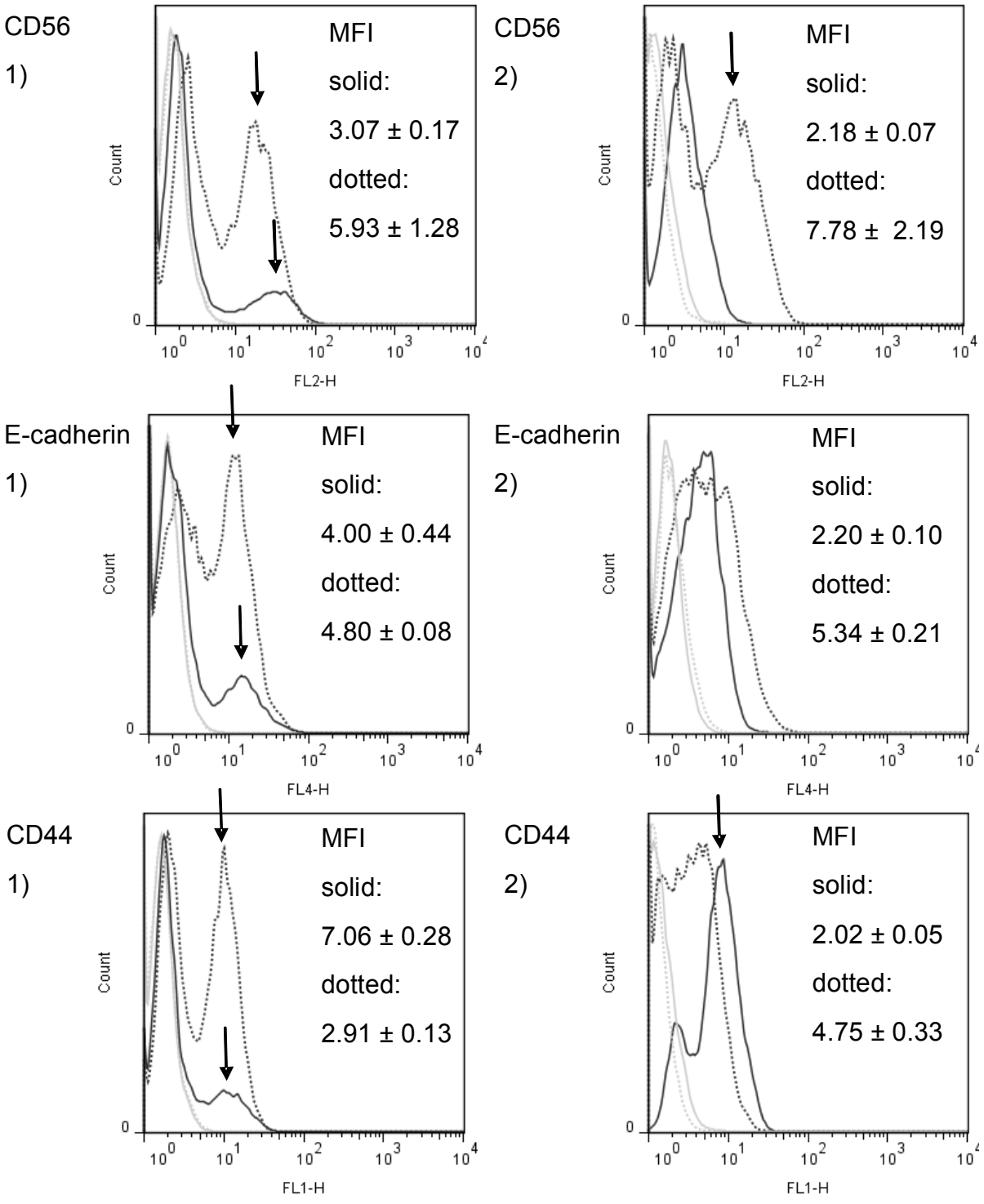

Figure 6.4: Variation in expression level of CD44,E-cadherin and CD56 on the cell surface of S cells

Left and right column denote independently repeated experiments; for each two different passages were stained on the same day. Light grey lines in histogram show unstained samples, dark grey lines stained samples. Histograms show single samples, representative of triplicates (duplicates for unstained) measured. Forward/ Side scatter gate (not shown) was applied. Average of median fluorescence intensities (MFI) for overall populations of stained samples are given. Arrows indicate bimodal staining distribution in sample.

6.5 Discussion: flow cytometric analysis of adhesion molecule expression levels

Ahram *et al*. (2005) have previously shown that CD44 and NCAM are expressed on adherent CHO cells, which is an accordance with the flow cytometric analysis of cell surface protein expression demonstrated here. Also, the expression of cadherins on CHO suspensions cells as suggested by the mass spectrometry results (see chapter 5) has been confirmed for E-cadherin by the flow cytometric analysis.

As can be clearly seen in figure 6.3, there is a large variation in expression levels between different passages of S cells with respect to CD44, CD5 and E-cadherin expression. In contrast to the S cells, CCL61 cells show a bimodal expression pattern only for E-cadherin with a small, brighter stained population in both passages tested, whereas for the S cells for all adhesion molecules analysed bimodal distributions were found in at least two of the four passages tested. The difference in the protein expression can be regarded as a clear indication of a difference in the cell surface composition of the two CHO cell lines tested. The variation in protein expression seen here could not have been analysed using a quantitative mass spectrometry based approach, as the bimodal distribution would have been seen as an overall lower expression of the proteins in question on the cell lines analysed. As the variation in expression is as large as shown between different passages of the S cells, it is not possible to perform a quantitative comparison of the expression levels between the suspension and adherent cell lines based on the fluorescence intensities. The fluctuation in expression on the S cells seen for the adhesion molecules tested is an indication that those proteins are not necessary for growth in suspension, as the variation in expression shows that the proteins are not conserved on the cell surface. This idea is strengthened by the data gained for S cell growth characteristics showing no difference in reachable viable cell density when comparing different passages (see figure 4.4), as the expression differs between passages while the growth characteristics remain stable over culture. It should be noted that the changes in expression seen for CD44 might be due to expression of different isoforms of this molecule (Liu and Jiang, 2006) as the antibody clone used might not recognise all possible isoforms.

In conclusion, it can be said that CD44, NCAM and E-cadherin expression are neither necessary for growth in suspension nor counterproductive. As they are not a necessary part on the cell surface of suspension adapted CHO cells, these adhesion molecules play no major part in the suspension

phenotype. It cannot be concluded whether these molecules play a role during the actual process of suspension adaptation as only the end points of the adaptation process have been analysed based on the two cell lines.

7. Chapter

Integrins: cell to extra-cellular matrix interaction

In this chapter the structure, role and characteristics of integrins as cell surface molecules are described. The methodology used to analyse integrin expression level and conformation are explained. Results on the expression level, differences in outside-in signalling and integrin conformation for the model CHO cell lines are given and their relevance for the CHO suspension phenotype is demonstrated.

7.1 Integrin structure and ligands

Integrins form a group of cell surface proteins that mainly interact with the extra-cellular matrix in tissue and serum components in cell culture. Integrins are heterodimers, consisting of an alpha and beta unit. The two units are non-covalently bound. Both units are transmembrane proteins (Etzioni, 1999) with a single hydrophobic transmembrane domain (Hynes, 1992), a large ectodomain and a short cytoplasmic tail (Regent *et al.*, 2010). The alpha unit size varies between 120 -180 kDa and the beta unit size between 90-110 kDa (Hynes, 1992). There are 8 known beta chains and around 20 alpha units have been identified so far (Regent *et al.*, 2010). The subunits can be expressed in a variety of combinations; each of the known beta subunits can dimerize with different alpha units and some of the alpha subunits can also associate with different beta subunits (Ruoslathi, 1991). As the binding region is formed by the alpha and beta chain (Hynes, 1992) the different subunit combinations bind to different ligands, making the integrins a varied and complex family of cell surface receptor proteins, which allows them to play a role in cell adhesion, proliferation and differentiation (Streuli, 2009). So far, the largest known group of integrins comprises those containing the beta 1 subunit and most mammalian cells express one or more beta 1 integrins constitutively (Hynes, 1992). Table 7.1 below shows the possible alpha subunits interacting with the beta 1 subunit and lists which ligands are recognised by the resulting integrin.

Table 7.1 Integrin alpha units interacting with the integrin beta 1 chain and the resulting ligands.

(after Hynes (1992); Stupack and Cheresh (2002); reactome.org (2012))

* VCAM-1: vascular cell adhesion protein 1, expressed on activated endothelial cells

** requires magnesium ions

Integrin alpha unit	Integrin beta unit	Ligand
alpha 1	beta 1	fibrillar collagen domain, laminins **
alpha 2	beta 1	collagens, laminins **
alpha 3	beta 1	collagens, laminins (different epitops to Alpha 2)
alpha 4	beta 1	fibronectin, VCAM-1*
alpha 5	beta 1	fibronectin, fibrin
alpha 6	beta 1	laminins (laminin-5, laminin-1)
alpha 7	beta 1	laminins (laminin-2, laminin-1)
alpha 8	beta 1	fibronectin
alpha 9	beta 1	VCAM-1*
alpha 10	beta 1	collagen **
alpha 11	beta 1	collagen **
alpha V	beta 1	vitronectin, fibronectin

Newer studies indicate that most integrins containing the integrin beta 1 subunit, e.g. integrin alpha 5 beta 1, integrin alpha 4 beta 1 and integrin alpha V beta 1, bind to the RGD tri-peptide motif that is found in most extra-cellular matrix components such as fibronectin (Wiesner *et al.*, 2005; Regent *et al.*, 2010; Stupack and Cheresh, 2002).

7.2 Integrin function, expression level and conformation

In contrast to the reversible growth arrest seen in fibroblasts when transferred into suspension, Francis and Frisch (1994) demonstrated that epithelial cells in suspension undergo anoikis and hence proved that the extra-cellular matrix is a survival factor for epithelial cells. Meredith *et al.* (1993) showed that for epithelial cells attachment to integrin alpha antibodies offered protection from anoikis, indicating that integrin outside-in signalling (Legate *et al*., 2009) is necessary for cell survival. Extensive research by Ruoslathi (Giancotti and Ruoslathi, 1990; Zhang *et al*., 1995; Lee

and Ruoslathi, 2005) links integrin alpha 5 beta 1 in different epithelial cells to apoptosis regulation via the protein Bcl-2. In the study by Giancotti and Rouslathi (1990) the integrin alpha 5 beta 1 expression level was also linked to the capacity of the cells to adhere. Furthermore, increased integrin alpha 5 beta 1 expression correlated inversely with the maximal achievable cell density of the adherent cell line. As the above studies clearly link integrin expression level to adhesion capability and survival in suspension, the integrin expression level of three integrins (integrin beta 1, integrin alpha 1 and integrin alpha 4) was analysed for the four model cell lines using flow cytometry.

The different roles of integrins have been described in more detail by Stupack and Cheresh (2002) which describe integrins as important biosensors regulating the survival/ death response of cells as a function of the surrounding extra-cellular matrix. The complexity of this regulation is demonstrated by the fact that integrin alpha 5 beta 1 and integrin alpha V beta 3 outside-in signalling can provide resistance to serum withdrawal whereas integrin alpha V beta 1 cannot (Stupack and Cheresh, 2002). More recently, the integrin beta 1 cytoplasmic domain has been associated with the regulation of cell adhesion on fibronectin (Green *et al.*, 2009). This study indicated that for constitutively expressed integrins different regulating mechanisms, such as modulation of interactions on the cytoplasmic tail, might play a role besides ligand binding and outside-in signalling. A similar idea is the concept of a bidirectional signalling process via integrins proposed by Regent *et al*. (2010).

Askari *et al.* (2009) suggest that this idea has to be extended as integrins have different conformational states of which they describe three in more detail: inactive (showing low affinity to ligand), primed (showing high affinity to ligand) and active (bound to ligand). Priming is described by them as either an inside-out signalling process, with the activation being controlled by interaction between integrin beta 1 cytoplasmic domain and talin, or outside-in activation due to ligand binding; furthermore, they stress that integrin activity can be modulated by other factors such as divalent cations, mechanical force and monoclonal antibodies and that these different ways of activation might lead to different integrin conformations. They explicitly mention that it might be possible to distinguish between integrins signalling inside-out and outside-in by conformation. This idea has been developed further by Regent *et al.* (2010) which describe three conformations: bent closed conformation, intermediate extended with closed head piece (referring to the ligand binding site between alpha and beta sub-units) and extended open conformation. They linked these three different conformations to different activation and signalling stages: low-affinity, activated and

ligand occupied, respectively. They also describe integrin activation as insufficient to control cell adhesion processes. Studies of negative regulators of beta 1 integrins have strengthened the possibility that conformational changes triggered by proteins interacting with the cytoplasmic beta 1 domain are the starting point of integrin activation but that the full activation is a multi-step process requiring not only conformational changes but also clustering of integrins on the cell surface (Regent *et al.*, 2010).

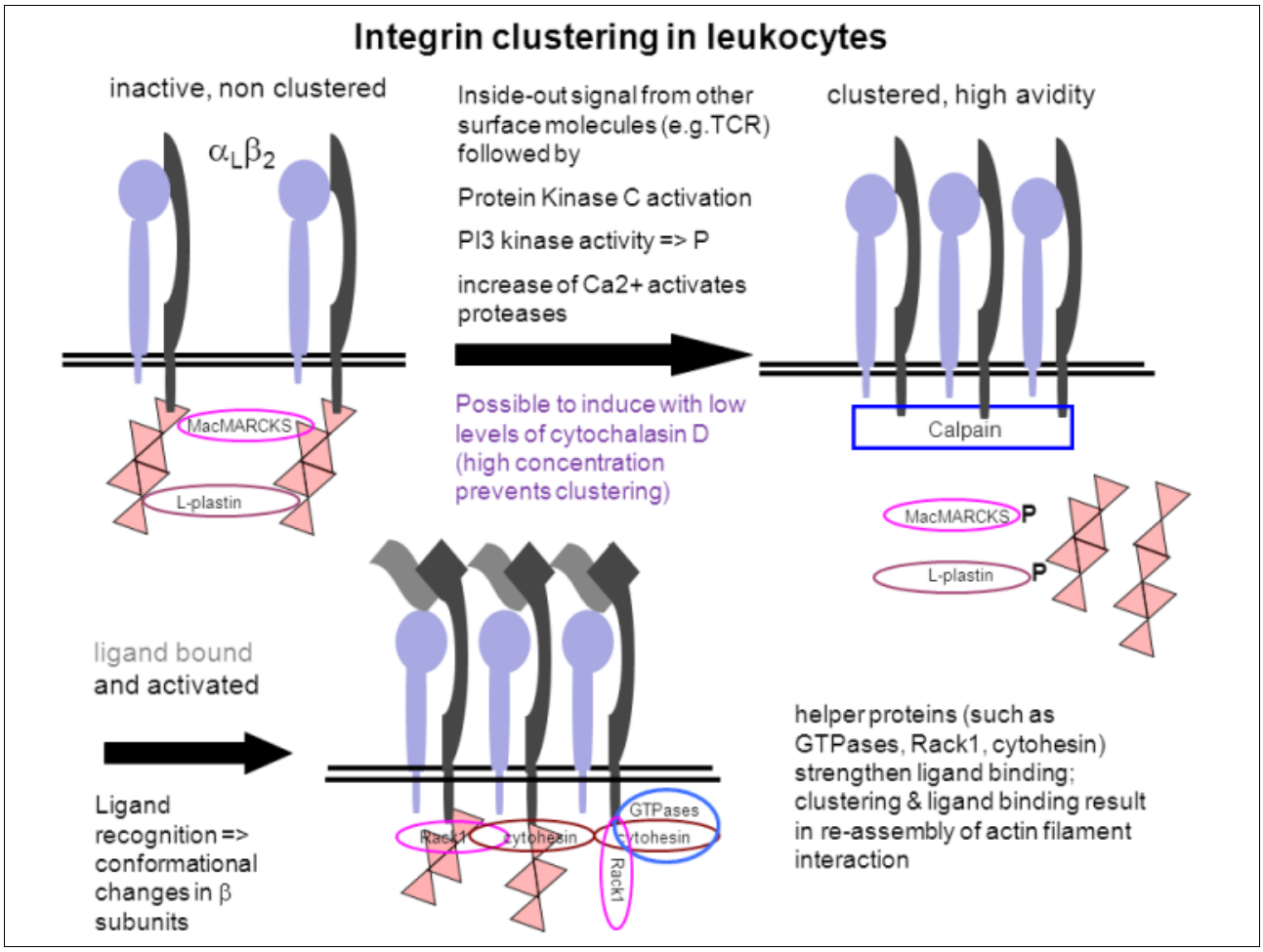

Figure 7.1 Model of integrin clustering in leukocytes.

How integrin clustering occurs in leukocytes and leads to activation of integrin alpha L beta 2: Extracellular signals from cell surface receptors, such as T-cell receptors (TCR), lead to Protein Kinase C activation and increased PI-3 activity resulting in dissociation of actin cytos-keleton from the integrin beta 2 cytoplasmic tail. Ligand binding induces conformational changes of the integrin beta subunit which allows binding of helper proteins such as GTPases on the intracellular side, inducing clustering of the integrins. Clustering and ligand binding result in re-assembly of integrin beta 1 and actin interaction (van Kooyk and Figdor (2000); Green *et al.* (1998)).

The idea of activation through inside-out signalling events has been proposed earlier by van Kooyk and Figdor (2000) for integrins involved in leukocyte adhesion. They proposed clustering as a major step in integrin activation and described release of cytoskeletal restrain as a necessary step for clustering. Their model stresses the importance of the intracellular interaction partners of the integrin. More details with respect to the process of clustering can be found in Figure 7.1.

The idea of clustering of integrin on lymphoctes was used in a study by Lub *et al.* (1997). They used confocal microscopy to study clustering of integrin alpha L beta 2 on a variety of cell lines and lymphocytes. Their results indicated a correlation between clustering of integrins and adhesion capability and demonstrated that cytochalasin D treatment induced clustering of integrins on the surface of resting lymphocytes. To analyse integrin conformation on the cell surface a confocal study has been conducted for the four model cell lines investigated in this study, analysing integrin beta 1, integrin alpha 1 and integrin alpha 4 conformation on the cell surfaces.

7.3 Anti-integrin antibodies and analysis methodology used

A number of antibodies were tested for use on CHO cells and their details are presented in table 7.2.

Table 7.2 List of antibodies tested for analysis of integrin expression on CHO cells
Bold indicates the antibodies that have been found in this study to actually recognise a cell population in CHO cells.

integrin	antibody	clone	supplier
integrin alpha 2	anti mouse CD49b	DX5	Miltenyi Biotec
integrin alpha 4	anti human CD49d	MZ18-24A9	Miltenyi Biotec
integrin alpha X	anti mouse CD11c	N418	Miltenyi Biotec
integrin alpha 5	anti mouse CD49e	5H10-27 (MFR5)	BD Biosciences
integrin alpha 3	anti human CD49c	C3 II.1	BD Biosciences
integrin alpha 4	**anti mouse CD49d**	**R1-2**	**Miltenyi Biotec**
integrin alpha 1	**anti rat/mouse CD49a**	**Ha31/8**	**BD Biosciences**
integrin beta 1	**anti mouse CD29**	**9EG7**	**BD Biosciences**

Only the last three antibodies gave a visible shift in the staining intensities between unstained and stained cells. For staining with integrin beta 1 and integrin alpha 4 the use of secondary antibodies was necessary as direct fluorochrome conjugates were not available (see also chapters 3.8.1, 3.9.1 and 3.10.1). This made a modification in the analysis of the expression level necessary

as secondary antibodies introduce an increased background signal to the staining. As shown in Figure 7.2 this background signal was subtracted for the analysis from the expression levels and the resulting difference in fluorescence intensity(Δ FI) was used for comparison of expression levels.

For integrin beta 1 an isotype control (ITC) was available. The results of the isotype control staining are shown in Figure 7.3. As can be seen in this figure the integrin beta 1 antibody recognises a specific antigen on the cell surface of the S cells, as staining with the specific antibody is brighter than the staining from the isotype control.

A)

unstained

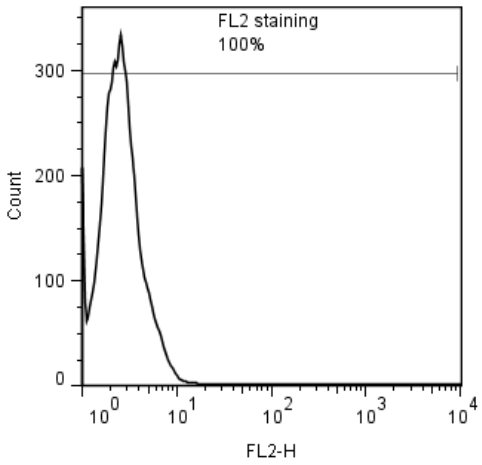

B)

secondary antibody only

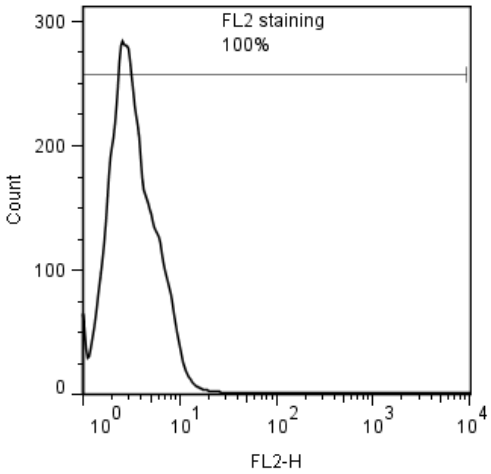

C)

integrin beta 1 staining

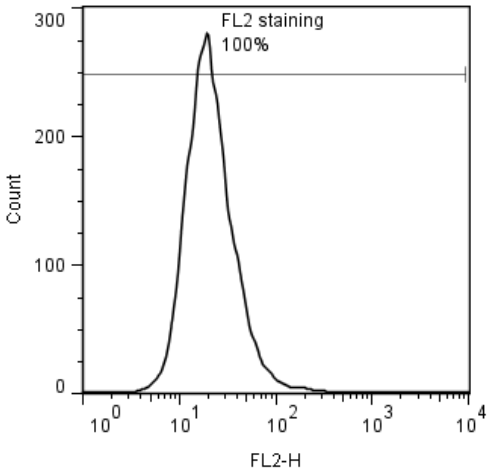

	median FI
A) unstained	2.49
B) sec. ab only	3.04
C) integrin beta 1	19.08
Δ FI [C) - B)]	16.04

Figure 7.2: Example of staining for integrin beta 1 with mouse anti rat IgG2a PE as secondary antibody.

Histograms show one set of results for staining on fixed S cells. Data is based on FSC gate (not shown). A) shows results of unstained S cells, B) shows results of staining with secondary antibody only. There is only a small shift in fluorescence intensity (FI) compared to unstained cells, indicating that no unspecific binding of the secondary antibody to the cells occurs. C) shows results of complete staining for integrin beta 1. The single population is considerably shifted. Δ FI can be calculated based on median fluorescence intensity of B) and C).

A) Unstained cells (light grey) and
cells stained with secondary antibody only (black).

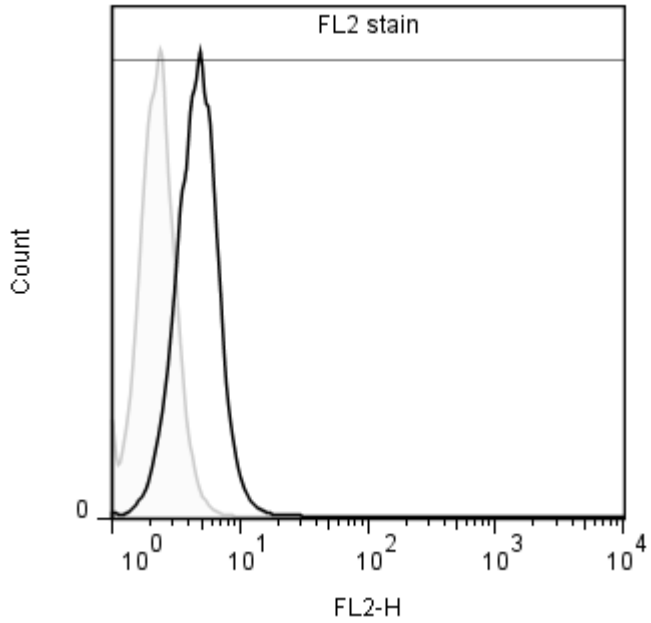

median fluorescence intensity

	FL2 stain
unstained	2.22 ± 0.06
sec. ab only	4.31 ± 0.29

B) Cells stained with ITC plus secondary antibody (dashed)
and CD29 antibody plus secondary antibody (dotted).

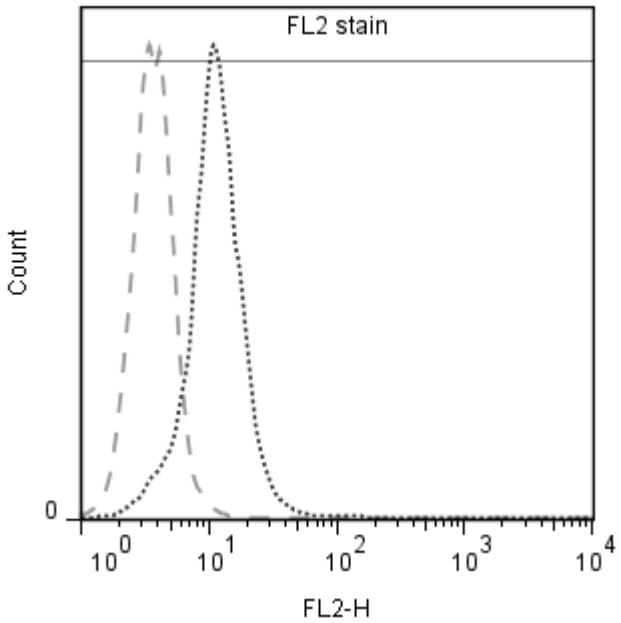

median fluorescence intensity

	FL2 stain
ITC	3.97 ± 0.72
CD29	11.33 ± 0.32

Figure 7.3: Isotype control staining for integrin beta 1 with mouse anti rat IgG2a PE as secondary antibody.

Histograms show one set of results for staining on fixed S cells. Upper overlay A) compares unstained vs. secondary antibody only (SO). Lower overlay B) compares isotype control (ITC) vs. staining with CD29 antibody. Standard deviations were calculated from three different samples for each set up. Data is based on FSC gate (not shown). Median fluorescence intensity of ITC and SO are comparable.

7.4 Stability of expression level of integrin beta 1, integrin alpha 1 and integrin alpha 4 over different passages of S cells and CCL61

As a large variation in the expression level was seen between passages in the analysis of the cell-to-cell adhesion molecules, demonstrating an unstable heterogeneous bimodal distribution, the stability of the expression of the three integrins was analysed for S cells and CCL61. Figure 7.4 shows the result of staining different passages of S cells and CCL61 with integrin alpha 4, which is a direct conjugate. The variation in expression as previously seen for cell-to-cell adhesion molecules with regard to the bimodal distribution pattern on S cells is not seen for integrin alpha 4. In all passages tested a single stained peak can be identified. This peak differs in shape between the passages of S cells, leading to a larger difference in median fluorescence intensity between the passages whereas peak form and median fluorescence intensities are very similar for the two passages of CCL61. This indicates a larger heterogeneity between cells in one passage in the suspension adapted S cells compared to cells in one passage of CCL61.

In figure 7.5 the results with respect to stability of expression between different passages for integrin alpha 1 are shown. As the staining with the recommended secondary antibody did not show a sufficient shift in staining intensities, the primary antibody had to be biotinylated and stained with Streptavidin FITC to reach measurable fluorescence intensity. The biotinylation introduced an additional variation into the set-up of the experiment because the biotinylation reaction had to be done for each staining experiment separately, as the biotinylated primary antibody was unstable when stored. The appearance of a small side peak in staining results for both cell lines is assumed to be due to a less efficient biotinylation of the primary antibody, as a slightly prolonged biotinylation reaction did not show this. The large variation seen in Δ FI for integrin alpha 1 when comparing passages is presumably due to the biotinylation step.

In figure 7.6 the results of the passage comparison for integrin beta 1 are shown. Only a single stained peak is seen in both cell lines for both passages with less variation in peak size compared to integrin alpha 4. No variation in expression, such as a bimodal distribution pattern as previously found before on S cells when analysing cell-to-cell adhesion molecules, is seen. The variation in Δ FI between passages is smaller for the CCL61, as seen for integrin alpha 4.

Overall the above results show that integrin beta 1, integrin alpha 1 and integrin alpha 4 are constitutively expressed on the whole population of both cell lines, CCL61 and S cells. This allows detailed analysis of the expression level. In combination with a comparison of the three suspension

CCL61

integrin alpha 4

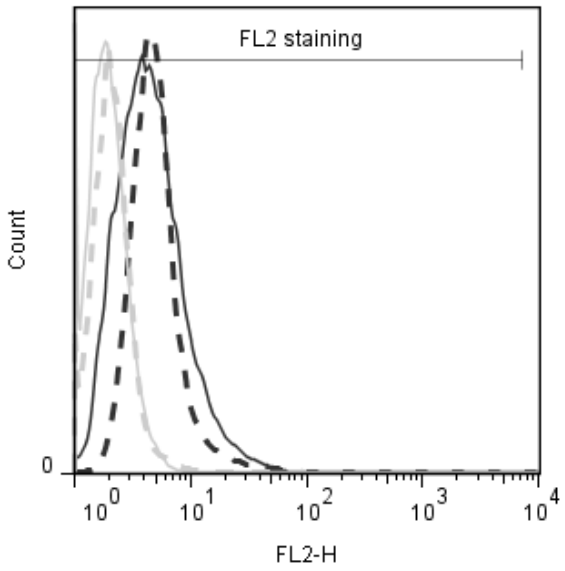

median fluorescence intensity (MFI)

solid dark grey line: 4.01 ± 0.2

dashed dark grey line: 5.12 ± 0.59

S cells

integrin alpha 4

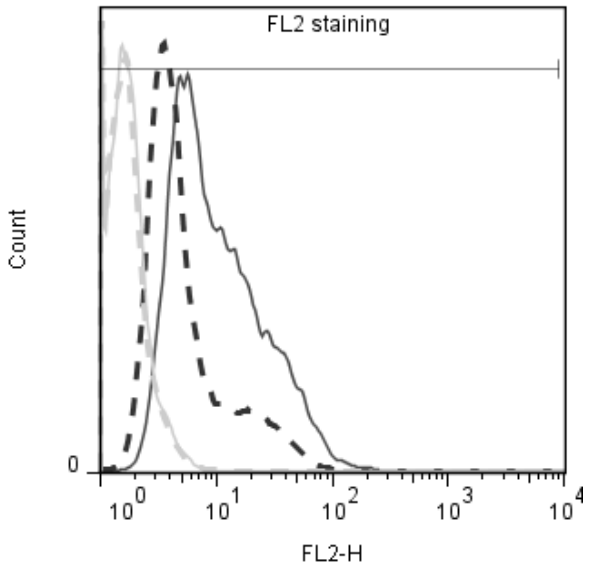

median fluorescence intensity (MFI)

solid dark grey line: 7.88 ± 0.76

dashed dark grey line: 3.94 ± 0.54

Figure 7.4: Comparison of fluorescence intensities for integrin alpha 4 for two different passages of CCL61 and S cells.

Histograms show staining results for integrin alpha 4 on two different passages. Light grey lines in histograms show unstained samples, dark grey lines (dotted or solid) stained samples. Histograms show single samples, representative of triplicates (unstained: duplicates) analysed. Average of fluorescence intensities of the population (FSC gate not shown) including standard deviations are given. For both cell lines only single peaks, no bimodal distributions, are seen.

CCL61

integrin alpha 1

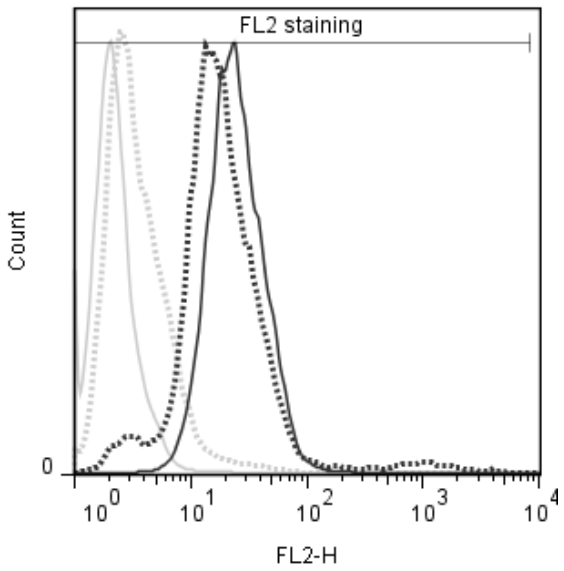

Δ FI

solid lines: 21.52

dotted lines: 14.14

S cells

integrin alpha 1

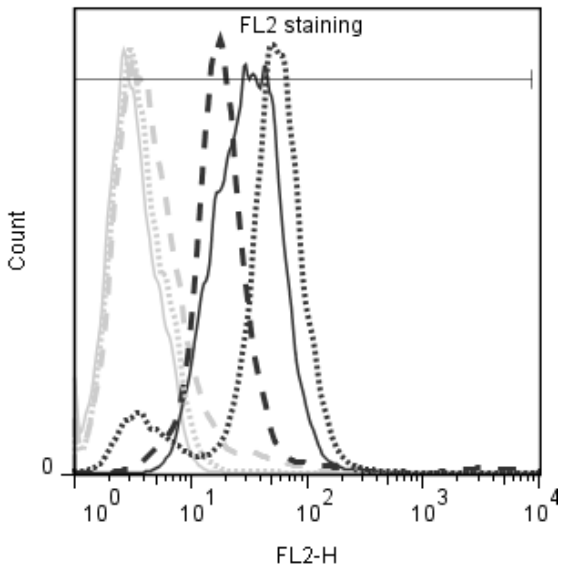

Δ FI

solid lines: 28.01

dotted lines: 47.16

dashed lines: 13.87

Figure 7.5: Comparison of fluorescence intensities for integrin alpha 1 between different passages of CCL61 and S cells.
Histograms show staining results for integrin alpha 1 on two (CCL61) or three (S cells) different passages. Secondary antibody staining (light grey) and specific staining (dark grey) are given and were used to calculate Δ FI based on median fluorescence intensities. For integrin alpha 1 the specific antibody needed to be biotinylated first; this could explain the small and less stained population seen in some passage (dotted lines) and the larger variance of the Δ FI between the different passages.

CCL61

integrin beta 1

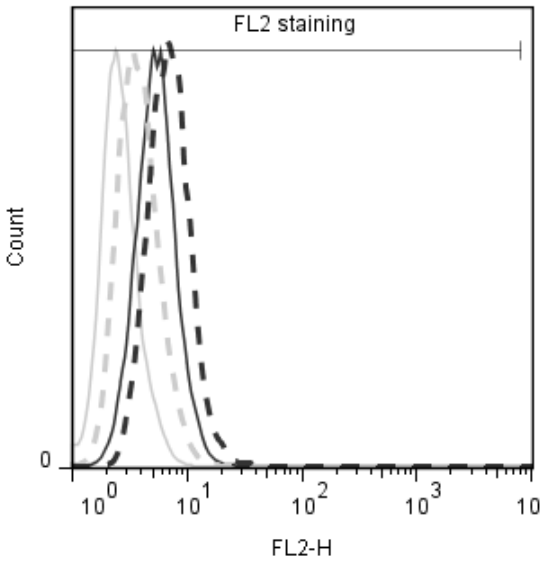

Δ FI

solid lines: 2.33 ± 1.14

dashed lines: 2.73 ± 0.48

S cells

integrin beta 1

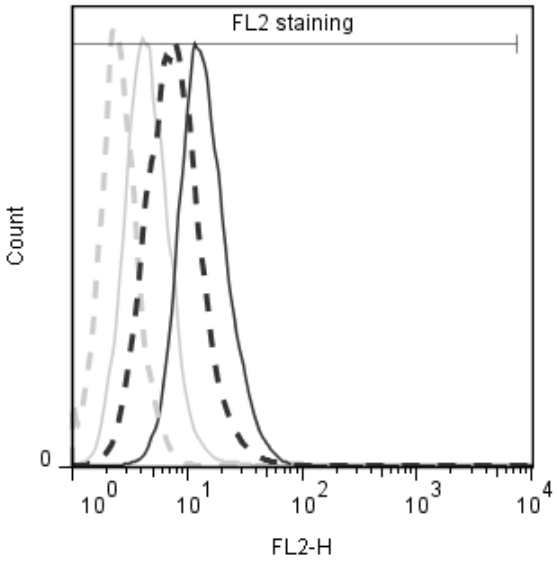

Δ FI

solid lines: 7.44 ±1.6

dashed lines: 4.48 ± 0.45

Figure 7.6: Comparison of fluorescence intensities for integrin beta 1 between different passages of CCL61 and S cells.

Histogram overlays show staining results for integrin beta 1 on two different passages. Top histograms show results for CCL61; lower histograms show result for S cells. Secondary antibody staining (light grey) and specific staining (dark grey) are given and were used to calculate Δ FI based on median fluorescence intensities. Histograms show single samples, representative of triplicates analysed. Average of Δ FI of the populations (FSC gate not shown) including standard deviation are given. For both cell lines only single peaks, not bimodal distributions, are seen.

adapted S cells, CHO-S and AML against the non-suspension adapted CCL61 it should be possible to test the hypothesis that integrins become down-regulated during suspension adaptation of CHO cells.

7.5 Comparison of expression level of integrin beta 1, integrin alpha 1 and integrin alpha 4 on the model cell lines

After establishing that integrin beta 1, integrin alpha 1 and integrin alpha 4 are constitutively expressed on adherent and suspension CHO cells the next aim has been to compare expression levels of the three integrins on the four model cell lines. This analysis should test if integrin expression levels can be used to describe a suspension phenotype in CHO cells by verifying the hypothesis that integrin expression is down-regulated on suspension CHO cells in comparison to non-suspension adapted CHO cell lines.

7.5.1 Methodology: experimental set-up and analysis

As the integrin expression level showed some degree of variation between passages of the same cell line (see chapter 7.4) all four cell lines were stained on the same day using randomly chosen passages for the cell lines analysed. The experiment was repeated on different days: three times for integrin beta 1 and integrin alpha 4 and two times for integrin alpha 1, to minimise the influence of differences between passages on the results. For each experiment triplicates of the passages chosen were prepared. Expression levels were calculated as before using ΔFI, using the unstained samples as background control in the case of integrin alpha 4. The results of the experiment were normalised based on the ΔFI values of CCL61. Normalisation was used independently for each day to allow comparison of independent runs of this experiment on different days, as fluorescence intensities are also influenced by the day-to-day variation of the flow cytometer set-up.

7.5.2 Results: comparison of integrin expression levels

Apart from the variation between passages shown by the individual columns for each cell line in figure 7.7 there is a trend with regard to the expression level when comparing S cell and CCL61. In contrast to the hypothesis that integrins may be down-regulated on suspension adapted CHO cells, S cells show a comparable or even higher expression (up to a factor of 2) of integrin beta 1 and integrin alpha 4 in relation to adherent CCL61. Only for integrin alpha 1 is a weak down-regulation of expression seen when comparing S cells to CCL61. Hence, the hypothesis that integrin in

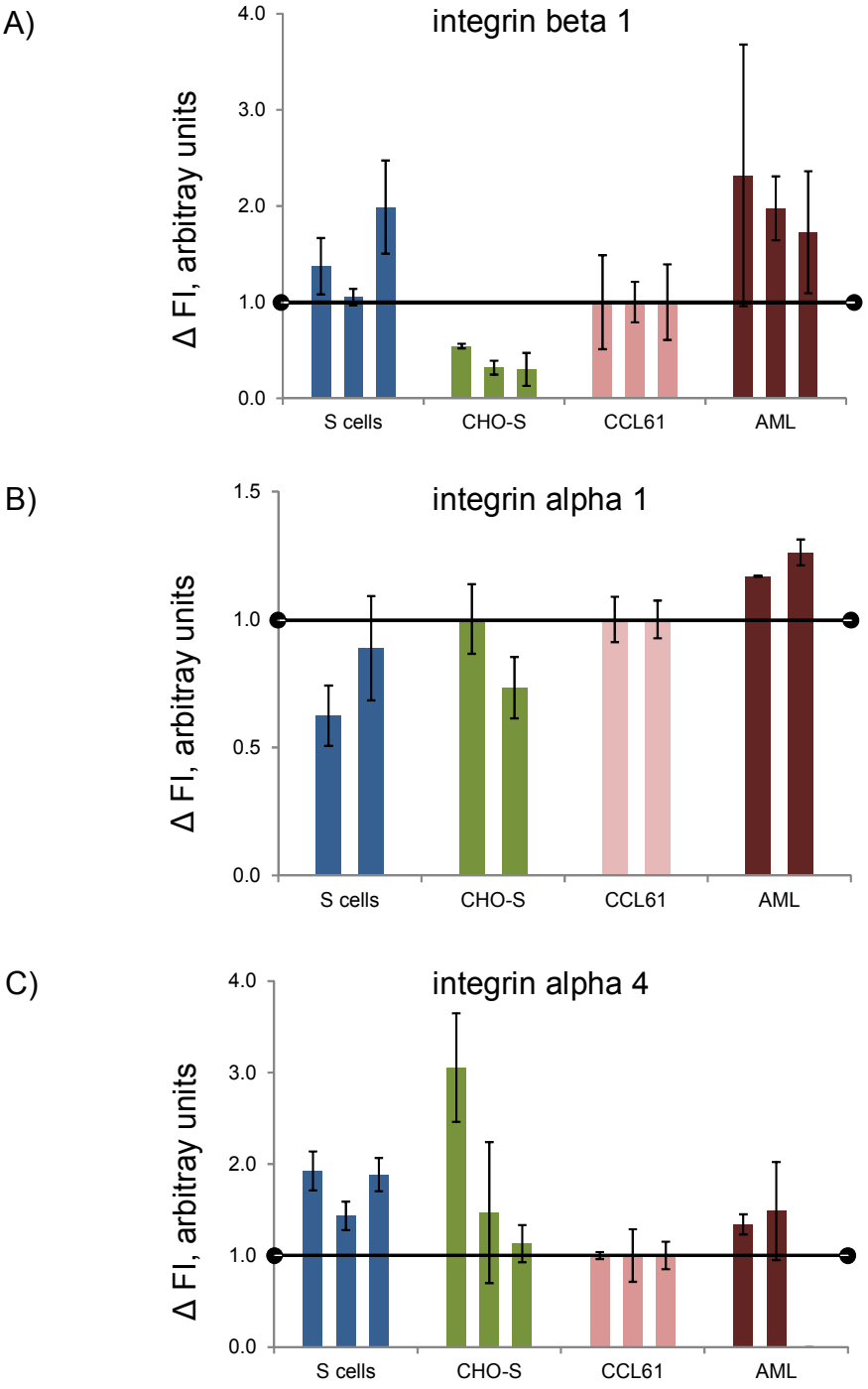

Figure 7.7: Differences in expression level for integrin alpha 1, integrin alpha 4 and integrin beta 1 between the four model cell lines.

Staining was done as described before. Stained samples were prepared as triplicates. ΔFI was calculated as described before. For each experiment, the average of ΔFI of CCL61 was used for normalisation to allow better comparison between results from different days.

No down-regulation of expression level is seen on both suspension cell lines for integrin alpha 4 compared to CCL61. S cells show also no down-regulation of expression level for integrin beta 1 compared to CCL61.

AML show higher expression level for all three surface proteins compared to CCL61.

suspension-adapted CHO cells are generally down-regulated is invalid. For the other suspension adapted CHO cell line, CHO-S, there is a clear down-regulation of integrin beta 1 compared to CCL61, only a small degree of down-regulation for integrin alpha 1 and comparable or higher expression for integrin alpha 4. Again, this indicates that there is no general down-regulation of integrin expression on suspension adapted CHO cells. Interestingly, the AML cells as an adherently growing cell line cloned from a suspension CHO cell line (S cells) show up-regulation of expression for all three integrins tested. The heterogeneity of the cells within one passage, which is partially represented by the standard deviation calculated from the triplicates prepared, can be assumed to be the underlying reason for the variation observed between the passages. As the variance seen is different from experiment to experiment and varies also between the cell lines in one experiment a statistical analysis of the results gained for integrin expression levels, using for example an ANOVA analysis, is not possible. These results indicate that integrins are not generally down-regulated on CHO cells growing in suspension; hence a further analysis of expression level for integrin beta 1 and integrin alpha 4 was done using AML cells grown in suspension.

As can be seen in figure 7.8 the AML cells after growth in suspension over a period of four days developed yet another phenotype with regard to expression level of integrin beta 1 and integrin alpha 4. They revealed a slight up-regulation for integrin beta 1 but a clear down-regulation for integrin alpha 4 when compared to CCL61. The down-regulation of integrin alpha 4 is in contrast to what was seen before when comparing corresponding expression levels of S cells and CCL61, even though AML cells were cloned from S cells and grown in the same suspension medium (PSM) in this experiment.

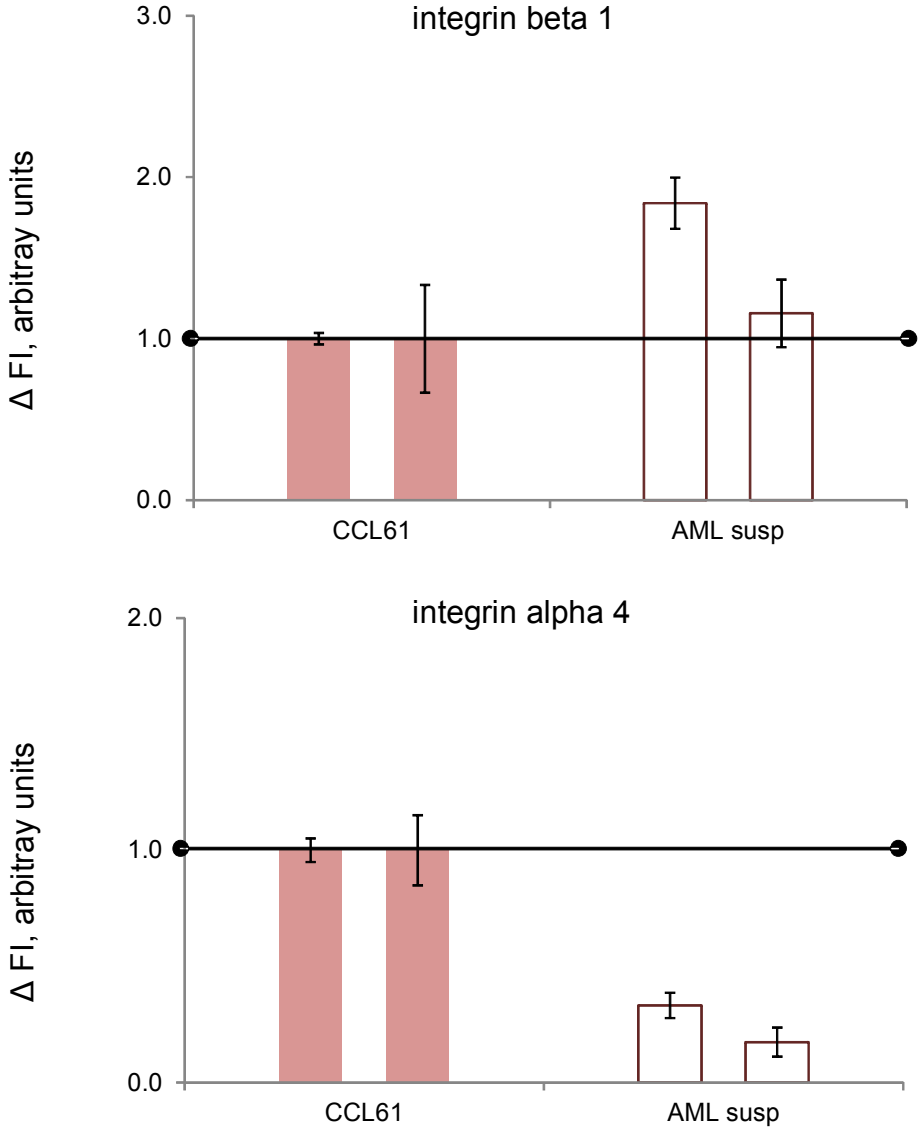

Figure 7.8: Expression level of integrin alpha 4 and integrin beta 1 on AML cells grown in suspension in comparison to CCL61.

AML cells were grown for four days in suspension using PSM. Two different set-ups of the cell lines were stained on different days. Stained samples were prepared as triplicates. Δ FI was calculated as described before. For each experiment the average Δ FI of CCL61 was again used for normalisation to allow better comparison between results from different days. Integrin beta 1 is higher expressed on AML cells grown in suspension compared to adherent CCL61; integrin alpha 4 is much lower expressed on AML cells grown in suspension compared to adherent CCL61.

7.6 Discussion: comparison of integrin expression levels

It has been clearly demonstrated that suspension adapted CHO cells express integrin beta 1, integrin alpha 4 and integrin alpha 1 on the cell surface although no extra-cellular matrix proteins have been added to the culture. The expression levels of these three integrins show no clear trend with respect to up- or down-regulation on suspension cells in comparison with adherent cells, as hypothesised: the three CHO cells lines capable of growing successfully in suspension (S cells, CHO-S and AML) all show a different phenotype with respect to the expression level of the three integrins in suspension culture. This might be due to the previously described phenotype differences (see chapter 4 and table 4.3) and the adaptation to a different media in the case of CHO-S cells. The result regarding the integrin expression levels is a clear indication that these cannot be used as criteria to describe a suspension CHO phenotype.

There are also variations of the expression levels between different passages of the same cell line and differences in the variance seen in the analysis of single passages. This indicates that a certain degree of heterogeneity exists within each cell line with respect to integrin expression level, as previously seen for the cell-to-cell adhesion molecule variation, but those showed a larger heterogeneity than the integrins. The phenomenon of heterogeneity in CHO cells has been shown to exist for various characteristics in CHO cells (Dahodwala *et al.*, 2012; Davies *et al.*, 2013).

As integrins are still expressed on CHO suspension cells, a further question is whether these surface proteins remain functionally active. As demonstrated in figure 4.5, all suspension adapted CHO cell lines used in this study are able to grow adherently, indicating that the expressed integrins could be functionally active. Adherent growth has been demonstrated to be related to integrin expression levels (Giancotti and Rouslathi, 1990), a result that is strengthened by the result of this study where CHO-S cells, with the lowest expression level of integrin beta 1, were the slowest to develop the adherent phenotype in comparison to the other suspension adapted CHO cell lines (see figure 4.5). To further study the functionality of the integrins found to be expressed on the surface of suspension adapted CHO cells it was analysed whether the integrin beta 1 antibody can block adherence of the cell lines as was previously demonstrated in other studies by Lenter *et al.* (1993) and Barkan *et al*. (2008) (see chapter 7.7).

As mentioned before, another approach to analyse the integrins found to be expressed on the cell surface of suspension adapted CHO cells is the analysis of the integrin conformation using confocal microscopy, as clustering of integrins has been shown to play a major role in adhesion formation

(Altrock *et al.*, 2012) and has been proposed to be indicative of activated integrins on the cell surface of suspension cells (Askari *et al.,* 2009; van Kooyk and Figdor, 2000) (see chapter 7.8).

7.7 Development of adherent phenotype – blocking with integrin beta 1 antibody (clone 9EG7)

To investigate if the integrin beta 1 found to be expressed on the suspension adapted CHO cell lines, S cells, AML cells and CHO-S, is functionally active it was tested if adherence development could be blocked with the integrin beta 1 antibody clone 9EG7.

7.7.1 Epitope characterisation of clone 9EG7 and previous use in adherence blocking

Lenter *et al.* (1993) used the integrin beta 1 clone 9EG7 to block adhesion of lymphocytes to endothelial cells and concluded that the integrin beta 1 epitope recognised by this clone was only accessible after integrin activation. Bazzoni *et al*. (1995) analysed the clone further and concluded that the epitope is inducible by fibronectin or depletion of calcium but is not a marker of integrin activation. Green *et al.* (2009) described the integrin beta 1 epitope recognised by clone 9EG7 as a cation and ligand influenced binding site and showed that binding of the antibody was reduced in cells expressing integrin beta 1 mutants that were assumed to have different conformations of the integrin beta 1 and did not show fibrillar adhesion and reduced spreading in adherent growth. Barkan *et al.* (2008) used the integrin beta 1 clone 9EG7 to neutralise integrin beta 1 function on cancer cells in three dimensional cultures. In their study the inhibition of integrin beta 1 led to a change in down-stream signalling. It was hence assumed that integrin beta 1 clone can block integrin dependent adhesion but does not block ligand binding and that a reduced binding capability of integrin beta 1 indicates changes in intracellular signalling of integrin beta 1.

7.7.2 Methodology of blocking experiment

Using the same concentration (150 µg/ml) as used by Barkan *et al.* (2008) all four cell lines were cultured in 6 well plates. For CCL61, CHO-S and S cells, cells were cultured in mF12 plus 10% FBS. AML cells were cultured in PAM plus 10% FBS. All cells were treated with trypsin/EDTA for 10 minutes before harvesting. To one set of each culture 150 µg/ml integrin beta 1 antibody was added and the difference in development of the adherent phenotypes documented.

7.7.3 Influencing adherence with integrin beta 1

As can be seen in figure 7.9, CCL61 and AML, that are cell lines with adherent growth mode as standard, show no difference in the development of the adherence phenotype after 3 hours and 6.5 hours, when cultures with and without integrin beta 1 antibody are compared; despite the cultures using different cell culture media, as described before. The same is true for S cells: there is no difference in the development of adherence after 3 and 6.5 hours. Hence, although these cells are capable of binding the integrin beta 1 clone 9EG7, as demonstrated in the flow cytometric analysis previously, there is no sign of inhibition of adherence, indicating no difference in the intracellular signalling via integrin beta 1 when comparing those three cell lines. In contrast to this, for CHO-S there is a blocking effect of the integrin beta 1 phenotype on the development of adherence growth: CHO-S cells incubated with the integrin beta 1 antibody do not become adherent even after 6.5 hours, despite being in the same media as S cells and AML cells in adherent culture.

This can bee seen as an indication of changes in the intracellular signalling downstream of integrin beta 1 of CHO-S in comparison to CCL61, as the antibody shows reduced binding to integrin beta 1 mutants that result in reduced cell spreading (Green *et al.,* 2009). CHO-S is the cell line showing the lowest expression of integrin beta 1 on the cell surface, as demonstrated before, but the largest effect of integrin beta 1 with regard to blocking adherence. CHO-S cells are hence noticeably different from the other suspension adapted cell lines (S cells and AML), as is also seen in the growth characterisation (see chapter 4).

The aim of this study was to define a CHO suspension surface phenotype in contrast to a CHO adherent surface phenotype; the above result can be seen as an indication that different suspension adapted CHO cells do not only show different integrin expression levels but these different expression levels might also be indicative of other differences, such as intracellular signalling, as previously indicated by Giancotti and Ruoslathi (1990) and Green *et al.* (2009).

Concentrating on the cell surface of suspension CHO cells, in the next step the conformation of the integrins on the cell surface was analysed with confocal microscopy; the aim is to identify if there is a specific distribution of integrins shared by the suspension adapted CHO cell lines (S cells, CHO-S and AML).

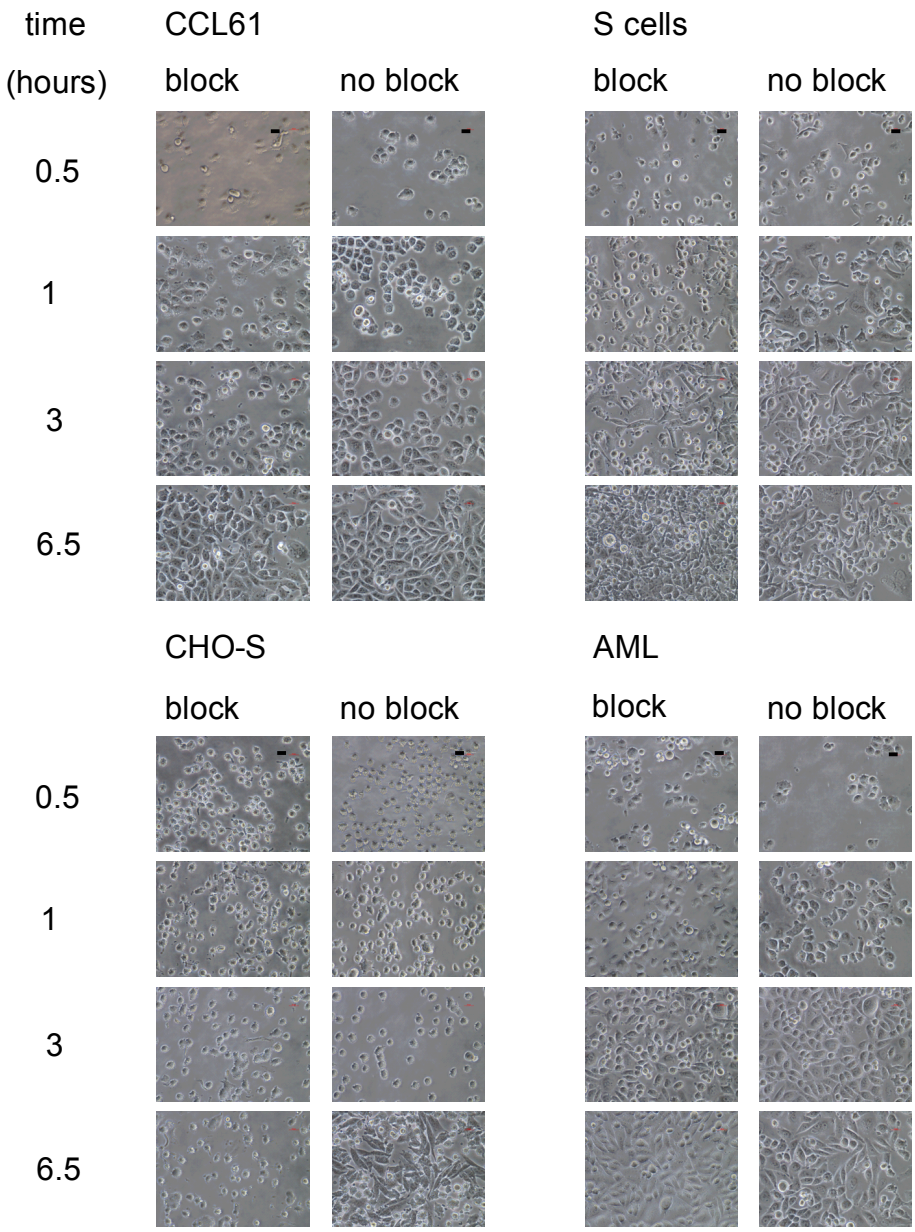

Figure 7.9: Influence of integrin beta 1 clone 9EG7 on development of adherence phenotype in the four model cell lines.

Blocking of development of adherence phenotype was tested by adding 150 µg/ml integrin beta 1 antibody. Cells were cultured in 6 well plates and images were taken with a Nikon Eclipse TS100 microscope with an attached camera and a 40x objective using the NIS Elements F2.30 software at the times indicated. Variation in development of the adherence morphology and the different influence of the integrin beta 1 antibody can be seen. Cells were treated with trypsin for 10 minutes before seeding. Scale bars in top rows equal 20 µm.

7.8 Methodology for confocal analysis of integrin conformation

For the analysis of the integrin conformation by confocal microscopy the staining systems had to be changed as some of the fluorochromes used in flow cytometry could not be used for confocal analysis. The final methodology used is described in chapters 3.8.2, 3.9.2 and 3.10.2. Table 7.3 shows a list of the secondary antibodies used for the three integrins.

Table 7.3 List of secondary antibodies used for confocal microscopy

isotype	fluorochrome	integrin used for
goat anti-mouse IgG2b	Alexa 488	integrin beta 1
anti-Armenian and Syrian hamster IgG	FITC	integrin alpha 1
Streptavidin	FITC	integrin alpha 4

A control experiment was done to ensure low background staining occurred with the secondary antibodies in the confocal set-up. Figure 7.10 confirms that all three secondary antibodies chosen give only a very weak background signal when imaged with the same set-up used for the specific staining, making the chosen antibodies suitable for confocal analysis of the integrin conformation.

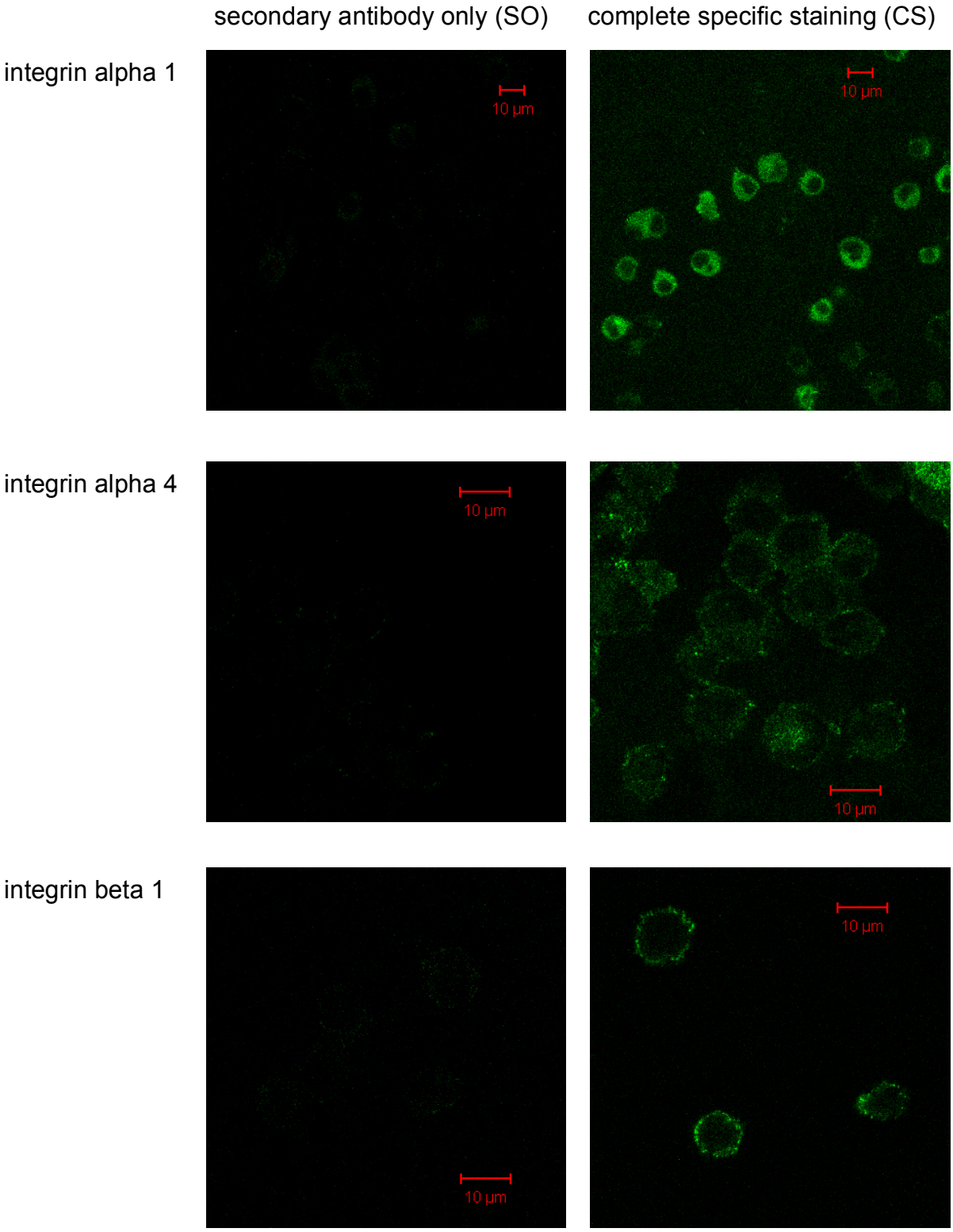

Figure 7.10: Background control staining for integrin alpha 1, integrin alpha 4 and integrin beta 1 demonstrated on S cells.
Set-up for SO and CS was identical. Analysis was done using an inverted Zeiss LSM510 Meta confocal microscope. Mounted cell samples were analysed using a plan apochromat 63x/ 1.4 oil DIC objective. Excitation of fluorochrome was at 488 nm by an argon laser. Emission was collected using a band pass 500-550 IR filter. All scale bars equal 10 µm.

7.9 Analysing the conformation of integrins known to be expressed on the cell surface of CHO cells

Single staining and confocal analysis of integrin beta 1, integrin alpha 1 and integrin alpha 4 was performed twice on all four model cell lines grown in standard conditions. Single slides were prepared using the methodology described before and images taken with the instrumentation set-up described previously. For each image an optimisation process with respect to the laser transmission, detector gain and amplifier offset was performed to optimise signal and to avoid over- and underexposure of image pixels. The pinhole defining the optical slice imaged was set as close as possible to 1 Airy unit as the optimal size, while still reaching maximum signal intensities. Line averaging was set to either 1 or 2 for integrin beta 1 and to 2 or 4 for integrin alpha 1 and integrin alpha 4. Frame size and pixel dwell time were optimised automatically by the software after adjustment of the above parameters.

In figure 7.11 the results for the conformation analysis of integrin beta 1, integrin alpha 4 and integrin alpha 1 on the adherent cell lines CCL61 and AML, growing in mF12 plus 10% FBS and PAM plus 10% FBS respectively, are compared. Representative examples of images have been chosen. The signal intensities for all three integrin stainings were very weak, with integrin alpha 4 and integrin alpha 1 requiring a laser transmission of above 35% and a detector gain around 1,000 to allow imaging with a pinhole below 1.8 Airy units. This also increased the background signals for those two integrins and made it difficult to distinguish the adherent cells from the slide. From the images shown in figure 7.11 one can conclude that the conformation seen for the analysed integrins is very similar for the adherent cells CCL61 and AML. For integrin beta 1 in particular the distribution of the integrin is clearly regular over the entire cell surface, showing the stretched-out morphology of adherent cells for both cell lines. Only very small clusters of integrins are visible as green spots; slightly larger clusters show no distinctive distribution pattern. This is the typical conformation one would expect for focal adhesions (Wiesner *et al.*, 2005).

In figure 7.12 the results for the conformation of the three integrins on the suspension cell lines CHO-S and S cells are shown. Both are grown in their standard growth conditions. For all three integrins a clear clustering of the signal on the cell surface can be seen; the dot-like clustering is most distinct for integrin beta 1 on the S cells but it is also visible for integrin beta 1 on CHO-S. This difference in signal intensity of the dot-like clusters might be due to the lower expression level of integrin beta 1 on CHO-S already demonstrated in the flow cytometric analysis of the expression

level. The integrin beta 1 signals are clustered evenly over the entire surface of the cells visible in the image. The clustering is less well defined for integrin alpha 4, and integrin alpha 1 shows less distinctive spots and some larger patches of clustering. Nevertheless, those integrins are regularly distributed over the entire cell surface of the suspension cells.

The regular clustering over the cell surface of the entire cell was confirmed by taking so-called *z*-stacks of integrin beta 1 stained S cells, CHO-S and AML cells grown in suspension. With *z*-stacks images in the *z* direction of the sample are taken with the exciting laser beam focusing on successive planes, creating a series of confocal single images with each slice representing a cross-section through the sample at a different depth. This allows visualisation of the integrin beta 1 over the complete surface of cells grown in suspension, enabling a three-dimensional model of the suspension cells in question to be gathered.

In addition the three suspension adapted cell lines S cells, CHO-S and AML grown in suspension could be compared with respect to their integrin beta 1 conformation. Using integrin beta 1 minimised problems with background in *z*-stack imaging due to the higher signal intensities compared to integrin alpha 1 and integrin alpha 4. *Z*-stacks were set up using the interval optimisation offered by the program to ensure coverage of the entire cell. Representative results of *z*-stacks are shown in figures 7.13 for S cells, 7.14 for AML and 7.15 for CHO-S. For presentation in this report only every n^{th} slice image from the *z*-stacks is shown.

In figure 7.13 the clustering for integrin beta 1 on the S cells is easily visible. For all three cells imaged in the *z*-stack the even distribution of the clusters over the entire cell surface can be seen. In a three-dimensional reconstruction the integrin clusters form a sphere. This means that the cell surface of S cells is covered with regularly distributed integrin beta 1 clusters. A similar distribution is seen in figure 7.14 for the AML cells when they are grown in suspension; this is a large change of conformation compared to what was seen when AML cells were grown adherently, indicating an influence of the culture environment on the conformation of integrin beta 1. Both cell lines show the same specific conformation of evenly distributed integrin beta 1 clusters on the cell surface.

In figure 7.15 the results for the integrin beta 1 conformation on CHO-S cells is shown. As expected from the flow cytometry results, the signal intensities are lower than those for S cells, requiring a higher laser transmission and leading to a higher background signal. Nevertheless, integrin clusters on the cell surface can be seen and are distributed over the entire surface of the cell. Hence, the sphere-like distribution of integrin beta 1 clusters as seen in S cells and AML is also present on the CHO-S cells.

CCL61

integrin beta 1 integrin alpha 1 integrin alpha 4

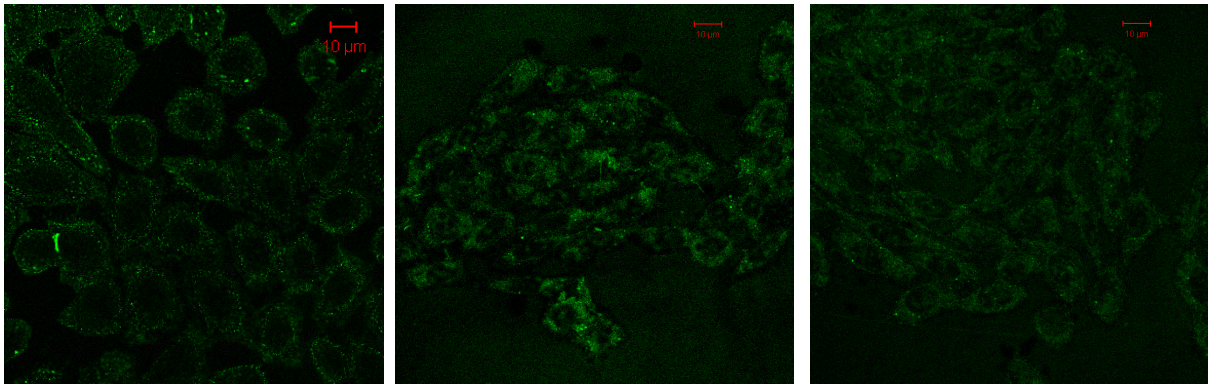

AML

integrin beta 1 integrin alpha 1 integrin alpha 4

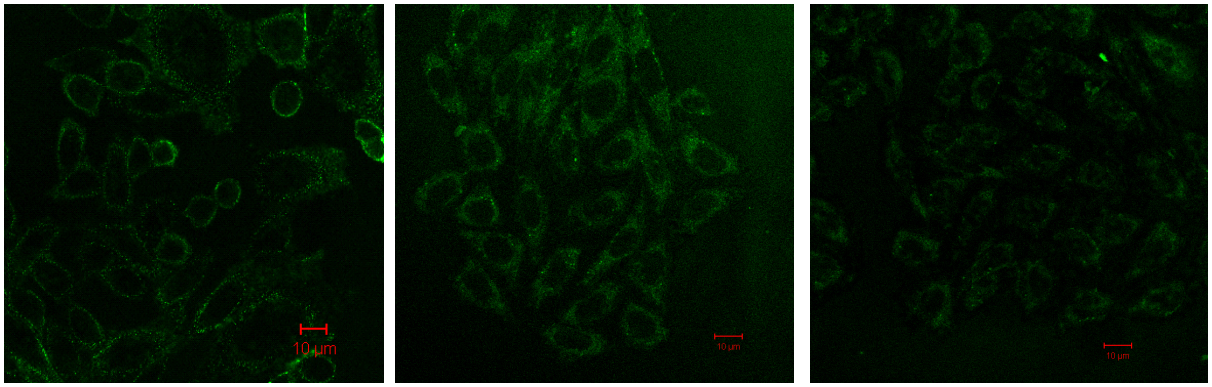

Figure 7.11: Conformation of integrin beta 1, alpha 1 and alpha 4 on the adherent model CHO cell lines, CCL61 and AML.
Cells were grown on cover-slips in 6 well plates and stained as described. Imaging was performed using an inverted Zeiss LSM510 Meta confocal microscope. Mounted cell samples were analysed using a plan apochromat 63x/ 1.4 oil DIC objective. Excitation of the fluorochrome was at 488nm by an argon laser. Emission was collected using a band pass 500-550 IR filter.
For integrin alpha 1 and alpha 1 laser transmission had to be used at between 35% and 40% due to a very low staining signal. Laser transmission for integrin beta 1 was around 32%. Scale bars equal 10µm.

S cells

integrin beta 1 integrin alpha 1 integrin alpha 4

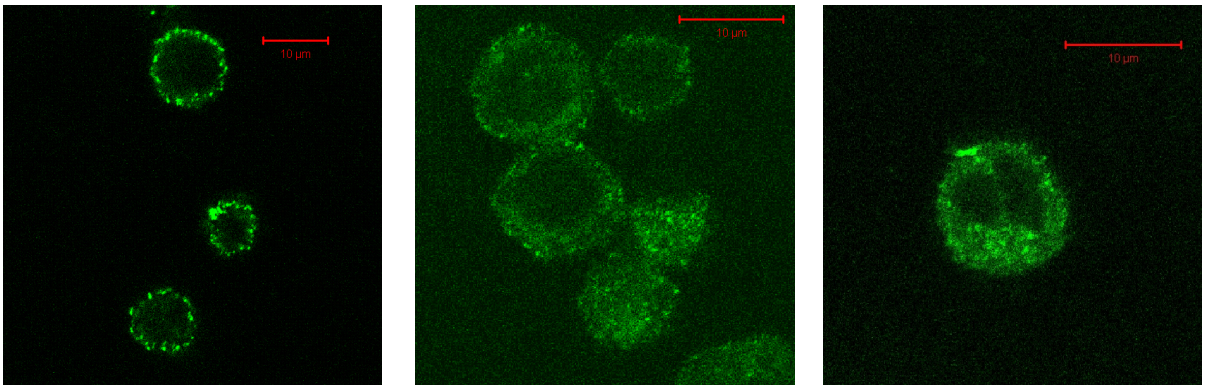

CHO-S

integrin beta 1 integrin alpha 1 integrin alpha 4

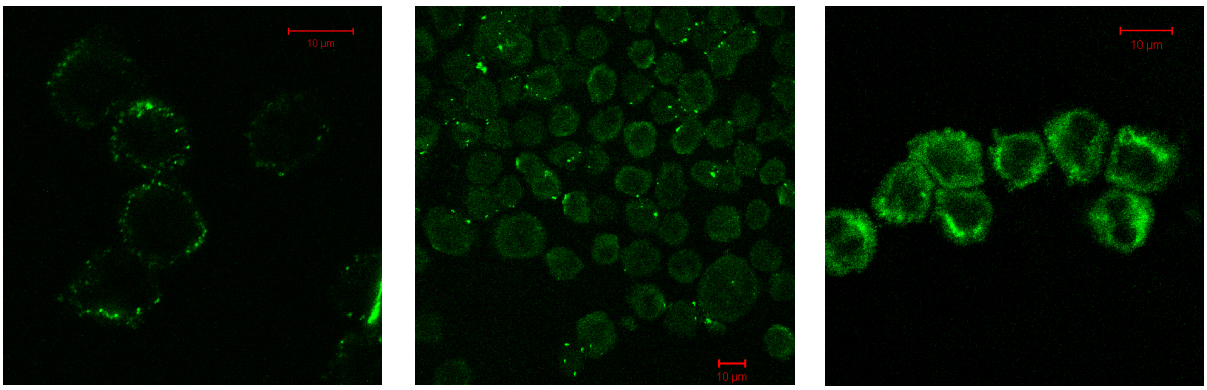

Figure 7.12: Conformation of integrin beta 1, alpha 1 and alpha 4 on S cells and CHO-S cells.
Cells were grown in standard suspension conditions and stained as described before. Imaging was performed using an inverted Zeiss LSM510 Meta confocal microscope. Mounted cell samples were analysed using a plan apochromat 63x/ 1.4 oil DIC objective. Excitation of fluorochrome was at 488nm by an argon laser. Emission was collected using a band pass 500-550 IR filter. For integrin beta 1 a specific conformation with regularly distributed clusters of integrin beta 1 on the cell surface can be seen for both suspension cell lines. A similar but less distinct conformation is visible for integrin alpha 1 and integrin alpha 4. For integrin alpha 1 and alpha 4 laser transmission had to be used at between 35% and 40% due to the very low staining signal. Laser transmission for integrin beta 1 was around 32%. Scale bars equal 10µm.

The conformation of integrin beta 1 on suspension CHO cells as seen in the confocal analysis in figures 7.13, 7.14 and 7.15 indicates sphere-like distribution of integrin clusters on the cell surface common to all three suspension adapted cell lines. In the next step the question to be addressed was whether this distribution is a common feature occurring for all cells, i.e. also for non-suspension adapted CCL61 when cultured in suspension, and whether the evenly distributed integrin beta 1 clusters are a reaction to the media environment as suggested by the result for AML cells grown in suspension.

A) scale

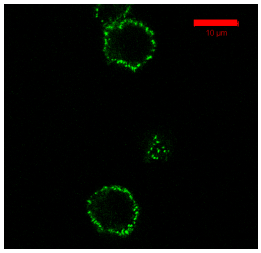

scale bar: 10 µm

B) *z*-stack

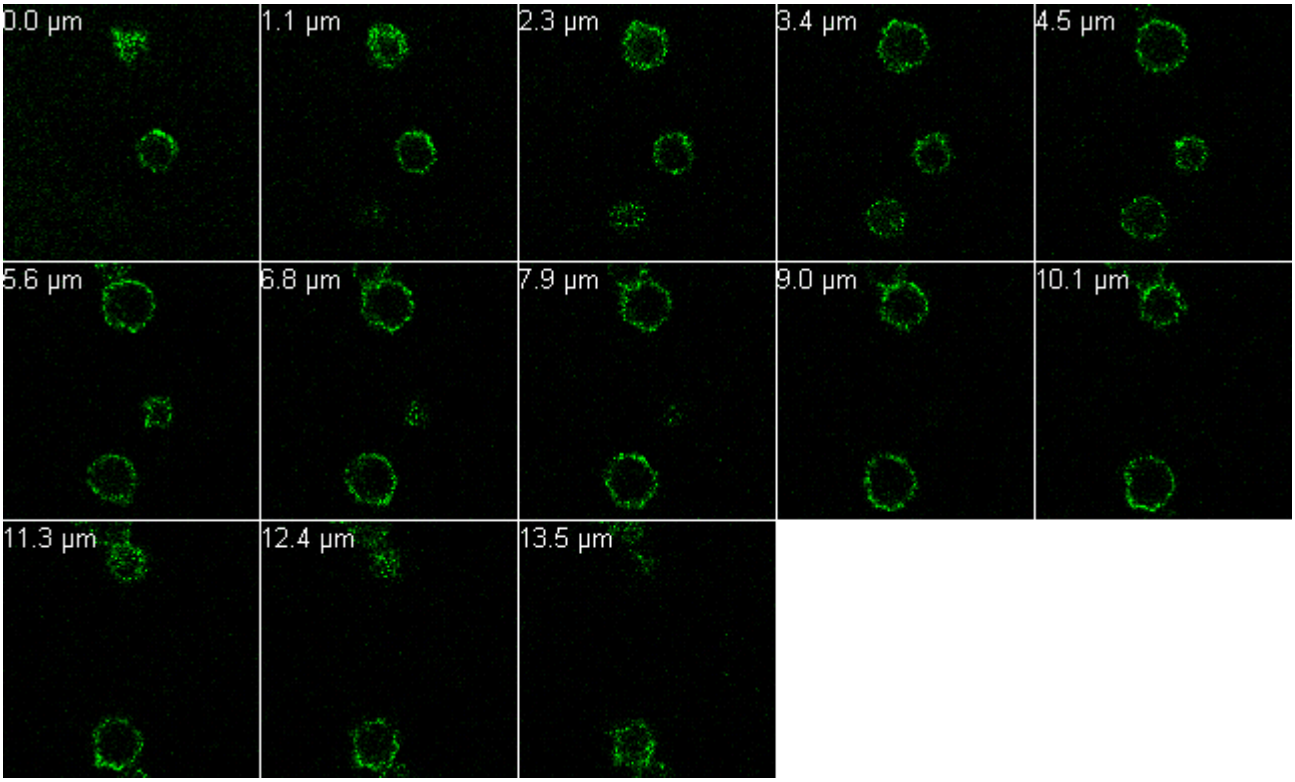

Figure 7.13: Three dimensional conformation of integrin beta 1 clusters on S cells
Z-stacks were taken with an inverted Zeiss LSM510 Meta confocal microscope to analyse the three dimensional distribution of integrin beta 1 clusters on the cell surface. Every third image of the *z*-stack is presented.
Set up: image size: 512 x 512 pixels/ 58.4 µm x 58.4 µm
pixel time: 25.6 µs,
pinhole: 96 µm,
laser transmission : 29.6%

A) scale

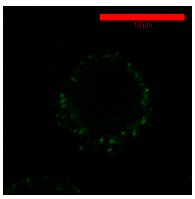

scale bar: 10 µm

B) *z*-stack

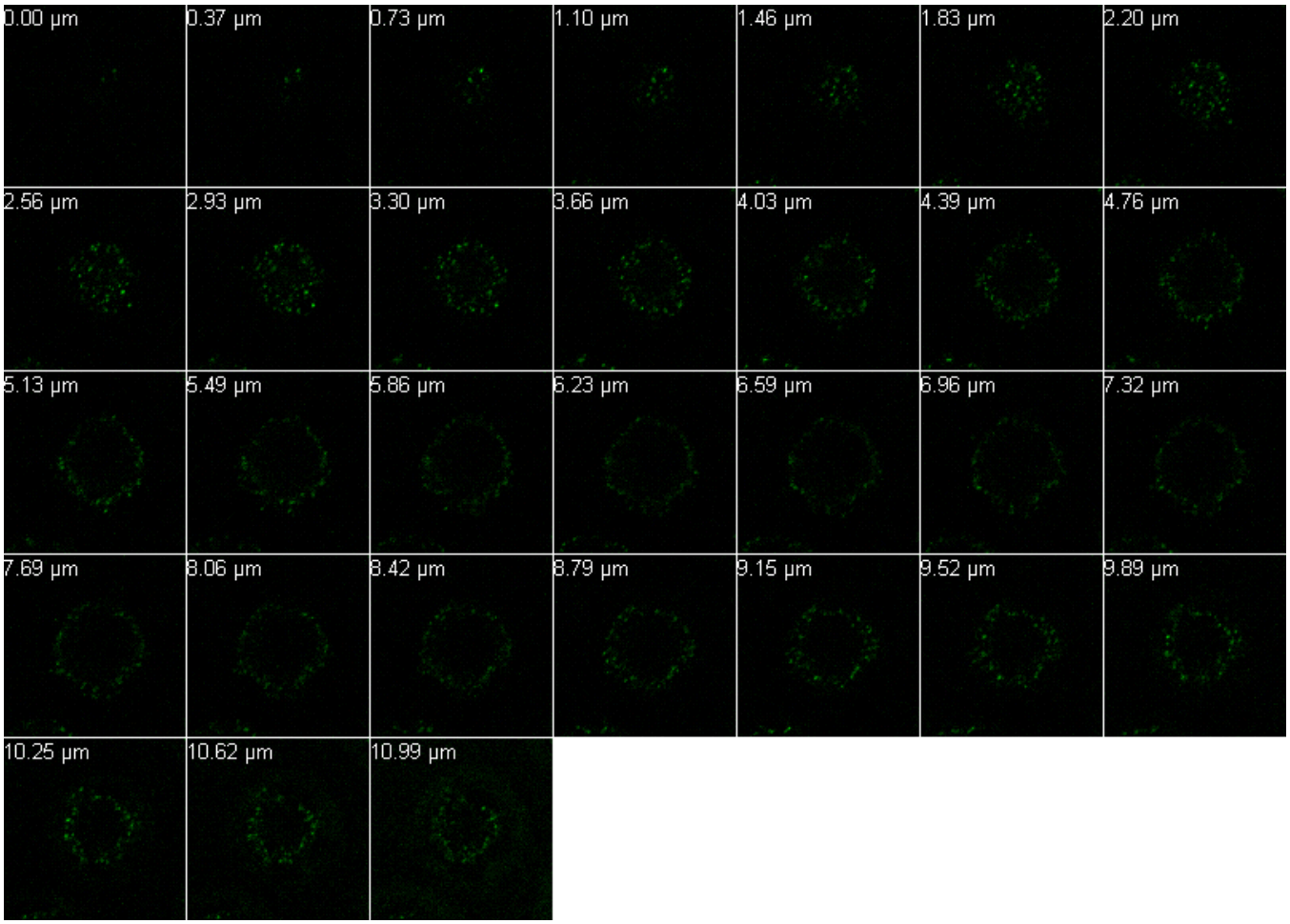

Figure 7.14: Three dimensional conformation of integrin beta 1 clusters on AML cells grown in suspension

Z-stacks were taken with an inverted Zeiss LSM510 Meta confocal microscope to analyse the three dimensional distribution of integrin beta 1 clusters on the cell surface. Every third image of the *z*-stack is presented.

Set up: image size: 228 x 228 pixels/ 22.6 µm x 22.6 µm
pixel time: 28.6 µs,
pinhole: 96 µm,
laser transmission : 35%

A) scale

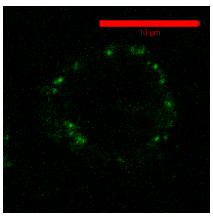

scale bar: 10 µm

B) *z*-stack

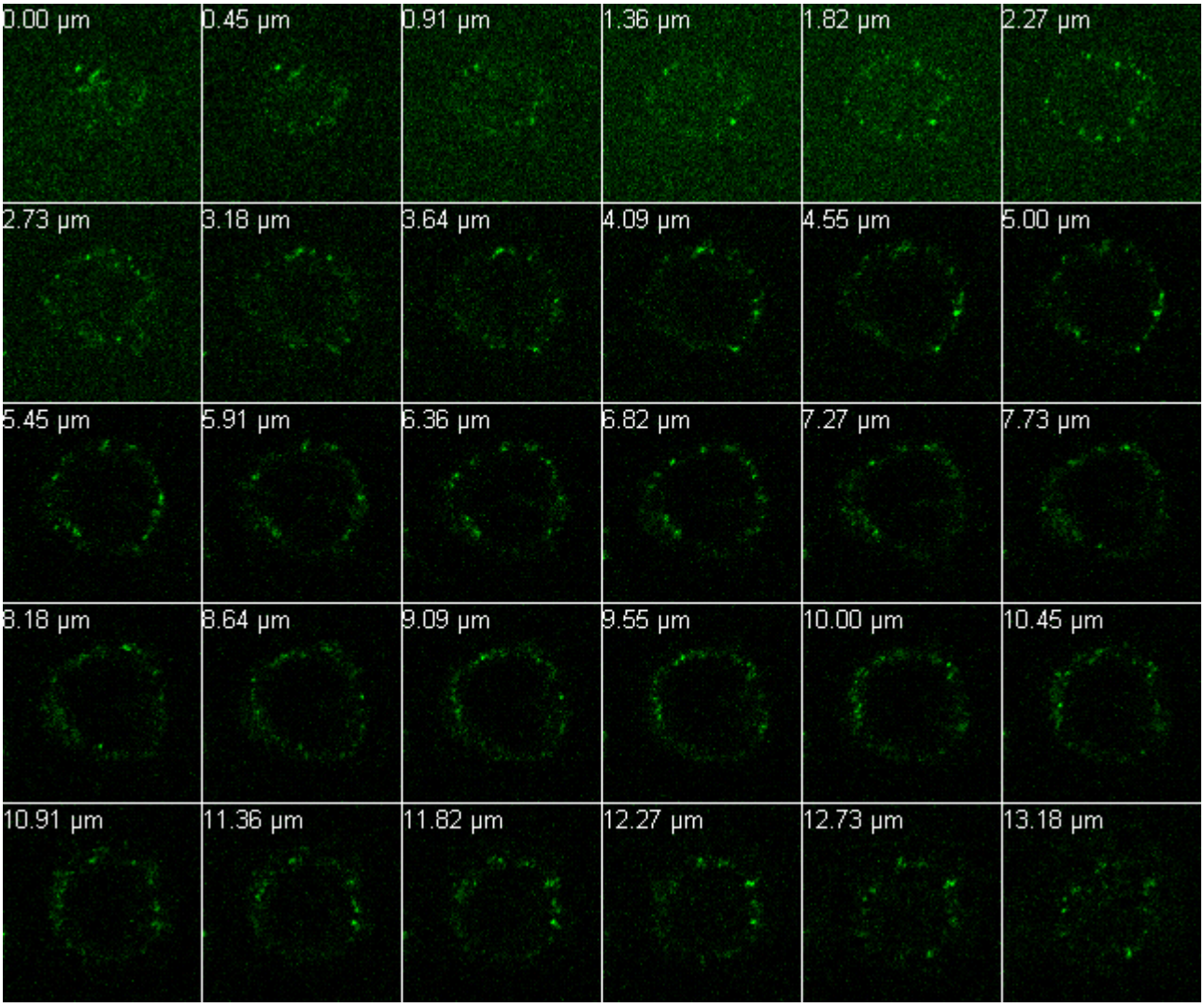

Figure 7.15: Three dimensional conformation of integrin beta 1 clusters on CHO-S
Z-stacks were taken with an inverted Zeiss LSM510 Meta confocal microscope to analyse the three dimensional distribution of integrin beta 1 clusters on the cell surface. Every second image of the *z*-stack is presented.
Set up: image size: 212 x 212 pixels/ 20.9 µm x 20.9 µm
pixel time: 15.4 µs,
pinhole: 121 µm,
laser transmission: 35%

7.10 Integrin beta 1 conformation as a reaction to the cell culture environment

To prove that the demonstrated integrin beta 1 conformation in suspension cells (figures 7.12 -7.15) is really due to the process of suspension adaptation it has to be verified that the conformation is a reaction of suspension adapted CHO cells to the cell culture environment.

7.10.1 Methodology: conformation as reaction to cell culture environment

S cells were cultured first in suspension growth conditions, then in adherent growth conditions and after that transferred back into suspension growth. AML cells were transferred from adherent into suspension growth conditions, and non-suspension adapted CCL61 were also transferred from adherent into suspension growth conditions. All three cell lines were treated in the same way when transferring them from adherent growth conditions into suspension growth conditions using a trypsin/EDTA harvest with a subsequent blocking of the trypsin using the adherent growth media. In all growth conditions the three cell lines were analysed for conformation of integrin beta 1 using confocal microscopy.

7.10.2 Result: conformation is a reaction to cell culture environment

As the results in figure 7.16 show, S cells change their conformation of integrin beta 1 when grown in adherent conditions. In adherent conditions the integrin conformation is comparable to what is seen for AML and CCL61 when these grow in their standard adherent mode, with smaller, less distinct cluster of integrin beta 1. Taking S cells back into suspension leads to re-formation of the integrin beta 1 conformation typical of suspension growth, with regularly distributed distinctive integrin beta 1 clusters on the cell surface. This conformation also develops when AML cells are grown in suspension. This is a clear indication that the demonstrated specific integrin beta 1 conformation is a reaction of the two CHO cell lines to their growth environment, confirming that the conformation plays a role in the suspension phenotype. This result is strengthened by the fact that when transferring non-suspension adapted CCL61 cells into suspension growth the integrin beta 1 conformation changes to a different type of integrin beta 1 conformation, as shown in figure 7.6. Large patches of integrin beta 1 clusters appear mainly on the connecting points where cells clump together. These cell clumps repeatedly appeared, to a varying degree, when CCL61 cells were cultured in suspension, for example during analysis of the cell growth characteristics. In

CCL61 cells grown in suspension, integrin beta 1 becomes concentrated at these contact points between the cells, indicating an interaction between cells and leaving the rest of the cell surface free of integrin beta 1 clusters. This conformation of CCL61 in suspension is apparently different from the conformation seen on S cells and AML cells growing in suspension. While the conformation of integrin beta 1 changes for all three cell lines in reaction to the environment, only the suspension adapted cell lines S cells and AML show the specific evenly clustered distribution of integrin beta 1 on the cell surface when growing in suspension.

7.11 Discussion: role of integrin conformation in suspension adaptation

A specific conformation of integrins, in particular integrin beta 1, on the cell surfaces of the suspension adapted CHO cell lines (S cells, CHO-S and AML) has been found. This specific conformation is characterised by dot-like clusters of integrins that are evenly distributed over the entire cell surface, providing a sphere-like network of integrins on the cell surface similar to results seen for activated lymphocytes by Lub *et al.*(1997). The even distribution of integrin beta 1 clusters on leukocytes has also been demonstrated by Altrock *et al.* (2013).

It has been shown that this conformation is a reaction of the S cells and AML cells upon their cell culture environment and that both cell lines are capable of switching reversibly back and forth between the conformation seen in adherent growth and the one seen in suspension growth; similar processes of cell surface protein rearrangement have been shown for adherence of leukocytes by Shahal *et al.* (2012); in their study focal adhesion growth was influenced by RGD peptide density and EGF factor type (soluble, immobilised) and concentration. As S cells and AML cells in adherent conditions have been cultured in different media the conformation is clearly influenced by the suspension culture conditions seen, which for both cell lines used PSM media. The main factor for the demonstrated integrin conformation found can be assumed to be the suspension culture, independently of the media used, because CHO-S cells show a comparable integrin conformation in suspension, though being cultured in a different media. The switch seen between adherent and suspension confirms the importance of the integrin conformation for suspension growth. This idea is further strengthened by the fact that the non-suspension adapted CHO cell line CCL61 shows an entirely different conformation of integrin beta 1 when cultured in suspension using PSM media, lacking the evenly distributed dot-like clusters of integrin beta 1 on the cell surface and showing instead non-regularly distributed patches of integrin beta 1 that accumulate where the cells touch. Hence, it can be concluded that the non-suspension adapted cell line CCL61 lacks the capability to

change the integrin conformation to the dot-like clustering of integrins covering the entire cell surface, seen to exist for all three suspension adapted cell lines. Hence, CCL61 can be described as being less similar to leukocytes with regard to rearrangement capability of surface proteins compared to S cells, AML cells and CHO-S cells. Most studies (Lub *et al.*, 1997, Bakker *et al.*, 2012) concentrated on the rearrangement of integrin beta 2 as the major beta chain involved in immune function, and not integrin beta 1; Altrock *et al.* (2012) showed a very similar integrin beta 1 conformation as seen here for HSC cells.

Considering that integrins are constitutively expressed on suspension adapted CHO cells, although no ligand is provided by the cell culture environment, and the specific conformation type seen for integrins, it can be assumed that integrins, especially integrin beta 1, play an important role in suspension CHO cells. It is hence proposed that the described conformation of integrin beta 1 on the cell surface of suspension cells is part of a general suspension phenotype. The question remains what function the integrins have in the specific conformation demonstrated to exist on the surface of suspension adapted CHO cells.

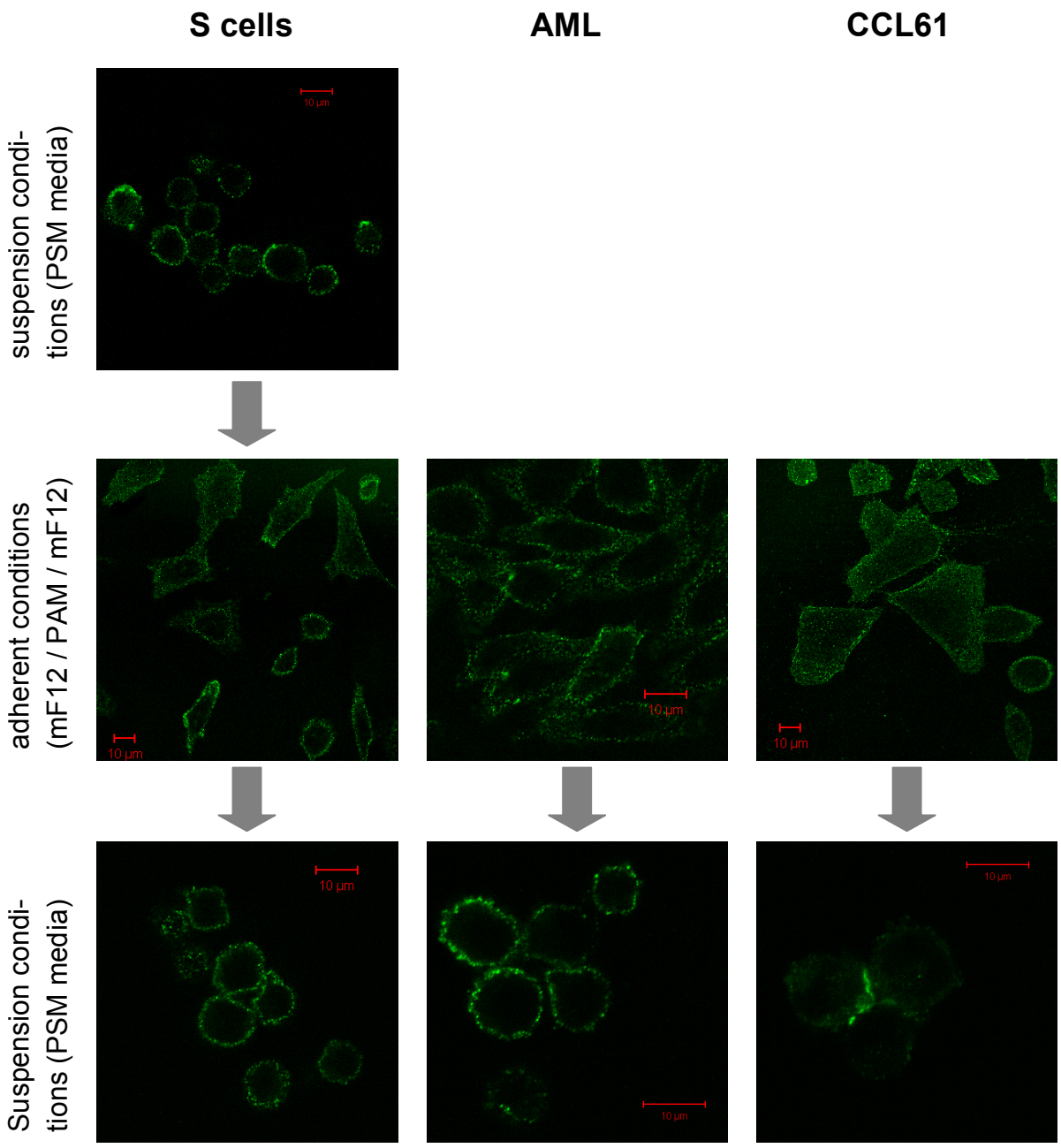

Figure 7.16: Conformation of integrin beta 1 clusters on the cell surfaces of S cells, AML cells and CCL61 as a reaction to cell culture environment.
Top row shows conformation of integrin beta 1 on S cells in their standard growth condition (suspension). Middle row shows conformation of integrin beta 1 on: S cells grown in adherent conditions using mF12, AML cells grown in standard growth condition (PAM), CCL61 grown in standard growth condition (mF12). Bottom row shows integrin beta 1 conformation on: S cells in suspension after having previously grown in adherent conditions, AML cells growing in suspension and CCL61 growing in suspension. All imaging was done after three days in culture. All scale bars equal 10µm.

8. Chapter

Intracellular interaction of integrins with the cytoskeleton

In this chapter the possible interactions between integrins and the actin cytoskeleton are described. Methods to analyse actin content and conformation are introduced. Then results on actin content and conformation for the model CHO cell lines are presented. The dependence of actin conformation on cell line and adaptation status is shown and the interplay between integrin and actin conformation is demonstrated as being relevant for suspension adaptation.

8.1 Interaction between integrins and actin cytoskeleton – role of cytoplasmic beta tail and associated proteins

Studies concentrating on the intracellular signalling side of integrins stress the role the interaction between integrins and actin cytoskeleton plays. Wiesner *et al.* (2005) describe the actin cytoskeleton as one of the most important targets of integrin mediated cell signalling. Streuli (2009) describes the role integrins play in cell division and organisation of the mitotic spindle; both are processes where the rearrangement of the cytoskeleton is highly relevant. Regent *et al*. (2011) explain the connection between adhesion strength to ligands and the actin cytoskeleton as based on the integrin working as an interface between the two. The assembly of focal adhesions, points of attachment to the extracellular matrix, requires tension signals from the actin filaments which result in the binding of vinulin and talin to integrin cytoplasmic tails (Regent *et al.,* 2011). Wiesner *et al.* (2005) describe the process of focal adhesion formation as a step-wise procedure that starts from focal complexes which are described as small dot-like dynamic structures (size around 100 nm) usually found in spreading cells. Focal adhesion, also called focal contact, is described as a mature focal complex with an elongated form and a size of around 1 µm in resting cells. Integrin cytoplasmic tail binding proteins have been found to play a major role in focal adhesion development; talin and vinculin are seen as key players within the group of integrin cytoplasmic tail

binding proteins. Furthermore, the Arp2/3 complex, a nucleator for actin polymerisation that binds to vinculin, links actin polymerisation to integrins interacting with the extracellular matrix. The process of actin polymerisation is particularly active when integrins newly engage with the extracellular matrix, e.g. when integrins start to cluster (DeMali *et al.*, 2003), and hence is more prominent in focal complexes. Delon and Brown (2007) describe the integrins as bidirectional acting proteins that on one hand act as classic receptors which allow the cell environment to influence the cell interior, while on the other hand the cell inside can also influence the integrins itself (concept of outside-in and inside-out signalling). Delon and Brown (2007) state that an active integrin conformation is required for integrin-actin interaction. They list several types of interaction:

1) binding and capping of pre-existing actin filaments, which increases the stability of the cell,
2) recruitment of proteins to polymerise new actin filaments (involving Arp2/3 complex),
3) inhibition of actin dependent processes by intersecting with Rho GTPases (also described by Wiesner *et al.*, 2005) and
4) cytoskeleton contraction, amplifying integrin adhesion.

Delon and Brown (2007) stress that the interaction between integrins and actin involves numerous (around 50) associated proteins and suggest that different integrins and different ligands might require different associated proteins and that adhesion site maturation might require a tightly regulated sequence of associated proteins. They list a few of those associated proteins as essential for integrin function, including talin and integrin-linked kinase. Talin is known to bind direcly to integrins by a specific binding domain, thereby increasing the affinity of integrin to its ligand (Delon and Brown, 2007). Talin has been shown to have a second integrin binding domain which might play a role in integrin clustering. Talin anchors integrins in the membrane and provides the initial cytoskeleton connection. Integrin-linked kinase (ILK) is also able to bind directly to integrin beta 1 tails but might also interact indirectly. Phosphorylation of ILK regulates one of the down-stream signalling pathways of integrin, protein kinase B/AKT3, and has also been indicated to phosphorylate integrins. ILK deficiency is linked to impaired adhesion to fibronectin (Wiesner *et al.*, 2005). Other proteins that have been found to have an actin binding domain are parvin, filamin, α-actinin and tensin. The conformation of those proteins might also influence their role in the integrin-cytoskeleton interaction. Most of the data presented in the articles above is based on results gained from two-dimensional cell cultures using adherent cell lines such as fibroblasts, a model similar to the CCL61 cell line used in this study. Figure 8.1 summarizes the possible interaction

partners involved in the link between integrins and cytoskeleton in cultured cells. Studies looking at the interaction between integrin and actin in tissue indicate differences in associated proteins and linkage between integrin and cytoskeleton in comparison to the two-dimensional models studied.

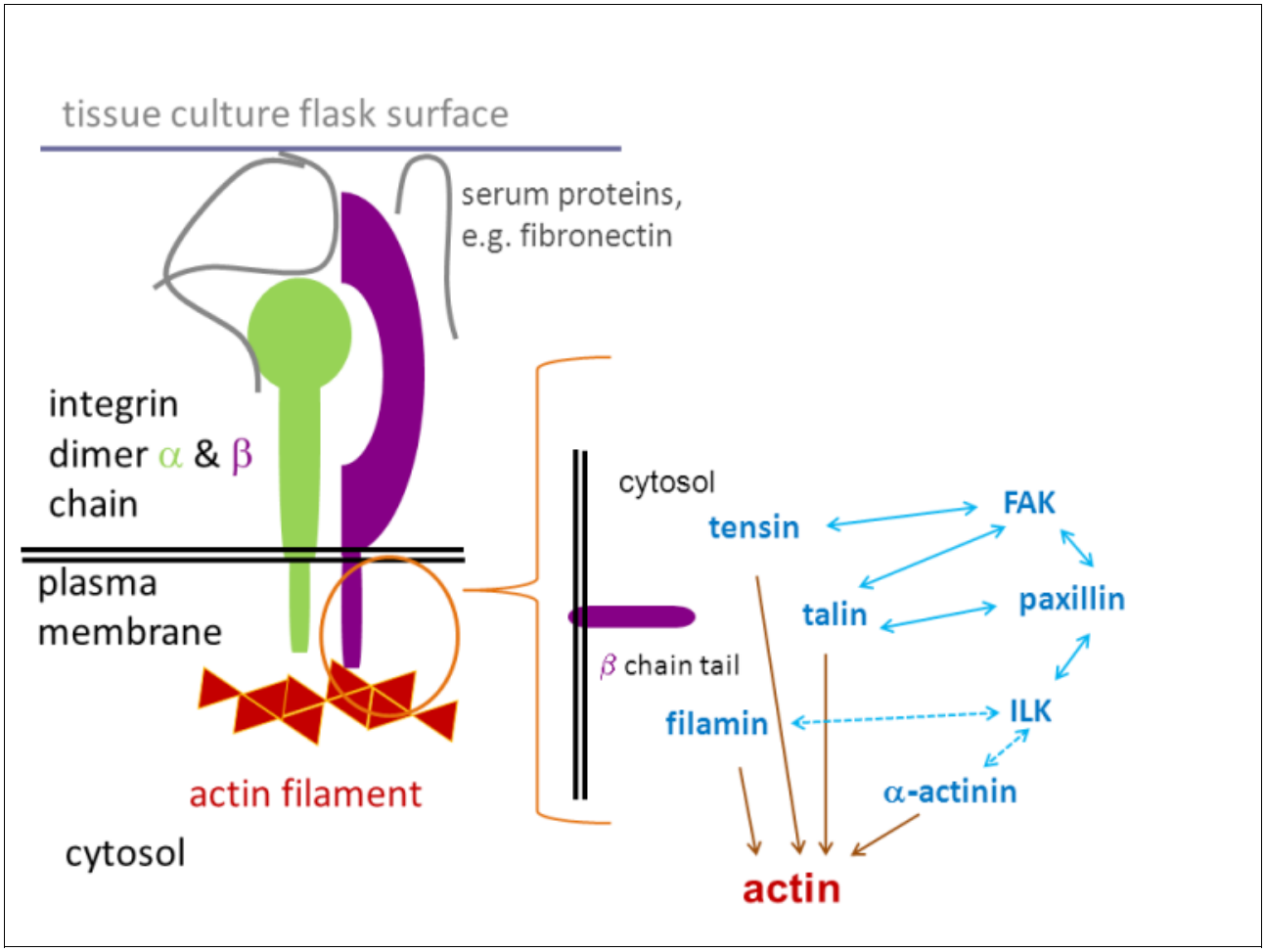

Figure 8.1 Model of integrin-actin interaction and associated proteins.
Integrins predominantly interact with the actin cytoskeleton via the integrin beta 1 cytoplasmic tail. Proteins associated with this interaction (tensin, talin, filamin, ILK, paxillin, FAK, α-actinin) are shown. All are capable of binding to the cytoplasmic beta tail. Of these only filamin, tensin, talin and α-actinin can bind to actin. Furthermore, those proteins can interact with each other either directly (solid blue line) or via other interaction proteins (dashed blue line). (Wiesner *et al.*, 2005).

Different interactions might also play a role in suspension growing cells, as summarized by van Kooyk and Figdor (2000) and shown in figure 7.1. Several studies (Pedersen *et al.*, 1999; Humphries *et al.*, 2007; Whitlock *et al.*, 2000; Lub *et al.*, 1997) have used cytoskeleton disrupting reagents such as cytochalasin D to study actin conformation, focal adhesion formation and

interaction between integrins and actin cytoskeleton in adherent and suspension cells. Most interesting in this context is the study by Lub *et al.* (1997) where clustering of integrins on lymphocytes was induced by cytochalasin D treatment. Cytochalasin D has been demonstrated frequently to disrupt the cytoskeleton of cells and this effect has been used to study the link between the actin cytoskeleton and numerous processes (Peterson and Mitchison, 2002; Mills *et al.*, 2000). Hayduk and Lee (2004b) used cytochalasin D to improve protein production in adherent CHO cells.

8.2 Conformation of the actin cytoskeleton in the four model cell lines

As integrins were shown in this study to be expressed on the suspension adapted cells lines in a specific conformation, the conformation of actin as the main intracellular interaction partner of the integrins has also been analysed using confocal microscopy. The question is if there is also a specific conformation of actin for successfully suspension adapted CHO cell lines – as seen for the integrins – that could be used to described a CHO suspension phenotype.

In a first step the four cell lines S cells, CHO-S, AML and CCL61 were analysed with respect to their actin conformation when grown in their standard growth conditions. In figure 8.2 both adherent cell lines, AML and CCL61, show actin fibres across the cells and strong actin fibre formation (stronger staining signal) at the cell edges, a pattern one would expect for an adherent cell line grown in two-dimensional culture condition (Shahal *et al.*, 2012). For the suspension cells no actin filaments can be seen across the intracellular part of the cells; instead, the actin cytoskeleton is concentrated in a sphere which from its diameter can be assumed to lie directly under the cell membrane; this is a conformation similar to what has been described to be found in activated T cells (Barda-Saad *et al.*, 2004) and has also bee previously described for lymphocytes (Mills *et al.*, 2000; Lub *et al.*, 2007). The ruffling of the cytoskeleton might be due to the permeabilisation step that needs to be performed for actin staining, which can lead to cell shrinking. To determine whether the difference in the actin cytoskeleton conformation demonstrated to exist between adherent and suspension CHO cells is a reaction to the cell culture environment, AML and CCL61 have also been cultured in suspension and their actin conformation was analysed.

In figure 8.3, both cell lines show a strong concentration of the actin cytoskeleton in a circle or sphere with no actin filaments across the inner area of the cells. The non-suspension adapted cell line CCL61 shows only small clumps of cells with most cell clusters being around three cells in size, in contrast to the suspension adapted AML cells the cells of which grow in single cell mode (only few clusters of two cells). These cell clumps appeared repeatedly to a varying degree when

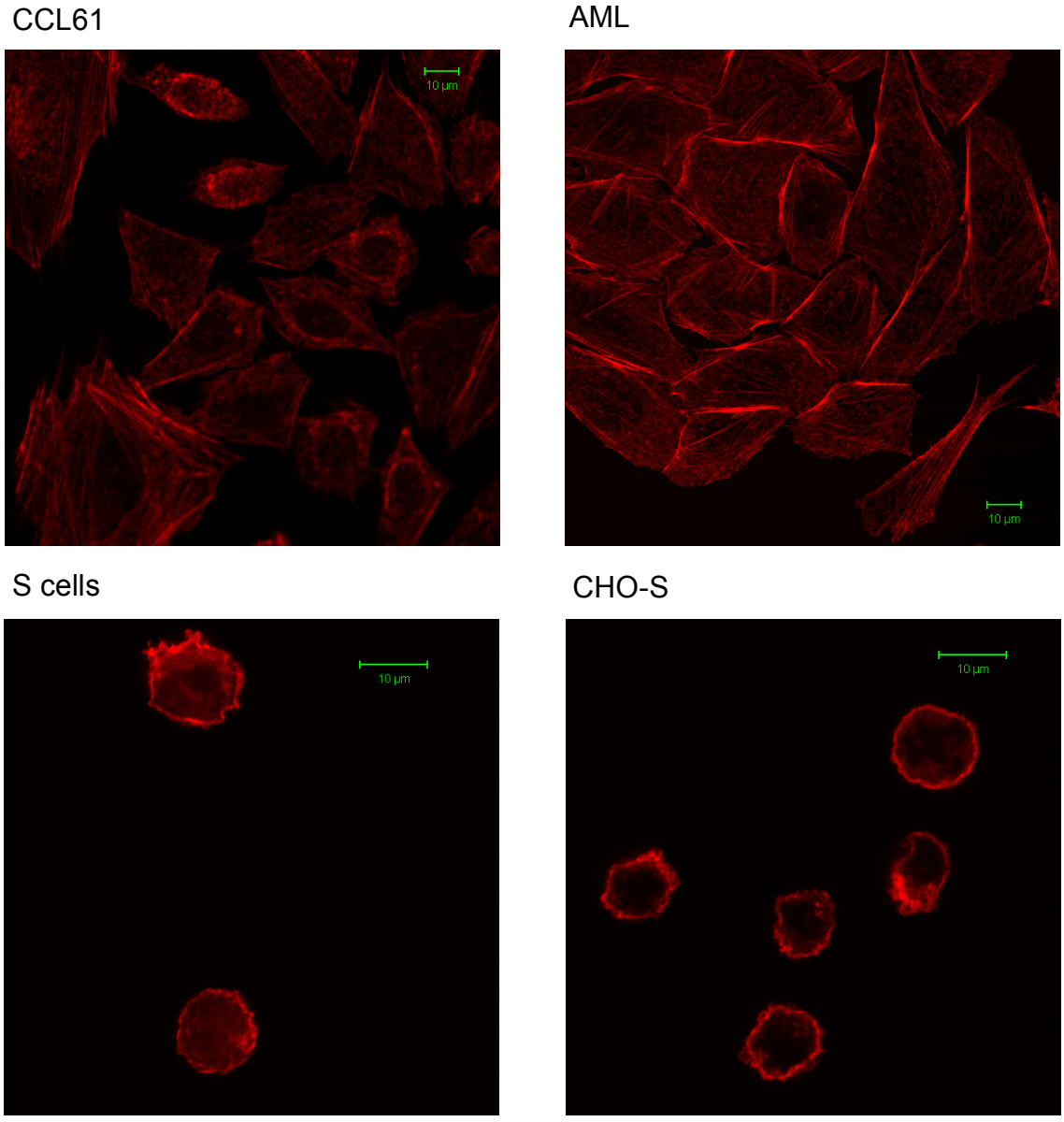

Figure 8.2: Conformation of actin in CCL61, AML, S cells and CHO-S in standard growth conditions.

Cells were stained using phalloidin Alexa 546 and analysed by confocal microscopy. Imaging was performed using an inverted Zeiss LSM510 Meta confocal microscope. Mounted cell samples were analysed using a plan apochromat 63x/ 1.4 oil DIC objective. Excitation of fluorochrome was at 514 nm by an argon laser. Emission was collected using a long pass 560 nm filter. Pinhole was at 106 µm (111 µm for AML), laser transmission was 13%. All scale bars equal 10 µm.

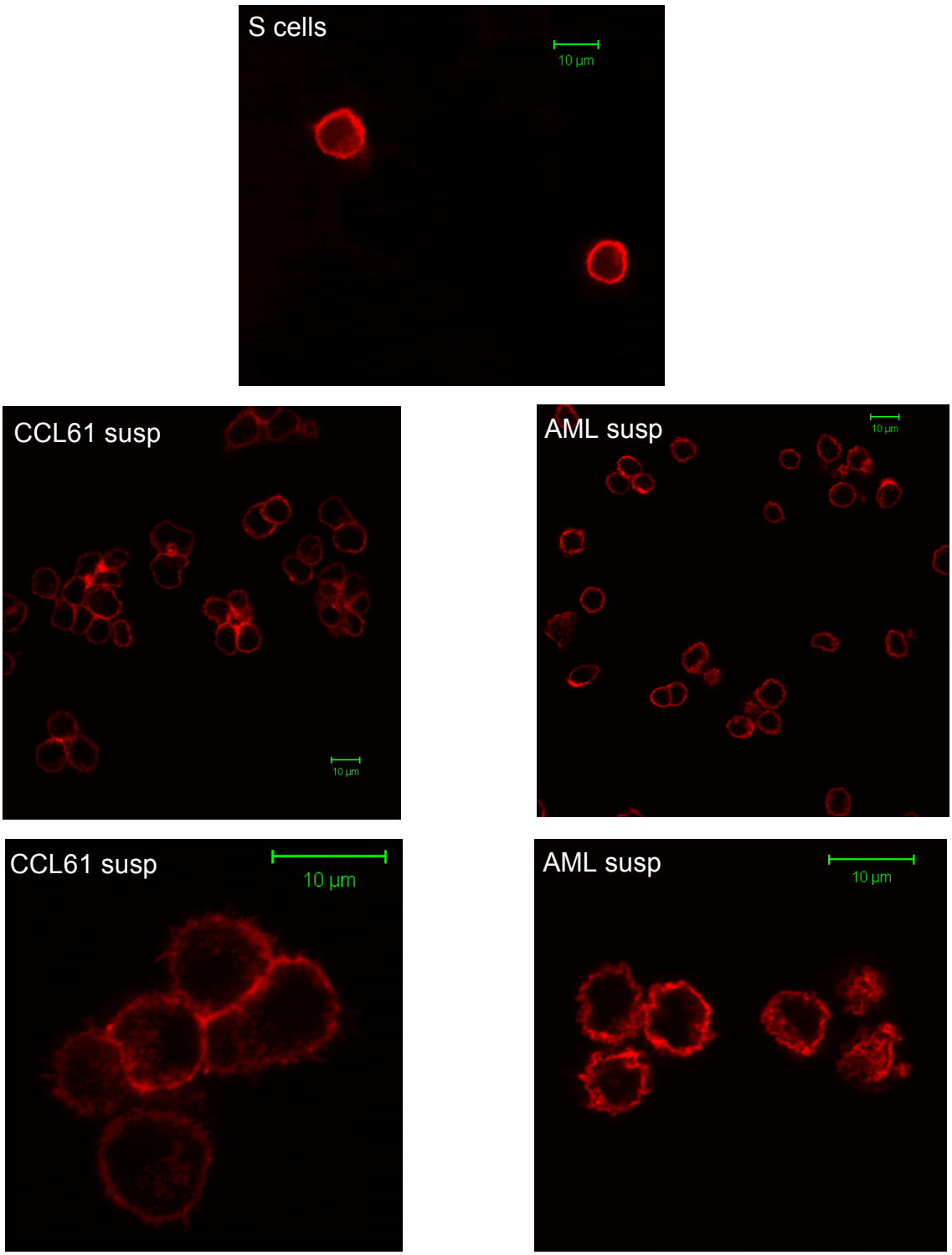

Figure 8.3: Conformation of actin: S cells in comparison to CCL61 and AML, both grown in suspension.

Cells were stained using phalloidin Alexa 546 and analysed by confocal microscopy. Imaging was performed using an inverted Zeiss LSM510 Meta confocal microscope. Mounted cell samples were analysed using a plan apochromat 63x/ 1.4 oil DIC objective. Excitation of fluorochrome was at 514 nm by an argon laser. Emission was collected using a long pass 560 nm filter. Pinhole was 106 µm for S cells and 111 µm for CCL61 and AML and laser transmission was 13%. All scale bars equal 10 µm.

CCL61 cells were cultured in suspension, for example during analysis of the cell growth characteristics. At the contact area of the CCL61 cell clumps the actin cytoskeleton is concentrated. This correlates with the result for the integrin beta 1 conformation seen in CCL61 cells grown in suspension where a concentration of the integrin beta 1 was also seen at the contact point of the clusters (compare figure 7.16). Hence, the conformations for actin and integrin beta 1 become similar when CCL61 are grown in suspension, indicating a strong linkage between integrin beta 1 and actin, as suggested by previously mentioned studies. The actin conformation seen for the AML cells is the same as seen for the S cells. Therefore, suspension CHO cells seem to have a common distribution of the actin cytoskeleton that differs to a high degree from the conformation they show in adherent growth. To further analyse the actin conformation *z*-stacks of S cells and AML grown in suspension were acquired to gain a three-dimensional model of the actin conformation.

Figure 8.4 clearly shows that the actin cytoskeleton of an S cell forms a strong sphere which is 1-2 µm thick and completely encloses the intracellular area of the cell. The same conformation of a ball-like cytoskeleton is seen in AML cells when growing in suspension, whereas in adherent growth they show filaments across the cells and strong actin fibre formation at the cell edges. The actin conformation seen is very similar for all four cell lines when grown in suspension, with the notable difference that CCL61 cells grown in suspension show a stronger signal for actin at the contact area of cells when small cell clumps are formed. The sphere-like actin conformation can be interpreted as a reaction of the cells lines to the culture conditions and seems to be linked to the integrin beta 1 conformation, as indicated by the comparable shift in distribution and conformation when switching AML and CCL61 from adherent to suspension growth. This is also in line with the literature where numerous studies have concentrated on the analysis of the integrin -cytoskeleton interaction (Pedersen *et al.*, 1999; Humphires, 2007; Hayes *et al.*, 2011, Bakker *et al.*, 2012). One reason for the observed conformation can be assumed to be the shear stress that cells experience in suspension culture, leading to a strong sub-cortical actin cytoskeleton. Due to the weakness of the integrin signal, its imaging requiring a high laser transmission, it was not possible to analyse double stained cells to further investigate the interaction between integrin and actin, as the Alexa 546 fluorochrome was also excited to a measurable extent by the 488 nm excitation wavelength at high laser transmission.

While imaging the actin in different cell lines it was noted that the signal intensity for the S cells seemed stronger compared to that of the other cell lines imaged. This may be an indication of a difference in actin content between the cell lines. The sphere-like actin conformation had shown to

be a feature seen not only for successfully suspension adapted CHO cell lines. As the confocal image intensities suggested a difference in actin content, the next question to address was if the successful suspension adapted CHO cell lines (S cells, AML and CHO-S) show a higher actin content compared to the non-suspension adapted cell line CCL61.

A) scale

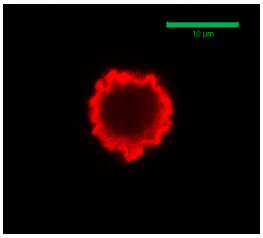

scale bar: 10 µm

B) *z*-stack

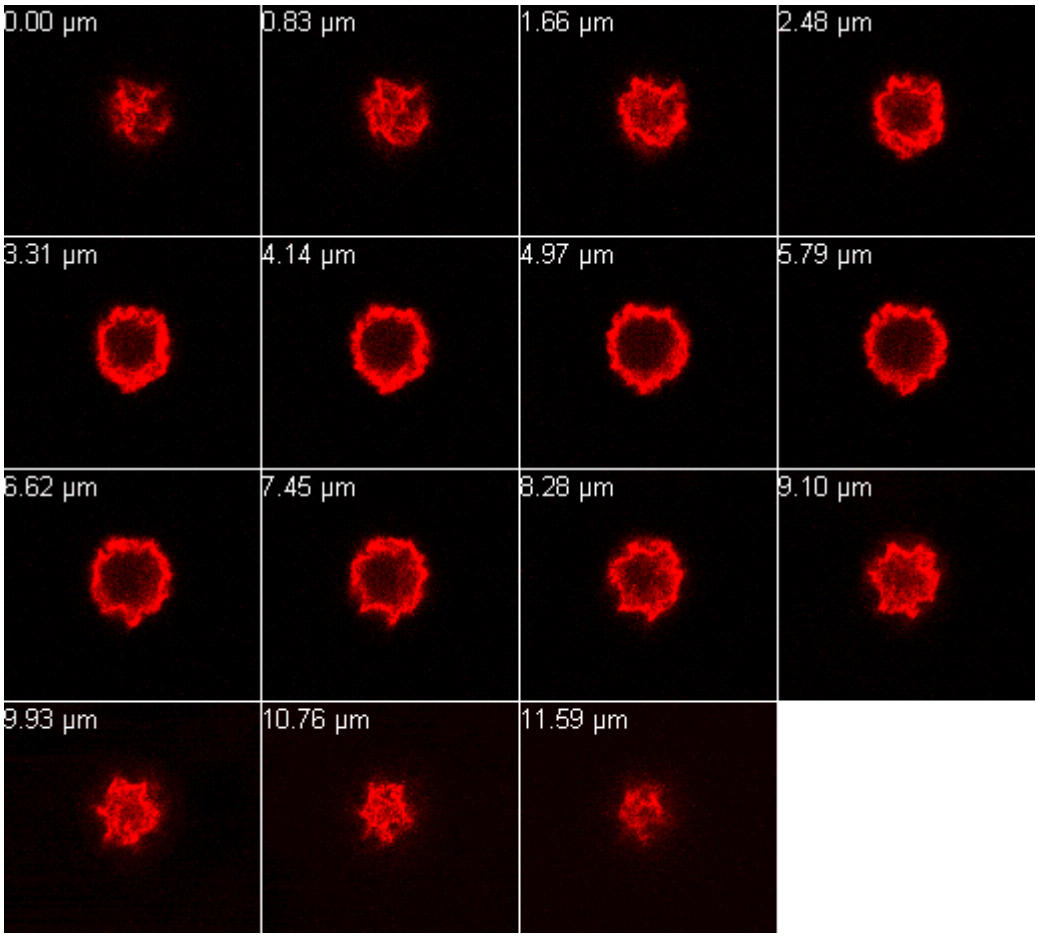

Figure 8.4: Three-dimensional conformation of actin in S cells.
Cells were stained using phalloidin Alexa 546 and analysed. *Z*-stacks were taken with an inverted Zeiss LSM510 Meta confocal microscope to analyse the three-dimensional conformation of actin. Mounted cell samples were analysed using a plan apochromat 63x/ 1.4 oil DIC objective. Excitation of fluorochrome was at 514nm by an argon laser. Emission was collected using a long pass 560 nm filter. Every second image of the *z*-stack is presented.

Set up: image size: 512 x 459 pixels/ 36.6 µm x 32.8 µm ,
pixel time: 25.6 µs,
pinhole: 106 µm,
laser transmission : 13%

A) scale

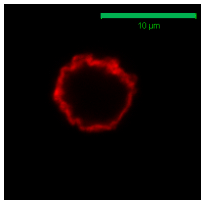

scale bar: 10 µm

B) *z*-stack

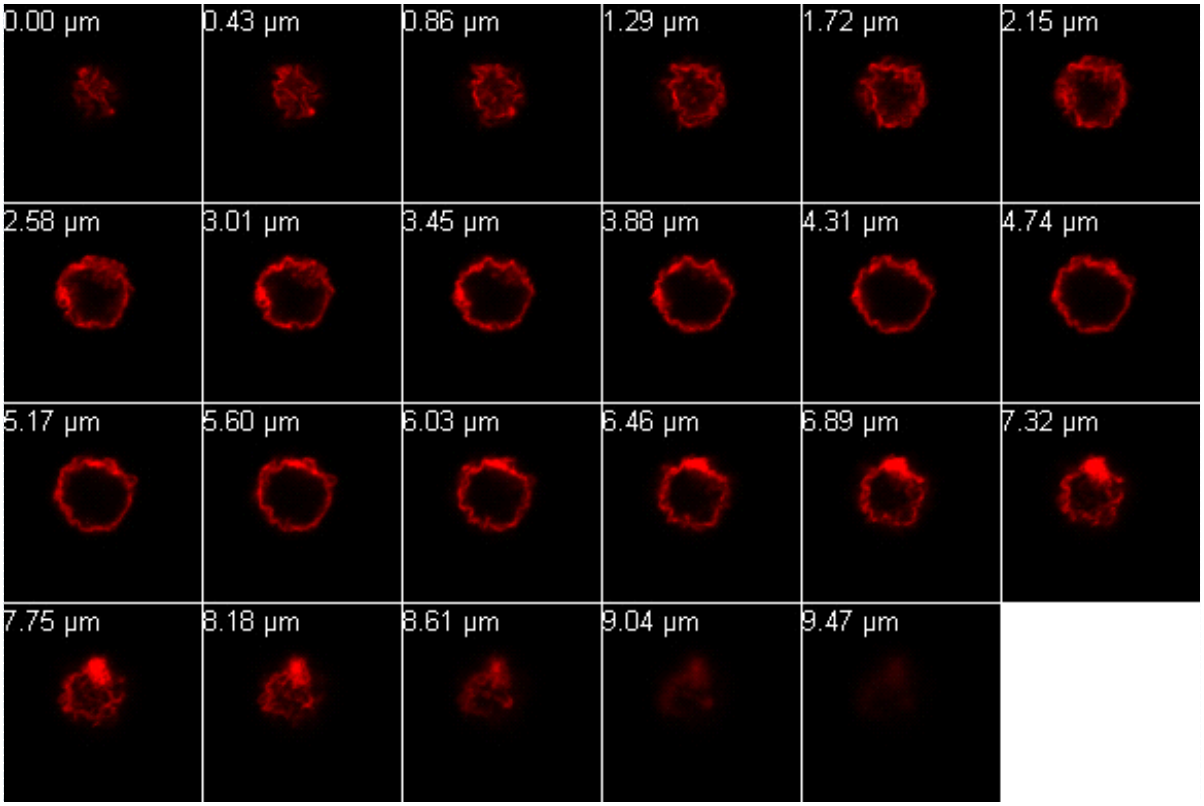

Figure 8.5: Three-dimensional conformation of actin in AML grown in suspension. Cells were stained using phalloidin Alexa 546 and analysed. *Z*-stacks were taken with an inverted Zeiss LSM510 Meta confocal microscope to analyse the three dimensional conformation of actin. Mounted cell samples were analysed using a plan apochromat 63x/ 1.4 oil DIC objective. Excitation of fluorochrome was at 514nm by an argon laser. Emission was collected using a long pass 560 nm filter. Every image of the *z*-stack is presented.

Set up: image size: 224 x 224 pixels/ 24.4 µm x 24.4 µm,
pixel time: 14.4 µs,
pinhole: 111 µm,
laser transmission : 13%

8.3 Comparison of the actin content of the four model cell lines by flow cytometry

The actin content of the four model cell lines was quantitatively measured by flow cytometry to address the question if, despite the four cell S cells, AML, CHO-S and CCL61 showing a comparable actin conformation when grown in suspension, the actin content could be used to distinguish a CHO suspension phenotype, as the conformation analysis had indicated a higher actin content in the S cells.

8.3.1 Methodology: analysis of actin content

Flow cytometry in combination with phalloidin staining has been used previously to determine the actin content of cells (Rao *et al.*, 1990; Knowles and McCulloch, 1992) and was adopted for this study as a reliable method to evaluate the actin content of the four model cell lines.

The protocol used in this study was based on the same staining protocol as used for confocal analysis because the Alexa 546 fluorochrome could also be measured with the flow cytometer. A typical flow cytometry result for the actin staining of S cells and CCL61 cells is shown in figure 8.6. As the actin staining yielded a clear and easily visible shift in both cell lines the staining results were analysed using two markers in histogram analysis, with one marker (no actin stain) defining the unstained (= negative) population and the other marker (actin staining) defining the stained (= positive) population. For an unstained sample more than 98% of the cells lay within the no-actin-stain marker, whereas for a stained sample 98% of the cells lay within the actin-stain marker. The use of two markers within one histogram, possible due to the very bright staining signal, made a subtraction of the background staining, as done previously for integrin staining, unnecessary. Hence, median fluorescence intensities (MFI) as given by the analysis program could be used to evaluate the actin content of the cell lines. To allow comparison of data sets measured on different days the MFI values were normalised using the MFI of S cells as reference. MFI of S cells was chosen as the reference point as those samples were expected to give the highest MFI values from the result in the confocal microscopy analysis.

8.3.2 Differences in actin content when comparing suspension adapted CHO cells lines to a non-suspension adapted CHO cell line

The actin content was analysed using the method described above. In the first set-up the cell lines were compared when grown in their standard growth conditions, i.e. S cells and CHO-S in

A) example of actin staining for S cells

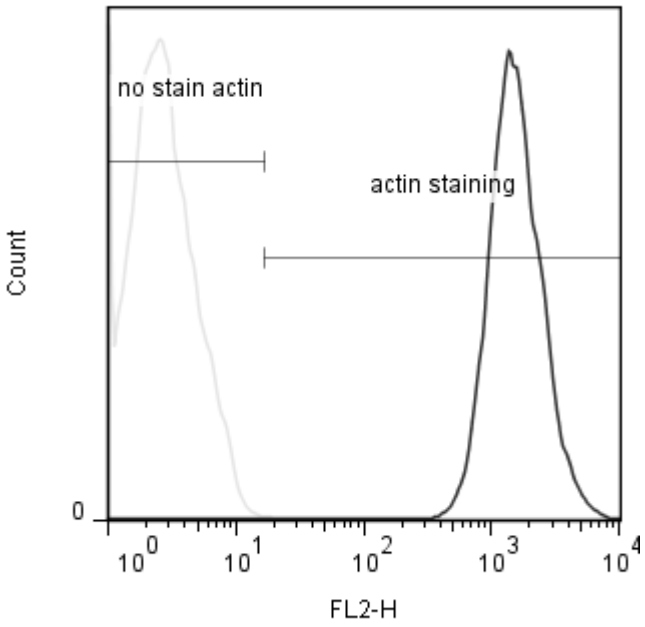

unstained	percentage	MFI
no actin stain	99.8	2.51
actin staining	0.2	22.3

stained	percentage	MFI
no actin stain	0.1 ± 0.0	4.2 ± 1.5
actin staining	99.9 ± 0.1	1470 ± 735.4

B) example of actin staining for CCL61

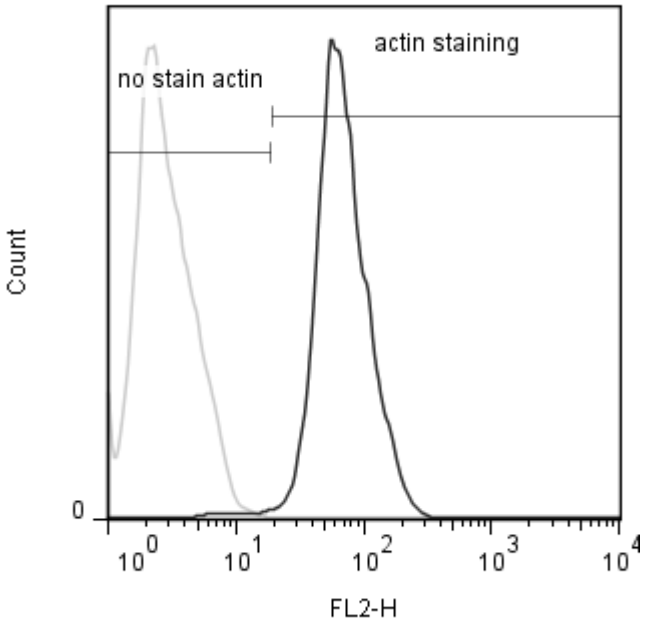

unstained	percentage	MFI
no actin stain	99.8	2.6
actin staining	0.2	28.0

stained	percentage	MFI
no actin stain	1.6 ± 0.2	8.7 ± 0.9
actin staining	98.4 ± 0.2	85.8 ± 45.3

Figure 8.6: Staining examples and analysis method for actin content analysis.
Cells were stained using phalloidin Alexa 546 and analysed by flow cytometry. Staining resulted in a single peak for the stained population with a well defined shift between unstained (light grey) and stained (dark grey) samples. Analysis was performed using two markers defining unstained and stained samples (no stain actin/ actin staining). Markers were kept constant for analysis of one experiment. Markers were set to include > 98% of the population within the FCS gate (not shown). Median fluorescence intensity of the population within the markers was used for analysis. Triplicates of stained samples were analysed. Calculated median fluorescence intensity was used for further analysis and normalisation.

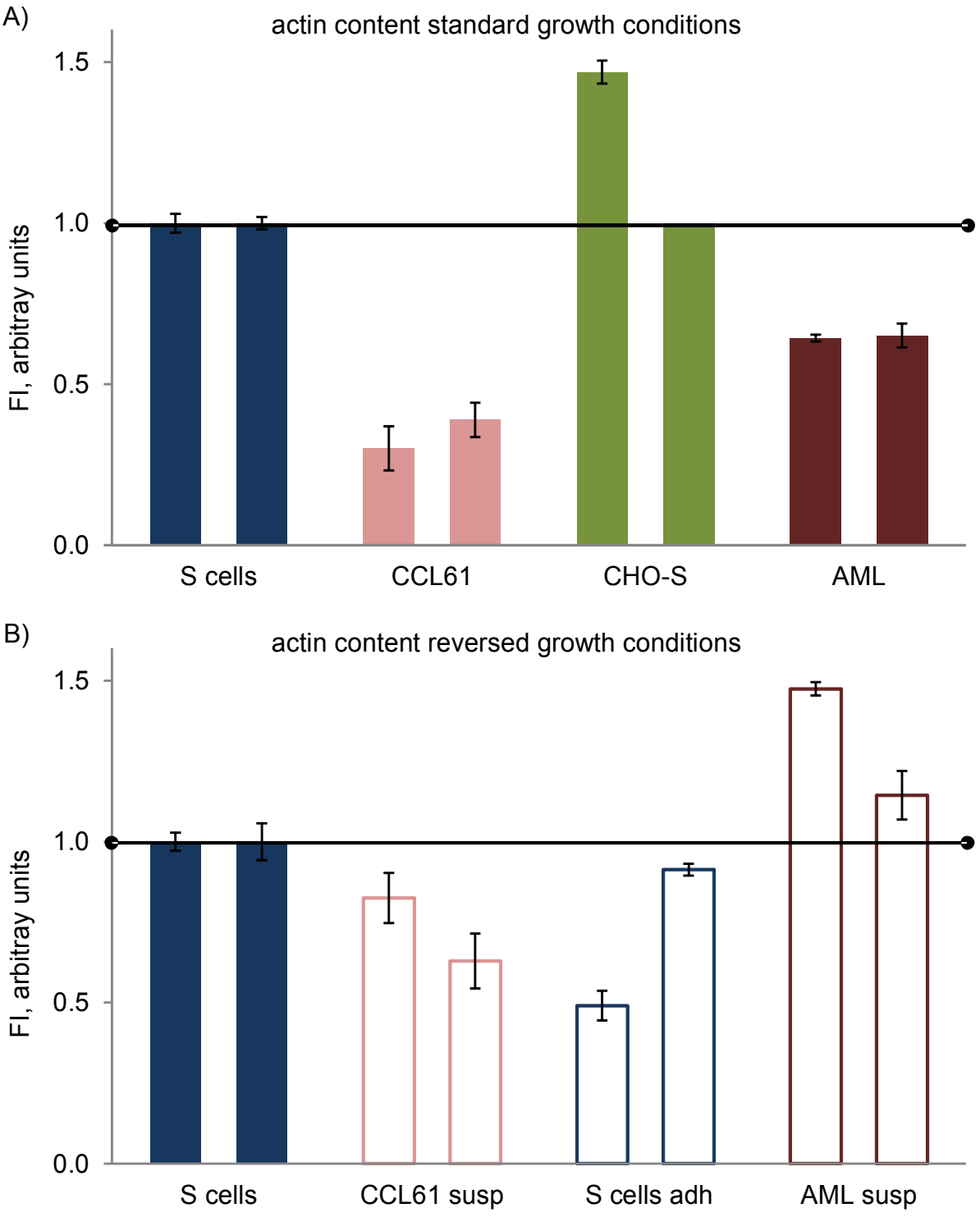

Figure 8.7: Actin content in standard and reversed growth conditions.
Actin content was determined with flow cytometry. For each experiment median fluorescence intensity of randomly chosen passages was determined and normalized against MFI of S cells. Standard deviation of MFI was calculated from triplicates of samples. Upper diagram A) shows results for cell lines grown in their standard growth conditions. Lower diagram B) compares cell lines grown in reversed growth conditions to S cells grown in standard conditions. Cells grown in suspension conditions have a higher actin content than cells grown in adherent conditions.

suspension, AML and CCL61 in adherent culture conditions. In the second set-up S cells, AML and CCL61 were grown in reversed growth conditions. The experiments were repeated twice; each time randomly chosen passages were analysed. As figure 8.7 A) clearly demonstrates, the actin content is higher in the suspension adapted cell lines CHO-S and S cells compared to adherently grown AML and CCL61. There is only a small degree of variation between different passages and the difference in actin content between S cells and CHO-S compared to CCL61 and AML is around a factor of 2, with CCL61 containing even less actin than AML cells.

To examine if the increase in actin content is typical for CHO cells cultured and proliferating in suspension, AML and CCL61 were also cultured in suspension, with the expectation of an increase of the actin content if the actin content was purely a reaction to the cell environment; if only AML cells grown in suspension showed an increase in actin content this would indicate the actin content was an attribute related to successful suspension adaptation. In addition, S cells were grown in adherent mode with the expectation of a decrease in actin content in the case the actin content was related to the cell culture environment.

As figure 8.6 B) demonstrates, CCL61 and the AML up-regulate their actin content although CCL61 are a non-suspension adapted cell lines, indicating that the actin content changes as a reaction to the cell culture environment. This is underlined by the fact that the S cells down-regulate the actin content when grown in adherent conditions. Nevertheless, the up-regulation for CCL61 and the down-regulation for S cells is not as high as seen before where adherent CCL61 cells showed an actin content around a factor of 2 smaller than the S cells.

8.3.3 Discussion of the differences in actin content

It was demonstrated that the amount of actin in the cytoskeleton is up-regulated when CHO cells are grown in suspension. Conformational analysis showed that the cytoskeleton is also rearranged to form a strong sub-cortical sheet of actin when CHO cells are grown in suspension. Hence, the actin cytoskeleton requires a complete rearrangement, from the actin fibre structures across the entire cells to a strong sphere-like actin cytoskeleton, when adherent CHO cells are transferred into suspension. The resulting sub-cortical actin sheet is stronger in the successfully suspension adapted cell lines, S cells, AML and CHO-S, than in CCL61 cells grown in suspension. Nevertheless, CCL61 show a conformation very similar to the described actin conformation when grown in suspension and show an increase in actin content. This indicates that both actin content and conformation are strongly influenced by the cell culture environment; it can be assumed that the

increase in shear stress cells experience in suspension growth conditions due to the continuous shaking plays a major role in this transformation.

The actin content might be used as a measure of successful suspension adaptation when comparing different cell lines if the necessary control samples are included in the measurements. As previous studies have shown the importance of actin cytoskeleton and integrins expressed on the cell surface, and the confocal data for the CCL61 cells grown in suspension indicated a parallel re-formation of the actin cytoskeleton with integrin beta 1 expressed on the cell surface, a further analysis to investigate this interaction has been performed.

8.4 Interrogating the interaction between actin cytoskeleton and integrin beta 1 with cytochalasin D

Lub *et al.* (1997) have demonstrated that it is possible to induce clustering of integrins by cytochalasin D treatment. It has been concluded in this study that suspension adapted CHO cell lines show a specific integrin beta 1 conformation characterised by evenly distributed integrin clusters on the cell surface. Furthermore, the results of the actin analysis has shown that the cytoskeleton is up-regulated in CHO cells grown in suspension and that the actin conformation is linked to the integrin beta 1 conformation. It is hence proposed that it should be possible to introduce the specific integrin beta 1 clustering on non-suspension adapted CHO cells by treating those cells during suspension adaptation with cytochalasin D. This should also allow further analysis of the interplay between integrin beta 1 conformation and actin conformation in suspension growing CHO cell lines.

8.4.1 Methodology: transfer into suspension growth with successive cytochalasin D treatment and recovery period

S cells and CCL61 cells were grown in adherent conditions for four days. Cells were then harvested using trypsin/EDTA followed by the blocking of the trypsin in adherent growth media with FBS and then transferred into PSM media at a seeding density of 0.4 x 10^6/ml (the required cell amount was spun down to avoid FBS supplementation). Cells were treated with 5 µM cytochalasin D (stock concentration 1 mg/ml in ethanol), a concentration that had been tested to show breakdown of the actin cytoskeleton without having a directly negative effect on the viability (see appendix). A control sample was treated with the equivalent amount of ethanol (EtOH). Cells were incubated with cytochalasin D for 8 hours. Samples were stained for actin and integrin beta 1

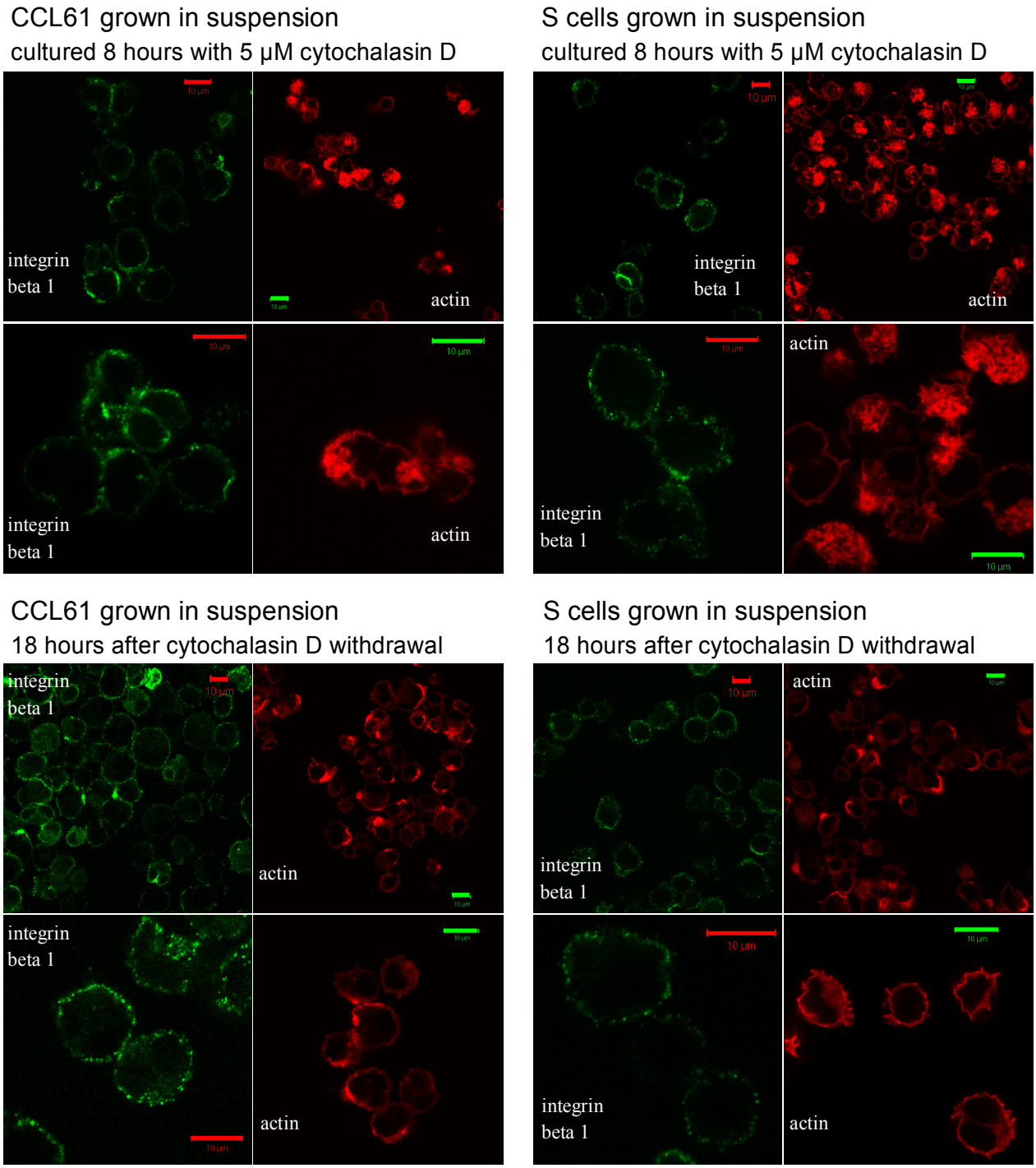

Figure 8.8: Effect of cytochalasin D on integrin and actin conformation in suspension and non-suspension adapted CHO cells.

CCL61 and S cells were transfered into PSM suspension culture with 5 µM cytochalasin D. After 8 hours of suspension culture, the cells were washed to remove cytochalasin D (CD) and cells were re-suspended in PSM and cultured for another 18 hours without CD.

One set of cell samples was analysed for integrin beta 1 and actin conformation after CD treatment and another set was done after the 18 hour recovery period. Imaging was performed using an inverted Zeiss LSM510 Meta confocal microscope. Mounted cell samples were analysed using a plan apochromat 63x/ 1.4 oil DIC objective. Excitation and emission was set as described before. All scale bars equal 10 µm.

confocal analysis at this time point to prove disruption of the actin cytoskeleton by the drug. Cells were spun down to remove cytochalasin D and re-suspended in PSM, re-adjusting the seeding density to 0.4 x 10^6/ml again. Cells were cultured in suspension mode for 18 hours and analysed again with regard to integrin beta 1 and actin conformation.

8.4.2 Influence of cytochalasin D on integrin beta 1 and actin conformation

Figure 8.8 demonstrates clearly that cytochalasin D breaks down the actin conformation of the cells in suspension growth, leading to large irregularly distributed clusters of actin. Nevertheless, no actin filaments have formed across the intracellular parts of the cells. The integrin beta 1 conformation shows irregularly distributed clusters for both cell lines, S cells and CCL61; and in the case of CCL61 also some diffuse, non-clustered expression on the cell surface is noticeable. Furthermore, both cell lines show membrane ruffles to some extent indicating that cells are undergoing an alteration of the properties of the actin network (Mills *et al.*, 2000). After withdrawal of cytochalasin D and culture in PSM media, the actin cytoskeleton conformation resembles very closely the conformation seen before in suspension cells, with a sphere-like sub-cortical sheet of actin, although there are a few areas showing a less even actin distribution than before. This is the case for both cell lines, S cells and CCL61 grown in suspension. The integrin beta 1 conformation after the recovery period shows small, quite regularly distributed clusters of integrins covering the entire cell surface for both cell lines. Hence, the previously seen sphere-like integrin beta 1 conformation has been successfully induced in the non-suspension adapted CCL61 cell line.

This conclusion is further strengthened by the data presented in figure 8.9 and 8.10 which show the three-dimensional conformation of integrin beta 1 on CCL61 cells after the recovery period, with figure 8.9 presenting the results after treatment with cytochalasin D and figure 8.10 presenting the results after treatment with the solvent control ethanol. While the treatment with cytochalasin D yields a *z*-stack for the CCL61 grown in suspension conditions similar to what was seen previously for S cells and AML grown in suspension (figures 7.13 and 7.14), the cells treated with the solvent control ethanol show concentration of the integrin beta 1 in form of large patches where two cells are in contact, as demonstrated previously for CCL61 cells grown in suspension without any treatment. The remaining cell surface is nearly entirely free of integrin beta 1 expression.

It has therefore been clearly demonstrated that integrin beta 1 clustering on CCL61 cells grown in suspension can be induced by treatment with cytochalasin D, resulting in a conformation that can

A) scale

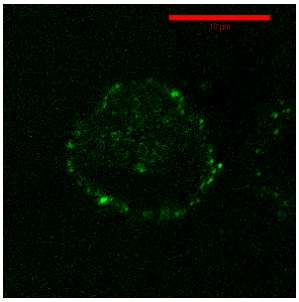

scale bar: 10 µm

B) *z*-stack

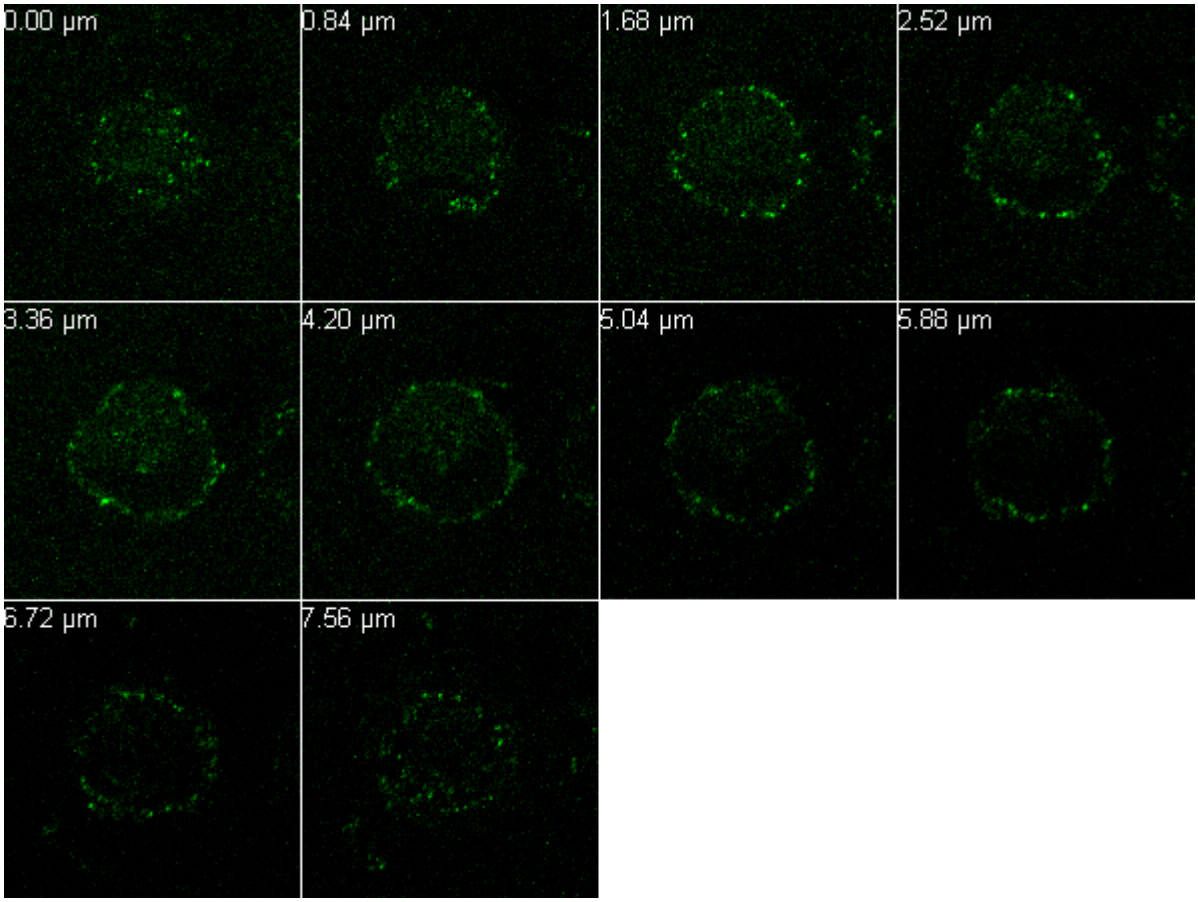

Figure 8.9: Three-dimensional integrin beta 1 conformation after cytochalasin D treatment in non-suspension adapted CCL61.

CCL61 were transferred into PSM suspension culture with 5 µM cytochalasin D. After 8 hours of culture, the cells were washed to remove cytochalasin D (CD) and cells were re-suspended in PSM and cultured for another 18 hours without CD. After the recovery period *z*-stacks were taken with an inverted Zeiss LSM510 Meta confocal microscope to analyse the three-dimensional conformation of integrin beta 1. Every second image of the *z*-stack is presented.

Set up: image size: 296 x 296 pixels; 29.3 µm x 29.3 µm,
pixel time: 11 µs
pinhole: 111 µm
laser transmission: 35%

A) scale

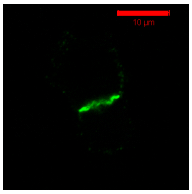

scale bar: 10 µm

B) *z*-stack

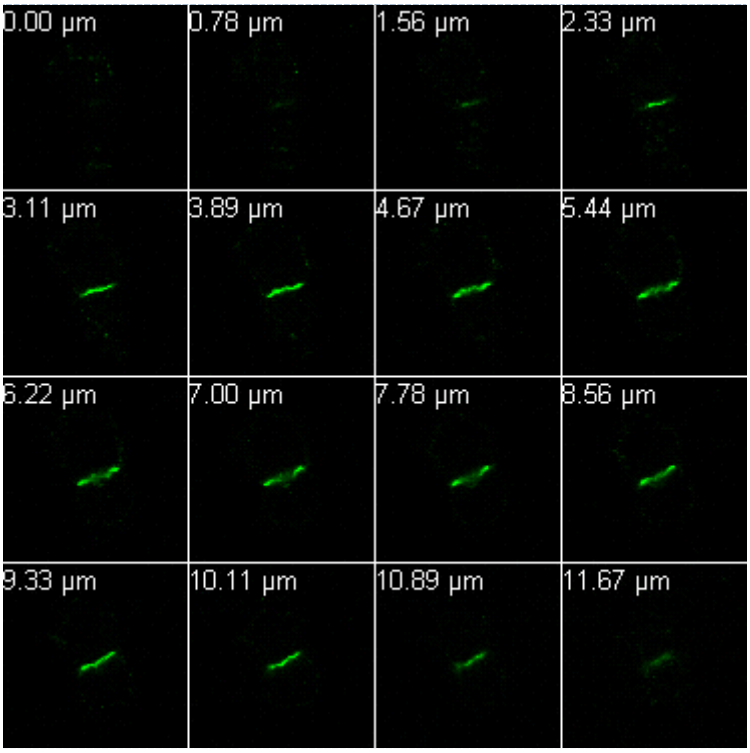

Figure 8.10: Three-dimensional integrin beta 1 conformation after treatment with EtOH (control to cytochalasin D) in non-suspension adapted CCL61.
CCL61 were transferred into PSM suspension culture adding 0.3% EtOH (solvent control). After 8 hours of suspension culture, the cells were washed to remove EtOH and cells were re-suspended in PSM and cultured for another 18 hours.
Z-stack was taken with an inverted Zeiss LSM510 Meta confocal microscope to analyse the three-dimensional conformation of integrin beta 1. Mounted cell samples were analysed using a plan apochromat 63x/ 1.4 oil DIC objective.
Set up: image size: 368 x 368 pixels, 36.6 µm x 36.6 µm
pixel time: 17.8 µs
pinhole: 101 µm
laser transmission: 35%

be regarded as a common feature of suspension adapted CHO cell lines. The successful induction of the integrin beta 1 conformation in CCL61 grown in suspension by cytochalasin D treatment indicates that for suspension adaptation a controlled rearrangement of the actin cytoskeleton in conjunction with a specific change in integrin beta 1 conformation needs to occur. While suspension adapted cells such as S cells, AML and CHO-S can switch the actin and integrin beta 1 conformation between the structures usually seen in adherent cells and the one described before for the suspension phenotype, non-suspension adapted CCL61 are only capable of doing so after breaking down the actin cytoskeleton with cytochalasin D. This difference between S cells, CHO-S and AML could indicate a difference in the proteins involved in the interplay between actin and integrin beta 1.

8.5 Growth of non-suspension adapted CCL61 after cytochalasin D treatment

It was demonstrated that the specific integrin beta 1 clustering typical for suspension adapted CHO cells can be induced by treatment with cytochalasin D on CCL61 cells grown in suspension. The next question to address was whether this switch in conformation allows CCL61 to grow in suspension.

8.5.1 Methodology: suspension growth characteristics after treatment with cytochalasin D

CCL61 cells and S cells were treated with cytochalasin D as described before. After washing out of cytochalasin D, growth characteristics were determined for four days using the same method as in chapter 4. As a control set-up both cell lines were treated with ethanol. The aim was to find out if cytochalasin D treatment allows suspension growth of CCL61 cell comparable to the growth seen in treated S cells.

8.5.2 Influence of cytochalasin D treatment on suspension growth of S cells and CCL61

As figure 8.11 A) shows, CCL61 treated with cytochalasin D do not grow in suspension to a viable cell density comparable to that of S cells treated with cytochalasin D. The result demonstrates that the change of integrin beta 1 conformation induced by cytochalasin D is not sufficient to allow the CCL61 cells to grow in suspension suggesting that the conformational

A) growth results in suspension after treatment with cytochalasin D

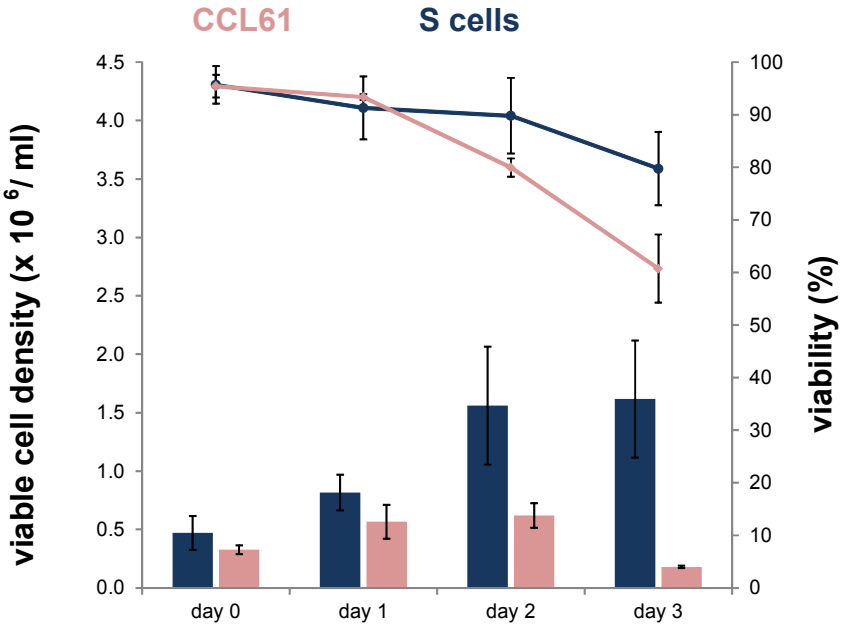

B) growth results: effect of cytochalasin D and solvent control (EtOH)

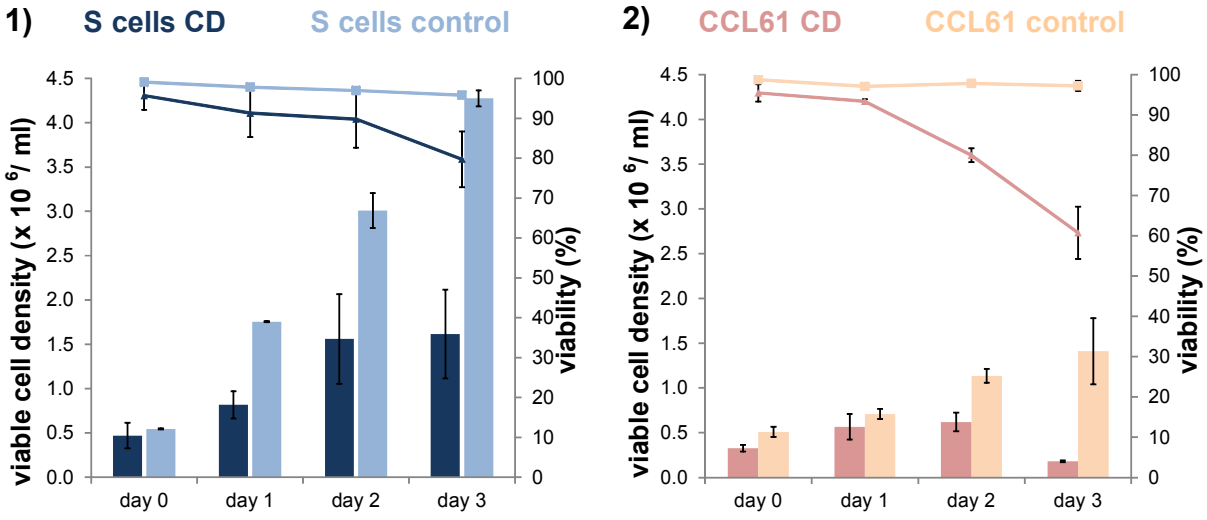

Figure 8.11: Growth results of S cells and CCL61 grown in suspension after treatment with cytochalasin D.

Both cell lines, S cells and CCL61, were grown adherently first. After trypsin harvest and transfer into suspension culture with PSM, 5 µM cytochalasin D (CD) was added to the culture. Controls were treated with equivalent amounts of EtOH (solvent). After 8 hours of suspension culture, the cells were washed to remove CD/EtOH and cells were re-suspended in PSM. Cell growth was monitored for three consecutive days. Viable cell density and viability are plotted. A) compares results of CD treated samples. B) compares effect of CD and EtOH in S cells (1, left) and CCL61 (2, right). Number of independent samples is 3 in all measurements.

change is probably coupled to a change in either downstream signalling from the integrin and/ or a change in the signalling between actin cytoskeleton and integrin and the relevant associated proteins involved. It is noticeable that both cell lines show an early drop in viability after the treatment with cytochalasin D which is very unusual when compared to the viability data seen in the previous growth characterisation. The treatment with cytochalasin D shows an overall negative effect on the growth of the two cell lines, as can also be seen in figure 8.11 B) where the growth of cells treated with the solvent (ethanol) alone is compared to the growth results of the cytochalasin D treated samples. The viability remains above 95% for the ethanol treated samples and the S cells reach a viable cell density of close to 4.5 x 10^6/ml, however, for both cell lines the viability drops below 80% on day 3 (around 60% for CCL61) and the cytochalasin D treated S cells only reach a viable cell density of maximal 1.5 x 10^6/ml. This indicates a loss of cell proliferation and survival signalling for the cytochalasin D treated cells.

8.6 Discussion: Interaction between integrins and actin cytoskeleton

From the specific integrin conformation found to exist on suspension adapted CHO cells as demonstrated in chapter 7 it was hypothesized that there might also be a specific actin conformation for suspension adapted CHO cells as integrins interact closely with the cytoskeleton via the help of numerous associated proteins (Wiesner *et al.*, 2005; Regent *et al.*, 2011). The analysis of the actin conformation with confocal microscopy revealed that all CHO cell lines, whether they were suspension-adapted or not, formed a sphere-like sub-cortical sheet of actin when grown in suspension, a conformation which has been demonstrated before for activated T cells (Barda-Saad *et al.*, 2005) and suspension adapted CHO cells (Hayes *et al.*, 2011). The change between the actin conformation from the adherent conformation characterised by actin fibres running across the entire cell to the sub-cortical sheet in suspension is influenced by the cell culture environment as demonstrated in figures 8.3 and 10.2. The conformational analysis also indicated an orchestrated rearrangement of integrin beta 1 and actin in the CCL61 grown in suspension, as the sphere-like sub-cortical actin sheet showed a higher concentration at the contact area between cells where, as previously demonstrated in figure 7.12, also integrin beta 1 occurs in larger patches. Further analysis of the actin content in the four model cell lines demonstrated that CHO cells grown in suspension up-regulate their actin content in comparison to adherent growth mode and that the actin content found in successfully suspension-adapted CHO cells as S cells, CHO-S and AML is higher than in the non-suspension adapted CCL61.

When probing the degree of interplay between integrin beta 1 and actin by treatment of CCL61 with cytochalasin D to induce integrin clustering as previously demonstrated for lymphocytes by Lub *et al.* (1997) it was found that the specific integrin beta 1 conformation previously seen on S cells, AML and CHO-S could indeed be induced with this treatment. Bakker *et al.* (2012) have also demonstrated an effect of cytochalasin D treatment on integrin clustering with respect to diffusion of integrin nano-clusters.

Nevertheless, when tested for cell growth in suspension conditions using PSM media the CCL61 cells with induced integrin beta 1 clustering were not capable of reaching viable cell densities comparable to those of S cells. One reason for this is clearly the detrimental effect of cytochalasin D on cell growth as seen by the reduced growth for S cells treated in the same way which did not reach their maximal viable cell density after the treatment. Furthermore, the results of the growth test after cytochalasin D treatment indicate that additional changes in, for example, the downstream signalling from integrins and/ or changes in the interaction between actin cytoskeleton and integrin and their associated proteins are necessary for successful suspension adaptation of CHO cells, involving for example MAP kinase and RhoA, which have been demonstrated by Hayes *et al.* (2011) to play a role in cytoskeletal remodelling in CHO cells.

9. Chapter

Conclusion and future work

This study aims to provide a better understanding of the changes the cell surface of CHO cells, major production vehicles in bioprocessing, undergoes in the process of suspension adaptation. Suspension adaptation plays an important part in the biopharmaceutical industry, as state-of-the-art production of recombinant proteins, such as antibodies and cytokines, requires production cell lines to be adapted to suspension and serum-free culture conditions, ideally in a chemically defined media. The transition from a parental adherent cell line such as CCL61 studied here, to a CHO suspension cell line, such as S cells studied here, is hence underlined by a significant change in cell culture environment. Previous studies in this area concentrated on single aspects, such as the influence of specific integrins on adhesion strength.

9.1 Conclusion: from cell characterisation to actin conformation

The four cell lines studied fall into two groups: the first one consisting of the non-suspension adapted CCL61 as the parental cell line, and the second group consisting of S cells, CHO-S and AML as suspension adapted cell lines. The second group can be further divided into two subgroups, with S cells and CHO-S usually cultured in suspension and AML usually being cultured in adherent conditions. It has been shown in this study that none of the suspension adapted cell lines has lost the capability to grow adherently but that adhesion strength varies, with CHO-S showing lowest adhesion capability.

Studying the cell surface of the four model cell lines by biotinylation has indicated that cells growing in suspension differ in the amount of cell surface proteins from adherently grown cells. Enrichment of the cell surface proteins has shown differences in the composition of the cell surface proteome between adherent and suspension cells but also differences of the cell surface proteome between CHO-S and S cells, as one might expect from the different cell growth characteristics. No large variation was noticeable between S cells and AML, two very closely related cell lines.

Unfortunately, enrichment of cell surface proteins from adherent cells proved to be insufficient for analysis by LC-MS/MS with a good proteome coverage. Although several approaches have been tested to yield comparable protein enrichment from suspension and adherent CHO cells, no sufficiently effective protocol could be established. Hence, the original plan of quantitative cell surface proteome analysis based on LC-MS/MS was not pursued further. Nevertheless, those results have established that there is indeed a difference in cell surface proteins between adherent and suspension cells. The results also confirmed that different suspension CHO cell lines differ in their surface proteome.

Flow cytometric analysis of cell-to-cell adhesion molecule expression has demonstrated that the three cell surface proteins CD44, CD56 and E-cadherin show a large variance with bimodal distribution patterns with respect to their expression level between different passages of S cells. This heterogeneity of expression is larger for the S cells than the variance of expression seen in CCL61 for these markers. The results demonstrated further that adaptation of cells to suspension growth conditions leads to a variety of changes in the cell surface proteome. The variable bimodal type of expression of the analysed markers seen for the S cells has had no influence on the growth characteristic of the cell lines as a comparison of different passages with respect to growth revealed no major change of viable cell density reached over time of culture. It has hence been concluded that the cell surface proteins CD44, CD56 and E-cadherin do not necessarily have to be expressed on successfully suspension adapted CHO cells, however, it is interesting to note that in this study the parental CCL61 cell line has shown only low (CD56 and E-cadherin) or non-existing expression (CD44) of these markers.

Integrins are cell surface proteins that on the extracellular side predominantly interact with the extracellular matrix in tissue and the serum proteins in two-dimensional cell culture. As suspension culture conditions exclude serum those cell surface proteins are of major interest in this study. It is known that integrins play a large role in apoptosis and anoikis regulation and that adherent cell lines with lower integrin expression levels are less adhesive in culture. In this study the expression level of integrin beta 1, integrin alpha 4 and integrin alpha 1 has been analysed. As the cell-to-cell adhesion marker expression proved too variable for a comparison of expression levels between cell lines, integrin expression was first studied with respect to expression stability of the three integrins on S cells and CCL61. It could be shown that there is some variation in expression level between

different passages of S cells and CCL61. The degree of variation was different for the three integrins analysed, with integrin beta 1 showing the smallest overall variation. The variation in expression level is larger for S cells than for CCL61 for all three integrins. This is similar to the larger heterogeneity seen for cell-to-cell adhesion molecule expression on S cells when compared to variations between cell-to-cell adhesion molecule expression on CCL61. Nevertheless, all three integrins analysed are expressed on both cell lines in all cells, a result that is underlined by the mass spectrometry results, which have shown expression of integrins on S cells. No bimodal expression pattern has been found for the three integrins, allowing analysis of the difference between the cell surface of suspension adapted cells and adherent cells with regard to integrin expression level using flow cytometry.

Table 9.1 Up- and down-regulation of the three integrins studied in suspension adapted CHO cells.

Reference point is the expression level on adherently grown CCL61. Integrin alpha 1 was not measured in AML suspension. ↓ indicates down-regulation, ↑ up-regulation, ~ nearly constant expression.

cell line	integrin alpha 1	integrin alpha 4	integrin beta 1
S cells	↓	↑	↑
CHO-S	~	↑	↓
AML suspension	n/a	↓	↑

As table 9.1 shows, the three integrins are expressed at different levels on suspension adapted CHO cell lines. No general trend of up- or down-regulation has been found in the data gathered. It is hence concluded that integrin expression levels cannot be used as a tool to describe successfully suspension-adapted CHO cell lines. To analyse if the integrins expressed on the cell surface are functionally active, the integrin beta 1 antibody was used in an adherence blocking experiment with S cells, CHO-S and AML. As mentioned before, these cell lines are all able to grow adherently (with some variation in adhesiveness).

The integrin beta 1 antibody used in this study has been shown to bind to an epitope which is induced by ligand binding or calcium depletion. Furthermore, reduced binding of the antibody has been found to be connected to a reduced adhesion capability of cells. Other studies have used the antibody to block adhesion. In this study the integrin beta 1 antibody only blocked adhesion of CHO-S to a noticeable degree. AML, S cells and CCL61 adhesion was not influenced by the

antibody. Hence, the CHO-S cell lines, which showed a reduced expression level of integrin beta 1 and loss of adhesion in the blocking experiment with integrin beta 1 antibody, are noticeable different from the other suspension-adapted cell lines, S cells and AML. As reduced integrin beta 1 binding has been described by Green *et al.* (2009) to be related to mutations in signalling down-stream of integrin beta 1, CHO-S might differ from S cells and AML not only in their integrin expression level but also in the signalling pathways down-stream of integrin - ligand binding. This is a further indication that different suspension CHO cells might react to suspension adaptation by changing cell surface proteins and intracellular signalling in different ways. Nevertheless, it can be assumed that some suspension-adapted CHO cells will show a decreased integrin beta 1 expression level (using clone 9EG7) combined with reduced adhesion capability, however, this needs not to be true for all suspension adapted CHO cell lines, as shown for S cells. It might also be that a decreased integrin beta 1 expression level is correlated to higher reachable viable cell density, as CHO-S cells have shown much higher viable cell density in the growth characterisation.

As no general trend for down-regulation of integrin across the CHO cell types tested has been found on suspension-adapted CHO cell lines and integrin conformation has been shown to be an important marker of integrin activation status, the integrin conformation was studied using confocal microscopy. The analysis of the three integrins alpha 1, alpha 4 and beta 1 has revealed a specific integrin conformation on CHO-S, S cells and AML in suspension. This conformation is characterised by dot-like clusters of integrins that are evenly distributed over the entire cell surface and hence form sphere-like nets on the cell surface. This conformation is most pronounced for integrin beta 1 on all suspension cell lines, however, the difference seen between integrin alpha 4 and integrin alpha 1 as compared to integrin beta 1 might be due to the differences in signal intensities in confocal analysis of the three markers. It has been demonstrated that the described conformation is a reaction of the cells to their environment, as for S cells and AML this conformation could be induced by changing from adherent cell culture conditions to suspension conditions. In contrast to this, CCL61 grown in suspension do not show this type of conformation. It is hence concluded that dot-like integrin clusters covering the cell surface in an even network are a substantial necessary condition for suspension-adapted CHO cells and might hence be used in the development of suspension cell lines as an endpoint analysis.

One of the main interaction partners of integrins on the intracellular side is the actin cytoskeleton. Integrins do not interact directly with actin but through a larger set of associated

proteins; for example, focal adhesion kinase, tensin and vinculin can bind to the integrin beta tail and actin. The protein interaction complex is thought to depend, with respect to its composition, on the cell type and the integrins and ligands involved. To analyse the role of the integrins expressed on the cell surface of suspension-adapted CHO cells more closely the actin conformation has been studied using confocal microscopy. For adherent cells actin stress fibres running across the entire cell interior could be identified, as one expects for attached cells. In suspension, the actin conformation is changed completely. Actin is then concentrated in sub-cortical ball-like structures enclosing the intracellular volume. This process of conformation change also occurs in CCL61 grown in suspension; there is a small difference to suspension adapted CHO cells, as CCL61 form clumps in suspension culture (three or more cells form groups) and actin is concentrated higher in the contact areas between the cells. This concentration of signal in the contact area of CCL61 clumps was also seen in the integrin beta 1 conformational analysis.

From a comparison of the signal intensity of the actin spheres seen in different cell lines it has been assumed that the actin content between different cell lines varies. Actin content analysis using flow cytometry has revealed that the amount of actin in cells increases when CHO cells are grown in suspension. The increase was strongest in CHO-S, but it was also measurable for S cells and AML grown in suspension. CCL61 grown in suspension also have shown an increase of actin content in comparison to adherent growth but have not reached values measured for fully suspension-adapted cells. The increase in actin content seen in suspension growing CHO cells can be assumed to be a reaction to the shear stress cells undergo by the constant shaking in suspension culture. Increase in actin content might hence be used as an indicator for suspension adaptation when using appropriate controls such as non-suspension adapted cells and suspension-adapted cells, both grown in suspension.

As results of integrin and actin conformation analyses have indicated a dependence between the conformational changes seen for both suspension and non-suspension adapted cells, this interplay has been analysed further with the help of cytochalasin D, an actin disrupting reagent. Cytochalasin D has been used here to induce integrin clustering in non-suspension adapted CCL61 by first breaking down the cytoskeleton with cytochalasin D, followed by a drug free recovery period of 18 hours. Confocal analysis of the integrin beta 1 conformation has revealed that a clustered network of integrin beta 1 could indeed be induced in CCL61 grown in suspension after breakdown of the cytoskeleton with cytochalasin D; also no larger cell clumps have been found in the treated CCL61

cells. S cells treated in the same way regained the specific integrin actin conformation after the recovery period. Hence, integrin clustering in CCL61 grown in suspension could be induced, indicating the need for a structural transformation of integrin conformation in combination with a change or disruption of actin-integrin interaction to allow for this conformation to form.

The strong interaction observed between cytoskeleton and integrin beta 1 in CHO cells could be the reason why a specific integrin conformation has been observed on suspension-adapted CHO cells; integrins might be required to retain the enforced cytoskeleton for suspension cells. As successfully inducing the specific integrin beta 1 conformation in CCL61 grown in suspension reduced the appearance of cell clumps, the integrin conformation might also play a role in reducing cell-to-cell contact and/ or capability of clumping.

Analysing the cell growth of CCL61 cells treated with cytochalasin D has shown that the induced integrin beta 1 conformation is not sufficient for successful growth in suspension. Although the rearrangement of conformation was demonstrated for the treated cells they were not able to grow in suspension and reached viable cell densities lower than those seen for S cells treated the same way. As a comparison with solvent-only treated samples has revealed that cytochalasin D has a negative effect on viable cell densities in S cells, perhaps a less toxic treatment inducing the transformation in conformation might be an alternative to yield better growth results. Nevertheless, as treated CCL61 have not shown growth comparable to treated S cells it can be assumed that additional changes apart from combined integrin/ actin conformation changes need to occur. As the results obtained reveal the importance of the integrin-actin interaction such additional changes might be found in the proteins linking actin and integrin.

9.2 Future work

In this study the emphasis was on the changes the cell surfaces of CHO cells undergo in the adaptation from adherent to suspension growth. As numerous different protocols are applied in this process it would be worthwhile to quantitatively compare the cell surface proteome of different suspension adapted CHO cells using mass spectrometry to prove the hypothesis indicated by this study that the cell surfaces of different suspension-adapted CHO cell lines varies in their cell surface proteome. This would allow using the same sample preparation process enabling comparable efficient cell surface protein enrichment. Data analysis would also be improved by the fact that the CHO genome has recently been sequenced (Baycin-Hizal *et al.*, 2012), thereby allowing proteomic data analysis against C*ricetulus griseus* proteins instead of rodents, as

attempted in this study, hence improving the reliability of protein identification. The results could give an overview of the differences and the similarities between suspension adapted CHO cells and one could try to link those to certain other cell line characteristics, such as growth, capability of transfection or protein secretion by using cell lines differing in those capabilities.

With regards to cell-to-cell adhesion molecule expression, a possible further line of investigation would be to monitor molecules such as CD44, CD56 and E-cadherin during a cell suspension adaptation process to see how the change from low expression on adherent cells to a bimodal distribution on suspension cells occurs, e.g. if a positive population builds up slowly or if within a few passages most cells express these proteins and later-on lose their expression again. If the latter is the case this might indicate changes in intracellular processes, such as DNA transcription or mRNA translation regulation, to play a role in suspension adaptation. It would also be interesting to analyse if the expression of the three markers is in some way correlated, e.g. if cells expressing CD44 also express CD56 and E-cadherin, as this would indicate that different specific sub-populations arise during suspension adaptation. Such an analysis was attempted in this study with the S cells but yielded unreliable data as the bimodal distribution at the time of analysis was predominantly shifted to non-expressing cells.

It would be useful to establish a more stable integrin expression analysis to generate data with a comparable variance as this would allow the results to be tested more rigorously with statistical methods. One way would be to stain more samples of unfixed cells in one experiment and measure these against internal standards such as fluorescent beads, to compare expression levels between cell lines. This would reduce sample preparation steps and differences possibly induced due to storage duration. On the other hand, the differences observed between passages might well be a naturally occurring fluctuation in expression level due to the heterogeneity of CHO cell lines.

Another route of investigation that would build on the results yielded in this study would be to investigate if integrin beta 1 expression and its down-regulation is generally correlated with higher viable cell density, as indicated by the results seen in this study for CHO-S. In conjunction with analysis of the integrin beta 1 conformation and actin content this approach might allow the establishment of threshold values for a suspension phenotype describing a CHO cell line with optimal growth characteristics. This analysis should also include fast growing suspension cell lines adapted to different media, e.g. with and without insulin or zinc, to allow a study of the influence of these factors on integrin expression and conformation. In addition, it would be important to analyse the influence of the integrin beta 1 conformation and expression level with regard to the

characteristic of clump formation in cell culture. This could yield a better understanding of the role of the cell surface protein expression and conformation of the process of cell clumping, which is a problem frequently encountered in bio-pharmaceutical industry.

As the treatment with cytochalasin D has demonstrated the importance of the interaction between integrin and actin cytoskeleton in suspension adaptation, it would be important to study this process in more detail to gain a better understanding of the changes in intracellular processes that are possibly important in suspension adaptation. This could include a detailed study of the proteins involved in integrin-actin interaction such as vinculin, talin, focal adhesion kinase, with regard to their respective expression, activation and localisation in the cell. The results might indicate how one could directly influence the changes necessary for suspension adaptation. Furthermore, such a study could be extended to the signalling pathways downstream of the integrins as the appearance of the suspension specific integrin clusters also indicates that changes in intracellular signalling might occur in suspension adaptation as has been attempted in a parallel PhD project.

The results gained here with regard to integrin conformation and expression are based on suspension adapted but non-producing cell lines. As establishing production cell lines includes numerous steps, thereby applying additional selection pressure, it would be important to analyse if the specific integrin conformation and actin up-regulation found for suspension adapted cells in this study can be found in industrial production cell lines as well. If the results indicated the same integrin conformation and actin up-regulation for production cell lines, this would strengthen the concept that these characteristics are important for suspension adapted cells. Furthermore, one could analyse the influence of different transfection and selection procedures on those characteristics and eventually optimise the choice of a certain cell clone for production by using integrin and actin conformation as an additional selection step ensuring that the cell line chosen will show a stable suspension phenotype.

10. Chapter

Appendix

10.1 Mass spectrometry: protein identification results

10.1.1 CCL61: List of proteins identified

Table 10.1 Proteins identified for CCL61 and designated to be localised in 'membrane'

Italics mark proteins identified more than once (in different organism).

Accession	Entry name	Protein names	Subcellular locations	Organism
Q5SSE9	ABCAD_MOUSE	ATP-binding cassette sub-family A member 13	Membrane; Multi-pass membrane protein;	Mus musculus (Mouse)
Q99PA3	BASI_CRIGR	Basigin (CD antigen CD147) (Fragment)	Cell membrane; Single-pass type I membrane protein; Melanosome;	Cricetulus griseus (Chinese hamster)
P54290	CA2D1_RAT	Voltage-dependent calcium channel subunit alpha-2/delta-1 (Voltage-gated calcium channel subunit alpha-2/delta-1)	Membrane; Single-pass type I membrane protein;	Rattus norvegicus (Rat)
P47934	CACP_MOUSE	Carnitine O-acetyltransferase (Carnitine acetylase) (EC 2;3;1;7) (Carnitine acetyltransferase) (CAT) (CrAT)	Endoplasmic reticulum; Peroxis-ome; Mitochon-drion inner mem-brane; Peri-pheral membrane protein; Matrix side;	Mus musculus (Mouse)
Q704S8	*CACP_RAT*	*Carnitine O-acetyltransferase (Carnitine acetylase) (EC 2;3;1;7) (Carnitine acetyltransferase) (CAT) (CrAT)*	*Endoplasmic re-ticulum; Peroxi-some; Mito-chondrion inner membran; Peri-pheal membrane protein; Matrix side;*	*Rattus norvegicus (Rat)*

Accession	Entry name	Protein names	Subcellular locations	Organism
Q3TVA9	CC136_MOUSE	Coiled-coil domain-containing protein 136	Membrane; Single-pass membrane protein;	Mus musculus (Mouse)
Q4V885	COL12_RAT	Collectin-12 (Collectin placenta protein 1) (CL-P1) (Nurse cell scavenger receptor 2)	Membrane; Single-pass type II membrane protein;	Rattus norvegicus (Rat)
P20816	CP4A2_RAT	Cytochrome P450 4A2 (CYPIVA2) (Cytochrome P-450 K-2) (Cytochrome P450 K-5) (Cytochrome P450-LA-omega 2) (Lauric acid omega-hydroxylase) (EC 1;14;15;3)	Endoplasmic reticulum membrane; Peripheral membrane protein; Microsome membrane; Peripheral membrane protein;	Rattus norvegicus (Rat)
P59764	DOCK4_MOUSE	Dedicator of cytokinesis protein 4	Endomembrane system; Peripheral membrane protein;	Mus musculus (Mouse)
Q8K3H0	DP13A_MOUSE	DCC-interacting protein 13-alpha (Dip13-alpha) (Adapter protein containing PH domain; PTB domain and leucine zipper motif 1)	Early endosome membrane; Peripheral membrane protein; Nucleus;	Mus musculus (Mouse)
P17182	ENOA_MOUSE	Alpha-enolase (EC 4;2;1;11) (2-phospho-D-glycerate hydro-lyase) (Enolase 1) (Non-neural enolase) (NNE)	Cytoplasm; Cell membrane;	Mus musculus (Mouse)
P39087	GRIK2_MOUSE	Glutamate receptor; ionotropic kainate 2 (Glutamate receptor 6) (GluR-6) (GluR6) (Glutamate receptor beta-2) (GluR beta-2)	Cell membrane; Multi-pass membrane protein; Cell junction ; synapse ; postsynaptic cell membrane; Multi-pass membrane protein;	Mus musculus (Mouse)
Q61647	HAS1_MOUSE	Hyaluronan synthase 1 (EC 2;4;1;212) (Hyaluronate synthase 1) (Hyaluronic acid synthase 1) (HA synthase 1)	Membrane; Multi-pass membrane protein;	Mus musculus (Mouse)
Q920H8	HEPH_RAT	Hephaestin (EC 1;-;-;-)	Membrane; Single-pass type I membrane protein;	Rattus norvegicus (Rat)
A2AAE1	K1109_MOUSE	Uncharacterized protein KIAA1109 (Fragile site-associated protein homolog)	Membrane; Single-pass membrane protein;	Mus musculus (Mouse)

Accession	Entry name	Protein names	Subcellular locations	Organism
P04104	K2C1_MOUSE	Keratin; type II cytoskeletal 1 (67 kDa cytokeratin) (Cytokeratin-1) (CK-1) (Keratin-1) (K1) (Type-II keratin Kb1)	Cell membrane;	Mus musculus (Mouse)
Q60675	LAMA2_MOUSE	Laminin subunit alpha-2 (Laminin M chain) (Laminin-12 subunit alpha) (Laminin-2 subunit alpha) (Laminin-4 subunit alpha) (Merosin heavy chain)	Secreted ; extracellular space; extracellular matrix; basement membrane;	Mus musculus (Mouse)
Q61092	LAMC2_MOUSE	Laminin subunit gamma-2 (Epiligrin subunit gamma) (Kalinin subunit gamma) (Kalinin/nicein/epiligrin 100 kDa subunit) (Laminin B2t chain) (Laminin-5 subunit gamma) (Nicein subunit gamma)	Secreted ; extracellular space; extracellular matrix; basement membrane;	Mus musculus (Mouse)
Q8BI84	MIA3_MOUSE	Melanoma inhibitory activity protein 3 (Transport and Golgi organization protein 1) (TANGO1)	Endoplasmic reticulum membrane; Single-pass type I membrane protein;	Mus musculus (Mouse)
O55164	MPDZ_RAT	Multiple PDZ domain protein (Multi-PDZ domain protein 1)	Endomembrane system; Cell junction ; tight junction; Apical cell membrane; Cell junction; synapse; Apical cell membrane; Cell junction; synapse; postsynaptic cell membrane ; postsynaptic density; Cell projection; dendrite; Cell junction ; synapse; synaptosome;	Rattus norvegicus (Rat)
Q9JLN9	MTOR_MOUSE	Serine/threonine-protein kinase mTOR (EC 2;7;11;1) (FK506-binding protein 12-rapamycin complex-associated protein 1) (FKBP12-rapamycin complex-associated protein) (Mammalian target of rapamycin) (mTOR) (Mechanistic target of rapamycin) (Rapamycin target protein 1) (RAPT1)	Endoplasmic reticulum membrane; Peripheral membrane protein; Cytoplasmic side; Golgi apparatus membrane; Mitochondrion outer membrane; Lysosome;	Mus musculus (Mouse)

Accession	Entry name	Protein names	Subcellular locations	Organism
A2AQP0	MYH7B_MOUSE	Myosin-7B (Myosin cardiac muscle beta chain) (Myosin heavy chain 7B; cardiac muscle beta isoform)	Membrane; Peripheral membrane protein;	Mus musculus (Mouse)
Q99MZ6	MYO7B_MOUSE	Myosin-VIIb	Apical cell membrane;	Mus musculus (Mouse)
Q7TN88	PK1L2_MOUSE	Polycystic kidney disease protein 1-like 2 (PC1-like 2 protein) (Polycystin-1L2)	Membrane; Multi-pass membrane protein;	Mus musculus (Mouse)
O88488	PTPRQ_RAT	Phosphotidylinositol phosphatase PTPRQ (EC 3;1;3;-) (Protein-tyrosine phosphatase receptor-type expressed by glomerular mesangial cells protein 1) (rPTP-GMC1) (Receptor-type tyrosine-protein phosphatase Q) (PTP-RQ) (R-PTP-Q) (EC 3;1;3;48)	Cell membrane; Single-pass type I membrane protein;	Rattus norvegicus (Rat)
Q9D620	RFIP1_MOUSE	Rab11 family-interacting protein 1 (Rab11-FIP1) (Rab-coupling protein)	Recycling endosome; Cytoplasmic vesicle ; phagosome membrane;	Mus musculus (Mouse)
O89026	ROBO1_MOUSE	Roundabout homolog 1	Membrane; Single-pass type I membrane protein;	Mus musculus (Mouse)
Q01887	RYK_MOUSE	Tyrosine-protein kinase RYK (EC 2;7;10;1) (Kinase VIK) (Met-related kinase) (NYK-R)	Membrane; Single-pass type I membrane protein;	Mus musculus (Mouse)
Q6QIY3	SCNAA_MOUSE	Sodium channel protein type 10 subunit alpha (Peripheral nerve sodium channel 3) (PN3) (Sensory neuron sodium channel) (Sodium channel protein type X subunit alpha) (Voltage-gated sodium channel subunit alpha Nav1;8)	Membrane; Multi-pass membrane protein;	Mus musculus (Mouse)
O35412	SI1L1_RAT	Signal-induced proliferation-associated 1-like protein 1 (SIPA1-like protein 1) (SPA-1-like protein p1294) (Spine-associated Rap GTPase-activating protein) (SPAR)	Cytoplasm; cytoskeleton; Cell junction ; synapse; postsynaptic cell membrane ; postsynaptic density; Cell junction; synapse ; synaptosome;	Rattus norvegicus (Rat)
P23739	SUIS_RAT	Sucrase-isomaltase; intestinal [Cleaved into: Sucrase (EC 3;2;1;48); Isomaltase (EC 3;2;1;10)]	Apical cell membrane; Single-pass type II membrane protein;	Rattus norvegicus (Rat)

Accession	Entry name	Protein names	Subcellular locations	Organism
Q6ZWR6	SYNE1_MOUSE	Nesprin-1 (Enaptin) (Myocyte nuclear envelope protein 1) (Myne-1) (Nuclear envelope spectrin repeat protein 1) (Synaptic nuclear envelope protein 1) (Syne-1)	Nucleus outer membrane; Single-pass type IV membrane protein; Cytoplasmic side; Cytoplasm; cytoskeleton; Cytoplasm ; myofibril; sarcomere;	Mus musculus (Mouse)
Q9EQU3	TLR9_MOUSE	Toll-like receptor 9 (CD antigen CD289)	Endoplasmic reticulum membrane; Single-pass type I membrane protein; Endosome; Lysosome; Cytoplasmic vesicle ; phagosome;	Mus musculus (Mouse)
Q2QI47	USH2A_MOUSE	Usherin (Usher syndrome type IIa protein homolog) (Usher syndrome type-2A protein homolog)	Cell projection; stereocilium membrane; Single-pass type I membrane protein; Secreted;	Mus musculus (Mouse)

10.1.2 S cells: List of proteins identified

Table 10.2 Proteins identified for S cells and designated to be localised in 'membrane' Italics mark the proteins identified more than once (in different organism);

Accession	Entry name	Protein names	Subcellular locations	Organism
Q9Z1T6	FYV1_MOUSE	1-phosphatidylinositol-3-phosphate 5-kinase (Phosphatidylinositol-3-phosphate 5-kinase) (EC 2;7;1;150) (FYVE finger-containing phosphoinositide kinase) (PIKfyve) (Phosphatidylinositol-3-phosphate 5-kinase type III) (PIPkin-III) (Type III PIP kinase) (p235)	Cytoplasmic vesicle membrane; Peripheral membrane protein; Endosome membrane;	Mus musculus (Mouse)
Q8K4S1	PLCE1_MOUSE	1-phosphatidylinositol-4;5-bisphosphate phosphodiesterase epsilon-1 (EC 3;1;4;11) (Phosphoinositide phospholipase C-epsilon-1) (Phospholipase C-epsilon-1) (PLC-epsilon-1)	Cytoplasm; cytosol; Cell membrane; Golgi apparatus membrane;	Mus musculus (Mouse)

Accession	Entry name	Protein names	Subcellular locations	Organism
Q99P84	*PLCE1_RAT*	*1-phosphatidylinositol-4;5-bisphosphate phosphodiesterase epsilon-1 (EC 3;1;4;11) (Phosphoinositide phospholipase C-epsilon-1) (Phospholipase C-epsilon-1) (PLC-epsilon-1)*	*Cytoplasm ;cytosol; Cell membrane; Golgi apparatus membrane;*	*Rattus norvegicus (Rat)*
A2AP18	PLCH2_MOUSE	1-phosphatidylinositol-4;5-bisphosphate phosphodiesterase eta-2 (EC 3;1;4;11) (Phosphoinositide phospholipase C-eta-2) (Phosphoinositide phospholipase C-like 4) (PLC-L4) (Phospholipase C-like protein 4) (Phospholipase C-eta-2) (PLC-eta2)	Cytoplasm; Cell membrane;	Mus musculus (Mouse)
Q60991	CP7B1_MOUSE	25-hydroxycholesterol 7-alpha-hydroxylase (Oxysterol 7-alpha-hydroxylase) (EC 1;14;13;100) (Cytochrome P450 7B1) (Hippocampal transcript 1 protein) (HCT-1)	Endoplasmic reticulum membrane; Peripheral membrane protein; Microsome membrane; Peripheral membrane protein;	Mus musculus (Mouse)
Q01237	HMDH_MOUSE	3-hydroxy-3-methylglutaryl-coenzyme A reductase (HMG-CoA reductase) (EC 1;1;1;34)	Endoplasmic reticulum membrane; Multi-pass membrane protein; Peroxisome membrane;	Mus musculus (Mouse)
P51639	*HMDH_RAT*	*3-hydroxy-3-methylglutaryl-coenzyme A reductase (HMG-CoA reductase) (EC 1;1;1;34)*	*Endoplasmic reticulum membrane; Multi-pass membrane protein;*	*Rattus norvegicus (Rat)*
P10852	4F2_MOUSE	4F2 cell-surface antigen heavy chain (4F2hc) (CD antigen CD98)	Apical cell membrane; Single-pass type II membrane protein; Melanosome;	Mus musculus (Mouse)
Q99J27	ACATN_MOUSE	Acetyl-coenzyme A transporter 1 (AT-1) (Acetyl-CoA transporter 1) (Solute carrier family 33 member 1)	Endoplasmic reticulum membrane; Multi-pass membrane protein;	Mus musculus (Mouse)
O54967	ACK1_MOUSE	Activated CDC42 kinase 1 (ACK-1) (EC 2;7;10;2) (Non-receptor protein tyrosine kinase Ack) (Tyrosine kinase non-receptor protein 2)	Cell membrane; Cell junction;adherens junction;	Mus musculus (Mouse)

Accession	Entry name	Protein names	Subcellular locations	Organism
Q9Z1K7	APC2_MOUSE	Adenomatous polyposis coli protein 2	Cytoplasm; Golgi apparatus membrane; Peripheral membrane protein; Cytoplasmic side; Cell membrane; Peripheral membrane protein; Cytoplasmic side; Cytoplasm ;cytoskeleton;	Mus musculus (Mouse)
Q8C0T9	ADCYA_MOUSE	Adenylate cyclase type 10 (EC 4;6;1;1) (Germ cell soluble adenylyl cyclase) (sAC) (Testicular soluble adenylyl cyclase)	Cell membrane; Peripheral membrane protein; Cytoplasmic side; Cytoplasm;cytoskeleton; Cytoplasm ;perinuclear region;	Mus musculus (Mouse)
Q9Z286	*ADCYA_RAT*	*Adenylate cyclase type 10 (EC 4;6;1;1) (Germ cell soluble adenylyl cyclase) (sAC) (Testicular soluble adenylyl cyclase)*	*Cell membrane; Peripheral membrane protein; Cytoplasmic side; Cytoplasm;cytoskeleton; Mitochondrion; ;perinuclear region; ;centrosome ;centriole;*	*Rattus norvegicus (Rat)*
P17182	ENOA_MOUSE	Alpha-enolase (EC 4;2;1;11) (2-phospho-D-glycerate hydro-lyase) (Enolase 1) (Non-neural enolase) (NNE)	Cytoplasm; Cell membrane;	Mus musculus (Mouse)
Q8C8R3	ANK2_MOUSE	Ankyrin-2 (ANK-2) (Brain ankyrin)	Cytoplasm;cytoskeleton; Membrane; Cyto-plasm; myofibril; sarcomere; M-band; Apical cell membrane; Cell membrane;	Mus musculus (Mouse)
P21958	TAP1_MOUSE	Antigen peptide transporter 1 (APT1) (ATP-binding cassette sub-family B member 2) (Histocompatibility antigen modifier 1) (Peptide transporter TAP1)	Endoplasmic reticulum membrane; Multi-pass membrane protein;	Mus musculus (Mouse)

Accession	Entry name	Protein names	Subcellular locations	Organism
P36370	*TAP1_RAT*	*Antigen peptide transporter 1 (APT1) (ATP-binding cassette sub-family B member 2) (Peptide transporter TAP1)*	*Endoplasmic reticulum membrane; Multi-pass membrane protein;*	*Rattus norvegicus (Rat)*
O35643	AP1B1_MOUSE	AP-1 complex subunit beta-1 (Adapter-related protein complex 1 subunit beta-1) (Adaptor protein complex AP-1 subunit beta-1) (Beta-1-adaptin) (Beta-adaptin 1) (Clathrin assembly protein complex 1 beta large chain) (Golgi adaptor HA1/AP1 adaptin beta subunit)	Golgi apparatus; Cytoplasmic vesicle ;clathrin-coated vesicle membrane; Peripheral membrane protein; Cytoplasmic side;	Mus musculus (Mouse)
P17426	AP2A1_MOUSE	AP-2 complex subunit alpha-1 (100 kDa coated vesicle protein A) (Adapter-related protein complex 2 alpha-1 subunit) (Adaptor protein complex AP-2 subunit alpha-1) (Alpha-adaptin A) (Alpha1-adaptin) (Clathrin assembly protein complex 2 alpha-A large chain) (Plasma membrane adaptor HA2/AP2 adaptin alpha A subunit)	Cell membrane; Membrane;coated pit; Peripheral membrane protein; Cytoplasmic side;	Mus musculus (Mouse)
Q9Z1T1	AP3B1_MOUSE	AP-3 complex subunit beta-1 (Adapter-related protein complex 3 subunit beta-1) (Adaptor protein complex AP-3 subunit beta-1) (Beta-3A-adaptin) (Clathrin assembly protein complex 3 beta-1 large chain)	Golgi apparatus; Cytoplasmic vesicle ;clathrin-coated vesicle membrane; Peripheral membrane protein; Cytoplasmic side; Golgi apparatus;	Mus musculus (Mouse)
Q9QWY8	ASAP1_MOUSE	Arf-GAP with SH3 domain; ANK repeat and PH domain-containing protein 1 (130 kDa phosphatidylinositol 4;5-biphosphate-dependent ARF1 GTPase-activating protein) (ADP-ribosylation factor-directed GTPase-activating protein 1) (ARF GTPase-activating protein 1) (Development and differentiation-enhancing factor 1) (DEF-1) (Differentiation-enhancing factor 1) (PIP2-dependent ARF1 GAP)	Cytoplasm; Membrane;	Mus musculus (Mouse)
Q1AAU6	*ASAP1_RAT*	*Arf-GAP with SH3 domain; ANK repeat & PH domain-containing protein 1 (130 kDa phosphatidylinositol 4;5-biphosphate-dependent ARF1 GTPase-activating protein) (ADP-ribosylation factor-directed GTPase-activating protein 1) (ARF GTPase-activating protein 1) (Development and differentiation-enhancing factor 1) (Diff-erentiation-enhancing factor 1)*	*Cytoplasm; Membrane;*	*Rattus norvegicus (Rat)*

Accession	Entry name	Protein names	Subcellular locations	Organism
Q03265	ATPA_MOUSE	ATP synthase subunit alpha; mitochondrial	Mitochondrion inner membrane;	Mus musculus (Mouse)
P56480	ATPB_MOUSE	ATP synthase subunit beta; mitochondrial (EC 3;6;3;14)	Mitochondrion; Mitochondrion inner membrane;	Mus musculus (Mouse)
Q5SSE9	ABCAD_MOUSE	ATP-binding cassette sub-family A member 13	Membrane; Multi-pass membrane protein;	Mus musculus (Mouse)
Q8K441	ABCA6_MOUSE	ATP-binding cassette sub-family A member 6	Membrane; Multi-pass membrane protein;	Mus musculus (Mouse)
Q91V24	ABCA7_MOUSE	ATP-binding cassette sub-family A member 7	Cell membrane; Multi-pass membrane protein; Golgi apparatus membrane; Endosome membrane;	Mus musculus (Mouse)
Q63563	ABCC9_RAT	ATP-binding cassette sub-family C member 9 (Sulfonylurea receptor 2)	Membrane; Multi-pass membrane protein;	Rattus norvegicus (Rat)
P16067	ANPRB_RAT	Atrial natriuretic peptide receptor 2 (EC 4;6;1;2) (Atrial natriuretic peptide receptor type B) (ANP-B) (ANPR-B) (NPR-B) (Guanylate cyclase B) (GC-B)	Membrane; Single-pass type I membrane protein;	Rattus norvegicus (Rat)
Q80YW5	BSPRY_MOUSE	B box and SPRY domain-containing protein	Cytoplasm; Membrane; Peripheral membrane protein;	Mus musculus (Mouse)
Q05793	PGBM_MOUSE	Basement membrane-specific heparan sulfate proteoglycan core protein (HSPG) [Cleaved into: Endorepellin; LG3 peptide]	Secreted;extracellular space ;extracellular matrix;basement membrane;	Mus musculus (Mouse)
Q99PA3	BASI_CRIGR	Basigin (CD antigen CD147) (Fragment)	Cell membrane; Single-pass type I membrane protein; Melanosome;	Cricetulus griseus (Chinese hamster)
Q9ES38	S27A5_RAT	Bile acyl-CoA synthetase (BACS) (EC 6;2;1;7) (Bile acid-CoA ligase) (BA-CoA ligase) (BAL) (Cholate--CoA ligase) (Fatty acid transport protein 5) (FATP-5) (Solute carrier family 27 member 5) (Very long-chain acyl-CoA synthetase-related protein) (VLACS-related) (VLACSR)	Endoplasmic reticulum membrane; Multi-pass membrane protein;	Rattus norvegicus (Rat)

Accession	Entry name	Protein names	Subcellular locations	Organism
Q9QY30	ABCBB_MOUSE	Bile salt export pump (ATP-binding cassette sub-family B member 11) (Sister of P-glycoprotein)	Membrane; Multi-pass membrane protein;	Mus musculus (Mouse)
Q3UHD1	BAI1_MOUSE	Brain-specific angiogenesis inhibitor 1	Cell membrane; Multi-pass membrane protein;	Mus musculus (Mouse)
Q8CGM1	BAI2_MOUSE	Brain-specific angiogenesis inhibitor 2	Cell membrane; Multi-pass membrane protein;	Mus musculus (Mouse)
Q80ZF8	BAI3_MOUSE	Brain-specific angiogenesis inhibitor 3	Cell membrane; Multi-pass membrane protein;	Mus musculus (Mouse)
Q9R0M0	**CELR2_MOUSE**	Cadherin EGF LAG seven-pass G-type receptor 2 (Flamingo homolog)	Cell membrane; Multi-pass membrane protein;	Mus musculus (Mouse)
Q91ZI0	**CELR3_MOUSE**	Cadherin EGF LAG seven-pass G-type receptor 3	Cell membrane; Multi-pass membrane protein;	Mus musculus (Mouse)
Q99PF4	**CAD23_MOUSE**	Cadherin-23 (Otocadherin)	Cell membrane; Single-pass type I membrane protein;	Mus musculus (Mouse)
P58365	*CAD23_RAT*	*Cadherin-23 (Otocadherin)*	*Cell membrane; Single-pass type I membrane protein;*	*Rattus norvegicus (Rat)*
Q08460	KCMA1_MOUSE	Calcium-activated potassium channel subunit alpha-1 (BK channel) (BKCA alpha) (Calcium-activated potassium channel; subfamily M subunit alpha-1) (K(VCA)alpha) (KCa1;1) (Maxi K channel) (MaxiK) (Slo-alpha) (Slo1) (mSlo1) (Slowpoke homolog) (Slo homolog) (mSlo)	Membrane; Multi-pass membrane protein;	Mus musculus (Mouse)
Q80TJ1	CAPS1_MOUSE	Calcium-dependent secretion activator 1 (Calcium-dependent activator protein for secretion 1) (CAPS-1)	Cytoplasmic vesicle membrane; Peripheral membrane protein; Cytoplasmic side; Cell junction ;synapse;	Mus musculus (Mouse)
Q62717	*CAPS1_RAT*	*Calcium-dependent secretion activator 1 (Calcium-dependent activator protein for secretion 1) (CAPS-1) (rCAPS)*	*Cytoplasmic vesicle membrane; Peripheral membrane protein; Cytoplasmic side; Cell junction;synapse;*	*Rattus norvegicus (Rat)*

Accession	Entry name	Protein names	Subcellular locations	Organism
Q8BYR5	CAPS2_MOUSE	Calcium-dependent secretion activator 2 (Calcium-dependent activator protein for secretion 2) (CAPS-2)	Cytoplasmic vesicle membrane; Peripheral membrane protein; Cytoplasmic side; Cell junction ;synapse;	Mus musculus (Mouse)
Q8VI47	MRP2_MOUSE	Canalicular multispecific organic anion transporter 1 (ATP-binding cassette sub-family C member 2)	Membrane; Multi-pass membrane protein;	Mus musculus (Mouse)
P18886	CPT2_RAT	Carnitine O-palmitoyltransferase 2; mitochondrial (EC 2;3;1;21) (Carnitine palmitoyltransferase II) (CPT II)	Mitochondrion inner membrane; Peripheral membrane protein; Matrix side;	Rattus norvegicus (Rat)
P26231	CTNA1_MOUSE	Catenin alpha-1 (102 kDa cadherin-associated protein) (Alpha E-catenin) (CAP102)	Cytoplasm;cytoskeleton; Cell junction ;adherens junction; Cell membrane; Peripheral membrane protein; Cytoplasmic side;	Mus musculus (Mouse)
Q07113	MPRI_MOUSE	Cation-independent mannose-6-phosphate receptor (CI Man-6-P receptor) (CI-MPR) (M6PR) (300 kDa mannose 6-phosphate receptor) (MPR 300) (Insulin-like growth factor 2 receptor) (Insulin-like growth factor II receptor) (IGF-II receptor) (M6P/IGF2 receptor) (M6P/IGF2R) (CD antigen CD222)	Lysosome membrane; Single-pass type I membrane protein;	Mus musculus (Mouse)
Q61490	CD166_MOUSE	CD166 antigen (Activated leukocyte cell adhesion molecule) (Protein DM-GRASP) (CD antigen CD166)	Membrane; Single-pass type I membrane protein;	Mus musculus (Mouse)
Q01062	PDE2A_RAT	cGMP-dependent 3';5'-cyclic phosphodiesterase (EC 3;1;4;17) (Cyclic GMP-stimulated phosphodiesterase) (CGS-PDE) (cGSPDE)	Membrane; Peripheral membrane protein;	Rattus norvegicus (Rat)
Q00657	CSPG4_RAT	Chondroitin sulfate proteoglycan 4 (Chondroitin sulfate proteoglycan NG2) (HSN tumor-specific antigen)	Cell membrane; Single-pass type I membrane protein; Extracellular side; Apical cell membrane; Cell projection lamellipodium; membrane;	Rattus norvegicus (Rat)

Accession	Entry name	Protein names	Subcellular locations	Organism
Q8VHY0	*CSPG4_MOUSE*	*Chondroitin sulfate proteoglycan 4 (Chondroitin sulfate proteoglycan NG2) (Proteoglycan AN2)*	*Apical cell membrane; Single-pass type I membrane protein; Extracellular side; Cell projection;lamellipodium membrane; Single-pass type I membrane protein; Extracellular side;*	*Mus musculus (Mouse)*
Q9Z261	CLD7_MOUSE	Claudin-7	Cell membrane; Multi-pass membrane protein; Lateral cell membrane; Cell junction ;tight junction;	Mus musculus (Mouse)
Q9QZE5	COPG_MOUSE	Coatomer subunit gamma (Gamma-coat protein) (Gamma-COP)	Cytoplasm; Golgi apparatus membrane; Peripheral membrane protein; Cytoplasmic side; Cytoplasmic vesicle;COPI-coated vesicle membrane; Peripheral membrane protein; Cytoplasmic side;	Mus musculus (Mouse)
Q3TVA9	CC136_MOUSE	Coiled-coil domain-containing protein 136	Membrane; Single-pass membrane protein;	Mus musculus (Mouse)
P02463	CO4A1_MOUSE	Collagen alpha-1(IV) chain [Cleaved into: Arresten]	Secreted ;extracellular space;extracellular matrix ;basement membrane;	Mus musculus (Mouse)
Q63870	CO7A1_MOUSE	Collagen alpha-1(VII) chain (Long-chain collagen) (LC collagen)	Secreted;extracellular space ;extracellular matrix;basement membrane;	Mus musculus (Mouse)

Accession	Entry name	Protein names	Subcellular locations	Organism
Q07563	COHA1_MOUSE	Collagen alpha-1(XVII) chain (180 kDa bullous pemphigoid antigen 2) (Bullous pemphigoid antigen 2) [Cleaved into: 120 kDa linear IgA disease antigen homolog]	Cell junction ;hemidesmosome; Membrane; Single-pass type II membrane protein; Secreted; extracellular space extracellular matrix basement membrane;	Mus musculus (Mouse)
Q99MQ5	COPA1_MOUSE	Collagen alpha-1(XXV) chain (CLAC-P) [Cleaved into: Collagen-like Alzheimer amyloid plaque component (CLAC)]	Membrane; Single-pass type II membrane protein;	Mus musculus (Mouse)
Q2UY11	COSA1_MOUSE	Collagen alpha-1(XXVIII) chain	Secreted;extracellular space extracellular matrix basement membrane;	Mus musculus (Mouse)
P08122	CO4A2_MOUSE	Collagen alpha-2(IV) chain [Cleaved into: Canstatin]	Secreted ;extracellular space;extracellular matrix ;basement membrane;	Mus musculus (Mouse)
Q9QZS0	CO4A3_MOUSE	Collagen alpha-3(IV) chain [Cleaved into: Tumstatin]	Secreted;extracellular space ;extracellular matrix;basement membrane;	Mus musculus (Mouse)
Q9QZR9	CO4A4_MOUSE	Collagen alpha-4(IV) chain	Secreted ;extracellular space extracellular matrix basement membrane;	Mus musculus (Mouse)
Q80YA9	CNKR2_MOUSE	Connector enhancer of kinase suppressor of ras 2 (Connector enhancer of KSR 2) (CNK homolog protein 2) (CNK2)	Cytoplasm; Membrane; Peripheral membrane protein;	Mus musculus (Mouse)
Q61330	CNTN2_MOUSE	Contactin-2 (Axonal glycoprotein TAG-1) (Axonin-1) (Transient axonal glycoprotein 1) (TAX-1)	Cell membrane; Lipid-anchor;GPI-anchor;	Mus musculus (Mouse)
Q9JMB8	CNTN6_MOUSE	Contactin-6 (Neural recognition molecule NB-3) (mNB-3)	Cell membrane; Lipid-anchor ;GPI-anchor;	Mus musculus (Mouse)
Q64535	ATP7B_RAT	Copper-transporting ATPase 2 (EC 3;6;3;4) (Copper pump 2) (Pineal night-specific ATPase) (Wilson disease-associated protein homolog)	Golgi apparatus;trans-Golgi net-work membrane; Multi-pass membrane protein;	Rattus norvegicus (Rat)

Accession	Entry name	Protein names	Subcellular locations	Organism
Q64446	ATP7B_MOUSE	Copper-transporting ATPase 2 (EC 3;6;3;4) (Copper pump 2) (Wilson disease-associated protein homolog)	Golgi apparatus ;trans-Golgi network membrane; Multi-pass membrane protein;	Mus musculus (Mouse)
P09605	KCRS_RAT	Creatine kinase S-type; mitochondrial (EC 2;7;3;2) (Basic-type mitochondrial creatine kinase) (Mib-CK) (Sarcomeric mitochondrial creatine kinase) (S-MtCK)	Mitochondrion inner membrane; Peripheral membrane protein; Intermembrane side;	Rattus norvegicus (Rat)
Q923L3	CSMD1_MOUSE	CUB and sushi domain-containing protein 1 (CUB and sushi multiple domains protein 1)	Membrane; Single-pass type I membrane protein;	Mus musculus (Mouse)
O70244	CUBN_RAT	Cubilin (460 kDa receptor) (Glycoprotein 280) (gp280) (Intrinsic factor-cobalamin receptor) (Intrinsic factor-vitamin B12 receptor)	Endosome membrane; Peripheral membrane protein; Lysosome membrane; Peripheral membrane protein;	Rattus norvegicus (Rat)
Q8CIM7	CP2DQ_MOUSE	Cytochrome P450 2D26 (EC 1;14;14;1) (CYPIID26)	Endoplasmic reticulum membrane; Peripheral membrane protein; Microsome membrane;	Mus musculus (Mouse)
Q45VK7	DYHC2_MOUSE	Cytoplasmic dynein 2 heavy chain 1 (Cytoplasmic dynein 2 heavy chain) (Dynein cytoplasmic heavy chain 2) (Dynein heavy chain 11) (mDHC11) (Dynein heavy chain isotype 1B)	Cytoplasm;cytoskeleton ;cilium axoneme; Cell membrane; Peripheral membrane protein; Cytoplasm;	Mus musculus (Mouse)
Q9JJ79	*DYHC2_RAT*	*Cytoplasmic dynein 2 heavy chain 1 (Cytoplasmic dynein 2 heavy chain) (Dynein cytoplasmic heavy chain 2) (Dynein heavy chain isotype 1B) (Dynein-like protein 4)*	*Cytoplasm;cytoskeleton ;cilium axoneme; Cell membrane; Peripheral membrane protein; Cytoplasm;*	*Rattus norvegicus (Rat)*
Q8BUR4	DOCK1_MOUSE	Dedicator of cytokinesis protein 1 (180 kDa protein downstream of CRK) (DOCK180)	Cytoplasm; Membrane;	Mus musculus (Mouse)

Accession	Entry name	Protein names	Subcellular locations	Organism
Q8C3J5	DOCK2_MOUSE	Dedicator of cytokinesis protein 2 (Protein Hch)	Endomembrane system; Peripheral membrane protein; Cytoplasm;cytoskeleton;	Mus musculus (Mouse)
O55111	DSG2_MOUSE	Desmoglein-2	Cell membrane; Single-pass type I membrane protein; Cell junction ;desmosome;	Mus musculus (Mouse)
Q80UP3	DGKZ_MOUSE	Diacylglycerol kinase zeta (DAG kinase zeta) (EC 2;7;1;107) (Diglyceride kinase zeta) (DGK-zeta)	Cytoplasm; Nucleus; Cell membrane;	Mus musculus (Mouse)
Q91ZV2	DCBD2_RAT	Discoidin; CUB and LCCL domain-containing protein 2 (Endothelial and smooth muscle cell-derived neuropilin-like protein)	Membrane; Single-pass type I membrane protein;	Rattus norvegicus (Rat)
Q61824	ADA12_MOUSE	Disintegrin and metalloproteinase domain-containing protein 12 (ADAM 12) (EC 3;4;24;-) (Meltrin-alpha)	Membrane; Single-pass type I membrane protein;	Mus musculus (Mouse)
Q9R1V6	ADA22_MOUSE	Disintegrin and metalloproteinase domain-containing protein 22 (ADAM 22)	Membrane; Single-pass type I membrane protein;	Mus musculus (Mouse)
Q8BPN8	DMXL2_MOUSE	DmX-like protein 2 (Rabconnectin-3)	Cytoplasmic vesicle;secretory vesicle ;synaptic vesicle membrane; Peri-pheral membrane protein;	Mus musculus (Mouse)
Q4VA61	DSCL1_MOUSE	Down syndrome cell adhesion molecule-like protein 1 homolog	Cell membrane; Single-pass type I membrane protein;	Mus musculus (Mouse)
P11531	DMD_MOUSE	Dystrophin	Cell membrane; Peripheral mem-brane protein; Cytoplasmic side; Cytoplasm cyto-skeleton;	Mus musculus (Mouse)
Q5U430	UBR3_MOUSE	E3 ubiquitin-protein ligase UBR3 (EC 6;3;2;-) (N-recognin-3) (Ubiquitin-protein ligase E3-alpha-3) (Zinc finger protein 650)	Membrane; Multi-pass membrane protein;	Mus musculus (Mouse)
Q2TL32	UBR4_RAT	E3 ubiquitin-protein ligase UBR4 (EC 6;3;2;-) (N-recognin-4) (Zinc finger UBR1-type protein 1)	Multi-pass mem-brane protein; Cyto-plasm; Cytoplasm ;cytoskeleton; Nucleus;	Rattus norvegicus (Rat)

Accession	Entry name	Protein names	Subcellular locations	Organism
A2AN08	*UBR4_MOUSE*	*E3 ubiquitin-protein ligase UBR4 (EC 6;3;2;-) (N-recognin-4) (Zinc finger UBR1-type protein 1) (p600)*	*Membrane; Multi-pass membrane protein; Cytoplasm; Cytoplasm;cytoskeleton; Nucleus;*	*Mus musculus (Mouse)*
Q8BL66	EEA1_MOUSE	Early endosome antigen 1	Cytoplasm; Early endosome membrane; Peripheral membrane protein;	Mus musculus (Mouse)
Q69ZW3	EHBP1_MOUSE	EH domain-binding protein 1	Cytoplasm; Membrane;	Mus musculus (Mouse)
Q6RI88	S4A5_RAT	Electrogenic sodium bicarbonate cotransporter 4 (Solute carrier family 4 member 5)	Cell membrane; Multi-pass membrane protein; Basolateral cell membrane; Multi-pass membrane protein;	Rattus norvegicus (Rat)
Q9JJ22	ERAP1_RAT	Endoplasmic reticulum aminopeptidase 1 (EC 3;4;11;-) (ARTS-1) (Adipocyte-derived leucine aminopeptidase) (A-LAP) (Aminopeptidase PILS) (Puromycin-insensitive leucyl-specific aminopeptidase) (PILS-AP)	Endoplasmic reticulum membrane; Single-pass type II membrane protein;	Rattus norvegicus (Rat)
Q9EQH2	*ERAP1_MOUSE*	*Endoplasmic reticulum aminopeptidase 1 (EC 3;4;11;-) (ARTS-1) (Adipocyte-derived leucine aminopeptidase) (A-LAP) (Aminopeptidase PILS) (Puromycin-insensitive leucyl-specific aminopeptidase) (PILS-AP) (VEGF-induced aminopeptidase)*	*Endoplasmic reticulum membrane; Single-pass type II membrane protein;*	*Mus musculus (Mouse)*
P54763	EPHB2_MOUSE	Ephrin type-B receptor 2 (EC 2;7;10;1) (Neural kinase) (Nuk receptor tyrosine kinase) (Tyrosine-protein kinase receptor EPH-3) (Tyrosine-protein kinase receptor SEK-3)	Membrane; Single-pass type I membrane protein;	Mus musculus (Mouse)
Q60902	EP15R_MOUSE	Epidermal growth factor receptor substrate 15-like 1 (Epidermal growth factor receptor pathway substrate 15-related sequence) (Eps15-rs) (Eps15-related protein) (Eps15R)	Cell membrane; Peripheral membrane protein; Nucleus; Membrane ;coated pit;	Mus musculus (Mouse)
Q6IE26	EPHX4_MOUSE	Epoxide hydrolase 4 (EC 3;3;-;-) (Abhydrolase domain-containing protein 7) (Epoxide hydrolase-related protein)	Membrane; Single-pass type II membrane protein;	Mus musculus (Mouse)

Accession	Entry name	Protein names	Subcellular locations	Organism
Q9JIM1	S29A1_MOUSE	Equilibrative nucleoside transporter 1 (Equilibrative nitrobenzylmercaptopurine riboside-sensitive nucleoside transporter) (Equilibrative NBMPR-sensitive nucleoside transporter) (Nucleoside transporter; es-type) (Solute carrier family 29 member 1)	Membrane; Multi-pass membrane protein;	Mus musculus (Mouse)
O70503	DHB12_MOUSE	Estradiol 17-beta-dehydrogenase 12 (EC 1;1;1;62) (17-beta-hydroxysteroid dehydrogenase 12) (17-beta-HSD 12) (3-ketoacyl-CoA reductase) (KAR) (EC 1;3;1;-) (KIK-I)	Endoplasmic reticulum membrane; Multi-pass membrane protein;	Mus musculus (Mouse)
Q3TZZ7	ESYT2_MOUSE	Extended synaptotagmin-2 (E-Syt2)	Cell membrane; Multi-pass membrane protein;	Mus musculus (Mouse)
Q80T14	FRAS1_MOUSE	Extracellular matrix protein FRAS1	Cell membrane; Single-pass type I membrane protein; Extracellular side;	Mus musculus (Mouse)
A3KGK3	FR1L4_MOUSE	Fer-1-like protein 4	Membrane; Single-pass membrane protein;	Mus musculus (Mouse)
Q6P6L0	FIL1L_MOUSE	Filamin A-interacting protein 1-like (Protein down-regulated in ovarian cancer 1 homolog) (DOC-1)	Cytoplasm; Membrane; Nucleus;	Mus musculus (Mouse)
O35346	FAK1_RAT	Focal adhesion kinase 1 (FADK 1) (EC 2;7;10;2) (Protein-tyrosine kinase 2) (pp125FAK)	Cell junction;focal adhesion; Cell membrane; Peripheral membrane protein; Cytoplasmic side;	Rattus norvegicus (Rat)
P35846	FOLR1_MOUSE	Folate receptor alpha (FR-alpha) (Folate receptor 1) (Folate-binding protein 1)	Cell membrane; Lipid-anchor ;GPI-anchor;	Mus musculus (Mouse)
Q6NVD0	FREM2_MOUSE	FRAS1-related extracellular matrix protein 2 (ECM3 homolog) (NV domain-containing protein 1)	Cell membrane; Single-pass type I membrane protein; Extracellular side;	Mus musculus (Mouse)
Q8BKG4	FZD10_MOUSE	Frizzled-10 (Fz-10) (CD antigen CD350)	Membrane; Multi-pass membrane protein;	Mus musculus (Mouse)
Q8BWQ4	FTSJ1_MOUSE	FtsJ methyltransferase domain-containing protein 1 (EC 2;1;1;-)	Membrane; Single-pass membrane protein;	Mus musculus (Mouse)

Accession	Entry name	Protein names	Subcellular locations	Organism
Q5SNZ0	GRDN_MOUSE	Girdin (Akt phosphorylation enhancer) (APE) (Coiled-coil domain-containing protein 88A) (G alpha-interacting vesicle-associated protein) (GIV) (Girders of actin filament) (Hook-related protein 1) (HkRP1)	Membrane; Cell membrane; Cytoplasm;cytosol; Cytoplasmic vesicle; Cell projection ;lamellipodium;	Mus musculus (Mouse)
Q8BMF8	GLDN_MOUSE	Gliomedin (Cancer-related gene liver 2 protein) (CRG-L2)	Cell membrane; Single-pass type II membrane protein;	Mus musculus (Mouse)
Q01097	NMDE2_MOUSE	Glutamate [NMDA] receptor subunit epsilon-2 (N-methyl D-aspartate receptor subtype 2B) (NMDAR2B) (NR2B)	Cell membrane; Multi-pass membrane protein; Cell junction;synapse ;postsynaptic cell membrane;	Mus musculus (Mouse)
Q01098	NMDE3_MOUSE	Glutamate [NMDA] receptor subunit epsilon-3 (N-methyl D-aspartate receptor subtype 2C) (NMDAR2C) (NR2C)	Cell membrane; Multi-pass membrane protein; Cell junction;synapse ;postsynaptic cell membrane;	Mus musculus (Mouse)
P35438	NMDZ1_MOUSE	Glutamate [NMDA] receptor subunit zeta-1 (N-methyl-D-aspartate receptor subunit NR1) (NMD-R1)	Cell membrane; Multi-pass membrane protein; Cell junction;synapse ;postsynaptic cell membrane; Cell junction;synapse ;postsynaptic cell membrane;postsynaptic density;	Mus musculus (Mouse)
P42264	GRIK3_RAT	Glutamate receptor; ionotropic kainate 3 (Glutamate receptor 7) (GluR-7) (GluR7)	Cell membrane; Multi-pass membrane protein; Cell junction ;synapse;postsynaptic cell membrane;	Rattus norvegicus (Rat)

Accession	Entry name	Protein names	Subcellular locations	Organism
Q925T6	GRIP1_MOUSE	Glutamate receptor-interacting protein 1 (GRIP-1)	Cytoplasmic vesicle; Endoplasmic reticulum; Cell junction ;synapse;postsynaptic cell membrane; Membrane; Lipid-anchor;	Mus musculus (Mouse)
Q9WU65	GLPK2_MOUSE	Glycerol kinase 2 (GK 2) (Glycerokinase 2) (EC 2;7;1;30) (ATP:glycerol 3-phosphotransferase 2) (Glycerol kinase; testis specific 2)	Mitochondrion outer membrane; Peripheral membrane protein; Cytoplasmic side; Cytoplasm;	Mus musculus (Mouse)
Q91VW5	GOGA4_MOUSE	Golgin subfamily A member 4 (tGolgin-1)	Cytoplasm; Golgi apparatus membrane; Peripheral membrane protein;	Mus musculus (Mouse)
Q9JJQ0	PIGB_MOUSE	GPI mannosyltransferase 3 (EC 2;4;1;-) (GPI mannosyltransferase III) (GPI-MT-III) (Phosphatidylinositol-glycan biosynthesis class B protein) (PIG-B)	Endoplasmic reticulum membrane; Multi-pass membrane protein;	Mus musculus (Mouse)
Q8VHN7	GPR98_MOUSE	G-protein coupled receptor 98 (Monogenic audiogenic seizure susceptibility protein 1) (Neurepin) (Very large G-protein coupled receptor 1)	Cell membrane; Multi-pass membrane protein; Secreted;	Mus musculus (Mouse)
Q8CHG3	GCC2_MOUSE	GRIP and coiled-coil domain-containing protein 2 (185 kDa Golgi coiled-coil protein) (GCC185)	Cytoplasm; Golgi apparatus ;trans-Golgi network membrane; Peripheral membrane protein;	Mus musculus (Mouse)
O70443	GNAZ_MOUSE	Guanine nucleotide-binding protein G(z) subunit alpha (G(x) alpha chain) (Gz-alpha)	Membrane; Lipid-anchor;	Mus musculus (Mouse)
P55205	GUC2G_RAT	Guanylate cyclase 2G (EC 4;6;1;2) (Guanylyl cyclase receptor G) (GC-G) (Kinase-like domain-containing soluble guanylyl cyclase) (ksGC)	Cell membrane; Single-pass type I membrane protein; Cytoplasm;	Rattus norvegicus (Rat)
Q6TL19	*GUC2G_MOUSE*	*Guanylate cyclase 2G (EC 4;6;1;2) (Guanylyl cyclase receptor G) (mGC-G)*	*Membrane; Single-pass type I membrane protein;*	*Mus musculus (Mouse)*

Accession	Entry name	Protein names	Subcellular locations	Organism
P52785	GUC2E_MOUSE	Guanylyl cyclase GC-E (EC 4;6;1;2) (Guanylate cyclase 2E)	Membrane; Single-pass type I membrane protein;	Mus musculus (Mouse)
P51840	*GUC2E_RAT*	*Guanylyl cyclase GC-E (EC 4;6;1;2) (Guanylate cyclase 2E)*	*Membrane; Single-pass type I membrane protein;*	*Rattus norvegicus (Rat)*
O35387	HAX1_MOUSE	HCLS1-associated protein X-1 (HS1-associating protein X-1) (HAX-1) (HS1-binding protein 1) (HSP1BP-1)	Mitochondrion; Endoplasmic reticulum; Nucleus membrane; Sarcoplasmic reticulum; Cytoplasmic vesicle;	Mus musculus (Mouse)
Q7TSE9	*HAX1_RAT*	*HCLS1-associated protein X-1 (HS1-associating protein X-1) (HAX-1) (HS1-binding protein 1) (HSP1BP-1)*	*Endoplasmic reticulum; Sarcoplasmic reticulum; Cytoplasmic vesicle; Mitochondrion; Nucleus membrane;*	*Rattus norvegicus (Rat)*
Q8BKN6	HS3SA_MOUSE	Heparan sulfate glucosamine 3-O-sulfotransferase 3A1 (EC 2;8;2;23) (Heparan sulfate D-glucosaminyl 3-O-sulfotransferase 3A1) (Heparan sulfate 3-O-sulfotransferase 3A1)	Golgi apparatus membrane; Single-pass type II membrane protein;	Mus musculus (Mouse)
Q3V1H3	HPHL1_MOUSE	Hephaestin-like protein 1 (EC 1;-;-;-)	Membrane; Single-pass type I membrane protein;	Mus musculus (Mouse)
Q6ZPR6	IBTK_MOUSE	Inhibitor of Bruton tyrosine kinase (IBtk)	Cytoplasm; Membrane; Peripheral membrane protein;	Mus musculus (Mouse)
P11881	ITPR1_MOUSE	Inositol 1;4;5-trisphosphate receptor type 1 (IP3 receptor isoform 1) (IP3R 1) (InsP3R1) (Inositol 1;4;5-trisphosphate-binding protein P400) (Protein PCD-6) (Purkinje cell protein 1) (Type 1 inositol 1;4;5-trisphosphate receptor) (Type 1 InsP3 receptor)	Endoplasmic reticulum membrane; Multi-pass membrane protein;	Mus musculus (Mouse)
Q9Z329	ITPR2_MOUSE	Inositol 1;4;5-trisphosphate receptor type 2 (IP3 receptor isoform 2) (IP3R 2) (InsP3R2) (Inositol 1;4;5-trisphosphate type V receptor) (Type 2 inositol 1;4;5-trisphosphate receptor) (Type 2 InsP3 receptor)	Endoplasmic reticulum membrane; Multi-pass membrane protein;	Mus musculus (Mouse)

Accession	Entry name	Protein names	Subcellular locations	Organism
P29995	*ITPR2_RAT*	*Inositol 1;4;5-trisphosphate receptor type 2 (IP3 receptor isoform 2) (IP3R 2) (InsP3R2) (Type 2 inositol 1;4;5-trisphosphate receptor) (Type 2 InsP3 receptor)*	*Endoplasmic reticulum membrane; Multi-pass membrane protein;*	*Rattus norvegicus (Rat)*
P70227	ITPR3_MOUSE	Inositol 1;4;5-trisphosphate receptor type 3 (IP3 receptor isoform 3) (IP3R 3) (InsP3R3) (Type 3 inositol 1;4;5-trisphosphate receptor) (Type 3 InsP3 receptor)	Endoplasmic reticulum membrane; Multi-pass membrane protein;	Mus musculus (Mouse)
Q63269	*ITPR3_RAT*	*Inositol 1;4;5-trisphosphate receptor type 3 (IP3 receptor isoform 3) (IP3R 3) (InsP3R3) (Type 3 inositol 1;4;5-trisphosphate receptor) (Type 3 InsP3 receptor)*	*Endoplasmic reticulum membrane; Multi-pass membrane protein;*	*Rattus norvegicus (Rat)*
Q60751	IGF1R_MOUSE	Insulin-like growth factor 1 receptor (EC 2;7;10;1) (Insulin-like growth factor I receptor) (IGF-I receptor) (CD antigen CD221) [Cleaved into: Insulin-like growth factor 1 receptor alpha chain; Insulin-like growth factor 1 receptor beta chain]	Membrane; Single-pass type I membrane protein;	Mus musculus (Mouse)
P24062	*IGF1R_RAT*	*Insulin-like growth factor 1 receptor (EC 2;7;10;1) (Insulin-like growth factor I receptor) (IGF-I receptor) (CD antigen CD221) [Cleaved into: Insulin-like growth factor 1 receptor alpha chain; Insulin-like growth factor 1 receptor beta chain]*	*Membrane; Single-pass type I membrane protein;*	*Rattus norvegicus (Rat)*
Q80UK8	INT2_MOUSE	Integrator complex subunit 2 (Int2)	Nucleus membrane; Single-pass membrane protein;	Mus musculus (Mouse)
P17852	**ITA3_CRIGR**	Integrin alpha-3 (CD49 antigen-like family member C) (Galactoprotein B3) (GAPB3) (VLA-3 subunit alpha) (CD antigen CD49c) [Cleaved into: Integrin alpha-3 heavy chain; Integrin alpha-3 light chain]	Membrane; Single-pass type I membrane protein;	Cricetulus griseus (Chinese hamster)
Q62470	***ITA3_MOUSE***	*Integrin alpha-3 (CD49 antigen-like family member C) (Galactoprotein B3) (GAPB3) (VLA-3 subunit alpha) (CD antigen CD49c) [Cleaved into: Integrin alpha-3 heavy chain; Integrin alpha-3 light chain]*	*Membrane; Single-pass type I membrane protein;*	*Mus musculus (Mouse)*
Q00651	**ITA4_MOUSE**	Integrin alpha-4 (CD49 antigen-like family member D) (Integrin alpha-IV) (Lymphocyte Peyer patch adhesion molecules subunit alpha) (LPAM subunit alpha) (VLA-4 subunit alpha) (CD antigen CD49d)	Membrane; Single-pass type I membrane protein;	Mus musculus (Mouse)

Accession	Entry name	Protein names	Subcellular locations	Organism
P11688	**ITA5_MOUSE**	Integrin alpha-5 (CD49 antigen-like family member E) (Fibronectin receptor subunit alpha) (Integrin alpha-F) (VLA-5) (CD antigen CD49e) [Cleaved into: Integrin alpha-5 heavy chain; Integrin alpha-5 light chain]	Membrane; Single-pass type I membrane protein;	Mus musculus (Mouse)
Q61738	**ITA7_MOUSE**	Integrin alpha-7 [Cleaved into: Integrin alpha-7 heavy chain; Integrin alpha-7 light chain]	Membrane; Single-pass type I membrane protein;	Mus musculus (Mouse)
Q3V0T4	**ITAD_MOUSE**	Integrin alpha-D (CD antigen CD11d)	Membrane; Single-pass type I membrane protein;	Mus musculus (Mouse)
P43406	**ITAV_MOUSE**	Integrin alpha-V (Vitronectin receptor subunit alpha) (CD antigen CD51) [Cleaved into: Integrin alpha-V heavy chain; Integrin alpha-V light chain]	Membrane; Single-pass type I membrane protein;	Mus musculus (Mouse)
Q9QXH4	**ITAX_MOUSE**	Integrin alpha-X (CD11 antigen-like family member C) (Leukocyte adhesion receptor p150;95) (CD antigen CD11c)	Membrane; Single-pass type I membrane protein;	Mus musculus (Mouse)
P09055	**ITB1_MOUSE**	Integrin beta-1 (Fibronectin receptor subunit beta) (VLA-4 subunit beta) (CD antigen CD29)	Cell membrane; Single-pass type I membrane protein;	Mus musculus (Mouse)
A2A863	**ITB4_MOUSE**	Integrin beta-4 (CD antigen CD104)	Membrane; Single-pass type I membrane protein;	Mus musculus (Mouse)
P22273	IL6RA_RAT	Interleukin-6 receptor subunit alpha (IL-6 receptor subunit alpha) (IL-6R subunit alpha) (IL-6R-alpha) (IL-6RA) (IL-6R 1) (CD antigen CD126)	Membrane; Single-pass type I membrane protein;	Rattus norvegicus (Rat)
Q02257	PLAK_MOUSE	Junction plakoglobin (Desmoplakin III) (Desmoplakin-3)	Cell junction; adherens junction; desmo-some; Cytoplasm cyto-skeleton; peripheral membrane protein;	Mus musculus (Mouse)
P04104	K2C1_MOUSE	Keratin; type II cytoskeletal 1 (67 kDa cytokeratin) (Cytokeratin-1) (CK-1) (Keratin-1) (K1) (Type-II keratin Kb1)	Cell membrane;	Mus musculus (Mouse)
Q6IMF3	*K2C1_RAT*	*Keratin; type II cytoskeletal 1 (Cytokeratin-1) (CK-1) (Keratin-1) (K1) (Type-II keratin Kb1)*	*Cell membrane;*	*Rattus norvegicus (Rat)*
Q9EQG6	KDIS_RAT	Kinase D-interacting substrate of 220 kDa (Ankyrin repeat-rich membrane-spanning protein)	Membrane; Multi-pass membrane protein;	Rattus norvegicus (Rat)

Accession	Entry name	Protein names	Subcellular locations	Organism
Q61097	KSR1_MOUSE	Kinase suppressor of Ras 1 (mKSR1) (Protein Hb)	Cytoplasm; Membrane; Peripheral membrane protein;	Mus musculus (Mouse)
Q3UVC0	KSR2_MOUSE	Kinase suppressor of Ras 2	Cytoplasm; Membrane; Peripheral membrane protein;	Mus musculus (Mouse)
Q8K1F9	LCTL_MOUSE	Lactase-like protein (Klotho/lactase-phlorizin hydrolase-related protein)	Endoplasmic reticulum membrane; Single-pass membrane protein;	Mus musculus (Mouse)
P19137	LAMA1_MOUSE	Laminin subunit alpha-1 (Laminin A chain) (Laminin-1 subunit alpha) (Laminin-3 subunit alpha) (S-laminin subunit alpha) (S-LAM alpha)	Secreted ;extracellular space;extracellular matrix ;basement membrane;	Mus musculus (Mouse)
Q60675	LAMA2_MOUSE	Laminin subunit alpha-2 (Laminin M chain) (Laminin-12 subunit alpha) (Laminin-2 subunit alpha) (Laminin-4 subunit alpha) (Merosin heavy chain)	Secreted;extracellular space ;extracellular matrix;basement membrane;	Mus musculus (Mouse)
Q61789	LAMA3_MOUSE	Laminin subunit alpha-3 (Epiligrin subunit alpha) (Kalinin subunit alpha) (Laminin-5 subunit alpha) (Laminin-6 subunit alpha) (Laminin-7 subunit alpha) (Nicein subunit alpha)	Secreted ;extracellular space;extracellular matrix ;basement membrane;	Mus musculus (Mouse)
Q61001	LAMA5_MOUSE	Laminin subunit alpha-5 (Laminin-10 subunit alpha) (Laminin-11 subunit alpha) (Laminin-15 subunit alpha)	Secreted;extracellular space ;extracellular matrix;basement membrane;	Mus musculus (Mouse)
Q61087	LAMB3_MOUSE	Laminin subunit beta-3 (Epiligrin subunit bata) (Kalinin B1 chain) (Kalinin subunit beta) (Laminin-5 subunit beta) (Nicein subunit beta)	Secreted ;extracellular space;extracellular matrix ;basement membrane;	Mus musculus (Mouse)
O88917	LPHN1_RAT	Latrophilin-1 (Calcium-independent alpha-latrotoxin receptor 1) (CIRL-1)	Cell membrane; Multi-pass membrane protein;	Rattus norvegicus (Rat)
Q9Z173	LPHN3_RAT	Latrophilin-3 (Calcium-independent alpha-latrotoxin receptor) (CIRL-3)	Cell membrane; Multi-pass membrane protein;	Rattus norvegicus (Rat)

Accession	Entry name	Protein names	Subcellular locations	Organism
Q5SGE0	LPPRC_RAT	Leucine-rich PPR motif-containing protein; mitochondrial (130 kDa leucine-rich protein) (LRP 130) (Leucine rich protein 157) (rLRP157)	Mitochondrion; Nucleus; Nucleus;nucleoplasm; Nucleus inner membrane; Nucleus outer membrane;	Rattus norvegicus (Rat)
Q8CBC6	LRRN3_MOUSE	Leucine-rich repeat neuronal protein 3 (Neuronal leucine-rich repeat protein 3) (NLRR-3)	Membrane; Single-pass type I membrane protein;	Mus musculus (Mouse)
Q8R502	LRC8C_MOUSE	Leucine-rich repeat-containing protein 8C (Protein AD158)	Endoplasmic reticulum membrane; Multi-pass membrane protein;	Mus musculus (Mouse)
P70193	LRIG1_MOUSE	Leucine-rich repeats and immunoglobulin-like domains protein 1 (LIG-1)	Membrane; Single-pass type I membrane protein;	Mus musculus (Mouse)
P97629	LCAP_RAT	Leucyl-cystinyl aminopeptidase (Cystinyl aminopeptidase) (EC 3;4;11;3) (GP160) (Insulin-regulated membrane aminopeptidase) (Insulin-responsive aminopeptidase) (IRAP) (Oxytocinase) (OTase) (Placental leucine aminopeptidase) (P-LAP) (Vesicle protein of 165 kDa) (Vp165)	Cell membrane; Single-pass type II membrane protein; Endomembrane system; Single-pass type II membrane protein;	Rattus norvegicus (Rat)
Q8CIV3	LIPH_MOUSE	Lipase member H (EC 3;1;1;-)	Secreted; Membrane; Peripheral membrane protein;	Mus musculus (Mouse)
Q9ESE1	LRBA_MOUSE	Lipopolysaccharide-responsive and beige-like anchor protein (Beige-like protein)	Cell membrane; Single-pass membrane protein; Endoplasmic reticulum; Golgi apparatus ;trans-Golgi network; Lysosome;	Mus musculus (Mouse)
Q9JI18	LRP1B_MOUSE	Low-density lipoprotein receptor-related protein 1B (LRP-1B) (Low-density lipoprotein receptor-related protein-deleted in tumor) (LRP-DIT)	Membrane; Single-pass type I membrane protein;	Mus musculus (Mouse)
P98158	LRP2_RAT	Low-density lipoprotein receptor-related protein 2 (LRP-2) (Glycoprotein 330) (gp330) (Megalin)	Cell membrane; Single-pass type I membrane protein; Membrane;clathrin-coated pit; Cytoplasm;	Rattus norvegicus (Rat)

Accession	Entry name	Protein names	Subcellular locations	Organism
Q8VI56	LRP4_MOUSE	Low-density lipoprotein receptor-related protein 4 (LRP-4) (LDLR dan)	Membrane; Single-pass type I membrane protein;	Mus musculus (Mouse)
Q9QYP1	*LRP4_RAT*	*Low-density lipoprotein receptor-related protein 4 (LRP-4) (Multiple epidermal growth factor-like domains 7)*	*Membrane; Single-pass type I membrane protein;*	*Rattus norvegicus (Rat)*
Q61830	MRC1_MOUSE	Macrophage mannose receptor 1 (MMR) (CD antigen CD206)	Membrane; Single-pass type I membrane protein;	Mus musculus (Mouse)
Q9WV57	MPEG1_RAT	Macrophage-expressed gene 1 protein (Macrophage gene 1 protein) (Mpg-1)	Membrane; Single-pass type I membrane protein;	Rattus norvegicus (Rat)
Q80U28	MADD_MOUSE	MAP kinase-activating death domain protein (Rab3 GDP/GTP exchange factor)	Membrane; Multi-pass membrane protein;	Mus musculus (Mouse)
O08873	*MADD_RAT*	*MAP kinase-activating death domain protein (Rab3 GDP/GTP exchange factor)*	*Membrane; Multi-pass membrane protein;*	*Rattus norvegicus (Rat)*
Q8BI84	MIA3_MOUSE	Melanoma inhibitory activity protein 3 (Transport and Golgi organization protein 1) (TANGO1)	Endoplasmic reticulum membrane; Single-pass type I membrane protein;	Mus musculus (Mouse)
Q9WVQ1	MAGI2_MOUSE	Membrane-associated guanylate kinase; WW and PDZ domain-containing protein 2 (Activin receptor-interacting protein 1) (Acvrip1) (Atrophin-1-interacting protein 1) (AIP-1)	Cell junction synapse synaptosome; Cell membrane; Peripheral membrane protein;	Mus musculus (Mouse)
Q9EQJ9	MAGI3_MOUSE	Membrane-associated guanylate kinase; WW and PDZ domain-containing protein 3 (Membrane-associated guanylate kinase inverted 3) (MAGI-3)	Cell membrane; Peripheral membrane protein; Cell junction ;tight junction; Nucleus;	Mus musculus (Mouse)
Q9R1L5	MAST1_MOUSE	Microtubule-associated serine/threonine-protein kinase 1 (EC 2;7;11;1) (Syntrophin-associated serine/threonine-protein kinase)	Cell membrane; Peripheral membrane protein; Cytoplasmic side; Cytoplasm;cytoskeleton;	Mus musculus (Mouse)
Q810W7	*MAST1_RAT*	*Microtubule-associated serine/threonine-protein kinase 1 (EC 2;7;11;1) (Syntrophin-associated serine/threonine-protein kinase)*	*Cell membrane; Peripheral membrane protein; Cytoplasmic side; Cytoplasm ;cytoskeleton;*	*Rattus norvegicus (Rat)*

Accession	Entry name	Protein names	Subcellular locations	Organism
Q60592	MAST2_MOUSE	Microtubule-associated serine/threonine-protein kinase 2 (EC 2;7;11;1)	Membrane; Peripheral membrane protein; Cytoplasmic side; Cytoplasm;cytoskeleton; Cell junction;	Mus musculus (Mouse)
P06795	MDR1_MOUSE	Multidrug resistance protein 1 (EC 3;6;3;44) (ATP-binding cassette sub-family B member 1) (P-glycoprotein 1) (CD antigen CD243)	Membrane; Multi-pass membrane protein;	Mus musculus (Mouse)
P43245	*MDR1_RAT*	*Multidrug resistance protein 1 (EC 3;6;3;44) (ATP-binding cassette sub-family B member 1) (P-glycoprotein 1) (CD antigen CD243)*	*Membrane; Multi-pass membrane protein;*	*Rattus norvegicus (Rat)*
P21449	MDR2_CRIGR	Multidrug resistance protein 2 (EC 3;6;3;44) (P-glycoprotein 2)	Membrane; Multi-pass membrane protein;	Cricetulus griseus (Chinese hamster)
Q8CG09	MRP1_RAT	Multidrug resistance-associated protein 1 (ATP-binding cassette sub-family C member 1) (Leukotriene C(4) transporter) (LTC4 transporter)	Cell membrane; Multi-pass membrane protein;	Rattus norvegicus (Rat)
Q69ZN7	MYOF_MOUSE	Myoferlin (Fer-1-like protein 3)	Cell membrane; Single-pass type II membrane protein; Nucleus membrane; Single-pass type II membrane protein; Cytoplasmic vesicle membrane;	Mus musculus (Mouse)
A2AQP0	MYH7B_MOUSE	Myosin-7B (Myosin cardiac muscle beta chain) (Myosin heavy chain 7B; cardiac muscle beta isoform)	Membrane; Peripheral membrane protein;	Mus musculus (Mouse)
Q9Z1N3	MYO9A_RAT	Myosin-IXa (Myr 7) (Unconventional myosin-9a)	Membrane; Single-pass membrane protein; Cytoplasm;	Rattus norvegicus (Rat)
Q8C170	*MYO9A_MOUSE*	*Myosin-IXa (Unconventional myosin-9a)*	*Membrane; Single-pass membrane protein;*	*Mus musculus (Mouse)*

Accession	Entry name	Protein names	Subcellular locations	Organism
Q64331	MYO6_MOUSE	Myosin-VI (Unconventional myosin-6)	Golgi apparatus ;trans-Golgi network membrane; Peripheral membrane protein; Nucleus; Cytoplasm;perinuclear region; Membrane ;clathrin-coated pit; Cell projection;ruffle; Cytoplasmic vesicle;	Mus musculus (Mouse)
Q99MZ6	MYO7B_MOUSE	Myosin-VIIb	Apical cell membrane;	Mus musculus (Mouse)
P28660	NCKP1_MOUSE	Nck-associated protein 1 (NAP 1) (Brain protein H19) (MH19) (Membrane-associated protein HEM-2) (p125Nap1)	Cell membrane; Single-pass membrane protein; Cytoplasmic side; Cell projection ;lamellipodium membrane; Cytoplasmic side;	Mus musculus (Mouse)
P55161	*NCKP1_RAT*	*Nck-associated protein 1 (NAP 1) (Membrane-associated protein HEM-2) (p125Nap1)*	*Cell membrane; Single-pass membrane protein; Cytoplasmic side; Cell projection;lamellipodium membrane; Cytoplasmic side;*	*Rattus norvegicus (Rat)*
Q6ZWR6	SYNE1_MOUSE	Nesprin-1 (Enaptin) (Myocyte nuclear envelope protein 1) (Myne-1) (Nuclear envelope spectrin repeat protein 1) (Synaptic nuclear envelope protein 1) (Syne-1)	Nucleus outer membrane; Single-pass type IV membrane protein; Cytoplasmic side; Cytoplasm ;cytoskeleton; myofibril; sarcomere;	Mus musculus (Mouse)

Accession	Entry name	Protein names	Subcellular locations	Organism
Q6ZWQ0	SYNE2_MOUSE	Nesprin-2 (Nuclear envelope spectrin repeat protein 2) (Nucleus and actin connecting element protein) (Protein NUANCE) (Synaptic nuclear envelope protein 2) (Syne-2)	Nucleus outer membrane; Single-pass type IV membrane protein; Cytoplasmic side; Sarcoplasmic reticulum membrane; Cell membrane; Cytoplasm; cytoskeleton; Mitochondrion;; nucleoplasm;	Mus musculus (Mouse)
Q4FZC9	SYNE3_MOUSE	Nesprin-3	Nucleus outer membrane; Single-pass type IV membrane protein;	Mus musculus (Mouse)
O35136	**NCAM2_MOUSE**	Neural cell adhesion molecule 2 (N-CAM-2) (NCAM-2) (Neural cell adhesion molecule RB-8) (R4B12)	Cell membrane; Single-pass type I membrane protein; Lipid-anchor;GPI-anchor;	Mus musculus (Mouse)
Q9EPN1	NBEA_MOUSE	Neurobeachin (Lysosomal-trafficking regulator 2)	Membrane; Peripheral membrane protein; Endomembrane system; Cell junction synapse ;postsynaptic cell membrane;	Mus musculus (Mouse)
Q80TN7	NAV3_MOUSE	Neuron navigator 3 (Pore membrane and/or filament-interacting-like protein 1)	Nucleus outer membrane;	Mus musculus (Mouse)
Q91XT9	ASAH2_RAT	Neutral ceramidase (N-CDase) (NCDase) (EC 3;5;1;23) (Acylsphingosine deacylase 2) (N-acylsphingosine amidohydrolase 2)	Cell membrane; Single-pass type II membrane protein;	Rattus norvegicus (Rat)
P29476	NOS1_RAT	Nitric oxide synthase; brain (EC 1;14;13;39) (BNOS) (Constitutive NOS) (NC-NOS) (NOS type I) (Neuronal NOS) (N-NOS) (nNOS) (Peptidyl-cysteine S-nitrosylase NOS1)	Cell membrane Peripheral membrane protein; Cell projection; dendritic spine;	Rattus norvegicus (Rat)
Q9Z0J4	*NOS1_MOUSE*	*Nitric oxide synthase; brain (EC 1;14;13;39) (Constitutive NOS) (NC-NOS) (NOS type I) (Neuronal NOS) (N-NOS) (nNOS) (Peptidyl-cysteine S-nitrosylase NOS1) (bNOS)*	*Cell membrane Peripheral membrane protein; Cell projection ;dendritic spine;*	*Mus musculus (Mouse)*

Accession	Entry name	Protein names	Subcellular locations	Organism
Q3TL44	NLRX1_MOUSE	NLR family member X1	Mitochondrion outer membrane;	Mus musculus (Mouse)
Q99P88	NU155_MOUSE	Nuclear pore complex protein Nup155 (155 kDa nucleoporin) (Nucleoporin Nup155)	Nucleus;nuclear pore complex; Nucleus membrane; Peripheral membrane protein; Cytoplasmic side; Nucleus membrane; Peripheral membrane protein; Nucleoplasmic side;	Mus musculus (Mouse)
P37199	*NU155_RAT*	*Nuclear pore complex protein Nup155 (155 kDa nucleoporin) (Nucleoporin Nup155) (P140)*	*Nucleus; nuclear pore complex; Nucleus membrane; Peripheral membrane protein; Cytoplasmic side; Nucleus membrane; Nucleoplasmic side;*	*Rattus norvegicus (Rat)*
P11654	PO210_RAT	Nuclear pore membrane glycoprotein 210 (Nuclear pore protein gp210) (Nuclear envelope pore membrane protein POM 210) (POM210) (Nucleoporin Nup210) (Pore membrane protein of 210 kDa)	Nucleus ;nuclear pore complex; Nucleus membrane; Single-pass type I membrane protein; Endoplasmic reticulum membrane; Single-pass type I membrane protein;	Rattus norvegicus (Rat)
Q9D2F7	P210L_MOUSE	Nuclear pore membrane glycoprotein 210-like (Nucleoporin 210 kDa-like) (Nucleoporin Nup210-like)	Membrane; Single-pass membrane protein;	Mus musculus (Mouse)
P31662	S6A17_RAT	Orphan sodium- and chloride-dependent neurotransmitter transporter NTT4 (Solute carrier family 6 member 17)	Membrane; Multi-pass membrane protein;	Rattus norvegicus (Rat)

Accession	Entry name	Protein names	Subcellular locations	Organism
Q9ESF1	OTOF_MOUSE	Otoferlin (Fer-1-like protein 2)	Cytoplasmic vesicle;secretory vesicle; synaptic vesicle membrane; Single-pass type II mem-brane protein; Baso-lateral cell membrane; Endo-plasmic reticulum mem-brane; Cell membrane;	Mus musculus (Mouse)
Q9ERC5	*OTOF_RAT*	*Otoferlin (Fer-1-like protein 2)*	*Cytoplasmic vesicle;secretory vesicle ;synaptic vesicle membrane; Single-pass type II membrane protein; Basolateral cell membrane; Endoplasmic reticulum membrane; Cell membrane;*	*Rattus norvegicus (Rat)*
Q9CWU2	ZDH13_MOUSE	Palmitoyltransferase ZDHHC13 (EC 2;3;1;-) (Huntingtin-interacting protein 14-related protein) (HIP14-related protein) (Zinc finger DHHC domain-containing protein 13) (DHHC-13)	Golgi apparatus membrane; Multi-pass membrane protein; Cytoplasmic vesicle membrane;	Mus musculus (Mouse)
Q3ULF4	SPG7_MOUSE	Paraplegin (EC 3;4;24;-)	Mitochondrion membrane; Multi-pass membrane protein;	Mus musculus (Mouse)
Q9Z340	PARD3_RAT	Partitioning defective 3 homolog (PAR-3) (PARD-3) (Atypical PKC isotype-specific-interacting protein) (ASIP) (Atypical PKC-specific-binding protein) (ASBP)	Endomembrane system; Cell junction;tight junction; Cytoplasm ; cell cortex; Cytoplasm; cytoskeleton;	Rattus norvegicus (Rat)
Q99NH2	*PARD3_MOUSE*	*Partitioning defective 3 homolog (PAR-3) (PARD-3) (Atypical PKC isotype-specific-interacting protein) (ASIP) (Ephrin-interacting protein) (PHIP)*	*Endomembrane system; Cell junction; tight junction; Cytoplasm ;cell cortex; Cytoplasm;cytoskeleton;*	*Mus musculus (Mouse)*

Accession	Entry name	Protein names	Subcellular locations	Organism
Q5BK26	PLPL7_RAT	Patatin-like phospholipase domain-containing protein 7 (EC 3;1;1;-) (Liver NTE-related protein 1) (NTE-related esterase)	Membrane; Single-pass membrane protein; Nucleus membrane; Mitochondrion membrane; Lysosome membrane; Microsome membrane;	Rattus norvegicus (Rat)
Q5DU28	PCX2_MOUSE	Pecanex-like protein 2	Membrane; Multi-pass membrane protein;	Mus musculus (Mouse)
Q9R155	S26A4_MOUSE	Pendrin (Sodium-independent chloride/iodide transporter) (Solute carrier family 26 member 4)	Membrane; Multi-pass membrane protein;	Mus musculus (Mouse)
Q9R154	S26A4_RAT	Pendrin (Sodium-independent chloride/iodide transporter) (Solute carrier family 26 member 4)	Membrane; Multi-pass membrane protein;	Rattus norvegicus (Rat)
Q63425	PRAX_RAT	Periaxin	Nucleus; Cell projection ;axon; Cytoplasm; Cell membrane; Peripheral membrane protein; Cytoplasmic side;	Rattus norvegicus (Rat)
Q62915	CSKP_RAT	Peripheral plasma membrane protein CASK (EC 2;7;11;1) (Calcium/calmodulin-dependent serine protein kinase)	Nucleus; Cytoplasm; Cell membrane; Peripheral membrane protein;	Rattus norvegicus (Rat)
Q9R269	PEPL_MOUSE	Periplakin	Cell junction;desmosome; Cytoplasm ;cytoskeleton; Cell membrane; Nucleus; Mitochondrion;	Mus musculus (Mouse)
Q2PFD7	PSD3_MOUSE	PH and SEC7 domain-containing protein 3 (Exchange factor for ADP-ribosylation factor guanine nucleotide factor 6) (Pleckstrin homology and SEC7 domain-containing protein 3)	Cell junction;synapse ;postsynaptic cell membrane;postsynaptic density;	Mus musculus (Mouse)

Accession	Entry name	Protein names	Subcellular locations	Organism
Q9WTR8	PHLP1_RAT	PH domain leucine-rich repeat protein phosphatase 1 (EC 3;1;3;16) (Pleckstrin homology domain-containing family E member 1) (PH domain-containing family E member 1)	Cytoplasm; Membrane; Peripheral membrane protein; Nucleus;	Rattus norvegicus (Rat)
P97573	SHIP1_RAT	Phosphatidylinositol-3;4;5-trisphosphate 5-phosphatase 1 (EC 3;1;3;n1) (SH2 domain-containing inositol-5'-phosphatase 1) (SH2 domain-containing inositol phosphatase 1)	Cytoplasm; Membrane; Peripheral membrane protein;	Rattus norvegicus (Rat)
Q61194	P3C2A_MOUSE	Phosphatidylinositol-4-phosphate 3-kinase C2 domain-containing subunit alpha (PI3K-C2-alpha) (PtdIns-3-kinase C2 subunit alpha) (EC 2;7;1;154) (Cpk-m) (Phosphoinositide 3-kinase-C2-alpha) (p170)	Cell membrane; Golgi apparatus; Cytoplasmic vesicle ;clathrin-coated vesicle; Nucleus; Cytoplasm;	Mus musculus (Mouse)
Q3TTY0	PLB1_MOUSE	Phospholipase B1; membrane-associated (Phospholipase B) (Phospholipase B/lipase) (PLB/LIP) [Includes: Phospholipase A2 (EC 3;1;1;4); Lysophospholipase (EC 3;1;1;5)]	Apical cell membrane; Single-pass type I membrane protein;	Mus musculus (Mouse)
O54728	*PLB1_RAT*	*Phospholipase B1; membrane-associated (Phospholipase B) (Phospholipase B/lipase) (PLB/LIP) [Includes: Phospholipase A2 (EC 3;1;1;4); Lysophospholipase (EC 3;1;1;5)]*	*Apical cell membrane; Single-pass type I membrane protein;*	*Rattus norvegicus (Rat)*
O08684	PLD1_CRIGR	Phospholipase D1 (PLD 1) (EC 3;1;4;4) (Choline phosphatase 1) (Phosphatidylcholine-hydrolyzing phospholipase D1)	Cytoplasm perinuclear region; Endoplasmic reticulum membrane; Lipid-anchor; Cytoplasmic side; Golgi apparatus membrane; Cytoplasmic side; Late endosome membrane; Lipid-anchor;	Cricetulus griseus (Chinese hamster)
P70496	*PLD1_RAT*	*Phospholipase D1 (PLD 1) (rPLD1) (EC 3;1;4;4) (Choline phosphatase 1) (Phosphatidylcholine-hydrolyzing phospholipase D1)*	*Cytoplasm perinuclear region; Endoplasmic reticulum membrane; Lipid-anchor; Golgi apparatus membrane; Lipid-anchor; Late endosome membrane; Lipid-anchor;*	*Rattus norvegicus (Rat)*

Accession	Entry name	Protein names	Subcellular locations	Organism
P11506	AT2B2_RAT	Plasma membrane calcium-transporting ATPase 2 (PMCA2) (EC 3;6;3;8) (Plasma membrane calcium ATPase isoform 2) (Plasma membrane calcium pump isoform 2)	Cell membrane; Multi-pass membrane protein;	Rattus norvegicus (Rat)
Q64542	AT2B4_RAT	Plasma membrane calcium-transporting ATPase 4 (PMCA4) (EC 3;6;3;8) (Plasma membrane calcium ATPase isoform 4) (Plasma membrane calcium pump isoform 4)	Cell membrane; Multi-pass membrane protein;	Rattus norvegicus (Rat)
Q8C115	PKHH2_MOUSE	Pleckstrin homology domain-containing family H member 2	Membrane; Single-pass membrane protein;	Mus musculus (Mouse)
P70206	PLXA1_MOUSE	Plexin-A1 (Plex 1) (Plexin-1)	Membrane; Single-pass type I membrane protein;	Mus musculus (Mouse)
P70207	PLXA2_MOUSE	Plexin-A2 (Plex 2) (Plexin-2)	Membrane; Single-pass type I membrane protein;	Mus musculus (Mouse)
Q9QZC2	PLXC1_MOUSE	Plexin-C1 (Virus-encoded semaphorin protein receptor) (CD antigen CD232)	Membrane; Single-pass type I membrane protein;	Mus musculus (Mouse)
O88422	GALT5_RAT	Polypeptide N-acetylgalactosaminyl-transferase 5 (EC 2;4;1;41) (Polypeptide GalNAc transferase 5) (GalNAc-T5) (pp-GaNTase 5) (Protein-UDP acetylgalactos-aminyltransferase 5)	Golgi apparatus membrane; Single-pass type II membrane protein;	Rattus norvegicus (Rat)
Q91WF7	FIG4_MOUSE	Polyphosphoinositide phosphatase (EC 3;1;3;-) (Phosphatidylinositol 3;5-bisphosphate 5-phos-phatase) (SAC domain-containing protein 3)	Endosome membrane;	Mus musculus (Mouse)
Q9Z258	KCNT1_RAT	Potassium channel subfamily T member 1 (Sequence like a calcium-activated potassium channel subunit)	Cell membrane; Multi-pass membrane protein;	Rattus norvegicus (Rat)
P15387	KCNB1_RAT	Potassium voltage-gated channel subfamily B member 1 (Delayed rectifier potassium channel 1) (DRK1) (Voltage-gated potassium channel subunit Kv2;1)	Membrane; Multi-pass membrane protein;	Rattus norvegicus (Rat)
Q03717	*KCNB1_MOUSE*	*Potassium voltage-gated channel subfamily B member 1 (Voltage-gated potassium channel subunit Kv2;1) (mShab)*	*Membrane; Multi-pass membrane protein;*	*Mus musculus (Mouse)*
Q9QWS8	KCNH8_RAT	Potassium voltage-gated channel subfamily H member 8 (Ether-a-go-go-like potassium channel 3) (ELK channel 3) (Voltage-gated potassium channel subunit Kv12;1)	Membrane; Multi-pass membrane protein;	Rattus norvegicus (Rat)

Accession	Entry name	Protein names	Subcellular locations	Organism
Q64436	ATP4A_MOUSE	Potassium-transporting ATPase alpha chain 1 (EC 3;6;3;10) (Gastric H(+)/K(+) ATPase subunit alpha) (Proton pump)	Membrane; Multi-pass membrane protein;	Mus musculus (Mouse)
P09626	*ATP4A_RAT*	*Potassium-transporting ATPase alpha chain 1 (EC 3;6;3;10) (Gastric H(+)/K(+) ATPase subunit alpha) (Proton pump)*	*Membrane; Multi-pass membrane protein;*	*Rattus norvegicus (Rat)*
Q80Y24	PRIC2_MOUSE	Prickle-like protein 2	Nucleus membrane;	Mus musculus (Mouse)
Q9EPE9	AT131_MOUSE	Probable cation-transporting ATPase 13A1 (CATP) (EC 3;6;3;-)	Membrane; Multi-pass membrane protein;	Mus musculus (Mouse)
Q5XF89	AT133_MOUSE	Probable cation-transporting ATPase 13A3 (EC 3;6;3;-)	Membrane; Multi-pass membrane protein;	Mus musculus (Mouse)
Q5XF90	AT134_MOUSE	Probable cation-transporting ATPase 13A4 (EC 3;6;3;-) (P5-ATPase isoform 4)	Membrane; Multi-pass membrane protein;	Mus musculus (Mouse)
Q9WVT0	GP116_RAT	Probable G-protein coupled receptor 116 (G-protein coupled hepta-helical receptor Ig-hepta)	Cell membrane; Multi-pass membrane protein;	Rattus norvegicus (Rat)
Q7TT36	GP125_MOUSE	Probable G-protein coupled receptor 125	Cell membrane; Multi-pass membrane protein;	Mus musculus (Mouse)
Q8K451	GP156_RAT	Probable G-protein coupled receptor 156 (GABAB-related G-protein coupled receptor)	Cell membrane; Multi-pass membrane protein;	Rattus norvegicus (Rat)
Q8C419	GP158_MOUSE	Probable G-protein coupled receptor 158	Cell membrane; Multi-pass membrane protein;	Mus musculus (Mouse)
A3FIN4	AT8B5_MOUSE	Probable phospholipid-transporting ATPase FetA (EC 3;6;3;1) (ATPase class I type 8B member 2-like protein) (ATPase class I type 8B member 5) (Flippase expressed in testis A)	Cytoplasmic vesicle;secretory vesicle ;acrosome membrane; Multi-pass membrane protein;	Mus musculus (Mouse)
P98195	ATP9B_MOUSE	Probable phospholipid-transporting ATPase IIB (EC 3;6;3;1) (ATPase class II type 9B)	Membrane; Multi-pass membrane protein;	Mus musculus (Mouse)
P01132	EGF_MOUSE	Pro-epidermal growth factor (EGF) [Cleaved into: Epidermal growth factor]	Membrane; Single-pass type I membrane protein;	Mus musculus (Mouse)

Accession	Entry name	Protein names	Subcellular locations	Organism
Q91ZX7	LRP1_MOUSE	Prolow-density lipoprotein receptor-related protein 1 (LRP-1) (Alpha-2-macroglobulin receptor) (A2MR) (CD antigen CD91) [Cleaved into: Low-density lipoprotein receptor-related protein 1 85 kDa subunit (LRP-85); Low-density lipoprotein receptor-related protein 1 515 kDa subunit (LRP-515); Low-density lipoprotein receptor-related protein 1 intracellular domain (LRPICD)]	Cell membrane; Single-pass type I membrane protein; Membrane;coated pit; Peripheral membrane protein; Extracellular side; Membrane ;coated pit; Cytoplasm; Nucleus;	Mus musculus (Mouse)
P41413	PCSK5_RAT	Proprotein convertase subtilisin/kexin type 5 (EC 3;4;21;-) (Proprotein convertase 5) (PC5) (Proprotein convertase 6) (PC6) (Subtilisin/kexin-like protease PC5) (rPC5) (Fragment)	Secreted; Endomembrane system; Single-pass type I membrane protein;	Rattus norvegicus (Rat)
Q04592	PCSK5_MOUSE	Proprotein convertase subtilisin/kexin type 5 (EC 3;4;21;-) (Proprotein convertase 5) (PC5) (Proprotein convertase 6) (PC6) (Subtilisin-like proprotein convertase 6) (SPC6) (Subtilisin/kexin-like protease PC5)	Secreted; Endomembrane system; Single-pass type I membrane protein;	Mus musculus (Mouse)
Q62786	FPRP_RAT	Prostaglandin F2 receptor negative regulator (Prostaglandin F2-alpha receptor regulatory protein) (Prostaglandin F2-alpha receptor-associated protein) (CD antigen CD315)	Endoplasmic reticulum membrane; Single-pass type I membrane protein; Golgi apparatus;trans-Golgi network membrane;	Rattus norvegicus (Rat)
Q6R0H6	ALEX_MOUSE	Protein ALEX (Alternative gene product encoded by XL-exon)	Cell membrane; Peripheral membrane protein; Cell projection ;ruffle;	Mus musculus (Mouse)
P38660	PDIA6_MESAU	Protein disulfide-isomerase A6 (EC 5;3;4;1) (Protein disulfide isomerase P5)	Endoplasmic reticulum lumen; Cell membrane; Melanosome;	Mesocricetus auratus (Golden hamster)
Q5DTZ0	NYNRI_MOUSE	Protein NYNRIN (NYN domain and retroviral integrase catalytic domain-containing protein) (Pol-like protein)	Membrane; Multi-pass membrane protein;	Mus musculus (Mouse)
Q9JIG4	PPR3F_MOUSE	Protein phosphatase 1 regulatory subunit 3F	Membrane; Single-pass membrane protein;	Mus musculus (Mouse)

Accession	Entry name	Protein names	Subcellular locations	Organism
Q0KL00	PIEZ1_RAT	Protein PIEZO1 (Membrane protein induced by beta-amyloid treatment) (Mib) (Protein FAM38B)	Endoplasmic reticulum membrane; Multi-pass mem-brane protein; Endo-plasmic reticulum-Golgi intermediate compartment;Cell membrane;	Rattus norvegicus (Rat)
Q80U72	SCRIB_MOUSE	Protein scribble homolog (Scribble) (Protein LAP4)	Cell membrane; Peripheral membrane protein; Cell junction;adherens junction; Cytoplasm;	Mus musculus (Mouse)
Q7TP36	SHRM2_RAT	Protein Shroom2 (Liver regeneration-related protein LRRG167) (Protein Apxl)	Apical cell membrane; Cell junction ;tight junction; Cytoplasm;cytoskeleton;	Rattus norvegicus (Rat)
Q3UH53	SDK1_MOUSE	Protein sidekick-1	Membrane; Single-pass membrane protein;	Mus musculus (Mouse)
Q6V4S5	SDK2_MOUSE	Protein sidekick-2	Membrane; Single-pass type I membrane protein;	Mus musculus (Mouse)
Q91VM4	SPNS2_MOUSE	Protein spinster homolog 2	Membrane; Multi-pass membrane protein;	Mus musculus (Mouse)
Q0VGY8	TANC1_MOUSE	Protein TANC1 (Tetratricopeptide repeat; ankyrin repeat and coiled-coil domain-containing protein 1)	Cell junction ;synapse;postsynaptic cell membrane ;postsynaptic density;	Mus musculus (Mouse)
Q6F6B3	*TANC1_RAT*	*Protein TANC1 (TPR domain; ankyrin-repeat and coiled-coil domain-containing protein 1)*	*Cell junction;synapse ;postsynaptic cell membrane;postsynaptic density;*	*Rattus norvegicus (Rat)*

Accession	Entry name	Protein names	Subcellular locations	Organism
Q3UPL0	SC31A_MOUSE	Protein transport protein Sec31A (SEC31-like protein 1) (SEC31-related protein A)	Cytoplasm; Cytoplasmic vesicle ;COPII-coated vesicle membrane; Peripheral membrane protein; Cytoplasmic side; Endoplasmic reticulum membrane;	Mus musculus (Mouse)
Q9Z2Q1	*SC31A_RAT*	*Protein transport protein Sec31A (SEC31-like protein 1) (SEC31-related protein A) (Vesicle-associated protein 1)*	*Cytoplasm; Cytoplasmic vesicle;COPII-coated vesicle membrane; Peripheral membrane protein; Cytoplasmic side; Endoplasmic reticulum membrane;*	*Rattus norvegicus (Rat)*
Q62768	UN13A_RAT	Protein unc-13 homolog A (Munc13-1)	Cytoplasm; Cell membrane; Peripheral membrane protein; Cell junction ;synapse;presynaptic cell membrane;	Rattus norvegicus (Rat)
Q8K0T7	UN13C_MOUSE	Protein unc-13 homolog C (Munc13-3)	Cytoplasm; Membrane; Peripheral membrane protein; Cell junction ;synapse;presynaptic cell membrane;	Mus musculus (Mouse)
Q62770	*UN13C_RAT*	*Protein unc-13 homolog C (Munc13-3)*	*Cytoplasm; Membrane; Peripheral membrane protein; Cell junction ;synapse;presynaptic cell membrane; ;*	*Rattus norvegicus (Rat)*
Q0KK59	UNC79_MOUSE	Protein unc-79 homolog	Membrane; Multi-pass membrane protein;	Mus musculus (Mouse)

Accession	Entry name	Protein names	Subcellular locations	Organism
Q8BLN6	UNC80_MOUSE	Protein unc-80 homolog (mUNC-80)	Membrane; Multi-pass membrane protein;	Mus musculus (Mouse)
Q5RJS8	TPST2_RAT	Protein-tyrosine sulfotransferase 2 (EC 2;8;2;20) (Tyrosylprotein sulfotransferase 2) (TPST-2)	Golgi apparatus membrane; Single-pass type II membrane protein;	Rattus norvegicus (Rat)
O88277	**FAT2_RAT**	Protocadherin Fat 2 (Multiple epidermal growth factor-like domains protein 1) (Multiple EGF-like domains protein 1)	Cell membrane; Single-pass membrane protein;	Rattus norvegicus (Rat)
Q8BNA6	FAT3_MOUSE	Protocadherin Fat 3 (FAT tumor suppressor homolog 3)	Membrane; Single-pass type I membrane protein;	Mus musculus (Mouse)
Q8R508	*FAT3_RAT*	*Protocadherin Fat 3 (FAT tumor suppressor homolog 3)*	*Membrane; Single-pass type I membrane protein;*	*Rattus norvegicus (Rat)*
P35546	RET_MOUSE	Proto-oncogene tyrosine-protein kinase receptor Ret (EC 2;7;10;1) (Proto-oncogene c-Ret)	Membrane; Single-pass type I membrane protein;	Mus musculus (Mouse)
Q9D620	RFIP1_MOUSE	Rab11 family-interacting protein 1 (Rab11-FIP1) (Rab-coupling protein)	Recycling endosome; Cytoplasmic vesicle;phagosome membrane;	Mus musculus (Mouse)
P31750	AKT1_MOUSE	RAC-alpha serine/threonine-protein kinase (EC 2;7;11;1) (AKT1 kinase) (Protein kinase B) (PKB) (Proto-oncogene c-Akt) (RAC-PK-alpha) (Thymoma viral proto-oncogene)	Cytoplasm; Nucleus; Cell membrane;	Mus musculus (Mouse)
Q8CHG7	RPGF2_MOUSE	Rap guanine nucleotide exchange factor 2 (Neural RAP guanine nucleotide exchange protein) (nRap GEP) (PDZ domain-containing guanine nucleotide exchange factor 1) (PDZ-GEF1) (Fragment)	Cell membrane;	Mus musculus (Mouse)
Q9QUH6	SYGP1_RAT	Ras GTPase-activating protein SynGAP (Neuronal RasGAP) (Synaptic Ras GTPase-activating protein 1) (Synaptic Ras-GAP 1) (p135 SynGAP)	Membrane; Peripheral membrane protein; Cell junction ;synapse;	Rattus norvegicus (Rat)
Q9JKF1	IQGA1_MOUSE	Ras GTPase-activating-like protein IQGAP1	Cell membrane;	Mus musculus (Mouse)

Accession	Entry name	Protein names	Subcellular locations	Organism
P35285	RB22A_MOUSE	Ras-related protein Rab-22A (Rab-22) (Rab-14)	Endosome membrane; Lipid-anchor; Cell membrane; Lipid-anchor;	Mus musculus (Mouse)
Q9ERD6	RGPS2_MOUSE	Ras-specific guanine nucleotide-releasing factor RalGPS2 (Ral GEF with PH domain and SH3-binding motif 2) (RalA exchange factor RalGPS2)	Cytoplasm; Cell membrane;	Mus musculus (Mouse)
P60603	ROMO1_MOUSE	Reactive oxygen species modulator 1 (ROS modulator 1) (Protein MGR2 homolog)	Mitochondrion membrane; Single-pass membrane protein;	Mus musculus (Mouse)
Q62799	ERBB3_RAT	Receptor tyrosine-protein kinase erbB-3 (EC 2;7;10;1) (Proto-oncogene-like protein c-ErbB-3)	Membrane; Single-pass type I membrane protein;	Rattus norvegicus (Rat)
B2RU80	PTPRB_MOUSE	Receptor-type tyrosine-protein phosphatase beta (Protein-tyrosine phosphatase beta) (R-PTP-beta) (EC 3;1;3;48) (Vascular endothelial protein tyrosine phosphatase) (VE-PTP)	Membrane; Single-pass type I membrane protein;	Mus musculus (Mouse)
Q64487	PTPRD_MOUSE	Receptor-type tyrosine-protein phosphatase delta (Protein-tyrosine phosphatase delta) (R-PTP-delta) (EC 3;1;3;48)	Membrane; Single-pass type I membrane protein;	Mus musculus (Mouse)
P49446	PTPRE_MOUSE	Receptor-type tyrosine-protein phosphatase epsilon (Protein-tyrosine phosphatase epsilon) (R-PTP-epsilon) (EC 3;1;3;48)	Cell membrane; Single-pass type I membrane protein; Cytoplasm;	Mus musculus (Mouse)
A2A8L5	PTPRF_MOUSE	Receptor-type tyrosine-protein phosphatase F (EC 3;1;3;48) (Leukocyte common antigen related) (LAR)	Membrane; Single-pass membrane protein;	Mus musculus (Mouse)
Q64604	*PTPRF_RAT*	*Receptor-type tyrosine-protein phosphatase F (EC 3;1;3;48) (Leukocyte common antigen related) (LAR)*	*Membrane; Single-pass type I membrane protein;*	*Rattus norvegicus (Rat)*
Q05909	PTPRG_MOUSE	Receptor-type tyrosine-protein phosphatase gamma (Protein-tyrosine phosphatase gamma) (R-PTP-gamma) (EC 3;1;3;48)	Membrane; Single-pass type I membrane protein;	Mus musculus (Mouse)
Q6Y5D8	RHG10_MOUSE	Rho GTPase-activating protein 10 (PH and SH3 domain-containing rhoGAP protein) (PS-GAP) (PSGAP) (Rho-type GTPase-activating protein 10)	Cytoplasm; Cytoplasm;perinuclear region; Cell membrane;	Mus musculus (Mouse)

Accession	Entry name	Protein names	Subcellular locations	Organism
Q6DFV3	RHG21_MOUSE	Rho GTPase-activating protein 21 (Rho GTPase-activating protein 10) (Rho-type GTPase-activating protein 21)	Golgi apparatus membrane; Peripheral membrane protein; Cell junction; Cytoplasmic vesicle membrane; Peripheral membrane protein; Cytoplasm ;cytoskeleton;	Mus musculus (Mouse)
Q6TLK4	RHG27_RAT	Rho GTPase-activating protein 27 (CIN85-associated multi-domain-containing Rho GTPase-activating protein 1) (Rho-type GTPase-activating protein 27)	Cytoplasm; Membrane; Peripheral membrane protein;	Rattus norvegicus (Rat)
Q811P8	RHG32_MOUSE	Rho GTPase-activating protein 32 (Brain-specific Rho GTPase-activating protein) (GAB-associated Cdc42/Rac GTPase-activating protein) (GC-GAP) (Rho-type GTPase-activating protein 32) (Rho/Cdc42/Rac GTPase-activating protein RICS) (RhoGAP involved in the beta-catenin-N-cadherin and NMDA receptor signaling) (p200RhoGAP) (p250GAP)	Cell junction; synapse post-synaptic cell membrane post-synaptic density; Cell projection dendritic spine; Cytoplasm;cell cortex; Endosome membrane; Golgi apparatus membrane; Endoplasmic reticulum membrane; Membrane;	Mus musculus (Mouse)
P97393	RHG05_MOUSE	Rho GTPase-activating protein 5 (Rho-type GTPase-activating protein 5) (p190-B)	Cytoplasm; Membrane; Peripheral membrane protein;	Mus musculus (Mouse)
Q61210	ARHG1_MOUSE	Rho guanine nucleotide exchange factor 1 (Lbc's second cousin) (Lymphoid blast crisis-like 2)	Cytoplasm; Membrane;	Mus musculus (Mouse)
Q63644	ROCK1_RAT	Rho-associated protein kinase 1 (EC 2;7;11;1) (Liver regeneration-related protein LRRG199) (Rho-associated; coiled-coil-containing protein kinase 1) (p150 RhoA-binding kinase ROK beta) (p160 ROCK-1) (p160ROCK)	Cytoplasm; Cytoplasm ;cyto-skeleton;centro-some ;centriole; Golgi apparatus membrane; Peripheral membrane protein;	Rattus norvegicus (Rat)

Accession	Entry name	Protein names	Subcellular locations	Organism
P70336	ROCK2_MOUSE	Rho-associated protein kinase 2 (EC 2;7;11;1) (Rho-associated; coiled-coil-containing protein kinase 2) (p164 ROCK-2)	Cytoplasm; Cell membrane; Peripheral membrane protein;	Mus musculus (Mouse)
Q62868	*ROCK2_RAT*	*Rho-associated protein kinase 2 (EC 2;7;11;1) (Rho-associated; coiled-coil-containing protein kinase 2) (RhoA-binding kinase 2) (p150 ROK-alpha) (ROKalpha) (p164 ROCK-2)*	*Cytoplasm; Cell membrane; Peripheral membrane protein;*	*Rattus norvegicus (Rat)*
P0C6P5	RGNEF_RAT	Rho-guanine nucleotide exchange factor (190 kDa guanine nucleotide exchange factor) (p190-RhoGEF) (p190RhoGEF)	Cytoplasm; Cell membrane;	Rattus norvegicus (Rat)
Q99PL5	RRBP1_MOUSE	Ribosome-binding protein 1 (Ribosome receptor protein) (RRp) (mRRp)	Endoplasmic reticulum membrane; Single-pass type III membrane protein;	Mus musculus (Mouse)
P0C219	SLMAP_RAT	Sarcolemmal membrane-associated protein	Cell membrane;sarcolemma; Single-pass type IV membrane protein; Cytoplasm ;cytoskeleton;centrosome;	Rattus norvegicus (Rat)
Q62028	PLA2R_MOUSE	Secretory phospholipase A2 receptor (PLA2-R) (PLA2R) (180 kDa secretory phospholipase A2 receptor) (M-type receptor) [Cleaved into: Soluble secretory phospholipase A2 receptor (Soluble PLA2-R) (Soluble PLA2R)]	Cell membrane; Single-pass type I membrane protein; Secreted;	Mus musculus (Mouse)
P42346	MTOR_RAT	Serine/threonine-protein kinase mTOR (EC 2;7;11;1) (FK506-binding protein 12-rapamycin complex-associated protein 1) (FKBP12-rapamycin complex-associated protein) (Mammalian target of rapamycin) (mTOR) (Mechanistic target of rapamycin) (Rapamycin target protein 1) (RAPT1)	Endoplasmic reticulum membrane; Peripheral membrane protein; Cytoplasmic side; Golgi apparatus membrane; Mitochondrion outer membrane; Cytoplasmic side; Lysosome;	Rattus norvegicus (Rat)

Accession	Entry name	Protein names	Subcellular locations	Organism
Q6ZQ29	TAOK2_MOUSE	Serine/threonine-protein kinase TAO2 (EC 2;7;11;1) (Thousand and one amino acid protein 2)	Cytoplasmic vesicle membrane; Multi-pass membrane protein; Cytoplasm ;cytoskeleton; Cell projection;dendrite;	Mus musculus (Mouse)
Q9JLS3	*TAOK2_RAT*	*Serine/threonine-protein kinase TAO2 (EC 2;7;11;1) (Thousand and one amino acid protein 2)*	*Cytoplasmic vesicle membrane; Multi-pass membrane protein; Cytoplasm ;cytoskeleton; Cell projection;dendrite;*	*Rattus norvegicus (Rat)*
Q9WV48	SHAN1_RAT	SH3 and multiple ankyrin repeat domains protein 1 (Shank1) (GKAP/SAPAP-interacting protein) (SPANK-1) (Somatostatin receptor-interacting protein) (SSTR-interacting protein) (SSTRIP) (Synamon)	Cytoplasm; Cell junction ;synapse; Cell junction;synapse ;postsynaptic cell membrane	Rattus norvegicus (Rat)
Q925N2	SFXN2_MOUSE	Sideroflexin-2	Mitochondrion membrane; Multi-pass membrane protein;	Mus musculus (Mouse)
Q8C0T5	SI1L1_MOUSE	Signal-induced proliferation-associated 1-like protein 1 (SIPA1-like protein 1)	Cytoplasm;cyto-skeleton; Cell junc-tion ;synapse;post-synaptic cell membrane ;post-synaptic density; Cell junction; ;synaptosome;	Mus musculus (Mouse)
O35412	*SI1L1_RAT*	*Signal-induced proliferation-associated 1-like protein 1 (SIPA1-like protein 1) (SPA-1-like protein p1294) (Spine-associated Rap GTPase-activating protein) (SPAR)*	*Cytoplasm;cytoskeleton; Cell junction ;synapse;postsynaptic cell membrane ;postsynaptic density; Cell junction;synapse ;synaptosome;*	*Rattus norvegicus (Rat)*
P0C1S9	DGLB_RAT	Sn1-specific diacylglycerol lipase beta (DGL-beta) (EC 3;1;1;-)	Cell membrane; Multi-pass membrane protein;	Rattus norvegicus (Rat)

Accession	Entry name	Protein names	Subcellular locations	Organism
Q6QIY3	SCNAA_MOUSE	Sodium channel protein type 10 subunit alpha (Peripheral nerve sodium channel 3) (PN3) (Sensory neuron sodium channel) (Sodium channel protein type X subunit alpha) (Voltage-gated sodium channel subunit alpha Nav1;8)	Membrane; Multi-pass membrane protein;	Mus musculus (Mouse)
O88457	SCNBA_RAT	Sodium channel protein type 11 subunit alpha (NaN) (Sensory neuron sodium channel 2) (Sodium channel protein type XI subunit alpha) (Voltage-gated sodium channel subunit alpha Nav1;9)	Membrane; Multi-pass membrane protein;	Rattus norvegicus (Rat)
Q9ER60	SCN4A_MOUSE	Sodium channel protein type 4 subunit alpha (Sodium channel protein skeletal muscle subunit alpha) (Sodium channel protein type IV subunit alpha) (Voltage-gated sodium channel subunit alpha Nav1;4)	Membrane; Multi-pass membrane protein;	Mus musculus (Mouse)
Q9WTU3	SCN8A_MOUSE	Sodium channel protein type 8 subunit alpha (Sodium channel protein type VIII subunit alpha) (Voltage-gated sodium channel subunit alpha Nav1;6)	Membrane; Multi-pass membrane protein;	Mus musculus (Mouse)
Q6Q760	NALCN_RAT	Sodium leak channel non-selective protein (Four domain-type voltage-gated ion channel alpha-1 subunit) (Voltage gated channel-like protein 1)	Membrane; Multi-pass membrane protein;	Rattus norvegicus (Rat)
Q8BXR5	*NALCN_MOUSE*	*Sodium leak channel non-selective protein (Voltage gated channel-like protein 1)*	*Membrane; Multi-pass membrane protein;*	*Mus musculus (Mouse)*
Q8C3K6	SC5A1_MOUSE	Sodium/glucose cotransporter 1 (Na(+)/glucose cotransporter 1) (High affinity sodium-glucose cotransporter) (Solute carrier family 5 member 1)	Membrane; Multi-pass membrane protein;	Mus musculus (Mouse)
Q8BLV3	SL9A7_MOUSE	Sodium/hydrogen exchanger 7 (Na(+)/H(+) exchanger 7) (NHE-7) (Solute carrier family 9 member 7)	Golgi apparatus;trans-Golgi network membrane; Multi-pass membrane protein; Recycling endosome membrane;	Mus musculus (Mouse)
Q6PIE5	AT1A2_MOUSE	Sodium/potassium-transporting ATPase subunit alpha-2 (Na(+)/K(+) ATPase alpha-2 subunit) (EC 3;6;3;9) (Na(+)/K(+) ATPase alpha(+) subunit) (Sodium pump subunit alpha-2)	Membrane; Multi-pass membrane protein; Cell membrane;	Mus musculus (Mouse)

Accession	Entry name	Protein names	Subcellular locations	Organism
Q3UHA3	SPTCS_MOUSE	Spatacsin (Spastic paraplegia 11 protein homolog)	Membrane; Multi-pass membrane protein; Cytoplasm ;cytosol; Nucleus;	Mus musculus (Mouse)
Q62261	SPTB2_MOUSE	Spectrin beta chain; brain 1 (Beta-II spectrin) (Embryonic liver fodrin) (Fodrin beta chain) (Spectrin; non-erythroid beta chain 1)	Cytoplasm;cytoskeleton; Cytoplasm ;myofibril;sarcomere ;M-band; Cell membrane; Peripheral membrane protein; Cytoplasmic side;	Mus musculus (Mouse)
Q9QWI6	SRCN1_MOUSE	SRC kinase signaling inhibitor 1 (SNAP-25-interacting protein) (SNIP) (p130Cas-associated protein) (p140Cap)	Cytoplasm; Cytoplasm;cytoskeleton; Cell projection ;axon; Cell projection;dendrite; Cell junction ;synapse; Cell junction;synapse ;postsynaptic cell membrane;postsynaptic density;	Mus musculus (Mouse)
Q9QXY2	*SRCN1_RAT*	*SRC kinase signaling inhibitor 1 (SNAP-25-interacting protein) (SNIP) (p130Cas-associated protein) (p140Cap)*	*Cytoplasm; Cytoplasm ;cytoskeleton; Cell projection;axon; Cell projection ;dendrite; Cell junction;synapse; Cell junction ;synapse;postsynaptic cell membrane ;postsynaptic density;*	*Rattus norvegicus (Rat)*
Q4QR83	STRA6_RAT	Stimulated by retinoic acid gene 6 protein homolog	Cell membrane; Multi-pass membrane protein;	Rattus norvegicus (Rat)

Accession	Entry name	Protein names	Subcellular locations	Organism
Q8K4L3	SVIL_MOUSE	Supervillin (Archvillin) (p205/p250)	Cell membrane; Peripheral membrane protein; Cytoplasmic side; Cytoplasm;cytoskeleton; Cell projection;invadopodium; Cell projection;podosome;	Mus musculus (Mouse)
P0C6B8	SVEP1_RAT	Sushi; von Willebrand factor type A; EGF and pentraxin domain-containing protein 1	Secreted; Cytoplasm; Membrane; Peripheral membrane protein;	Rattus norvegicus (Rat)
A2AVA0	*SVEP1_MOUSE*	*Sushi; von Willebrand factor type A; EGF and pentraxin domain-containing protein 1 (Polydom)*	*Secreted; Cytoplasm; Membrane; Peripheral membrane protein;*	*Mus musculus (Mouse)*
Q80X82	SYMPK_MOUSE	Symplekin	Cytoplasm ;cytoskeleton; Cell junction; tight junction; Cell membrane; Peripheral membrane protein; Cytoplasmic side; Nucleus;nucleoplasm;	Mus musculus (Mouse)
Q63564	SV2B_RAT	Synaptic vesicle glycoprotein 2B (Synaptic vesicle protein 2B)	Cytoplasmic vesicle ;secretory vesicle;synaptic vesicle membrane; Multi-pass membrane protein; Cytoplasmic vesicle ;secretory vesicle;acrosome;	Rattus norvegicus (Rat)
Q5SV85	SYNRG_MOUSE	Synergin gamma (AP1 subunit gamma-binding protein 1) (Gamma-synergin)	Cytoplasm ;cytosol; Golgi apparatus;trans-Golgi network membrane; Peripheral membrane protein;	Mus musculus (Mouse)

Accession	Entry name	Protein names	Subcellular locations	Organism
Q9JKC9	*SYNRG_RAT*	*Synergin gamma (AP1 subunit gamma-binding protein 1) (Gamma-synergin)*	*Cytoplasm; Golgi apparatus ;trans-Golgi network membrane; Peripheral membrane protein;*	*Rattus norvegicus (Rat)*
P26039	TLN1_MOUSE	Talin-1	Cell projection;ruffle membrane; Peripheral membrane protein; Cytoplasmic side; Cytoplasm ;cytoskeleton;	Mus musculus (Mouse)
Q71LX4	TLN2_MOUSE	Talin-2	Cell junction;focal adhesion; Cell junction ;synapse; Cell membrane; Peripheral membrane protein; Cytoplasmic side; Cytoplasm;cytoskeleton;	Mus musculus (Mouse)
Q5SVR0	TBC9B_MOUSE	TBC1 domain family member 9B	Membrane; Single-pass membrane protein;	Mus musculus (Mouse)
Q9R1K2	TEN2_RAT	Teneurin-2 (Ten-2) (Neurestin) (Protein Odd Oz/ten-m homolog 2) (Tenascin-M2) (Ten-m2)	Membrane; Single-pass type II membrane protein;	Rattus norvegicus (Rat)
Q9WTS5	*TEN2_MOUSE*	*Teneurin-2 (Ten-2) (Protein Odd Oz/ten-m homolog 2) (Tenascin-M2) (Ten-m2)*	*Membrane; Single-pass type II membrane protein;*	*Mus musculus (Mouse)*
Q9WTS6	TEN3_MOUSE	Teneurin-3 (Ten-3) (Protein Odd Oz/ten-m homolog 3) (Tenascin-M3) (Ten-m3)	Membrane; Single-pass type II membrane protein;	Mus musculus (Mouse)
Q3UHK6	TEN4_MOUSE	Teneurin-4 (Ten-4) (Downstream of CHOP4) (Protein Odd Oz/ten-m homolog 4) (Tenascin-M4) (Ten-m4)	Membrane; Single-pass type II membrane protein;	Mus musculus (Mouse)
Q9JM61	THSD1_MOUSE	Thrombospondin type-1 domain-containing protein 1 (Transmembrane molecule with thrombospondin module)	Membrane; Single-pass type I membrane protein;	Mus musculus (Mouse)
Q9QX05	TLR4_RAT	Toll-like receptor 4 (Toll4) (CD antigen CD284)	Membrane; Single-pass type I membrane protein;	Rattus norvegicus (Rat)

Accession	Entry name	Protein names	Subcellular locations	Organism
Q91YD4	TRPM2_MOUSE	Transient receptor potential cation channel subfamily M member 2 (EC 3;6;1;13) (Long transient receptor potential channel 2) (LTrpC-2) (LTrpC2) (Transient receptor potential channel 7) (TrpC7)	Membrane; Multi-pass membrane protein;	Mus musculus (Mouse)
Q8CIR4	TRPM6_MOUSE	Transient receptor potential cation channel subfamily M member 6 (EC 2;7;11;1) (Channel kinase 2) (Melastatin-related TRP cation channel 6)	Membrane; Multi-pass membrane protein;	Mus musculus (Mouse)
Q925B3	TRPM7_RAT	Transient receptor potential cation channel subfamily M member 7 (EC 2;7;11;1) (Long transient receptor potential channel 7) (LTrpC-7) (LTrpC7) (Transient receptor potential-phospholipase C-interacting kinase) (TRP-PLIK)	Membrane; Multi-pass membrane protein;	Rattus norvegicus (Rat)
Q8R455	TRPM8_RAT	Transient receptor potential cation channel subfamily M member 8 (Cold menthol receptor 1)	Membrane; Multi-pass membrane protein;	Rattus norvegicus (Rat)
Q56A06	TMTC2_MOUSE	Transmembrane and TPR repeat-containing protein 2	Membrane; Multi-pass membrane protein;	Mus musculus (Mouse)
Q80WF4	T132A_RAT	Transmembrane protein 132A (GRP78-binding protein) (HSPA5-binding protein 1)	Golgi apparatus membrane; Single-pass type I membrane protein; Endoplasmic reticulum membrane; Single-pass type I membrane protein;	Rattus norvegicus (Rat)
Q91VX9	TM168_MOUSE	Transmembrane protein 168	Membrane; Multi-pass membrane protein;	Mus musculus (Mouse)
Q9DBS1	TMM43_MOUSE	Transmembrane protein 43 (Protein LUMA)	Endoplasmic reticulum; Nucleus inner membrane; Multi-pass membrane protein;	Mus musculus (Mouse)
Q9ESN3	TMM8A_MOUSE	Transmembrane protein 8A (M83 protein) (Transmembrane protein 8)	Membrane; Multi-pass membrane protein;	Mus musculus (Mouse)
P52332	JAK1_MOUSE	Tyrosine-protein kinase JAK1 (EC 2;7;10;2) (Janus kinase 1) (JAK-1)	Endomembrane system; Peripheral membrane protein;	Mus musculus (Mouse)

Accession	Entry name	Protein names	Subcellular locations	Organism
Q07014	LYN_RAT	Tyrosine-protein kinase Lyn (EC 2;7;10;2)	Cell membrane; Nucleus; Cytoplasm; Cytoplasm ;perinuclear region; Golgi apparatus;	Rattus norvegicus (Rat)
P55144	TYRO3_MOUSE	Tyrosine-protein kinase receptor TYRO3 (EC 2;7;10;1) (Etk2/tyro3) (TK19-2) (Tyrosine-protein kinase DTK) (Tyrosine-protein kinase RSE)	Cell membrane; Single-pass type I membrane protein;	Mus musculus (Mouse)
A2AVR2	CA175_MOUSE	Uncharacterized protein C1orf175 homolog	Membrane; Multi-pass membrane protein;	Mus musculus (Mouse)
A2RUW0	*CA175_RAT*	*Uncharacterized protein C1orf175 homolog*	*Membrane; Multi-pass membrane protein;*	*Rattus norvegicus (Rat)*
Q6NZL0	CF174_MOUSE	Uncharacterized protein C6orf174 homolog	Membrane; Single-pass membrane protein;	Mus musculus (Mouse)
A2AAE1	K1109_MOUSE	Uncharacterized protein KIAA1109 (Fragile site-associated protein homolog)	Membrane; Single-pass membrane protein;	Mus musculus (Mouse)
Q2QI47	USH2A_MOUSE	Usherin (Usher syndrome type IIa protein homolog) (Usher syndrome type-2A protein homolog)	Cell projection;stereocilium membrane; Single-pass type I membrane protein; Secreted;	Mus musculus (Mouse)
A1A535	MELT_MOUSE	Ventricular zone-expressed PH domain-containing protein 1 (Protein melted homolog)	Cell membrane; Peripheral membrane protein; Cytoplasmic side;	Mus musculus (Mouse)
P50544	ACADV_MOUSE	Very long-chain specific acyl-CoA dehydrogenase; mitochondrial (EC 1;3;99;-) (MVLCAD) (VLCAD)	Mitochondrion inner membrane;	Mus musculus (Mouse)
P45953	*ACADV_RAT*	*Very long-chain specific acyl-CoA dehydrogenase; mitochondrial (VLCAD) (EC 1;3;99;-)*	*Mitochondrion inner membrane;*	*Rattus norvegicus (Rat)*
P98166	VLDLR_RAT	Very low-density lipoprotein receptor (VLDL receptor) (VLDL-R)	Membrane; Single-pass type I membrane protein; Membrane ;clathrin-coated pit; Single-pass type I membrane protein;	Rattus norvegicus (Rat)

Accession	Entry name	Protein names	Subcellular locations	Organism
Q64727	VINC_MOUSE	Vinculin (Metavinculin)	Cytoplasm;cytoskeleton; Cell junction ;adherens junction; Cell membrane; Peripheral membrane protein; Cytoplasmic side; Cell junction;	Mus musculus (Mouse)
P54290	CA2D1_RAT	Voltage-dependent calcium channel subunit alpha-2/delta-1 (Voltage-gated calcium channel subunit alpha-2/delta-1)	Membrane; Single-pass type I membrane protein;	Rattus norvegicus (Rat)
Q01815	CAC1C_MOUSE	Voltage-dependent L-type calcium channel subunit alpha-1C (Calcium channel; L type; alpha-1 polypeptide; isoform 1; cardiac muscle) (MELC-CC) (Mouse brain class C) (MBC) (Voltage-gated calcium channel subunit alpha Cav1;2)	Membrane; Multi-pass membrane protein; Cell membrane;	Mus musculus (Mouse)
P22002	*CAC1C_RAT*	*Voltage-dependent L-type calcium channel subunit alpha-1C (Calcium channel; L type; alpha-1 polypeptide; isoform 1; cardiac muscle) (Rat brain class C) (RBC) (Voltage-gated calcium channel subunit alpha Cav1;2)*	*Membrane; Multi-pass membrane protein; Cell membrane;*	*Rattus norvegicus (Rat)*
P27732	CAC1D_RAT	Voltage-dependent L-type calcium channel subunit alpha-1D (Calcium channel; L type; alpha-1 polypeptide; isoform 2) (Voltage-gated calcium channel subunit alpha Cav1;3)	Membrane; Multi-pass membrane protein;	Rattus norvegicus (Rat)
Q02485	CAC1S_RAT	Voltage-dependent L-type calcium channel subunit alpha-1S (Calcium channel; L type; alpha-1 polypeptide; isoform 3; skeletal muscle) (ROB1) (Voltage-gated calcium channel subunit alpha Cav1;1) (Fragment)	Membrane; Multi-pass membrane protein;	Rattus norvegicus (Rat)
Q02789	*CAC1S_MOUSE*	*Voltage-dependent L-type calcium channel subunit alpha-1S (Calcium channel; L type; alpha-1 polypeptide; isoform 3; skeletal muscle) (Voltage-gated calcium channel subunit alpha Cav1;1)*	*Membrane; Multi-pass membrane protein;*	*Mus musculus (Mouse)*
Q02294	CAC1B_RAT	Voltage-dependent N-type calcium channel subunit alpha-1B (Brain calcium channel III) (BIII) (Calcium channel; L type; alpha-1 polypeptide isoform 5) (Voltage-gated calcium channel subunit alpha Cav2;2)	Membrane; Multi-pass membrane protein;	Rattus norvegicus (Rat)

Accession	Entry name	Protein names	Subcellular locations	Organism
P54282	CAC1A_RAT	Voltage-dependent P/Q-type calcium channel subunit alpha-1A (Brain calcium channel I) (BI) (Calcium channel; L type; alpha-1 polypeptide; isoform 4) (Rat brain class A) (RBA-I) (Voltage-gated calcium channel subunit alpha Cav2;1)	Membrane; Multi-pass membrane protein;	Rattus norvegicus (Rat)
Q07652	CAC1E_RAT	Voltage-dependent R-type calcium channel subunit alpha-1E (BII) (Brain calcium channel II) (Calcium channel; L type; alpha-1 polypeptide; isoform 6) (RBE-II) (RBE2) (Voltage-gated calcium channel subunit alpha Cav2;3)	Membrane; Multi-pass membrane protein;	Rattus norvegicus (Rat)
Q61290	*CAC1E_MOUSE*	*Voltage-dependent R-type calcium channel subunit alpha-1E (Brain calcium channel II) (BII) (Calcium channel; L type; alpha-1 polypeptide; isoform 6) (Voltage-gated calcium channel subunit alpha Cav2;3)*	*Membrane; Multi-pass membrane protein;*	*Mus musculus (Mouse)*
Q9Z0Y8	CAC1I_RAT	Voltage-dependent T-type calcium channel subunit alpha-1I (CaVT;3) (Voltage-gated calcium channel subunit alpha Cav3;3)	Membrane; Multi-pass membrane protein;	Rattus norvegicus (Rat)
Q9EPR5	SORC2_MOUSE	VPS10 domain-containing receptor SorCS2	Membrane; Single-pass type I membrane protein;	Mus musculus (Mouse)
P15920	VPP2_MOUSE	V-type proton ATPase 116 kDa subunit a isoform 2 (V-ATPase 116 kDa isoform a2) (Immune suppressor factor J6B7) (ISF) (Lysosomal H(+)-transporting ATPase V0 subunit a2) (ShIF) (Vacuolar proton translocating ATPase 116 kDa subunit a isoform 2)	Cell membrane; Multi-pass membrane protein; Endosome membrane;	Mus musculus (Mouse)
Q6PDJ1	CAHD1_MOUSE	VWFA and cache domain-containing protein 1 (Cache domain-containing protein 1)	Membrane; Single-pass type I membrane protein;	Mus musculus (Mouse)
Q9R037	WDR44_RAT	WD repeat-containing protein 44 (Rabphilin-11)	Cytoplasm;cytosol; Cytoplasm ;perinuclear region; Endosome membrane; Golgi apparatus;trans-Golgi network;	Rattus norvegicus (Rat)

Accession	Entry name	Protein names	Subcellular locations	Organism
Q9EPL0	XYLT2_MOUSE	Xylosyltransferase 2 (EC 2;4;2;26) (Peptide O-xylosyltransferase 2) (Xylosyltransferase II)	Endoplasmic reticulum membrane; Single-pass type II membrane protein; Golgi apparatus membrane; Single-pass type II membrane protein;	Mus musculus (Mouse)
Q9EPI0	*XYLT2_RAT*	*Xylosyltransferase 2 (EC 2;4;2;26) (Peptide O-xylosyltransferase 2) (Xylosyltransferase II)*	*Endoplasmic reticulum membrane; Single-pass type II membrane protein; Golgi apparatus membrane;*	*Rattus norvegicus (Rat)*
O88799	ZAN_MOUSE	Zonadhesin	Cell membrane; Single-pass type I membrane protein;	Mus musculus (Mouse)

10.2 Structure of sulfo-NHS-SS-biotin

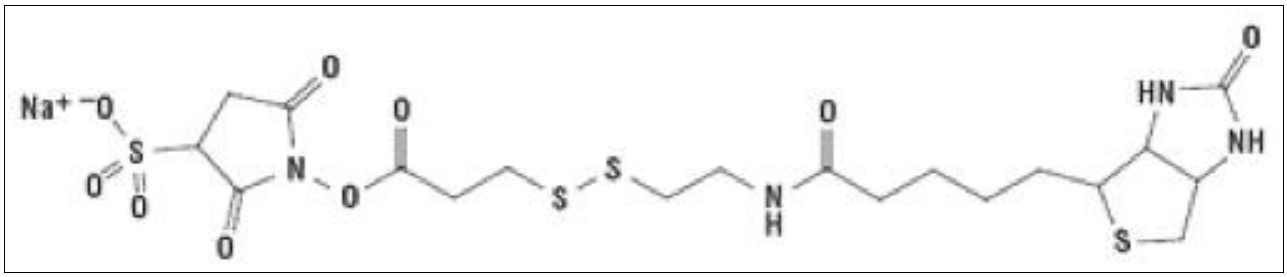

Figure 10.1 Structure of sulfo-NHS-SS-biotin.

To the left the sulfo-NHS-ester group is shown, in the middle the spacer containing a cleavable disulfide bridge, to the right the biotin molecule itself.

10.3 Actin conformation in reversed growth conditions – S cells and CHO-S

Figure 10.2 shows the actin conformation of CHO-S and S cells in adherent growth conditions in comparison to the conformation seen in CCL61.

10.4 Determination of cytochalasin D concentration

Figure 10.3 shows the effect of different cytochalasin D concentrations on the actin and integrin beta 1 conformation in CCL61 and S cells grown in suspension. This experiment was used to determine a suitable cytochalasin D concentration to induce integrin beta 1 clustering on CCL61 in suspension growth conditions.

CHO-S in adherent conditions

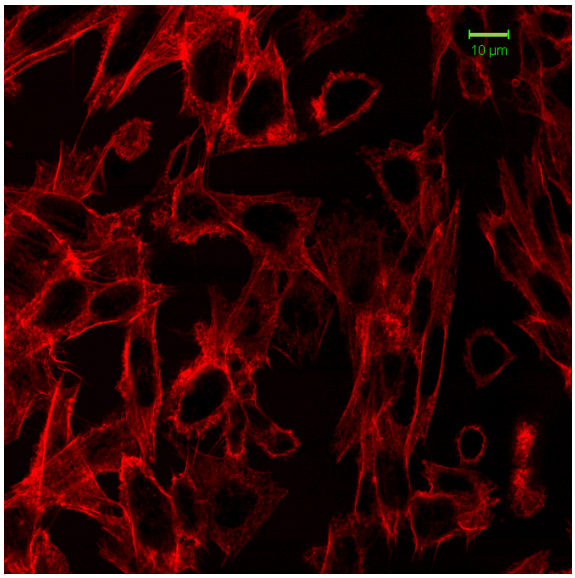

S cells in adherent conditions

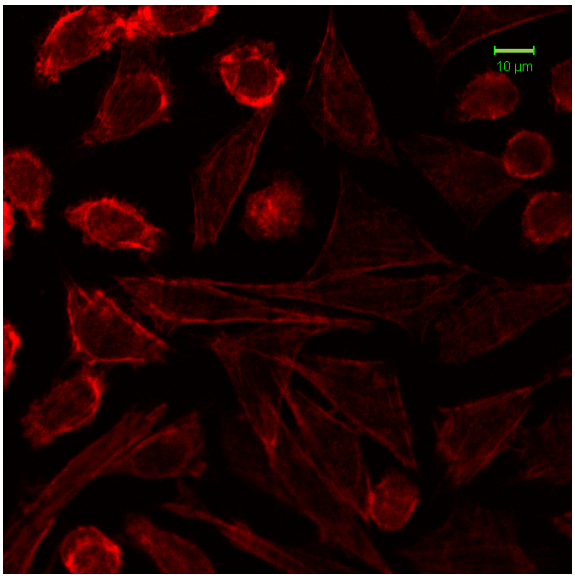

CCL61

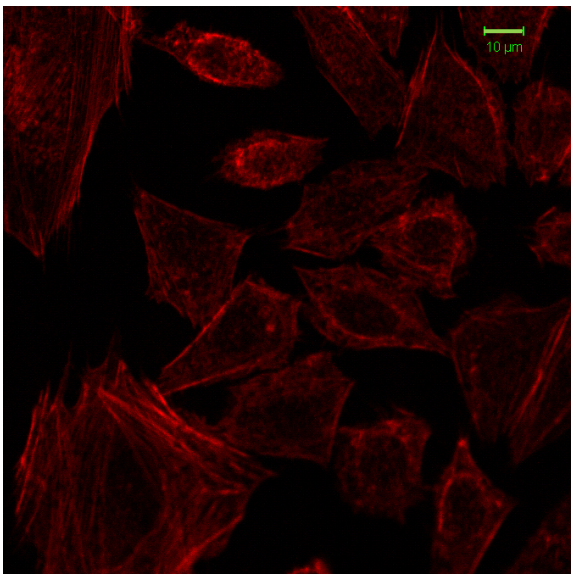

Figure 10.2: Conformation of actin in S cells and CHO-S under adherent conditions compared to adherent CCL61

Cells were stained using phalloidin Alexa 546 after a culture period of three days. Imaging was performed using an inverted Zeiss LSM510 Meta confocal microscope. Mounted cell samples were analysed using a plan apochromat 63x/ 1.4 oil DIC objective. Excitation of the fluorochrome was at 514nm by an argon laser. Emission was collected using a long pass 560 nm filter. Pinhole was 106 µm for S cells and CCl61, and 111 µm for CHO-S. Laser transmission was 13%. All scale bars equal 10 µm.

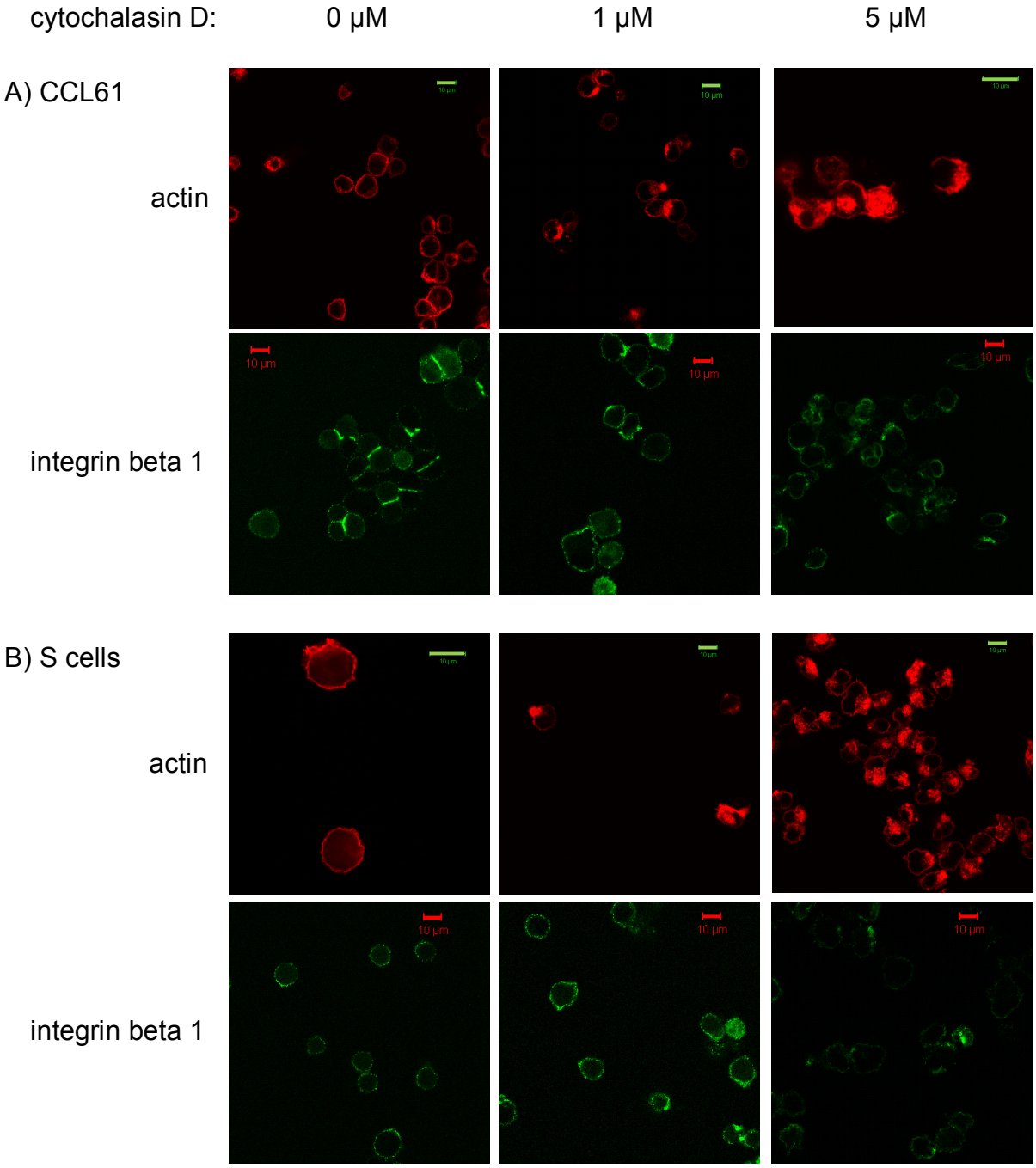

Figure 10.3: Variation of cytochalasin D concentration and its effect on actin and integrin beta 1 conformation for CCL61 and S cells in suspension.

CCL61 and S cells were transferred into PSM suspension culture with different cytochalasin D concentrations After 8 hours of suspension culture, the cells were washed to remove cytochalasin D (CD) and cells were analysed for actin and integrin beta 1 conformation after CD treatment. Imaging was performed using an inverted Zeiss LSM510 Meta confocal microscope. Mounted cell samples were analysed using a plan apochromat 63x/ 1.4 oil DIC objective. Excitation and emission was set as described before. As 5 µM cytochalasin D had an effect on the actin and the integrin beta 1 conformation this concentration was chosen for further experiments. All scale bars equal 10 µm.

References

Aebersold, R and Mann, M (2003) Mass spectrometry-based proteomics. *Nature*, **422**:198-207

Ahram, M *et al.* (2005) Identification of shed proteins from Chinese hamster ovary cells: Applications of statistical confidence using human and mouse databases. *Proteomics*, **5**:1815-1826

Ahram, M *et al.* (2005b) A proteomic approach to characterize protein shedding. *Proteomics*, **5:** 121-131

Altrock, E *et al.* (2012) The significance of integrin ligand nanopatterning on lipid raft clustering in hemapoietic stem cells. *Biomaterials*, **33**:3107-3118

Arnaout, MA *et al.* (2002) Coming to grisp with integrin binding to ligands, Opinion. *Current Opinion in Cell Biology*, **14**: 641-651

Arribas, J and Borroto, A (2002) Protein ectodomain shedding. *Chemical Reviews*, **102**: 4627-4637

Arun, I *et al.* (2010) Visual inspection versus quantitative flow cytometry to detect aberrant CD2 expression in malignant T cells. *Cytometry B Clinical Cytometry*, **78**:169–175

Askari, JA *et al.* (2009) Linking integrin conformation to function. *Journal of Cell Science*, **122**: 165-170

Auersperg, N *et al.* (2001) Ovarian surface epithelium: Biology, Endocrinology, and Pathology. *Endocrine Reviews*, **22**:255-288

Bakker, GJ *et al.* (2012) Lateral mobility of individual integrin nanoclusters orchestrates the onset of leukocytes adhesion. *Proceedings of the National Academy of Sciences*, **10**: 4869-4874

Barda-Saad, M *et al*. (2005) Dynamic molecular interactions linking the T cell antigen receptor to the actin cytoskeleton. *Nature Immunology*, **6**: 80-89

Barkan, D *et al.* (2008) Inhibition of metastatic outgrowth from single dormant tumor cells by targeting the cytoskeleton. *Cancer Research*, **68**: 6241-6250

Baycin-Hizal *et al.* (2012) Proteomic Analysis of Chinese hamster ovary cells. *Journal of proteome research*, **11**: 5265-5276

Bazzoni, G *et al.* (1995) Monoclonal antibody 9EG7 defines a novel beta 1 integrin epitope induced by soluble ligand and manganese, but inhibited by calcium. *The Journal of Biological Chemistry*, **270**: 25570-25577

Berro *et al.* (2007) Identifying the membrane proteome of HIV-1 latently infected cells. *Journal of Biological Chemistry*, **282**:8207-8218

Birch, JR and Racher, AJ (2006) Antibody production. *Advanced Drug Delivery Reviews*, **58**: 671-685

Blonder, J *et al.* (2002) Enrichment of integral membrane proteins for proteomic analysis using liquid chromatography-tandem mass spectrometry. *Journal of Proteome Research*, **1**:351-360

Blonder, J *et al.* (2006) Identification of membrane proteins from mammalian cell/tissue using methanol-facilitated solubilization and tryptic digestion coupled with 2D-LC-MS/MS. *Nature Protocols*, **1**:27842790

Browne, SM and Al-Rubeai, M (2007) Selection methods for high-producing mammalian cell lines. *Trends in Biotechnology*, **25**: 425-432

Butler, M (2005) Animal cell cultures: recent achievements and perspectives in the production of biopharmaceuticals. *Applied Microbiological Biotechnology*, **68**: 283-291

Carter, DL *et al.* (1999) CD56 identifies monocytes and not natural killer cells in Rhesus Macaques. *Cytometry*, **37**: 41-50

Chen, CS *et al.* (1997) Geometric control of cell life and death. *Science*, **276**: 1425-1429

Cheung,E and Juliano, RL(1984) CHO cell aggregation induced by fibronectin-coated beads. E*xperimental Cell Research*, **152**:127-133

Chiarugi, P and Giannoni, E (2008) Anoikis: A necessary death program for anchorage-dependent cells. *Biochemical Pharmacology*, **76**: 1325-1364

Conn, EM *et al.* (2008) Cell surface proteomics identifies molecules functionally linked to tumor cell intravasation. *Journal of Biological Chemistry*, **238**: 26518-26527

Copper, GM and Hausmann, RE (2006) The cell: a molecular approach. 4th ed., Sunderland, USA, Sinauer Associates

Costa, AR *et al*. (2013) The impact of microcarrier culture optimization on the glycosylation profile of a monoclonal antibody. *SpringerPlus*, **2**: (ten pages)

D'Anna, JA *et al.*(1996) Synchronization of Mammalian Cells in S Phase by Sequential Use of Isoleucine-Deprivation G1-or Serum-Withdrawal G0-Arrest and Aphidicolin Block. *Methods in Cell Science*, **18**:115-125

Dahodwala, H *et al.* (2012) Effects of clonal variation on growth, metabolism, and productivity in reponse to trophic factor stimulation: a study of Chinese hamster ovary cells producing a recombinant monoclonal antibody. *Cytotechnology*, **64**: 27-41

Dalton, SL *et al.* (1992) Cell attachment controls fibronectin and intergin alpha 4 beta 1 integrin levels in fibroblasts. *The Journal of Biological Chemistry*, **267**: 8186-8191

Davies, SL *et al.* (2013) Functional heterogeneity and heritability in CHO cell populations. *Biotechnology and Bioengineering*, **10**: 260-274

Delon, I and Brown, NH (2007) Integrins and the actin cytoskeleton. *Current Opinion in Cell Biology*, **19**:43-50

DeMali, KA *et al* (2003) Integrin signaling to the actin cytoskeleton. *Current Opinion in Cell Biology*, **15**: 572-582

Dinnis, DM and James, DC (2005) Engineering mammalian cell factories for improved recombinant monoclonal antibody production: lessons from nature? *Biotechnology and Bioengineering*, **91**: 180-189

Eble, AE and Haier, J (2006) Integrins in cancer treatment. *Current Cancer Drug Targets,* **6**: 89-105

Elia, G (2008) Biotinylation reagents for the study of cell surface proteins. *Proteomics*, **8**: 4012-4024

Etzioni, A (1999) Integrin - the glue of life. *The Lancet*, **353**: 341-343

Farges, B *et al.* (2008) Kinetics of INF gamma producing CHO cells and other industrially relevant cell lines in rapeseed-supplemented batch cultures. *Process Biochemistry*, **43**: 945-953

Ferro, M *et al.* (2000) Organic solvent extraction as a versatile procedure to identify hydrophobic chloroplast membrane proteins. *Electrophoresis*, **21**:3517-3526

Francis, SM and Frisch, H (1994) Disruption of epithelial Cell-Matrix interactions induces apoptosis. *The Journal of Cell Biology*, **124**: 619-626

Freitas,AA and Rocha, B. (1999) Peripheral T cell survival. *Current Opinion in Immunology*, **11**:152-156

Frisch, SM and Francis, H (1994) Disruption of epithelial cell-matrix interactions induces apoptosis. *The Journal of Cell Biology*, **124**:619-626

Gauthier, DJ *et al.* (2004) Utilization of a new biotinylation reagent in the development of a nondiscriminatory investigative approach for the study of cell surface proteins. *Proteomics*, **4**: 3783-3790

Geng, F *et al.* (2012) Multiple post-translational modifications regulate E-cadherin transport during apoptosis. *Journal of Cell Science*, **125**: 2615-2625

Giancotti, FG and Rouslathi, E (1990) Elevated levels of integrin alpha 5 beta 1 fibroncetin receptor supress the transformed phenotype of Chinese hamster ovary cells. *Cell*, **60**: 849-859

Gilmor, AP (2005) Anoikis. *Cell Death and Differentiation*, **12**:1473-1477

Glassy, MC *et al*. (1988) Serum-free media in hybridoma culture and monoclonal antibody production. *Biotechnology and Bioengineering*, **32**: 1015-1028

Godia, F and Cairó, JJ (2001) Metabolic engineering of animal cells. *Bioprocess and Biosystems Engineering*, **24**: 289-298

Green, JA *et al.* (2009) Beta 1 integrin cytoplasmic domain residues selectively modulate fibronectin matrix assembly and cell spreading through talin and AKT-1. *The Journal of Biological Chemistry*, **284**: 8148-8159

Green, LJ et.al. (1998) The integrin beta subunit. *The international Journal of Biochemistry and Cell Biology*, **30**: 179-184

Guilherme, A, Torres, K and Czech, MP (1998) Cross-talk between insulin receptor and integrin alpha 5 beta 1 signaling pathways. *The Journal of Biological Chemistry,* **273**:22899-22903.

Guo, L *et al.* (2002) A proteomic approach for the identification of cell-surface proteins shed by metalloproteases. *Molecular & Cellular Proteomics,* **1**: 30-36

Ham, RG (1964) Clonal growth of mammalian cells in chemically defined, synthetic medium. *Microbiology,* **53**: 288-293

Han, CL *et al.* (2008) A mulitplexed quantitative strategy for membrane proteomics. *Molecular and Cellular proteomics*, **7**: 1983-1997

Hayduk, EJ *et al.* (2004) A two-dimensional electrophoresis map of Chinese hamster ovary cell proteins based on fluorescence staining. *Electrophoresis*, **25**:2545-2556

Hayduk, EJ and Lee, KH (2004d) Cytochalasin D can improve heterologous protein productivity in adherent Chinese Hamster ovary cells. *Biotechnology and Bioengineering*, **90**:354-364

Hayes, NVL *et al.* (2011) Modulation of phosducin-like protein 3 (PhLP3) levels promotes cytoskeletal remodelling in a MAPK and RhoA-dependent manner. *PLoS one*, **6**:e28271-1-e28271-11

Herzenberger, LA *et al.* (2006) Interpreting flow cytometry data: a guide for the perplexed. *Nature Immunology,* **7**: 681-685

Hossler, P *et al.* (2009) Optimal and consistent protein glycosylation in mammalian cell culture. *Glycobiology,* **19**:936-949

Humphries, JD *et al.* (2007) Vinculin controls focal adhesion formation by direct interactions with talin and actin. *The journal of cell biology*, **179**:1043-1057

Hynes, RO (1992) Integrins: versatility, modulation and signaling in cell adhesion. *Cell,* **69**:11-25

Josic, D and Clifton, JG (2007) Mammalian plasma membrane proteomics. *Proteomics,* **7**:3010-3029

Yu, MJ *et al.* (2006) LC-MS/MS analysis of apical and basolateral plasma membranes of rat renal collecting duct cells. *Molecular and Cellular Proteomics*, **5:** 2131-2145

Knowles, GC and McCulloch, CAG (1992) Simultaneous localization and quantification of relative G and F actin content: optimization of fluorescence labeling methods. *The Journal of Histochemistry and Cytochemistry*, **40**:1605-1612

Kuystermans, D *et al.* (2007) Using cell engineering and omic tools for the improvement of cell culture processes. *Cytotechnology*, **53**: 3-22

Lee, BH and Ruoslathi, E (2005) Integrin alpha 5 beta 1 integrin stimulates Bcl-2 expression and cell survival through AKT, Focal Adhesion Kinase, and Ca^{2+}/Calmodulin-dependent protein kinase IV. *Journal of Cellular Biochemistry*, **95**: 1214-1223

LeFloch, F *et al.* (2006) Related effect of cell adaptation to serum-free conditions on murine EPO production and glycosylation by CHO cells. *Cytotechnology*, **52**:39-53

Legate, KR *et al.* (2009) Genetic and cell biological analysis of integrin outside-in signaling. *Genes and Development*, **23**: 397-418

Lenter, M *et al.* (1993) A monoclonal antibody against an activation epitope on mouse integrin chain beta 1 blocks adhesion of lymphocytes to the epithelial integrin alpha 5 beta 1. *Proceedings of the national academy of science of the United States of America,* **90**: 9051-9055

Li, G *et al.*(2001) Downregulation of E-cadherin and Desmoglein 1 by auticrine hepatocyte growht factor during melanoma development. *Oncogene*, **20**: 8125-8135

Liu, J and Jiang, G (2006) CD44 and hematologic malignancies. *Cellular and Molecular Immunology*, **3**: 359-365

Lub, M *et al.* (1997) Dual role of the actin cytoskeleton in regulating cell adhesion mediated by the integrin lymphocyte function-associated molecule-1. *Molecular Biology of the Cell,* **8**:341-351

Macher, BA and Yen, TY (2007) Proteins at membrane surfaces – a review of approaches. *Molecular BioSystems*, **3**: 705-713

Matters, M and Ruoslathi, E (2001) A signalling pathway from $\alpha_5\beta_1$ and $\alpha_V\beta_3$ integrins that elevates bcl-2 transcription. *The Journal of Biological Chemistry*, **276**: 27757-27763

Meredith, JE *et al.* (1993)The extracellular matrix as a cell survival factor. M*olecular Biology of the Cell*, **4**: 953-961

Mills, JW *et al.* (2000) Effect of cytochalasins on F-actin and morphology of Ehrlich Ascites tumor cells. *Experimental Cell Research*, **261**: 209-219

Mirza, SP *et al.* (2007) Improved method for the analysis of membrane proteins by mass spectrometry. *Physiological Genomics*, **30**:89-94

Morigi, M *et al.* (1995) Fluid shear stress modulates surface expression of adhesion molecules by endothelial cells. *Blood,* **85**: 1696-1703

Niessen, CM and Gumbier, BM (2002) Cadherin-mediated cell sorting not determined by binding or adhesion specificity. *The Journal of Cell Biology*, **156**: 389-399

Nolan, JP and Yang, L (2007) The flow of cytometry into systems biology. *Briefings in functional genomics and proteomics*, **6**: 81-90

Nunomura, K *et al.* (2005) Cell surface Labeling and Mass Spectrometry reveal diversity of cell surface markers and signalling molecules expressed in undifferentiated mouse embryonic stem cells. *Molecular and Cellular Proteomics*, **4**:1968-1976

Pedersen, SF *et al.* (1999) Role of F-actin cytoskeleton in the RVD and RVI process in Ehrlich Ascites tumor cells. *Experimental Cell Research*, **252**: 63-74

Peirce, MJ *et al.* (2004) Expression profiling of lymphocyte plasma membrane proteins. *Molecular & Cellular Proteomics*, **3**: 56-65

Peterson, JR and Mitchison, TJ (2000) Small molecules, big impact a history of chemical inhibitors and the cytoskeleton. *Chemistry & Biology*, **9**: 1275-1285

Pontier, SM and Muller, WJ (2009) Integrins in mammary-stem-cell biology and breast-cancer progression – a role in cancer stem cells? *Journal of Cell Sciences*, **122**: 207-214

Prag, S *et al.* (2002) NCAM regulates cell motility. *Journal of Cell Science*, **115**: 283-292.

Puck, TT, *et al.* (1958) Genetics of somatic mammalian cells III. Long-term cultivation of euploid cells from human and animal subject. *Journal of Experimental Medicine*, **108**: 945–56.

Rao, JY *et al.* (1990) Cellular F-actin levels as a marker for cellular transformation: relationship to cell divison and differentiation. *Cancer Research*, **50**: 2215-2220

Reactome [www.reactome.org/ReactomeGWT/entrypoint.html] (November 2012) Cell ECM interaction; *Mus Musculus*, Cold Spring Harbor Laboratory & Ontario Institute for Cancer Research & European Bioinformatics Institute

Redding, PJ and Juliano, RL (2005) Clinging to life; cell to matrix adhesion and cell survival. *Cancer and Metastasis Review*, **24**: 425-439

Regent, M *et al.* (2010) Specificities of integrin beta 1 signaling in the control of cell adhesion and adhesive strength. *European Journal of Cell Biology*, **90**:261-269

Ritchie, JL *et al.* (2000) Flow cytometry analysis of platelet P-selectin expression in whole blood-methodological considerations. *Clincial Laboratory Haematology*, **22**: 359-363

Rodrigues, ME *et al.* (2013) Advances and drawbacks of the adaptation to serum-free culture of CHO-K1 cells for monoclonal antibody production. *Applied Biochemistry and Biotechnology*, **169**:1279-1291

Ruoslathi, E (1991) Integrins. *Journal of Clinical Investigation*, **87**: 1-5

Ruoslathi, E and Reed, JC (1994) Anchorage dependence, integrin and apoptosis. *Cell*, **77**: 447-478

Ruoslathi, E and Vaheri, A (1997) Cell-to-cell contact and extracellular matrix. *Current Opinion in Cell Biology*, **9**: 605-607

Santoni, V *et al.* (200) Membrane proteins and proteomics: Un amour impossible? *Electrophoresis*, **21**: 1054-1070

Satymoorthy, K *et al.* (2001) Insulin-like Growth Factor-1 induces survival and growth of biologically early melanoma cells through both the mitogen-activated protein kinase and β-catenin pathways. *Cancer Research*, **61**: 7318-7324

Schindler, J *et al.* (2006) Enrichment of integral membrane proteins from small amounts of brain tissue. *Journal of Neural transmsstion*, **113**:995-1013

Schymeinsky, J et al. (2011) The mammalian actin-binding protein-1 (mAbp1): a novel molecular player in leukocyites biology. *Trends in Cell Biology*, **21**: 247-255

Shahal, T *et al.* (2012) Regulation of integrin adhesion by varying the density of substrate-bound epidermal growth factor. *Biointerphases*, **7**: (eleven pages)

Sinacore, MS *et al.* (2000) Adaptation of mammalian cells to growth in serum-free media. *Molecular Biotechnology*, **15**: 249-257

Sostaric, E *et al.* (2006) Global profiling of surface plasma membrane proteome of oviductal epithelial cells. *Journal of Proteome Research*, **5**: 3029-3037

Spearman, M et al. (2005) Production and Glycosylation of recombinant beta-interferon in suspension and cytopore microcarrier cultures of CHO cells. *Biotechnology Progress*, **21**: 31-39

Speers, AE and Wu, CW (2007) Proteomics of integral membrane proteins – theory and application. *Chemical Reviews*, **107**: 3687-3714

Streuli, CH (2009) Intergrins and cell-fate determination. *Journal of Cell Science*, **122**: 171-177

Stupack, DG and Cheresh, DA (2002) Get a ligand, get a life: integrins, signaling and cell survival. *Journal of Cell Science*, **115**: 3729-3738

Tan, S *et al.* (2008) Membrane proteins and membrane proteomics. *Proteomics*, **8**: 3924-3932

Thomas, J (ed.) (2009) 'practical proteomics' coursebook, University of York

Thorne, RF *et al.* (2004) The role of the CD44 transmembrane and cytoplasmic domains in co-ordinating adhesive and signalling events. *Journal of Cell Science*, **117**: 373-380

Van Kooyk, Y and Figdor, CG (2000) Avidity regulation of integrins: the driving force in leucocyte adhesion. *Current Opinion in Cell Biology*, **12**: 542-547

Whitlock, BB *et al.* (2000) Differential roles of alpha M beta 2 integrin clustering or activation in the control of apoptosis via regulation of Akt and ERK survival mechanisms. *The Journal of Cell Biology*, **151**:130-1320

Wiesner, S *et al.* (2005) Integrin-actin interactions. *Cellular and Molecular Life Sciences*, **62**:1081-1099

Wiśniewski, JR et al. (2009) Combination of FASP and StageTip-based fractionation allows in-depth analysis of the hippocampal membrane proteome. *Journal of Proteome Research*, **8**:5674-5678

Wong, VVT *et al.* (2004) Evaluation of insulin-mimetic trace metals as insulin replacements in mammalian cell cultures. *Cytotechnology*, **45**: 107-115

Wu, CC and Yates, JR (2003) The application of mass spectrometry to membrane proteins. *Nature Biotechnology*, **21**: 262-267

Wurm, FM (2004) Production of recombinant protein therapeutics in cultivated mammalian cells. *Nature Biotechnology*, **22**: 1393-1398

Yagi, T and Takeichi, M (2000) Cadherin superfamily genes: functions, genomic organization and neurologic diversity. *Genes and Development*, **14**: 1169-1180

Yanez-Mo, M *et al.* (2000) Tetraspanins in intercellular adhesion of polarized epithelial cells: spatial and functional relationship to integrins and cadherins. *Journal of Cell Science*, **114**:577-587

Yap, AS *et al.* (2007) Making and breaking contacs: the cellular biology of cadherin regulation. *Current Opinion in Cell Biology*, **19**: 508-514

Yilmaz, M and Christofoir, G (2010) Mechanisms of motility in metastasizing cells. *Molecular Cancer Research*, **8**: 629-642

Zhang, W *et al.* (2003) Affinity enrichment of plasma membrane for proteomic analysis. *Electrophoresis*, **24**: 2855-2863

Zhang, ZH *et al.* (1995) The alpha 5 beta 1 integrin supports survival of cells on fibronectin and up-regulates Bcl-2 expression. *Proceedings of the national academy of science of the United States of America*, **92**: 6161-6165

Zhao, Y *et al.* (2004) Proteomic analysis of integral plasma membrane proteins. *Analytical Chemistry*, **76**: 1817-1823